New Genes Involved in the Synthesis of Diphthamide, a Modification of Eukaryotic Translation Elongation Factor 2 with Roles in Diphtheria Disease and Ovarian Cancer Formation

A thesis submitted for the degree of
Doctor of Philosophy

by

Shanow Uthman MSc

Department of Genetics
University of Leicester
November 2012

New Genes Involved in the Synthesis of Diphthamide, a Modification of Eukaryotic Translation Elongation Factor 2 with Roles in Diphtheria Disease and Ovarian Cancer Formation

Shanow Uthman

Department of Genetics, University of Leicester
Thesis submitted for the degree of Doctor of Philosophy, November 2012

ABSTRACT

Diphthamide, the target of Diphtheria toxin, is a unique post-translational modification on His_{699} (*S. cerevisiae*) of translation elongation factor 2 (eEF2) found in eukarya and archaea. It serves as the unique target for bacterial ADP-ribosylating toxins such as Diphtheria Toxin, Exotoxin A and Cholix toxin. So far six genes have been known to be involved in the complex three-step biosynthesis pathway: *bona fide* diphthamide genes *DPH1-DPH5* and the recently identified *YBR246w*. While the latter was shown to be involved in the final step of the pathway, its exact role remains unclear. Dph1-Dph4 facilitate the initial step of the pathway and the methytransferase, Dph5, the second step. Surprisingly, after almost four decades of intensive research the enzyme catalyzing the final step, the conversion of the intermediate diphthine into the final product diphthamide, has remained elusive. We sought to exploit yeast genetic interaction and chemical genomic databases in order to identify novel diphthamide biosynthesis genes. A novel candidate gene *YLR143w* was identified and we here present genetic, phenotypic and biochemical analyses that clearly identify *YLR143w* as a novel diphthamide biosynthesis gene. Our observations implicate that *YLR143w* is the main catalytic enzyme necessary for the third step of the pathway, while *YBR246w* has a regulatory role involving Dph5-EF2 interaction.

Furthermore, we demonstrate that Dph1 is likely the primary catalytic enzyme which generates the initial modification on the His_{699} residue.

In addition to the implications in bacterial pathogenesis, diphthamide and the biosynthesis genes *DPH1*, *DPH3* and *DPH4* are associated with cancer formation as well as defects in embryonic development and cell proliferation control. We here demonstrate that diphthamide deficient yeast cells display a significant increase in -1 frameshifting during translation and propose that this is the underlying cause of the phenotypes seen in mammalian organisms.

New Genes Involved in the Synthesis of Diphthamide, a Modification of Eukaryotic Translation Elongation Factor 2 with Roles in Diphtheria Disease and Ovarian Cancer Formation

Shanow Uthman

COMMUNICATIONS

Publications

1. UTHMAN, S., BAER, C., JABLONOWSKI, D. & SCHAFFRATH, R. (2011). Growth Inhibition Strategies Based on Antimicrobial Microbes/Toxins. In: *Science against Microbial Pathogens: Communicating Current Research and Technological Advances*, Mendez-Vilas A (ed.), Formatex Research Center, Vol 2, pp. 1321-1329, ISBN 978-84-939843-2-8.

2. UTHMAN, S., LIU, S., GIORGINI, F., STARK, M., COSTANZO, M. & SCHAFFRATH, R. (2012). Diphtheria Disease and Genes Involved in Formation of Diphthamide, Key Effector of the Diphtheria Toxin. In: *Infectious Disease*, Kumar R (ed.), INTECH Open Access Publisher, pp. 333-356, ISBN 979-953-307-497-8.

3. UTHMAN, S., BAER, C., SCHEIDT, V., LIU, S., ten HAVE, S., GIORGINI, F., STARK, M. & SCHAFFRATH, R. (2013). The Amidation Step of Diphthamide Biosynthesis in Yeast Requires *DPH6* and *DPH7*, Genes Identified through Mining the *DPH1-DPH5* Interaction Network. *PLoS Genetics 9(2): e1003334.*

Scientific Meetings

UTHMAN, S., STARK, M. & SCHAFFRATH, R. (2012). Novel Diphthamide Synthesis Genes from Budding Yeast *Saccharomyces cerevisiae*. 2nd Molecular Microbiology Meeting, 25-27 April 2012, Würzburg, Germany

Shanow Uthman, Christian Bär, Shihui Liu, Sara ten Have, Flaviano Giorgini, Michael J.R. Stark and Raffael Schaffrath (2012). Novel Novel Genes for Diphthamide Synthesis and Antifungal Cell Death Pathways in Yeast. 9th International Meeting on Yeast Apoptosis, 16-20 Septemeber 2012, Rome, Italy

BÄR, C. UTHMAN, S., SCHEDIT, V., M.J.R. Stark3 & SCHAFFRTAH, R. (2012) A Yeast Model for Pathobiological Protein Modification Pathways Reveals New *Corynebacterium diphtheriae* Toxin Effector Genes. 2nd International Congress on Antimicrobial Research (ICAR), 21-23 November 2012, Lisbon, Portugal

Acknowledgements

There are many people who supported me throughout the past 4 years without whom I would not have been able to complete this journey. Firstly, I would like to thank my supervisor, Prof. Raffael Schaffrath, whose patience and excellent supervision, even after his transfer to the University of Kassel, kept me going and allowed me to complete my PhD. This thesis was only possible because of your guidance and support throughout the years. Special thanks to my second supervisor, Dr. Flaviano Giorgini, who kindly agreed to take over my supervision half way through my PhD and guided me through rough times. Without your kind words and encouragement I would not have been able to reach this stage. Thank you for always keeping an eye on me and my project. A very special thank you to my thesis examiners Prof. Mick Tuite and Dr. Kayoko Tanaka for their valuable advice and help, which greatly improved the quality of my thesis.

Thank you to our collaborators, Prof. Mike Stark (University of Dundee), I could not have completed this thesis without your insight and dedication to the MS analyses of our data. Thank you to Dr. Charlie Boone and Dr. Michael Costanzo (University of Toronto) and Dr. Shihui Liu (Bethesda, USA) for your collaboration and valuable suggestions. This project would not have been possible without the support of the HOPE Against Cancer foundation, especially Barbara North, who not only provided the financial basis for my research but whose dedication to the fight against cancer inspired me to keep going whenever things looked grim.

During my PhD I met many people who were wonderful to work with and who made the past 4 years fly by. Daniel and Christian, who patiently taught me genetics, were the best colleagues I ever had the pleasure of working with. I can honestly say you soon became friends; I will terribly miss your company and the Austro-German discussions. Mathura and Amit, though you are on the other side of the world, I will always cherish the laughs we shared. After you left, tea breaks were never the same again. Gurdeep,

though we only shared a short time working in the same lab, thank you for always putting a smile on my face. Mariaelena, my role model, there were times I thought I would not be able to carry on with my project; without your support, kind words and invaluable advice I would not have had the strength to finish this journey. When you run your own lab, I hope you give me a call. Mahdieh and Alex, I will miss all the fun we had while waiting for endless rounds of western blots to run; thank you for the smiles and laughs. Rob, thank you for your patience and advice whenever I came running with new technical problems, your scientific knowledge never ceased to amaze me.

I made many close friends during my time at the University of Leicester, many of whom will always stay close to my heart. Fabricio and Eva, you became my friends, my family and my support system. Thank you for being there whenever I needed a shoulder to cry on and for all the lovely times together. I hope to always be close to you and will cherish the memories of our journey together, I could not have asked for better friends! A big thank you to my friend Dave for sharing your home with me, for listening patiently and for always being on my side! Valeria, Chiara, Angelica, Pierpaolo, Danielle, Mahmut and Pille, I will miss our improvised dinners, the in depth discussions and the silly laughs we shared. You all taught me to view the world and myself from a different perspective and made me look outside the box. I hope to always be surrounded by such lovely friend like you.

Special thanks to my dear friends in Austria: Tina, Christian, Nini and Bernhard. Though I have spent the last six years abroad, you will always be the ones who know me best and I will always carry your friendship with me wherever I go. You are home to me.

Last but never the least, thank you to my wonderful family! Ata, who always kept me focused on what's important in life. Azad and Bakhteyar thank you for your support throughout the past 5 years. Thank you to my favourite cousin, Roza, whose kind words and encouragement never failed to brighten up my days. My dad, my mum and my sister, without your unconditional love and support I would not have been able to complete this journey. You all shaped my past and my future, you make me who I am.

ABBREVIATIONS

Amp	Ampicillin
ADP	Adenosine Diphosphate
ART	ADP-Ribosylating Toxins
ATP	Adenosine triphosphate
bp	base pairs
co-IP	co-immunoprecipitation
DNA	Deoxyribonucleic acid
DPT	Diphtheria–Pertussis–Tetanus
DT	Diphtheria toxin
DTT	Dithiotreitol
ECL	Electrogenerated chemiluminescence
EDTA	Ethylenediaminetetraacetic acid
ETA	Exotoxin A from *Pseudomonas aeruginosa*
HCl	Hydrochloric Acid
HEPES	4-(2-hydroxyethyl)-1-piperazineethanesulfonic acid
HIV	Human immunodeficiency virus
His	Histidine
KCl	Potassium chloride
kb	kilobases
kDa	Kilodalton
LB	Luria Bertani Medium
mRNA	messenger Ribonucleic acid
NAD+	Nicotinamide adenine dinucleotide
NP-40	Nonidet P-40
ONPG	Ortho-Nitrophenyl-β-galatoside
ORF	Open reading frame
OD	Optical density
PAGE	Polyacrylamide gelelectrophoresis
PCR	Polymerase chain reaction
PEG	Polyethylene glycol
PMSF	Phenylmethylfulfonylfluoride
PTM	Post-translational modification
RNA	Ribonucleic acid
SD	Synthetic dropout
SDS	Sodium dodecyl sulphate
TAP	Tandem affinity purification
TBE	Tris Borate EDTA
TBST	Tris-buffered saline Tween 20
tRNA	transfer Ribonucleic acid
UV	Ultraviolet light
YEPD	Yeast extract peptone dextrose medium

TABLE OF CONTENTS

1 Introduction 1
1.1 Post-translational modifications - diversifying the proteome 1
1.2 Diphthamide, a peculiar amino acid variation 3
1.3 Mono-ADP-ribosylation of diphthamide - friend or foe? 6
1.4 Microbial Competition 7
1.5 eEF2 - key player in the translation machinery 9
1.6 The multi-step pathway of diphthamide biosynthesis 12
1.7 Archael diphthamide synthesis 15
1.8 Dph3 and Dph4 – two versatile little proteins 17
1.9 YBR246w – the new guy in the neighbourhood 18
1.10 Sordarin and ricin, two powerful diphthamide indicator drugs 19
1.11 Diphthamide mouse models 21
1.12 *OVCA1*, tumour suppressor gene 22
1.13 Aims and Objectives 24

2 Mapping a Dph1 region crucial for the interaction with Dph2 and Dph3 26
2.1 Introduction 26
2.2 Results 33
2.2.1 DT phenotype of Dph1 constructs 33
2.2.2 Sordarin phenotype of Dph1 constructs 36
2.2.3 Co-Immunoprecipitation assay reveals interaction profile of Dph1 39
2.3 Conclusion 45

3 Identification of novel putative Diphthamide Biosynthesis genes 50
3.1 Introduction 50
3.2 Results 54
3.2.1 SGA analysis reveals novel candidate diphthamide biosynthesis genes 54
3.2.2 YLR143w and YBR246w phenocluster with bona fide diphthamide genes 60
3.3 Conclusion 65

4 Investigating the role of *YLR143w* and *YBR246w* in diphthamide biosynthesis ... 68
4.1 Introduction 68
4.2 Results 70
4.2.1 YLR143w and YBR246w phenocopy diphthamide synthesis genes 70
4.2.2 YLR243w and YBR246w cannot be ADP-Ribosylated in vitro 75
4.2.3 eEF2 tandem affinity purification 77
4.2.4 Mass spectrometry identifies YLR143w and YBR246w as diphthamide synthesis genes 79
4.2.5 The YLR143w/DPH6 gene product 93
4.2.6 The YBR246w/DPH7 gene product 97
4.2.7 Ylr143w and Ybr246w do not directly interact with each other or other Dph proteins 101
4.2.8 Ylr143w/Dph6 interacts with eEF2 independent of Ybr246w/Dph7 105
4.2.9 Deletion of DPH7 enhances interaction between Dph5 and eEF2 107
4.2.10 Excess Dph6 cannot by-pass the trimethylation step 110
4.2.11 Physiological role of diphthamide 112
4.3 Discussion 117

5 Discussion 124
5.1 Dph1 mutagenesis reveals a central role for the iron-sulfur enzyme 125
5.2 Data mining of genetic interaction database reveals novel *DPH* genes 128
5.3 The physiological role of diphthamide in normal cellular function 133
5.4 Concluding remarks and future directions 136

6 Materials and Methods 139
6.1 Materials 139
6.1.1 Escherichia coli strains 139
6.1.2 Saccharomyces cerevisiae strains 139
6.1.3 Plasmids 141
6.1.4 Oligonucleotides 143
6.1.5 Antibodies 147
6.1.6 Cultivation of bacterial strains 147
6.1.7 Cultivation of yeast strains 147
6.2 Methods 148
6.2.1 Isolation of plasmid DNA from bacterial cultures 148
6.2.2 Isolation of genomic DNA from yeast cultures 148
6.2.3 Transformation protocols for E.coli 149
6.2.4 S. cerevisiae transformation procedures 149
6.2.5 Polymerase chain reaction 151
6.2.6 Agarose gel electrophoresis 153
6.2.7 DNA isolation from agarose gels 153
6.2.8 Restriction Digestion 153
6.2.9 Ethanol precipitation of PCR products 154
6.2.10 Ligation 154
6.2.11 Gene manipulation procedures 154
6.2.12 Phenotype assays for S. cerevisiae 156
6.2.13 Protein biochemistry 158
6.2.14 Bioinformatic data mining of DPH genes 165
6.2.15 Multi-alignment tool 166
6.2.16 Statistical Analysis 166

7 Appendices 168
7.1 Appendix 1: Mass spectrometry analyses of TAP-isolated eEF2 from wt, *dph1*Δ and *ylr143w*Δ strains 168
7.2 Appendix 2: The amidation step of diphthamide biosynthesis in yeast requires DPH6, a gene identified through mining the DPH1-DPH5 interaction network 172

8 Bibliography 189

CHAPTER 1

INTRODUCTION

1 Introduction

1.1 Post-translational modifications - diversifying the proteome

One of the fundamental laws of genetics postulates that DNA is transcribed into RNA and RNA in turn is translated into protein. It is the basis of molecular biology and a beautifully simple principle, but soon becomes very complex when looked upon in detail. The end product of this cycle is the formation of proteins, which carry out most of the work in a cell. Proteins determine cell structure, function and regulation and therefore the synthesis of proteins is a fundamental process to every living organism.

The regulation of gene expression is highly sophisticated and allows the translation of genes into their gene products. Every single step from DNA to RNA and the final protein product is meticulously regulated in order to ensure proper cell function. First, transcription initiation at alternative promoters allows the tissue specific expression of genes and together with differential regulation of transcription termination represents important mechanisms of gene expression at the DNA level (Ayoubi and Van De Ven 1996). Next, alternative mRNA splicing delivers several isoforms of proteins translated from the same template RNA and finally alterations of the freshly synthesized protein, which undergoes so called post-translational modifications (PTMs). The regulation of these three main stages of translation enables the increase of complexity from the genome with ~25,000 human genes to the transcriptome (~100,000 transcripts) and finally an estimated one million proteins in the proteome (Jensen 2004). Here we

focus on post-translational modifications (PTM) which in contrast to the first two steps of gene expression regulation, present a much faster way for the cell to respond to intra- and extracellular signals. PTMs are chemical changes to the structure of the newly synthesized protein thereby regulating its function. The importance of PTMs is reflected in the number of genes that are assigned to them. The human genome includes more than 500 hundred protein kinases, more than 500 protein phosphatases and numerous methyltransferases, ubiquitinyl ligases, acetylases and deacetylases (reviewed by (Lin H. 2008; Lin and Begley 2011). In general, PTMs are additions of functional groups to side chains of amino acids in a protein, which in turn determines its activity, localization and interaction with other components of the cell. PTMs are generated by enzymatic activity and can occur at any point – right after translation the chemical modification of the newly synthesized peptide ensures the proper folding and localization of the protein. Kinases and proteases on the other hand act as an ON/OFF switch and shift the protein from an active into an inactive state. These are reversible forms of PTM whereas the irreversible addition of tags, such as during ubiquitination, is irreversible and leads to the degradation of the tagged protein. Errors in the vast network of PTM can impair protein function and even lead to disease, such as the deregulated phosphorylation cascade in the MAPK/ERK pathway, which is implicated in the formation of many cancers. Therefore investigating and targeting PTM provide us with invaluable therapeutic approaches for heart diseases, cancer and neurodegenerative diseases. Inhibitors of kinases and proteases for example have been used as a treatment for cancer, inflammation as well as infection by viruses such as HIV (reviewed by (Lin and Begley 2011).

PTMs can be classified according to their underlying chemistry (phosphorylation, acetylation, methylation, etc.), the target residue (Ser/Thr, Lys, Arg, etc.) or the biological function they regulate. The latter includes changes that act as an ON/OFF switch for enzymatic activity, the addition of protein tags like ubiquitin, creation or masking of recognition sites and the cleavage of proteins into smaller fragments (proteolysis). The list of PTM and the resulting amino acid variations is very long, some of which are more common and others are unique to a single protein (reviewed by (Lin H. 2008).

1.2 Diphthamide, a peculiar amino acid variation

Translation elongation factor 2 (EF2) from both archaea and eukayotes (eEF2) carries a unique PTM on His^{699} in yeast and His^{715} in mammalian cells, called diphthamide (Figure 1.1) (Van Ness et al. 1980b; Moehring et al. 1984; Chen et al. 1985b). It is an unusual amino acid variation, not only because it is exclusively found on eEF2, but also because it is generated in a complex pathway involving enzymes encoded by more than five diphthamide biosynthesis genes, *DPH1-DPH5* (Pappenheimer 1977; Chen et al. 1985b; Liu and Leppla 2003a). In 1974 Robinson *et al.* first reported the discovery of this histidine derivate as the unique target for diphtheria toxin, which hence was named diphthamide (Robinson et al. 1974; Van Ness et al. 1980b). Even though diphthamide was identified almost 4 decades ago, its role in cell physiology remains elusive. However, it is associated with several distinct phenotypes which will be discussed here. Adding to its peculiar nature is that diphthamide is subject to a secondary PTM: it can be mono-ADP-ribosylated by

endogenous and exogenous ADP-ribosyltransferases (ARTs) (Figure 1.3) (Honjo et al. 1968; Van Ness et al. 1980a; Sitikov et al. 1984; Fendrick and Iglewski 1989a). In contrast to the unique diphthamide, mono-ADP-ribosylated proteins can be found in every major compartment of the cell, which highlights its diverse application as a PTM. In the case of eEF2, the tandem of PTMs (diphthamide formation and its consequent ADP-ribosylation) renders the translation factor inactive, which in turn arrests *de novo* protein synthesis and ultimately leads to cell death (Pappenheimer 1977; Oppenheimer and Bodley 1981).

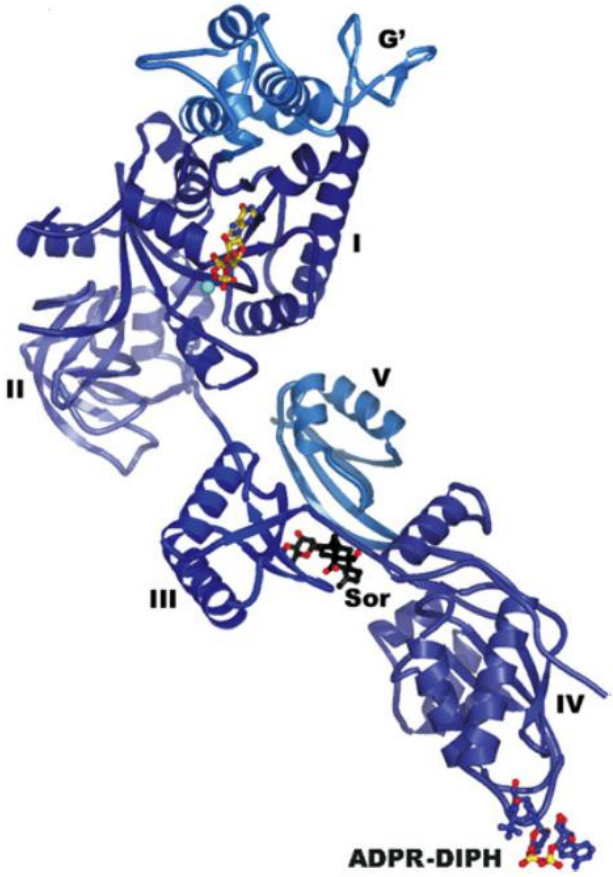

Figure 1.1. Ribbon diagram of ADP-ribosylated eukaryotic translation elongation factor 2 (eEF2) from *S.cerevisiae* (Jorgensen et al. 2006). eEF2 contains 6 domains (I-V and G'), which move relative to each other in order to perform conformational changes essential for eEF2 function. The diphthamide modification is located at the tip of domain IV, whereas the binding site for the antifungal sordarin (black) is at the interface between domains III, IV and V. Normal eEF2 function requires binding of GDP (yellow) to its binding site in domain I. ADPR-DIPH, ADP-ribosylated diphthamide.

1.3 Mono-ADP-ribosylation of diphthamide - friend or foe?

If ADP-ribosylation (ADP-R) of diphthamide causes translation inhibition and results in cell death, why would the cell put so much effort into the formation of a complex modification like diphthamide in the first place? The answer lies in the difference of the nature of the ADP-R catalyzed by cellular ATRs (ADP-ribosyl transferases) versus exogenous ARTs. While the endogenous process is reversible, ADP-R via exogenous transferases like diphtheria toxin is an irreversible PTM (Pappenheimer 1977; Corda and Di Girolamo 2003). It has been proposed that the reversible manner of cellular diphthamide ADP-R could act as an ON/OFF switch for eEF2 function, which could serve as a regulatory mechanism during translation. This putative regulatory role for diphthamide is supported by the discovery of endogenous ADP-ribosylation of eEF2 in the absence of bacterial toxins (Fendrick and Iglewski 1989b; Fendrick et al. 1992). Recently, Jaeger et al. reported that inteleukin-1β (IL-1β) ADP-ribosylates diphthamide in cardiomyocytes in a similar way to toxin mediated ADP-ribosylation and thereby might regulate eEF2 function (Jager et al. 2011). However, cellular mono-ADP-ribosylation of diphthamide is still poorly understood and deserves further attention before we can draw conclusions regarding the diphthamide modification. Nevertheless, mimicking this process allows bacterial toxins to target a vital cellular function and blocking it in an irreversible manner. What we know about diphthamide to date mainly stems from studies on bacterial protein toxins, therefore it seems compelling to take a closer look at microbial pathology.

1.4 Microbial Competition

Microorganisms have developed various mechanisms to secure survival in competitive environments. Amongst them is the well-known strategy of bacterial toxin secretion, which allows the toxin producing organism to compete and flourish in the microbial jungle. They are classified as endotoxins, which act in the close proximity of the bacterial cell wall, and exotoxins, which are secreted in order to attack cellular components of competitors at a remote site. Based on the molecular mechanism of action, the latter can be allocated into specific categories, such as the rather large group of ADP-ribosyltransferase (ART) family of bacterial toxins. ARTs act by blocking specific components of the host's translational machinery such as mRNA synthesis at the initiation, elongation and termination step or the general ribosome machinery including rRNAs and tRNAs. Diphtheria Toxin (DT) from *Corynebacterium diphtheriae*, Exotoxin A (ETA) from *Pseudomonas aeruginosa* and Cholix Toxin from *Vibrio cholerae* make up the DT group of ADP-Ribosylating toxins, which shares a specific target protein: translation elongation factor 2 (eEF2) (Deng and Barbieri 2008; Uthman S. 2011). These DT toxins belong to the two-component A-B family of pathogenic bacterial toxins, where initially the B domain facilitates binding to surface receptors of the host cell and upon uptake is followed by the enzymatic action of the A domain. This enzymatic activity involves the above mentioned covalent transfer of a single ADP-Ribose moiety from NAD^+ to the diphthamide residue on eEF2 (Figure 1.1). The mechanistic action of DT, ETA and cholix toxin involves three main steps: receptor-mediated endocytosis, release of the catalytic fragment into the cytoplasm by cleavage of the disulfide bridge between the A and B components and finally the ADP-

ribosylation of the target eEF2 protein. In order to generate the ADP-R, the enzyme first binds and cleaves NAD^+ between the nicotinamide and the nicotinamide-ribose to sever an ADP-Ribose group and consequently transfer it to diphthamide on eEF2 (Yates et al. 2006). By covalent modification of a key player of the translational machinery, these microorganisms have developed a highly efficient way of eliminating their competitors. In fact, the uptake of a single molecule of DT is sufficient to kill a cell (Yamaizumi et al. 1978). Interestingly, eubacteria do not carry the diphthamide modification on their eEF2 homologue (EF-G), hence the toxin attacks the target cell without affecting the protein synthesis of toxin producing bacteria (Collier 2001). The very similar mode of action between DT, ETA and cholix toxin that share ART activity and the same target protein, suggests that they share functional domains. However, sequence analysis of DT and ETA reveals low similarity (20% sequence identity) within their catalytic domains and therefore BLAST search for cellular ARTs does not generate any putative hits (Yates et al. 2006).

The prototype and best characterized member of bacterial ADP-ribosylating toxins is diphtheria toxin (DT), the causative agent of diphtheria disease in humans. DT is secreted by the gram-positive bacterium, *Corynebacterium diphtheriae*, and causes respiratory and cutaneous lesions that in severe cases can cause life-threatening complications such as loss of motor function, myocarditis and peripheral neuropathy. In particular, human skin, throat and pharynx can be colonized by *C. diphtheriae* biotypes *gravis*, *intermedius* and *mitis* which differ in colony morphology, growth and virulence properties. The infectious nature of the pathogen caused epidemics prior to the routine use of the Diphtheria–Pertussis–Tetanus (DPT) vaccine, which now has nearly

eradicated new diphtheria disease incidences (reviewed by (Pappenheimer 1977; Murphy 1996).

Another prominent member of the bacterial A-B toxin family is Exotoxin A (ETA) secreted by the gram-negative bacillus *P. aeruginosa*. This prevalent pathogen is associated with multi-drug-resistant infections including urinary tract infections, pneumonia and sepsis in immuno-compromised patients. In fact it is the primary cause of death in individuals with cystic fibrosis. In contrast to diphtheria disease, there is no preventive vaccine available for *P. aeruginosa* infections which together with its resistance towards many antibiotics makes it a potent human pathogen ((Deng and Barbieri 2008). The prevalent and opportunistic nature of ETA stresses the significance of current research centered around the diphthamide modification on eEF2.

1.5 eEF2 - key player in the translation machinery

Eukaryotic translation elongation comprises the formation of the newly synthesised polypeptide on the ribosome with the help of two highly conserved GTPases - translation elongation factors eEF1A and eEF2. While eEF1A is responsible for the selection of the aminoacyl-tRNA and its delivery to the acceptor site (A-site) of the ribosome, eEF2 facilitates the translocation of the peptidyl-tRNA from the A-site to the P-site (peptidyl site) as well as the simultaneous translocation of the deacylated tRNA from the P-site to the E-site on the 80S ribosome thereby exposing the A-site for a consecutive round of polypeptide elongation (Gomez-Lorenzo et al. 2000; Taylor et al. 2007). In detail, once translation is initiated, the 80S ribosome carries an mRNA with its start codon and the corresponding methionine-tRNA at the P site of the

ribosome. The GTPase, eEF1A binds an aa-tRNA and transfers it to the A site of the ribosome. To do so the anticodon of the aa-tRNA binds the codon sequence of the mRNA. Next, ribosomal RNA in the peptidyl transferase center (PTC) facilitate peptide bond formation between the newly incorporated amino acid and the methionine, which is bound to the tRNA in the P site. Upon GTP hydrolysis eEF1A in its GDP bound state is released to covalently bind another aa-tRNA, which is dependent on a guanine nucleotide exchange factor to transform GDP-eEF1A to its GTP bound form (Dever and Green 2012). In order to translocate the bound tRNAs, the 40S and 60S subunits of the ribosome perform a rapid rotation motion relative to each other. This motion is dependant on the action of eEF2, which reaches into the decoding centre of the ribosome and upon GTP hydrolysis undergoes conformational changes that unlock the ribosome and allow the ratcheting movement of the subunits (Dever and Green 2012).Once the tRNAs are moved from the A to the P site and from the P to the E site (exit site), eEF2 locks the ribosomal subunits again for the next elongation cycle. At the end of the translocation step, the deacylated-tRNA occupies the E site, the peptidyl-tRNA the P site and the A site is free for the next round of the peptide elongation. Interestingly, yeast and fungi have a third translation elongation factor, eEF3, an ATPase with 2 ATP binding domains. eEF3 has been reported to bind to the 80S ribosome in its post-translocation stage (Andersen et al. 2006). The exact role of eEF3 is unclear, however it was shown to bind the 60S as well as the 40S subunit (where exactly) as well as the E site and therefore has been suggested to aid the dissociation of the de-acylated tRNA from the ribosome (Triana-Alonso et al. 1995; Andersen et al. 2006). To date, no homolog of eEF3 has been found in other species and though yeast

eEF1a and eEF2 can complement their mammalian counterparts, they in return cannot facilitate translation elongation in yeast in the absence of eEF3 (Skogerson and Engelhardt 1977). Translation elongation is a highly conserved process from bacteria to eukaryotes, however it is unclear why fungal protein synthesis selectively is dependant on the action of a third elongation factor, eEF3 (Rodnina and Wintermeyer 2009).

The accuracy and efficiency of the eEF2 mediated translocation of tRNAs within the ribosome is fundamental to the translation machinery. eEF2 is composed of six domains, I-V and G' that can move relative to each other, a property central to the enzymatic activity of eEF2 (Figure 1.1). Upon GTP hydrolysis eEF2 as well as the small and large ribosome subunits undergo large-scale conformational changes in order to facilitate the translocation of the mRNA and tRNAs relative to the ribosome (Aevarsson et al. 1994; Jorgensen et al. 2003). The diphthamide modification on eEF2 is located at the tip of domain IV, which reaches into the ribosomal decoding center. In fact, cryo-electron microscopy reconstruction of ribosome bound eEF2 demonstrated that the diphthamide containing loop of yeast eEF2 (His694-Ile698) is close enough to interact with the codon-anticodon interface between the P-site bound tRNA and mRNA (Figure 1.2) (Agrawal et al. 1999; Stark et al. 2000; Spahn et al. 2004). It has been proposed that the movement of diphthamide on eEF2 from the GTP- to GDP-bound state would disrupt the interaction between the decoding center and the mRNA-tRNA duplex during the translocation cycle, a property that contributes to the maintenance of the correct reading frame (Taylor et al. 2007). In line with this, data from Ortiz et al. and our own group showed that amino acid substitutions (D696A, I698A, H699N) as

well as the loss of the diphthamide modification on His^{699} alone showed an increase in -1 frameshifting (Ortiz et al. 2006a; Bar et al. 2008).

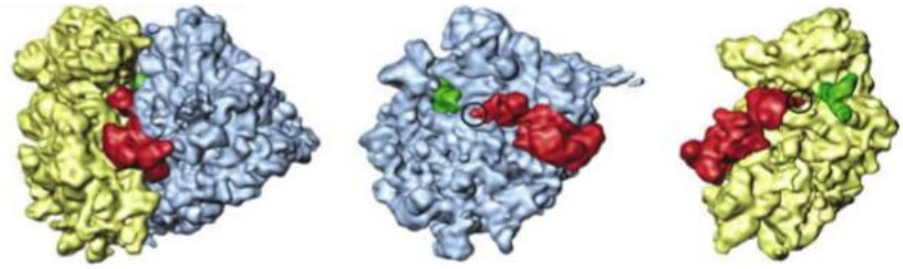

Figure 1.2. Cryo-EM reconstruction of ADP-ribosylated eEF2 in complex with the ribosome (Taylor et al. 2007). Cryo-EM derived densities are displayed in computationally separated structures of the 60S (grey) and 40S (yellow) ribosomal subunits, P/E site tRNA (green), ADP-ribosylated eEF2 (red) and the ADP-Ribose moiety is circled. The images visualize how close the tip of domain IV of eEF2 (with the diphthamide modification) reaches to the tRNA in the ribosomal decoding centre.

1.6 The multi-step pathway of diphthamide biosynthesis

The unique posttranslationally modified histidine residue, diphthamide or 2-[3-carboxyamido-3-(trimethylammonio)-propyl] histidine, is highly conserved from lower archaea to humans (Figure 1.3). It is found on His^{600} in the archaeon *Pyrococcus*

horikoshii, His^{699} in yeast and His^{715} in mammalian eEF2 (Moehring et al. 1984; Chen et al. 1985b; Liu et al. 2004b). The biosynthesis of diphthamide is a multi-step process of addition of chemical groups to the histidine precursor in eEF2. Initially a 3-amino-3-carboxypropyl group (ACP) from S-adenosylmethionine (SAM) is transferred to the C-2 position of the imidazole ring of the histidine residue resulting in the first product, the ACP-intermediate. The SAM-dependant tri-methylation of the amino-group follows and produces the second intermediate, diphthine (Chen and Bodley 1988; Mattheakis et al. 1992). In the 3rd and final step, the carboxyl group of the diphthine intermediate is amidated in an ATP-dependant manner, which completes the diphthamide modification (Liu et al. 2004b). The first 2 steps of the PTM are dependent upon SAM as a donor for functional groups: the ACP group and the methyl group. The genes involved in diphthamide synthesis were first identified in genome-wide screens for diphtheria toxin (DT) and *Pseudomonas* Exotoxin A (ETA) resistant mutants in yeast and CHO (Chinese hamster ovary) cells (Moehring et al. 1984; Chen et al. 1985a). The loss of diphthamide as a recognition motif makes them resistant to DT and ETA, and therefore resistant mutants can be considered to be involved in the synthesis of the PTM. DT resistant mutants were classified into 5 complementation groups, *dph1-dph5*. These diphthamide biosynthesis genes were assigned to the first 2 steps of the pathway, with *dph1-dph4* mutants lacking any modification on His^{699} and *dph5* blocking the modification after the formation of the ACP-intermediate. However, no mutants were found with the diphthine intermediate, most likely because diphthine can still be ADP-ribosylated by DT though it is a poor substrate compared to the final diphthamide modification (Moehring et al. 1984). Therefore the amidase at the end of the pathway

has repeatedly escaped DT and ETA screening. As for the other *dph* genes and their protein products, Dph1-Dph4 facilitate the initial transfer of the ACP group followed by the trimethylation by Dph5.

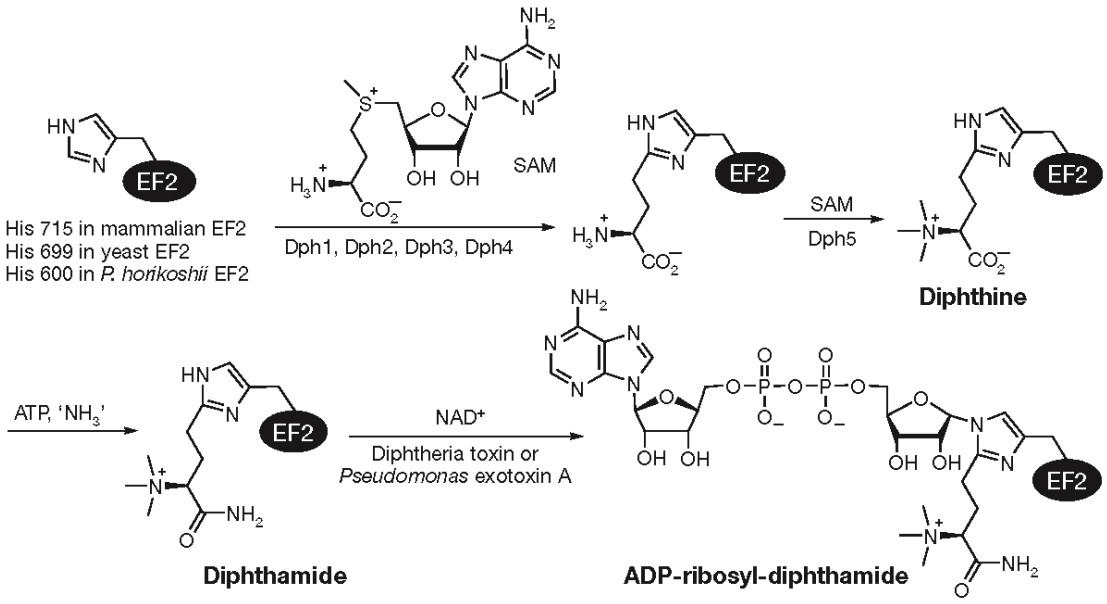

Figure 1.3. The proposed biosynthesis pathway and ADP-ribosylation of diphthamide (Zhang et al. 2010). The posttranslational modification of the histidine residue (*S.cerevisiae* His^{699}) on eEF2 is a 3 step process starting with the initial transfer of a 3-amino-3-carboxypropyl (ACP) group to the C2 position of the imidazole ring. Four protein products, Dph1-Dph4, are involved in the formation of the resulting ACP-intermediate, which further undergoes trimethylation by the methyltransferase, Dph5, and results in the second intermediate, diphthine. A yet unknown amidase generates the final diphthamide product by amidating the carboxyl group of diphthine. Diphthamide

is subject to a tandem posttranslational modification: ADP-ribosylation by bacterial toxins (diphtheria toxin, Pseudomonas exotoxin A and cholix toxin) and endogenous ADP-ribosyltransferases. eEF2, translation elongation factor 2.

1.7 Archael diphthamide synthesis

In an effort to further dissect the pathway, the archaeon *Pyrococcus horikoshii* (*P. horikoshii)* was used as a model organism for *in vitro* reconstruction of diphthamide formation. Two homologues of the yeast *Dph* genes can be found in *P. horikoshii*, termed *PhDph2* and *PhDph5*. PhDph2 forms a homodimer with 3 conserved cysteine residues (Cys59, Cys163 and Cys287), which are grouped together in the center and serve as binding sites for a [4Fe-4S] cluster (Figure 1.4). The cleavage of the ACP group from SAM is catalyzed by such a [4Fe-4S] cluster in the reduced state. Each PhDph2 can bind one [4Fe-4S] cluster, however only one such cluster is sufficient for the reaction (Zhang et al. 2010; Zhu et al. 2011). Interestingly, PhDph2 is more similar to *S. cerevisiae* Dph1, however Dph1 and Dph2 are homologous to each other. Therefore it was proposed that the archael PhDph2 homodimer evolved into a Dph1-Dph2 heterodimer in eukaryotes. The cleavage of an ACP radical from SAM and the formation of a C-C bond with the imidazole ring of His^{600} is followed by the activity of the archael diphthine synthase, PhDph5 (Zhu et al. 2010). This methyltransferase was shown to be sufficient to catalyze the mono-, di- and trimethylation in *P. horikoshii* with SAM as mehyl donor. Interestingly, even though the reconstitution of archael diphthine synthesis was successful, Zhu et al. (2010) reported that the resulting tri-methylamino group is readily eliminated *in vitro*. It will be interesting to see if this holds true for eukaryotic diphthine.

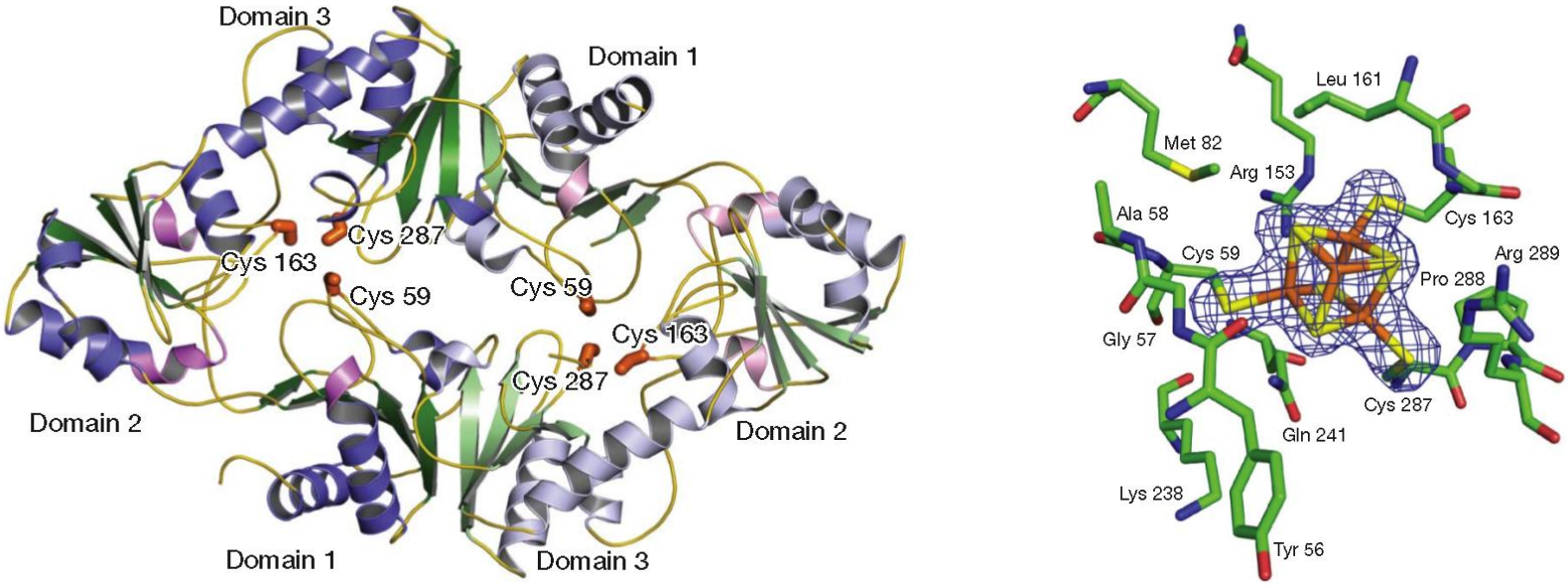

Figure 1.4. Ribbon diagram of PhDph2 homodimer and stereoview of the electron density assigned to a bound [4Fe-4S] cluster (Taylor et al. 2007). **A.** *Pyrococcus horikoshii* Dph2 forms a homodimer with 3 conserved cysteine residues (Cys59, Cys163 and Cys287) clustered in the center. **B.** Structural representation of a [4Fe-4S] cluster bound to the 3 cysteine residues of a single PhDph2 peptide. Fe: orange, S: yellow.

1.8 Dph3 and Dph4 – two versatile little proteins

Work from our own group and others has established that yeast Dph1, Dph2 and Dph3 interact with each other and form a complex in order to catalyze the formation of the ACP-intermediate (Fichtner et al. 2003b; Liu et al. 2004b; Baer et al. 2008; Zhang et al. 2010). Dph4, a J-domain protein, has been proposed to chaperone the correct assembly of the complex and its individual components. Type III J-proteins are a class of heat shock proteins that act as co-chaperones for Hsp70. In this role, Dph4 stimulates the ATPase activity of Hsp70 and is therefore involved in the chaperone regulation cycle (Thakur et al. 2012). The C-terminus of Dph4 contains a CSL-domain similar to full-length Dph3, allowing them to bind zinc and iron. Both Fe-Dph3 and Fe-Dph4 are redox active, which in light of the very recent findings in archael *in vitro* studies, might suggest that they act as electron reservoir for the [4Fe-4S] cluster thereby transforming it into the reduced state necessary for the cleavage of the ACP radical (Sun et al. 2005; Wu et al. 2008; Thakur et al. 2012). Moreover, their iron binding property indicates a putative iron donor role for the formation of the [4Fe-4S] cluster. Furthermore, Dph3 has been implicated in multiple biological processes. *DPH3* is allelic with *KTI11* (*Kluyveromyces lactis* killer toxin zymocin insensitive gene 11) and is a partner protein of the Elongator complex in yeast (Fichtner et al. 2003b). This Elongator complex has a diverse set of applications including the post-translational modification of tRNAs at the wobble position of the anticodon. Loss of Dph3 disrupts Elongator function and the consequent lack of tRNA modification renders the mutants resistant to the killer toxin zymocin. Therefore *dph3* deficient mutants are not only resistant to bacterial toxins but also the yeast killer toxin zymocin. Amongst the five diphthamide synthesis genes, *dph3*

deletion shows the most severe growth defects suggesting an involvement in multiple pathways (Bar et al. 2008). In line with this, the human homologue of Dph3 is DelGIP1 (DelGEF interacting protein 1), which interacts with deafness locus associated putative guanine nucleotide exchange factor. The Dph3-DelGEF complex is involved in the regulation of the secretion of proteoglycans which increases with the downregulation of human Dph3 (Sjolinder et al. 2002; Sjolinder et al. 2004). In summary, both Dph3 and Dph4 are essential for diphthamide formation but are also involved in multiple biological processes including regulation of the chaperone cycle, tRNA modification and secretion of proteoglycans.

1.9 YBR246w – the new guy in the neighbourhood

As mentioned above, the amidation of the carboxyl group in diphthine is most likely an enzymatic and ATP-dependant reaction with a yet unknown amidase that successfully escaped DT and sordarin screens for more than three decades. Recently, Carette et al. (2009) reported the finding of a novel putative diphthamide biosynthesis gene in human cells: mammalian *WDR85* and yeast *YBR246w* were proposed to act at the first step of the modification by aiding the formation of the ACP intermediate together with Dph1-Dph4. (Carette et al. 2009) identified *WDR85* in a genetic screen for mutants resistant to diphtheria and anthrax toxin in a human chronic myeloid leukemia cell. In contrast, more recent work by (Su et al. 2011) suggests the involvement of *YBR246w* in the final step of diphthamide formation. Mass spectrometric analysis revealed that the diphthamide pathway only progresses as far as diphthine in *ybr246wΔ* yeast strains. However, the exact role of *YBR246w* is still unkown. In parallel to the

above-mentioned findings, we identified *YBR246w* as a putative *DPH* gene in an independent search for novel candidate diphthamide genes and investigated its involvement in diphthamide biosynthesis. Our data is in agreement with Su at al. (2011) and will be discussed in chapter 3 and 4.

1.10 Sordarin and ricin, two powerful diphthamide indicator drugs

In addition to being the unique target for ADP-ribosylating bacterial toxins, diphthamide is also associated with the lethal properties of two toxic compounds sordarin and ricin. Not only does this indicate the significance of diphthamide in other biological processes, but also both agents are useful analytical tools for investigating the diphthamidation state of eEF2.

The antifungal compound sordarin is a product of the fungus *Sordaria araneosa*. Similar to bacterial toxins it targets the translation machinery, specifically the fungal elongation step. As mentioned above, eEF2's translocation activity depends on conformational changes of the protein. Sordarin targets eEF2 directly and binds at the interface between domain III, IV and V (Figure 1.1) (Dominguez et al. 1999; Jorgensen et al. 2003). Upon binding it cross-links eEF2 with the ribosome thereby immobilizing the elongation factor and inhibiting protein synthesis. Interestingly, a chemical genomic screen of the haploid yeast deletion mutant collection revealed that diphthamide formation is necessary for sordarin to target eEF2. Therefore *dph1-dph5* deficient cells lacking diphthamide are not only resistant to DT but also the antifungal translation

inhibitor, sordarin (Dominguez et al. 1999; Baer et al. 2008; Botet et al. 2008). Even though the binding site for sordarin is remote to the tip of domain IV, the lack of diphthamide as a recognition motif allows eEF2 to escape the inhibitory action of sordarin. In contrast to DT, selection for sordarin resistant mutations in *S. cerevisiae* generated a rather large list of genes (Botet et al. 2008). Nevertheless, many of them can be associated with the primary target eEF2 or other ribosomal proteins. Together with DT, sordarin has proven to be a valuable analytical tool for investigating the diphthamide modification. The cross-linking property of sordarin has been used in extensive cryo-EM studies to visualize stalled ribosomes and eEF2 conformations in different environments.

Another cytotoxic protein with relevance to diphthamide is the ribosome inactivating protein (RIP), ricin, from the plant *Ricinus communis*. Similar to the bacterial DT, ETA and cholix toxin it consists of 2 peptide chains, A and B, that harbour the enzymatically active (A) and the receptor-binding (B) properties of the protein toxin. It acts on the ribosome by breaking the 28S ribosomal RNA at a specific adenosine residue (A4324 in rat 28S rRNA). This region, termed sarcin/ricin domain, is also a binding site for eEF2. In fact, higher concentrations of eEF2 were shown to protect the 28S rRNA from the toxic cleavage by ricin (Fernandez-Puentes et al. 1976; Brigotti et al. 1989; Holmberg and Nygard 1994). Recently, Gupta et al. (2008) reported that this protective action of eEF2 is dependant on the diphthamide modification. CHO cells lacking Dph2, Dph3 and Dph5 were shown to be hypersensitive to the cytotoxic action of ricin (Gupta et al. 2008). Complementation and therefore reintroduction of the diphthamide modification regained wild-type levels of ricin tolerance. The difference in

ricin sensitivity of unmodified versus diphthamide eEF2 was threefold. This presents a novel role for diphthamide in cytoprotection of the ribosome towards RIPs.

1.11 Diphthamide mouse models

Despite the fact that Dph1-Dph5 are conserved in all eukaryotic organisms, the physiological role of diphthamide remains elusive. However mouse models of *DPH1*, *DPH3* as well as *DPH4* have proven a crucial role for the diphthamidation of eEF2 in early development. All three diphthamide deficient mouse models display distinct phenotypes where the homozygous deletion is embryonically lethal (Chen and Behringer 2004a; Liu et al. 2006; Webb et al. 2008). In agreement with the findings in yeast, *dph3*$^{-/-}$ mice show the most severe phenotype. They show a severe delay in embryonic development (2 - 3 days) and embryonic lethality by day 11.5. Furthermore, the embryos display increased degeneration and necrosis in neural tubes alongside with abnormal placenta development (Liu et al. 2006). *dph1*$^{-/-}$ and *dph4*$^{-/-}$ mice also display developmental delays of about 1 day and prenatal lethality. Interestingly they also share another distinct phenotype that is indicative of errors in the translation of specific proteins: the embryos from both homozygous mutations display preaxial polydactyly (duplication of the digit 1 of the hind foot) (Webb et al. 2008). The mammalian homologue of *DPH1, OVCA1* (ovarian cancer gene one), is a tumour suppressor gene and is closely linked to the formation of ovarian and other cancers. The heterozygous *Ovca1*$^{+/-}$ shows an increase in tumour development, predominantly lymphomas in contrast to ovarian tumours in humans. Consistent with this, mouse embryonic

fibroblasts (MEFs) from a *Ovca1*$^{+/-}$ background show cell proliferation defects (Chen and Behringer 2004a). In general, the role of diphthamide seems to become more apparent during early development, where cell proliferation is maintained at a maximum rate and is dependent on high translation levels.

1.12 *OVCA1*, tumour suppressor gene

The down-regulation of tumour suppressor genes (TSG) can be caused by gene deletion events, in particular LOH (loss of heterozygosity). The identification of the TSG, *OVCA1* (Ovarian Cancer Gene 1), has given rise to hope for new and specific treatment for ovarian cancer (Phillips et al. 1993; Phillips et al. 1996). Studies of frequent LOH events in human cancer established chromosome 17 as a hotspot for chromosomal aberrations, particularly in ovarian and breast cancer (Phillips et al. 1996; Schultz et al. 1996; Jorgensen et al. 2003). *OVCA1* on chromosome 17p13.3 is located in close proximity of *P53* and *HIC-1* (Hypermethylated in Cancer 1), which are also associated with various cancers (Schuijer and Berns 2003). Even though *P53* is the most frequently mutated gene (~50-70%) in epithelial ovarian tumours, it is only seen in advanced stages of ovarian cancer (Berchuck et al. 1994a; Berchuck et al. 1994b). Therefore the discovery of other genes involved in the onset of the disease is the main objective of current research. In this context, Phillips et al. (1993) reported the allelic deletion of human *OVCA1* to be associated with several types of cancer, in particular primary ovarian tumours. *OVCA1* expression is deleted or significantly reduced in ~80% (39 of 49) of ovarian tumours, including ~43% low malignant tumours and ~80%

non-metastatic tumours (Phillips et al. 1996). These findings suggest a crucial role for *OVCA1* in the prevention of tumour formation in the early stages of tumourigenesis. The molecular mechanism by which *OVCA1* prevents tumour formation is unclear together with the question of whether this property is dependent on its role as a diphthamide biosynthesis gene. Sequence analysis shows no homology to known functional domains, giving no indication about other diphthamide-independent functions of the protein.

Moreover, (Bruening et al. 1999) reported that the exogenous overexpression of *OVCA1* suppresses colony formation of ovarian cancer cell lines with an increased number of cells arrested in G1 phase, an effect that could be reversed by upregulation of cyclin D1 levels. In agreement with this, a recent finding suggests that *OVCA1* might prevent tumourigenesis by decreasing cyclin D1 and increasing p16 activity at both the mRNA and protein level (Kong et al. 2011). The p16/cyclin D1 cycle is one of the two main pathways that regulate cell proliferation and is implicated in virtually all human tumour types. It would be interesting to clarify if this is linked to the diphthamide modification on eEF2 or if it indicates *OVCA1*'s role in multiple cellular pathways.

1.13 Aims and Objectives

Despite the fact that the diphthamide modification on eEF2 was discovered more than three decades ago its biosynthesis has not been completely understood. Here we focus on the first and the final step of the pathway, where we sought to clarifying Dph1 function as well as identify the amidase that facilitates the conversion of diphthine into diphthamide.

1. Investigating functional domains of Dph1 by a systematic mutagenesis approach:

The systematic truncation of Dph1 from both the N- and C-terminal end in intervals of 30 amino acids was aimed at mapping functional domains of the protein. We sought to identify the minimal function unit of Dph1 and to elucidate its interaction profile with Dph2 and Dph3.

2. Identification of novel *DPH* genes by data mining of large scale yeast genetic and phenotypic screens:

Using data collected in two independent genetic and phenotypic yeast screens, we sought to identify putative candidate genes that are involved in diphthamide synthesis.

3. Validation of novel candidate Dph proteins using biochemical approaches:

The novel candidate diphthamide genes identified in the previous chapter were biochemically validated in order to elucidate their involvement in the synthesis of the post-translational modification on eEF2. Genetic, phenotypic and biochemical assays to clarify the role of the novel *DPH* genes in the diphthamide pathway.

CHAPTER 2

Mapping a Dph1 region crucial for the interaction with Dph2 and Dph3

2 Mapping a Dph1 region crucial for the interaction with Dph2 and Dph3

2.1 Introduction

The initial step of diphthamide formation on eEF2 requires the action of four diphthamide biosynthesis proteins, Dph1-Dph4. Together they facilitate the cleavage of an 3-amino-3-carboxypropyl group (ACP) group from S-adenosylmethionine (SAM) and subsequently facilitate its transfer to the C2 position of the imidazole ring of the histidine precursor (Chen and Bodley 1988; Mattheakis et al. 1992). Loss of Dph1 function results in a failure to form diphthamide and protects from diphtheria toxin (DT) as well as the antifungal drug, sordarin. Interestingly, the archael Dph1 homologue, PhDph2 (*P. horikoshii* Dph2) is an iron-sulfur enzyme, which generates the ACP radical with the help of a bound iron-sulfur cluster. In detail, PhDph2 contains three conserved cysteine residues (Cys59, Cys163 and Cys287, see Figure 2.2) that cluster in the center of the protein to form a triangular mould for binding of the [4Fe-4S] cluster (Zhang et al. 2010; Zhu et al. 2011). PhDph2 is more similar to Dph1 rather than Dph2 in *S. cerevisiae*, which is highlighted in the fact that ScDph1 carries all three conserved cysteine residues, whereas ScDph2 lacks the second one (Figure 2.2). In fact, yeast Dph1 and Dph2 are homologous to each other and seem to have evolved from the same ancestral protein (Zhang et al. 2010; Zhu et al. 2011).

Data from our own group and others show that Dph1, Dph2 and Dph3 form a complex and co-purify in immunoprecipitation assays (Fichtner et al. 2003b; Liu et al. 2004b; Baer et al. 2008; Zhang et al. 2010). It is very likely that *S. cerevisiae* Dph1 and Dph2 form a heterodimer similar to the PhDph2 homodimer in *P.horikoshii*, however the exact role of Dph3 and Dph4 in the formation of the ACP-intermediate is unclear. Sequence analysis and NMR studies revealed that both Dph3 and Dph4 are redox active and can bind iron and zinc. Therefore it was proposed that in the context of diphthamide synthesis they might act as electron donors for the [4Fe-4S] cluster, thereby keeping it in the reduced state necessary for the cleavage of ACP from SAM (Sun et al. 2005; Wu et al. 2008; Thakur et al. 2012). However, only Dph3 is part of the Dph1-Dph2-Dph3 complex, whereas Dph4 does not co-purify with the other three Dph proteins.

Even though Dph1 and Dph2 are homologous, they are both essential for diphthamidation of eEF2 in yeast and higher organisms. In order to gain further insight into the structure of the Dph1 protein, we decided to truncate *S. cerevisiae* Dph1 in a systematic manner to identify the shortest deletion mutant that confers loss of function, and thus the minimal functional unit of this protein. To do so, progressive N- and C-terminal truncations of Dph1 were generated using a PCR-based approach (see Methods). Figure 2.1 illustrates the genetic dissection of Dph1, with the HA-tagged full-length protein (N=N-terminal and C=C-terminal) and the truncations in intervals of 30 amino acids (N1-N4 and C1-C4). In order to assess the function of the Dph1 variants, the strains were subjected to diphtheria toxin (DT) and sordarin as well as used in co-immunoprecipitation assays. As shown in figure 2.3 and 2.4, the isogenic wildtype strain (W303) is sensitive to DT and sordarin, whereas the *dph1*Δ strain is resistant

which indicates the lack of diphthamide on eEF2. Hence we used both agents as analytic tools to verify the function of the Dph1 truncations. Co-Immunoprecipitation (co-IP) of proteins detects protein-protein interactions such as between Dph1, Dph2 and Dph3, which strongly interact with each other in a complex and co-purify. Here, we aimed to investigate if the Dph1 truncations are still able to interact with Dph2 and Dph3. In order to verify Dph1 binding activity, the mutagenesis was performed in two different strains carrying either Dph2-c-myc or Dph3-c-myc, which allowed us to study the interaction of the HA-tagged Dph1 with Dph2 and Dph3.

Immunoblot detection of the constructs is presented in Figure 2.1, where both Dph2-c-myc and Dph3-c-myc strains co-express wt-Dph1-HA and the N-terminal (N1-N4) as well as the C-terminal truncations (C1-C4). This allowed us to investigate which mutation causes loss of function of Dph1 and at the same time whether the mutation also affected protein-protein interaction between Dph1 and its partner proteins Dph2 and Dph3. Figure 2.2 highlights the position of the truncations in relation to the conserved cysteine sites of PhDph2 and homologues from other species (*C. griseus* CgDph2, *H. sapiens* HsDph2). We predicted that the N-terminal truncation upstream of the first cysteine residue (N1-N3) as well as the C-terminal truncation downstream of the region containing the third cysteine residue (C1) might not affect Dph1 function significantly, since all three conserved Cys residues are available for binding of the iron-sulfur cluster. The N-terminal truncations were expressed under the control of the conditional *GAL1* promoter and were expressed at a similar level as the full-length protein (Figure 2.2). The C-terminal truncations were expressed from the native promoter with the C2 and C3 truncation showing a significant decrease in expression

compared to the full-length Dph1, indicating an unstable protein. Alternatively, C2 and C3 levels might be lowered as a result of increased in mRNA decay. Interestingly, the C4 truncation lacking 120 amino acids at the C-terminus was detected as a clear band, but expressed at lower levels compared with C1 and C. Both HA-tagged full-length Dph1 (N and C) and the smallest truncations N1 and C1, were accompanied by smaller degradation products. Taken together, these experiments were designed to find the shortest non-functional deletion mutant of Dph1 as well as mapping a Dph1 region crucial for the interaction with Dph2 and Dph3.

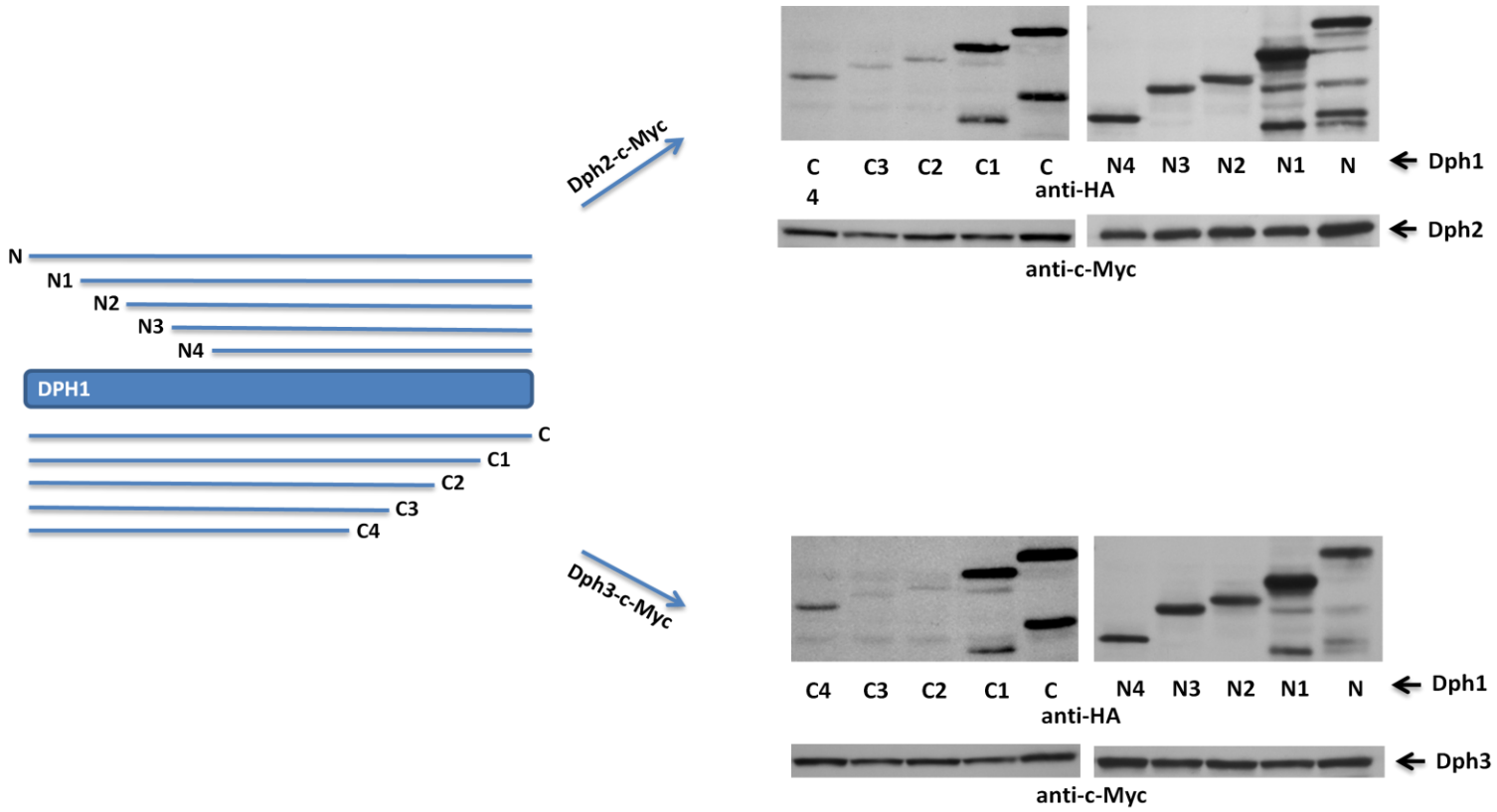

Figure 2.1. Systematic truncation of Dph1. N-terminal and C-terminal truncations of Dph1 in 30aa intervals (N1-N4 and C1-C4) as well as the HA tagged full-length Dph1 (N: N-terminal and C: C-terminal) are presented in a schematic diagram. Dph1 mutagenesis was performed in 2 strains: Dph2-c-Myc and Dph3-c-Myc. Expression of Dph1 variants are detected in western blot analysis using anti-HA antibody.

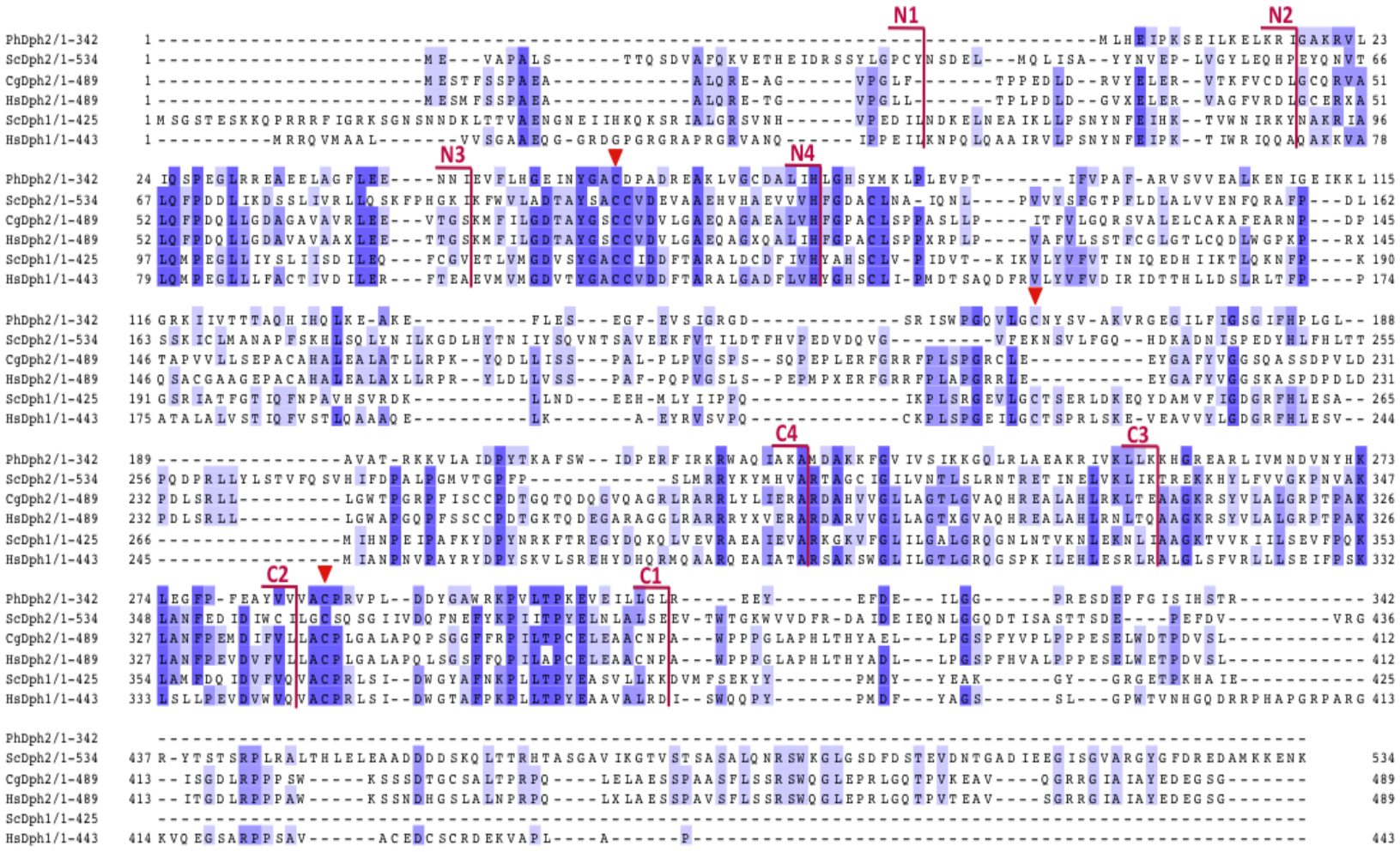
N1
N2
N3
N4
C4
C3
C2
C1
PhDph2/1-342
ScDph2/1-534
CgDph2/1-489
HsDph2/1-489
ScDph1/1-425
HsDph1/1-443

Figure 2.2. Sequence alignment of ScDph1 and homologues. Archael PhDph2 (*P. horikoshii*), mammalian chinese hamster (*C. griseus*) CgDph2, human HsDph1 and HsDph2, and *S. cerevisiae* ScDph2 are included for comparison of conserved regions. The highest degree of conservation between the six sequences is marked in dark blue. The three conserved cysteine residues in PhDph2, which bind the iron-sulfur cluster (Cys59, Cys163 and Cys287) are marked with a red triangle (Zhang et al. 2010; Zhu et al. 2011). The position of N-terminal truncations (N1-N4) as well as C-terminal truncations (C1-C4) of ScDph1 are highlighted. Sequence alignment was performed using Jalview.

2.2 Results

2.2.1 DT phenotype of Dph1 constructs

In order to investigate the DT phenotype of the Dph1 variants, the strains were exposed to endogenous expression of the DT F2 fragment from the plasmid pLMY101 under the control of the conditional *GAL1* promoter. 10-fold serial dilutions were spotted on plates containing glucose (control), which represses the *GAL1* promoter as well as galactose-containing media to turn on DT expression. The isogenic wt and *dph1*Δ strains were included as controls highlighting that the diphthamide containing wt strain is sensitive to DT, whereas the diphthamide-minus *dph1*Δ strain is resistant to the bacterial toxin. N- and C-terminal HA-tagging of full length Dph1 retained the DT sensitive phenotype and confirmed the presence of a functional protein, which is not affected by the HA tag. However, all truncations from the N-terminus as well as the C-terminus resulted in a DT resistant phenotype similar to a *dph1*Δ strain, indicating that diphthamide could not be formed. Seeing that all constructs apart from C2 and C3 are stably expressed, the lack of diphthamide is considered a direct result of the Dph1 truncations. These findings were confirmed in both background strains (DPh2-c-myc as well as Dph3-c-myc).

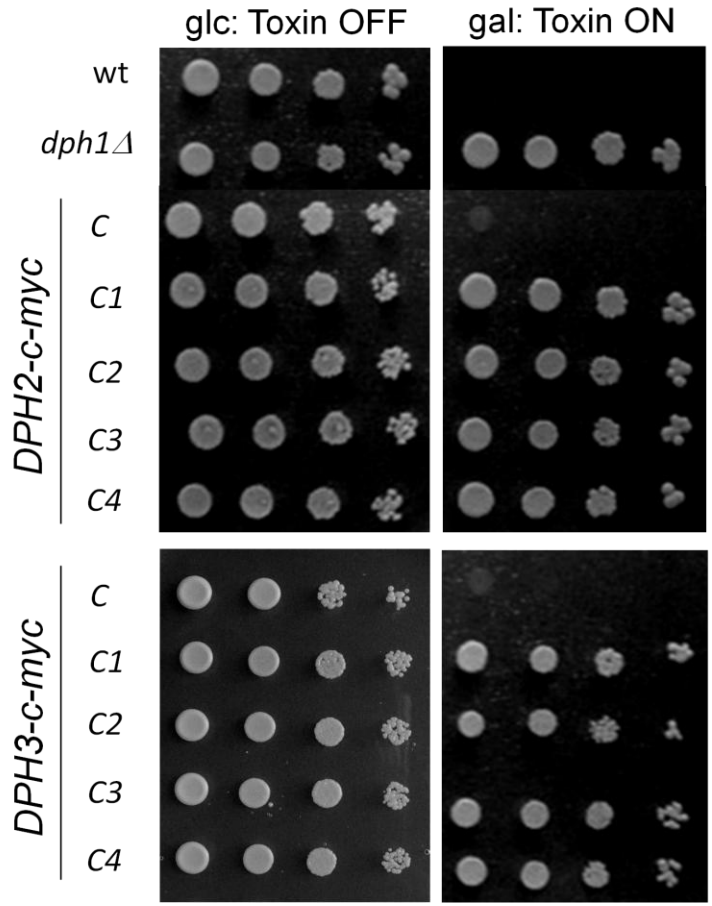
glc: Toxin OFF
gal: Toxin ON
wt
dph1Δ
DPH2-c-myc
C
C1
C2
C3
C4
DPH3-c-myc
C
C1
C2
C3
C4

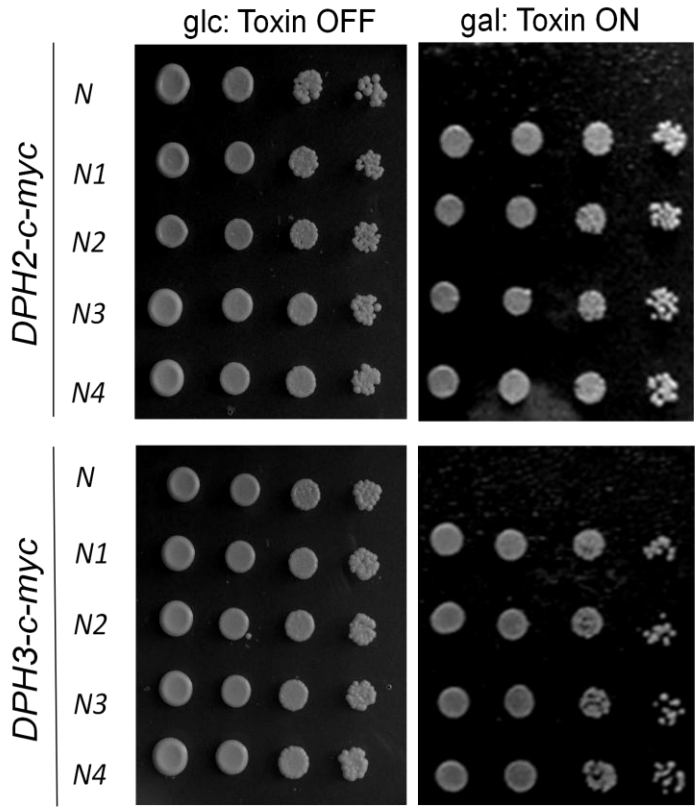
glc: Toxin OFF
gal: Toxin ON
DPH2-c-myc
N
N1
N2
N3
N4
DPH3-c-myc
N
N1
N2
N3
N4

Figure 2.3. Dph1 truncations fail to form diphthamide. 10-fold serial cell dilutions of isogenic wt, *dph1Δ* as well as Dph1 truncations were spotted on YPD plates supplemented with glucose (toxin off) as well as galactose (toxin on). N-terminal truncations (N1-N4) as well as C-terminal truncations (C1-C4) are resistant to diphtheria toxin (DT). Full-length HA-tagged Dph1 remains sensitive to the toxin, similar to the wt strain. DT phenotype of Dph1 variants are confirmed in both background strains (Dph2-c-Myc and Dph3-c-Myc).

2.2.2 Sordarin phenotype of Dph1 constructs

To address the functionality of the Dph1 truncations with a second diphthamide indicator drug, the constructs were exposed to the antifungal, sordarin. To do so, 10-fold serial cell dilutions were spotted on YPD plates supplemented with 20 µg/ml sordarin. As mentioned above, N-terminal truncations are under the control of the *GAL1* promoter and therefore required galactose to be expressed, which is supplemented in the YPD plates. However, when the strains were spotted on GalYPD containing 20 mg/ml sordarin, none of the strains grew including the *dph1*Δ mutant, a sordarin resistant strain. Glucose is the preferred carbon source for *S. cerevisiae,* which therefore show a slower growth on galactose. The combination of sordarin and galactose seems to potentiate toxicity dramatically and therefore the optimum concentration of sordarin in combination with galactose was identified as 5mg/ml where *dph1*Δ could grow and the wt strain was killed. All Dph1 variants survived in the presence of sordarin, which confirms the findings from the DT assay (Figure 2.4). Only the full length HA-tagged Dph1 constructs and the isogenic wt strain were killed by the translational inhibitor, which further indicates that none of the N- or C-terminal truncations could form diphthamide on eEF2.

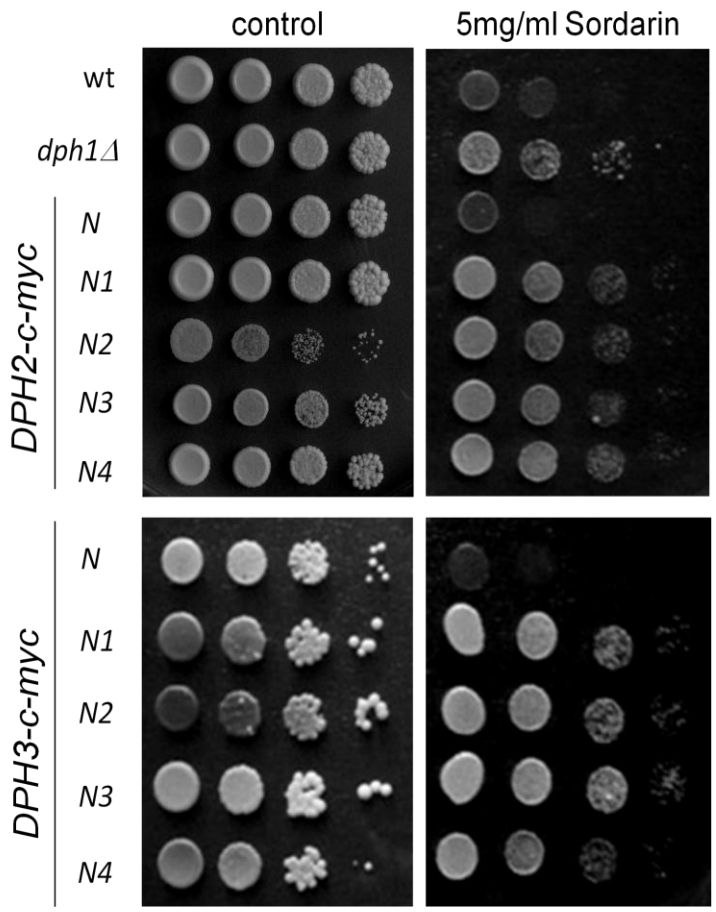
control
5mg/ml Sordarin
wt
dph1Δ
DPH2-c-myc
N
N1
N2
N3
N4
DPH3-c-myc
N
N1
N2
N3
N4

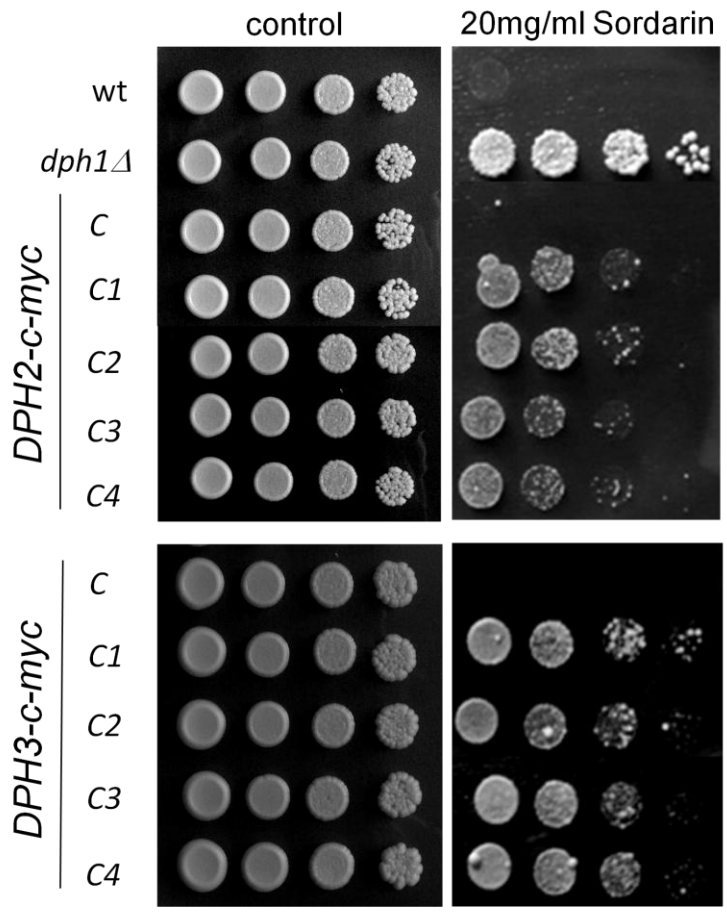
control
20mg/ml Sordarin
wt
dph1Δ
DPH2-c-myc
C
C1
C2
C3
C4
DPH3-c-myc
C
C1
C2
C3
C4

Figure 2.4. Sordarin assay confirms the lack of diphthamide formation due to the truncation of Dph1. 10-fold serial cell dilutions of isogenic wt, *dph1Δ* as well as Dph1 variants (N1-N4 and C1-C4) were spotted on YPD plates (control) as well as YPD media supplemented with 20mg/ml or 5mg/ml sordarin. N-terminal truncations (N1-N4) were spotted on GalYPD to switch on the expression of the constructs from the conditional *GAL1* promoter. Full-length HA-tagged Dph1 remains sensitive to the antifungal sordarin, similar to the wt strain. The sordarin phenotype of Dph1 variants were confirmed in both background strains (Dph2-c-Myc and Dph3-c-Myc).

2.2.3 Co-Immunoprecipitation assay reveals interaction profile of Dph1

2.2.3.1 C-terminal truncations

Interaction of full-length Dph1 and the truncated variants with Dph2 and Dph3 was investigated using Co-IP assays. Due to the DT and sordarin results, we hypothesized that only the full-length Dph1 construct would be able to interact with Dph2 and Dph3. Interestingly, C1-Dph1 was able to bind both Dph2 and Dph3, in fact when compared to binding of the full-length Dph1, this deletion does not alter binding to either proteins. As mentioned above, both C2 and C3 variants are expressed at low levels and are most likely unstable variants of Dph1, therefore it is not surprising that they do not co-purify with Dph2 or Dph3. C4 on the other hand is a stable construct but completely abolished the binding properties of Dph1. These data show that the removal of 30 amino acids from the C-terminus of Dph1 does not disrupt interactions between Dph1 and its partner proteins Dph2 and Dph3.

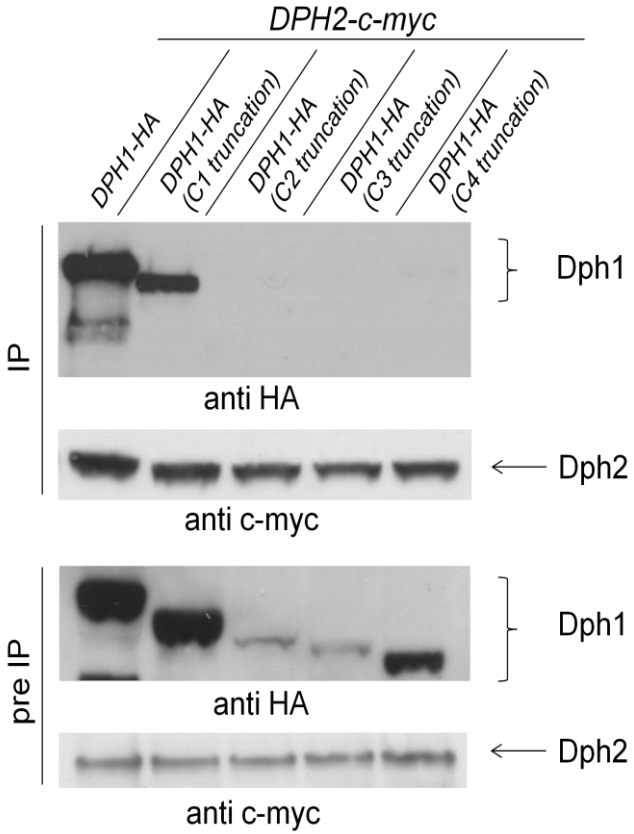
DPH2-c-myc
DPH1-HA
DPH1-HA (C1 truncation)
DPH1-HA (C2 truncation)
DPH1-HA (C3 truncation)
DPH1-HA (C4 truncation)
IP
Dph1
anti HA
Dph2
anti c-myc
pre IP
Dph1
anti HA
Dph2
anti c-myc

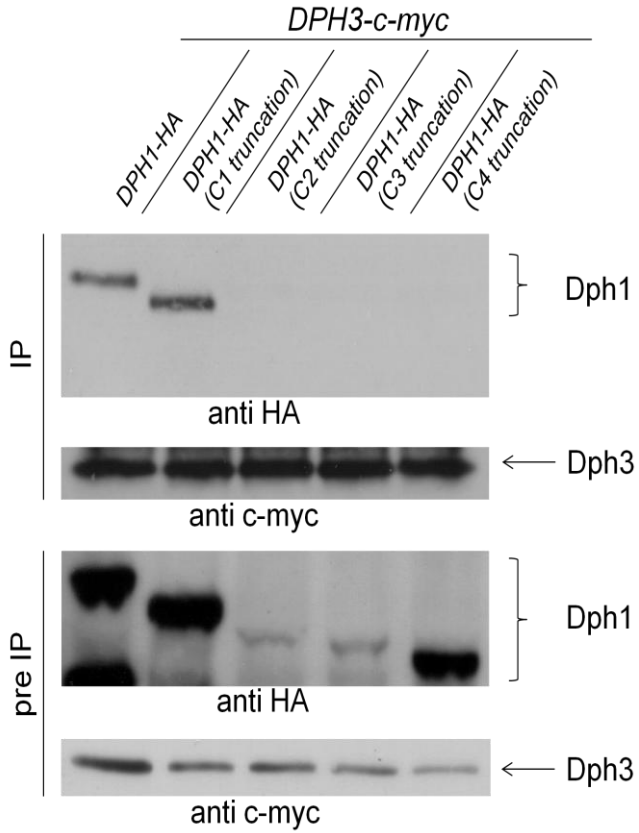
DPH3-c-myc
DPH1-HA
DPH1-HA (C1 truncation)
DPH1-HA (C2 truncation)
DPH1-HA (C3 truncation)
DPH1-HA (C4 truncation)
IP
Dph1
anti HA
Dph3
anti c-myc
pre IP
Dph1
anti HA
Dph3
anti c-myc

Figure 2.5. C1 truncation of Dph1 does not affect the interaction with Dph2 or Dph3. Co-Immunoprecipitation (co-IP) of C-terminal HA-tagged full-length Dph1 as well as truncations (C1-C4) with either Dph2-c-myc or Dph3-c-myc are shown. Anti-HA antibody is used for detection of the Dph1-HA constructs and anti-c-MYC antibody for Dph2-c-myc as well as Dph3-c-Myc. Co-IP analysis was performed with anti-c-Myc antibody. Co-purification of full-length Dph1-HA and C1-Dph1-HA with Dph2-c-Myc is presented in the top two panels on the left and with Dph3-c-Myc in the top two panels on the right. The bottom two panels represent immunoblot detection of the constructs in crude protein extracts prior to co-IP.

2.2.3.2 N-terminal truncations

Seeing that all N-terminal truncations of Dph1 proved to be DT and sordarin resistant we again hypothesized that they would fail to interact with Dph2 and Dph3. However, co-purification of N1-N4 with Dph2 and Dph3 revealed an even more surprising interaction profile. N1 and N3 variants co-purify with Dph2 and N1, N2 and N3-Dph1 interact with Dph3. The smallest truncation of 30 amino acids from the N terminus does not affect binding of Dph1 to either Dph2 or Dph3, as can be seen by the similar levels of interaction compared to the full length Dph1 construct. N2-Dph1 and N3-Dph1 lacking 60 and 90 amino acids, respectively, co-purified with Dph3, though weaker than N1-Dph1. However it is puzzling, that N3-Dph1 interacts with Dph2 but not N2-Dph1, which is 30 amino acids longer. Taken together the co-IP results indicate that the N-terminal region of Dph1 is less important for binding to Dph2 and Dph3 as compared with the C-terminus.

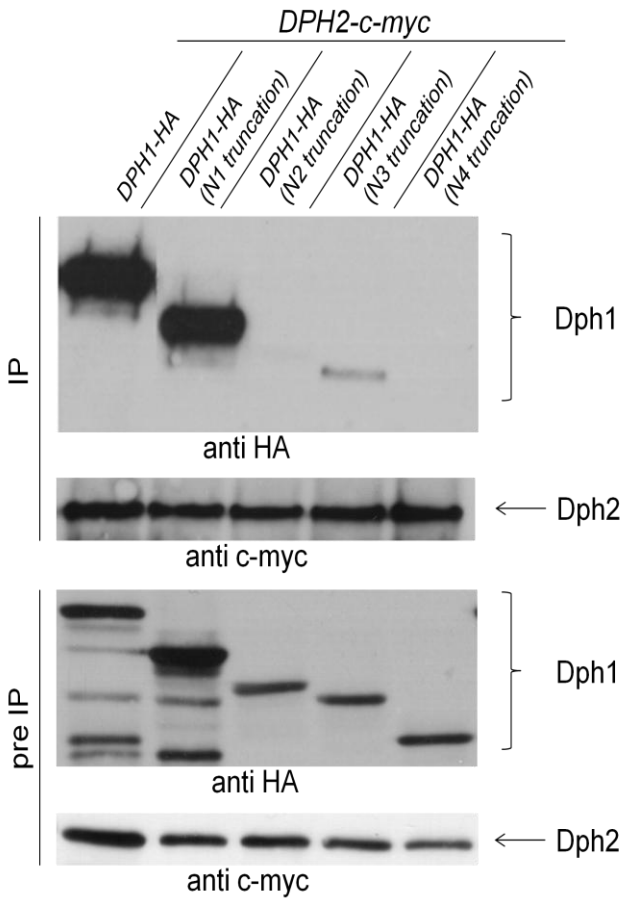
DPH2-c-myc
DPH1-HA
DPH1-HA (N1 truncation)
DPH1-HA (N2 truncation)
DPH1-HA (N3 truncation)
DPH1-HA (N4 truncation)
IP
Dph1
anti HA
Dph2
anti c-myc
pre IP
Dph1
anti HA
Dph2
anti c-myc

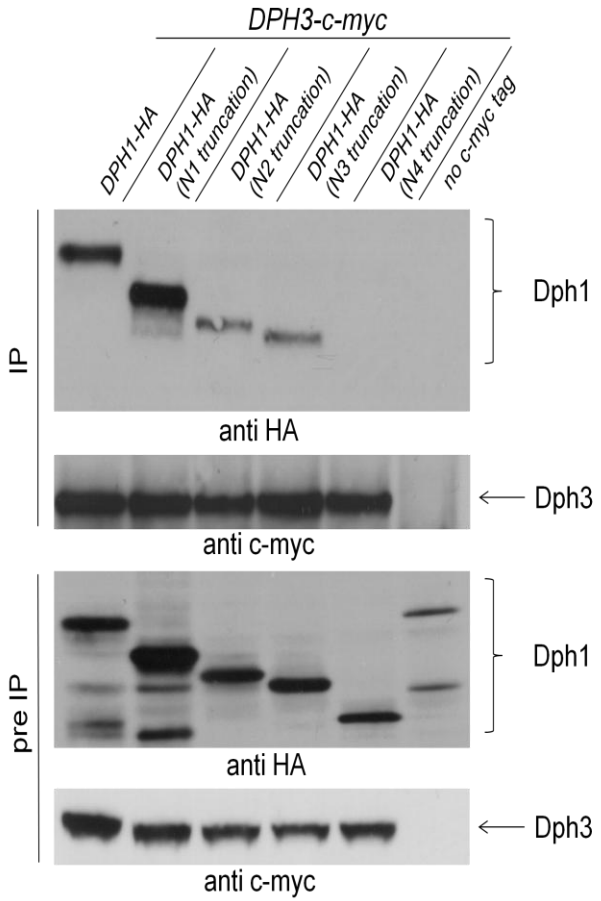
DPH3-c-myc
DPH1-HA
DPH1-HA (N1 truncation)
DPH1-HA (N2 truncation)
DPH1-HA (N3 truncation)
DPH1-HA (N4 truncation)
no c-myc tag
IP
Dph1
anti HA
Dph3
anti c-myc
pre IP
Dph1
anti HA
Dph3
anti c-myc

Figure 2.6. Dph1 N-terminal truncations interact with Dph2 and Dph3. Co-Immunoprecipitation (co-IP) of N-terminal HA-tagged full-length Dph1 as well as truncations (N1-N4) with either Dph2-c-myc or Dph3-c-myc are shown. Anti-HA antibody is used for detection of the Dph1-HA constructs and anti-c-MYC antibody for Dph2-c-myc as well as Dph3-c-Myc. Co-IP analysis was performed with anti-c-Myc antibody. Co-purification of full-length Dph1-HA as well as N1 and N3 variants with Dph2-c-Myc is presented in the top two panels on the left. Interaction of Dph3-c-Myc with full-length Dph1 and truncations N1-N3 are highlighted in the top two panels on the right. The bottom two panels represent immunoblot detection of the constructs in crude protein extracts prior to co-IP.

2.3 Conclusion

The aim of the experiments described in this chapter was to map functional regions of Dph1 by systematic truncation of the protein from both N- and C-terminal ends and to identify the smallest deletion mutant that confers resistance to DT and sordarin. Phenotypic assays with diphthamide indicator drugs DT and sordarin revealed that a removal of only 30 amino acids from either end of Dph1 renders the protein inactive in terms of diphthamide biosynthesis. With the exception of C-terminal truncations C2 and C3, lacking 60 and 90 amino acids respectively, all truncations were expressed in similar levels to the full-length Dph1 and were readily detected in protein immunoblots. Full-length Dph1-HA construct was shown to be functional and therefore it seems unlikely that the HA tag is interfering with Dph1 function. Hence we conclude that the genomic truncation of Dph1 resulted in the diphthamide-minus phenotype and that the full-length construct is necessary for proper Dph1 function.

Mapping the interaction profile of Dph1 with Dph2 and Dph3 revealed a different outcome to the above mentioned drug phenotypes. The truncated Dph1 variant C1 was still able to bind Dph2 as well as Dph3. Similarly N1, N2 and N3 can interact with Dph3 and truncations N1 and N3 with Dph2, though they all fail to promote diphthamidation of eEF2. Figure 2.2 highlights the deleted region in C1-Dph1, which is downstream of the third conserved cysteine residue of PhDph2, whereas the C2 constructs is upstream of *S. cerevisiae* Cys368. N-terminal truncations however are located upstream of the first conserved cysteine residue, except for N4 lacking 120 N-

terminal amino acids. Therefore mapping interaction regions of Dph1 indicates that the conserved regions, which contain the first and third [4Fe-4S] cluster binding cysteine residues are also crucial for the interaction between Dph1 and Dph2 or Dph3. In other words, C1 as well as N1-N3 variants are able to interact in the Dph1-Dph2-Dph3 complex, but fail to form diphthamide. Zhu et al. (2011) reported that the activity of a single iron-sulfur cluster bound to one of the PhDph2 subunits in the dimer is sufficient to facilitate the formation of the ACP-intermediate. Furthermore, mutating one out of the three cysteine residues did not affect PhDph2 activity, which still could bind the iron-sulfur cluster (Zhu et al. 2011). We hypothesize that the smallest deletion of 30 amino acids changes the structure of Dph1, which might not be able to form the triangular mold necessary for binding of a [4Fe-4S] cluster, even though it can still interact with Dph2 and Dph3.

Furthermore, Roy et al. (2010) recently reported a Dph2 mutant present in Chinese hamster ovary cells, Dph2(C-), which lacks 91aa from the C-terminus and fails to form diphthamide and therefore cannot be ADP-ribosylated *in vivo* when exposed to DT or ETA, or *in vitro* when incubated with DT in the presence of radiolabeled NAD. Interestingly, two other mutants, Dph2(N-) with a deletion of 158aa from the N-terminus as well as Dph2(Z-) lacking a putative leucine zipper motif in position 160-181, retained their enymatic activity and were phenotypically normal (Roy et al. 2010). These findings do not support the hypothesis that the 2 conserved cysteine residues are the main regions of interest for Dph2 function in rodents. In fact the diphthamide-minus Dph2(C-) deletion contains both cysteine residues, whereas the N-teminal truncation of 158 amino acids in Dph2(N-) removes the first and only leaves one cysteine residue,

however the former is non-functional and the latter does not alter diphthamide formation. These findings highlight the importance of the C-terminal end for CgDph2 function in diphthamide formation, however independent of the regions containing the conserved cysteine residues identified in PhDph2. Hence CgDph2 activity does not agree with the iron-sulfur enzyme model proposed by Zhu et al., which clearly shows the minimum requirement of 2 cysteine residues for binding of an iron-sulfur cluster (Zhu et al. 2011). In contrast, our data suggest that the smallest truncation of Dph1 fails to form diphthamide, hence we believe that Dph1 is the main iron-sulfur enzyme in yeast diphthamide synthesis. Even though the wt Dph2 could still bind a [4Fe-4S] cluster, by mutating Dph1, we abolish diphthamidation. In summary, even though Dph1 and Dph2 are fundamental to diphthamide synthesis, our data suggest that Dph1 is the main [4Fe-4S] enzyme and that conformational changes impair binding of a [4Fe-4S] cluster, hence render the truncated Dph1 variants inactive.

Some non-functional variants (N1-N3 as well as C1) resulting in a diphthamide-minus strain in phenotypic assays can still interact with Dph2 and Dph3 as shown by immunoblot. A possible explanation is that even though these mutant proteins can interact with other components of the Dph1-Dph2-Dph3 complex, they are unable to bind a [4Fe-4S] cluster and thus cannot generate the ACP radical necessary for the initiation of the diphthamide pathway. Interestingly, a PhDph2 heterodimer, containing one wt and one mutated PhDph2 copy, is more stable than the homodimer (Zhu et al. 2011). Here only one PhDph2 subunit can bind an iron-sulfur molecule. If the binding of only one iron-sulfur cluster indeed displays an advantage for the stability of the dimer, this might explain why in eukaryotes the homologues Dph1 and Dph2 evolved

differently and prompts the hypothesis that Dph2 might not act as an [4Fe-4S] cluster-binding enzyme.

CHAPTER 3

Identification of novel putative diphthamide biosynthesis genes

3 Identification of novel putative Diphthamide Biosynthesis genes

3.1 Introduction

In yeast approximately 80% of haploid mutations does not affect viability and it is possible to look into the phenotype of the deletion mutants, hence *S.cerevisiae* is an attractive model organism for large-scale studies assessing the biological role of genes (Hillenmeyer et al. 2008; Dixon et al. 2009). Exposure of the ~5000 non-essential gene deletions to genetic, chemical and environmental stresses and the resulting phenotype gives insight into the function of the deleted gene. In detail, screens for synthetic lethality have proven to be a powerful tool for identifying genetic interactions. Synthetic lethality arises when the combination of two mutations leads to an inviable organism, whereas the single mutation does not (Guarente 1993). By scoring the colony size of the double mutant it is possible to deduce genes whose products buffer one another and act in the same essential pathway.

Furthermore, the exposure of the same set of non-essential gene deletions to chemical and environmental stresses allows the identification of related genes that have similar phenotypic profiles (Hillenmeyer et al. 2008).

Here we use data from two large-scale screens to identify novel putative diphthamide biosynthesis genes. In collaboration with Prof. Charles Boone and Dr. Michael Costanzo, University of Toronto, who use the collection of viable *S.cerevisiae*

gene deletions for synthetic genetic array (SGA) analysis we aimed to identify genes that interact with known diphthamide biosynthesis genes, *DPH1-DPH5*. The Boone lab is in the process of generating 12.5 million different double mutations and scoring synthetic lethality or sickness via the colony size of each combination with the help of computational array analysis (Costanzo et al. 2010). To do so, a query strain containing a single mutation, e.g. *dph1*Δ, is crossed with the array of up to 4000 gene deletions. The diploid progeny are allowed to sporulate and the haploid cell containing both mutations is identified via selection for the appropriate markers (Tong et al. 2001; Tong et al. 2004). The resulting ~4000 double mutants are then scored for fitness defects (Figure 3.1). This process is repeated three times to ensure the significance of the outcome. The so-called interaction profile for each query strain, containing all negative and positive regulator genes, can be reviewed on the publically available database, DRYGIN (http://drygin.ccbr.utoronto.ca/; (Koh et al. 2010). Not surprisingly, genes that are biologically related have overlapping interaction profiles (Costanzo et al. 2010). So far, just over 5.4 million gene interactions have been studied highlighting that genes with related functions have highly related interaction profiles. We collaborated with Prof. Boone's lab to mine their SGA data for novel factors involved in the diphthamide pathway.

As mentioned above, the yeast single gene deletion collection not only serves as a starting point for genetic interaction studies, but also provides the basis for extensive chemical and environmental screens performed by Hillenmeyer *et al.* (Hillenmeyer et al. 2008; Hillenmeyer et al. 2010). Here the query strains were exposed to 1144 different chemical and environmental stresses. It was reported that even though only

20% of *S. cerevisiae* genes are essential for viability, approximately 97% of the yeast deletions conferred a phenotype under certain stress conditions and are therefore necessary for optimal growth (Hillenmeyer et al. 2008). Similar to the SGA analysis, related genes were shown to have related phenotype profiles, i.e. fitness defects towards specific agents were overlapping in gene deletions that are functionally related. The data is publically available in the Yeast Fitness Data Base (FitDB, http://fitdb.stanford.edu/) and was used to identify novel diphthamide related genes.

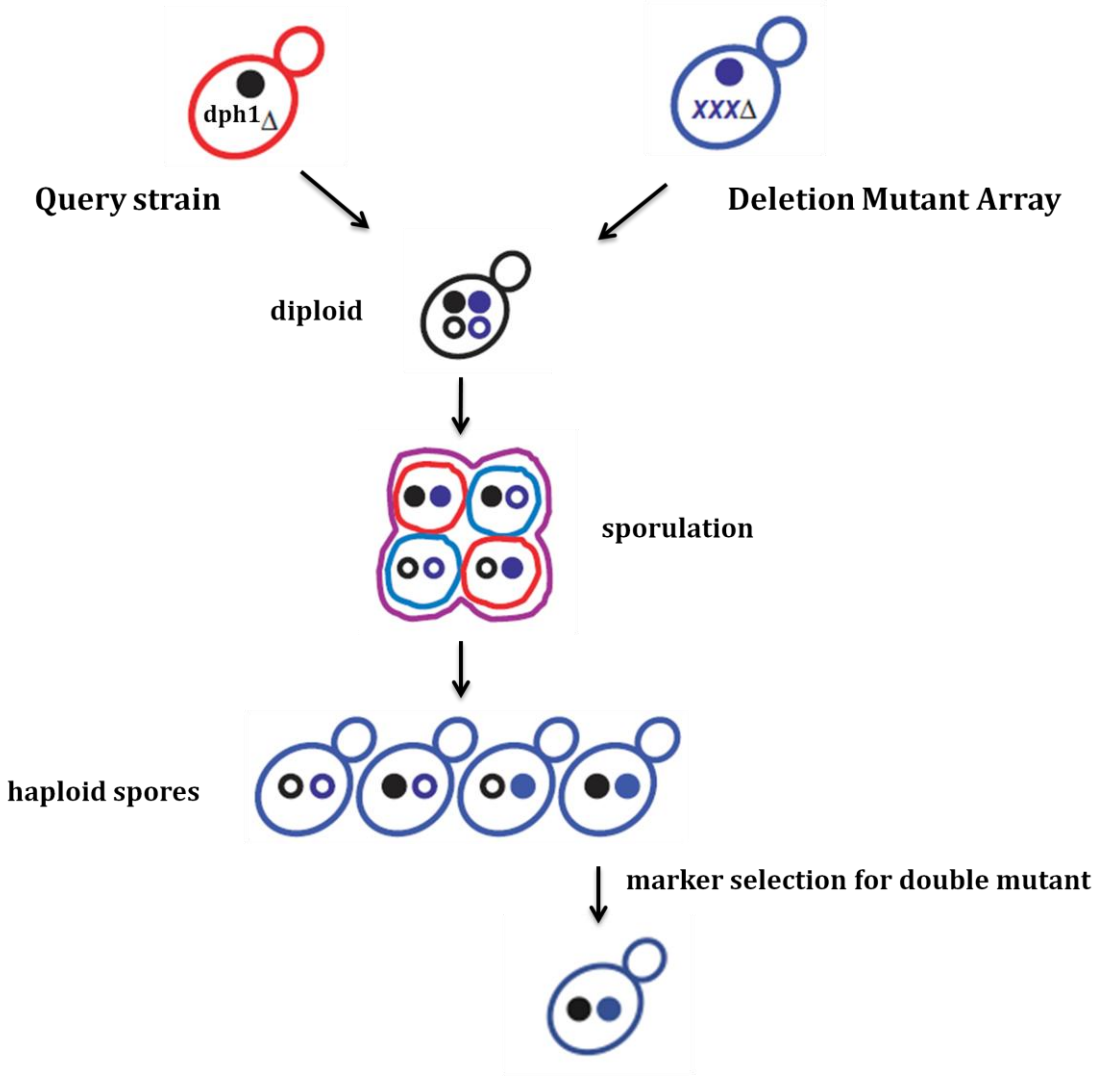

Figure 3.1. Simplified schematic representation of synthetic genetic array (SGA) methodology. *MATa* query strain *dph1*Δ (*natMX* selectable marker) is crossed with *MATa* deletion mutant array containing viable mutations linked to *kanMX* marker. The diploid zygote is sporulated and the haploid double mutant is selected for the dominant markers, *dph1*Δ::*natR* and *xxx*Δ::*kanR*, against nourseothricin and geneticin. Growth defects of the double mutant compared to the wild-type are measured. Schematic representation adapted from (Tong and Boone 2005).

3.2 Results

3.2.1 SGA analysis reveals novel candidate diphthamide biosynthesis genes

In order to identify novel genes involved in diphthamide biosynthesis we exploited the DRYGIN database to generate correlation profiles for *bona fide* diphthamide synthesis genes, *DPH1*, *DPH2*, *DPH4* and *DPH5*. Figure 3.2 contains the top ten hits of genetically correlated profiles of our query strains. The correlated profiles represent genes that have the closest genetic interaction profile for our query strains. In detail, *DPH1*, *DPH2*, *DPH4* and *DPH5* query strains all contain correlated profiles of each other, i.e. query strain *DPH1* top ten correlated profiles include *DPH2, DPH4* and *DPH5*. The same can be observed for query strains *DPH2*, *DPH4* and *DPH5*. This indicates a tightly clustered SGA-based network for diphthamide biosynthesis genes. The dipthamide gene *DPH3* was not included in this screen due to the mutant strain displaying a severe growth phenotype related to cumulative defects in pathways other than diphthamide, including tRNA wobble uridine modification (Fichtner and Schaffrath 2002; Fichtner et al. 2003b; Liu et al. 2004b; Baer et al. 2008; Zabel et al. 2008; Zhang et al. 2010). Furthermore, at least one paralogue copy of eEF2 encoding genes, *EFT1* or *EFT2*, scored amongst the top ten correlated profiles of *DPH1*, *DPH2* and *DPH4*. Strikingly, two uncharacterized ORFs, *YLR143w* and *YBR246w,* repeatedly scored highly in the correlated profiles of all diphthamide synthesis genes. This prompted us to look into query analyses using strains deleted for either *YLR143w* and *YBR246w.* Not surprisingly, the top ten correlated profiles for both ORFs contained all

diphthamide synthesis genes included in the SGA analysis (*DPH1*, *DPH2*, *DPH4* and *DPH5)*. Interaction profiles are correlated and ranked according to the highest Pearson Correlation Coefficient (PCC). Depending on the stringency of the PCC limit, a genetic landscape for each query strain can be designed. Figure 3.3 displays the genetic interaction landscape for *YLR143w* with a PCC cut-off ranging from <1.0 to <0.14. The former includes a wider landscape of correlated interactors together with diphthamide genes *DPH1-DPH5*, the novel candidate ORF *YBR246w* as well as eEF2 encoding genes *EFT1* and *EFT2*. By increasing the PCC cut-off to <0.14, it becomes apparent how closely related *YLR143w* and *YBR246w* are to each other and to the *DPH1-DPH5* network, which form a tightly related gene family cluster. These highly correlated profiles suggest that *YLR143w* and *YBR246w* are candidate genes related to the diphthamide pathway.

DPH1

	Query	Top 10	PCC
	DPH1	***DPH2***	0.303
	DPH1	***DPH4***	0.3
	DPH1	***DPH5***	0.275
	DPH1	*YGR205w*	0.241
	DPH1	***EFT2***	0.218
	DPH1	*FOB1*	0.215
	DPH1	***YBR246w***	0.21
	DPH1	*YHR210c*	0.202
	DPH1	*YDL121c*	0.191
	DPH1	*CRF1*	0.186
#26	***DPH1***	***YLR143w***	0.141

DPH2

	Query	Top 10	PCC
	DPH2	***DPH4***	0.316
	DPH2	***DPH1***	0.303
	DPH2	***YBR246w***	0.278
	DPH2	***DPH5***	0.234
	DPH2	***YLR143w***	0.188
	DPH2	*PBP1*	0.164
	DPH2	*SHO1*	0.156
	DPH2	***EFT1***	0.152
	DPH2	*CRP1*	0.148
	DPH2	*RLM1*	0.144
#104	***DPH2***	***EFT2***	0.088

DPH5

	Query	Top 10	PCC
	DPH5	***DPH1***	0.275
	DPH5	***YLR143w***	0.273
	DPH5	***DPH2***	0.234
	DPH5	***YBR246w***	0.222
	DPH5	***DPH4***	0.174
	DPH5	*MLP1*	0.165
	DPH5	*DOM34*	0.155
	DPH5	*YOL114c*	0.154
	DPH5	*FIR1*	0.147
	DPH5	*CMC1*	0.146
#228	***DPH5***	***EFT2***	0.072

DPH4

	Query	Top 10	PCC
	DPH4	***DPH2***	0.316
	DPH4	***DPH1***	0.3
	DPH4	*EDC2*	0.25
	DPH4	***YBR246w***	0.234
	DPH4	***YLR143w***	0.189
	DPH4	***DPH5***	0.174
	DPH4	*KRS1*	0.172
	DPH4	***EFT1***	0.171
	DPH4	*ERM6*	0.17
	DPH4	*CBF1*	0.158
#39	***DPH4***	***EFT2***	0.109

YLR143w

	Query	Top 10	PCC
	YLR143w	***DPH5***	0.273
	YLR143w	*HBS1*	0.199
	YLR143w	***DPH4***	0.189
	YLR143w	***DPH2***	0.188
	YLR143w	*PUS5*	0.168
	YLR143w	***YBR246w***	0.16
	YLR143w	*SNZ1*	0.155
	YLR143w	*NEJ1*	0.146
	YLR143w	***DPH1***	0.144
	YLR143w	*IPT1*	0.136
#29	***YLR143w***	***EFT2***	0.11

YBR246w

	Query	Top 10	PCC
	YBR246w	*ISW1*	0.434
	YBR246w	***DPH2***	0.278
	YBR246w	*IOC2*	0.27
	YBR246w	***DPH4***	0.234
	YBR246w	***DPH5***	0.222
	YBR246w	***DPH1***	0.21
	YBR246w	*PBP4*	0.197
	YBR246w	*NDE2*	0.174
	YBR246w	*PAT1*	0.17
	YBR246w	*TAE1*	0.166
#12	***YBR246w***	***YLR143w***	0.16

Figure 3.2. SGA-based correlated profiles for *DPH1-DPH5* and related ORFs *YLR143w* and *YBR246w*. Top 10 correlated profiles of the indicated query strains extracted from SGA-based DRYGIN database are ranked according to Pearson Correlation Coefficient determination (PCC) (see methods). Note that *DPH1-DPH5* genes repeatedly score highly and indicate a tightly clustered SGA-based diphthamide synthesis network. For clarity, *DPH1-DPH5*, *EFT1* and *EFT2* as well as related ORFs *YLR143w* and *YBR246w* are shown in bold.

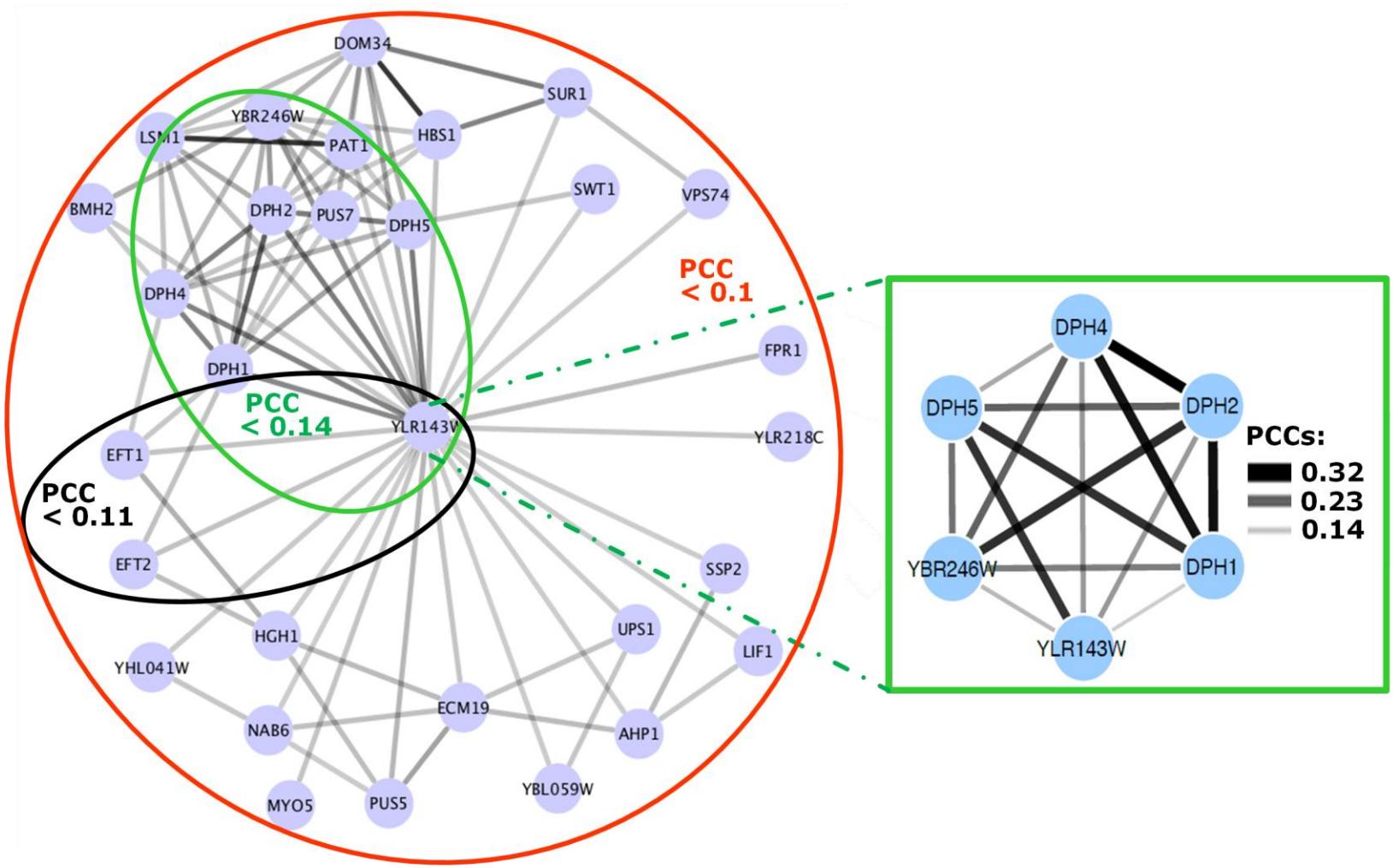
DOM34
SUR1
YBR246W
LSM1
PAT1
HBS1
SWT1
VPS74
BMH2
DPH2
PUS7
DPH5
DPH4
DPH1
PCC
< 0.14
YLR143W
PCC
< 0.1
FPR1
YLR218C
EFT1
PCC
< 0.11
EFT2
SSP2
HGH1
UPS1
LIF1
YHL041W
ECM19
NAB6
AHP1
MYO5
PUS5
YBL059W
DPH4
DPH5
DPH2
PCCs:
0.32
0.23
0.14
YBR246W
DPH1
YLR143W

Figure 3.3. *YLR143w* genetic interaction landscape. Schematic representation of interaction landscape of *YLR143w* according to SGA-based correlated profiles. Pearson Correlation Coefficient determination (PCC) cut offs (0.1 - 0.32) indicate how closely related the ORFs are to query strain *YLR143w*. PCC cut off <0.1 (red circle) displays the wider landscape of *YLR143w* containing 29 related ORFs, whereas at a slightly increased PCC <0.11 (black circle) eEF2 gene copies, *EFT1* and *EFT2*, are more closely related to *YLR143w*. The superimposed green square on the right includes all ORFs at a PCC <0.14, which only includes diphthamide synthesis genes *DPH1-DPH5* and closely related ORFs *YBR246w* and *YLR143w*. Figure kindly provided by Dr. Michael Costanzo.

3.2.2 *YLR143w* and *YBR246w* phenocluster with *bona fide* diphthamide genes

In order to find more evidence linking *YLR143w* and *YBR246w* to diphthamide synthetis, we examined data deposited at the FitDB for novel ORFs displaying correlated fitness defects to *DPH1-DPH5*. To do so, we collected the top ten hits of genes that phenocluster with query strains *DPH1*, *DPH2*, *DPH4*, *DPH5*, *YLR143w* and *YBR246w*. Hillenmeyer *et al.* (2008, 2010) generated these correlated fitness (co-fitness) profiles by comparing scored phenotypes across all experiments and ranked them according to their co-fitness values. Again, *DPH3* is not included in the database for the same reasons mentioned in the previous paragraph. Figure 3.4 contains the top ten sensitivity inducing conditions for *DPH1*, *DPH2*, *DPH4*, *DPH5*, *YLR143w* and *YBR246w* deletion strains and figure 3.5 lists the correlated fitness profiles for the above mentioned genes. The top ten hits are colour coded for *bona fide* and novel candidate diphthamide genes (yellow), genes that are shared by either two (blue) or four queries (green) and genes typical for only one query (transparent). With the exception of *DPH1*, all other query ORFs phenocluster with at least one diphthamide gene. Interestingly, *YBR246w* phenoclusters with *DPH2*, *DPH4* and *DPH5* while *YLR143w* phenoclusters with *DPH2*, *DPH4*, *DPH5* and *YBR246w*. The enriched GO terms for both ORFs listet in Figure 3.4 assign the process of peptidyl-diphthamide biosynthesis from peptidyl-histidine with P-values ranging from 2×10^{-3} (*YLR143w*) to 9×10^{-4} (*YBR246w*).

DPH1

Condition	Conc	Unit	Fitness Defect	P-value
synthetic complete for BY4743	0.78	uM	17.7743	0.0015752
synthetic complete for BY4743	29	uM	14.9808	< 1e-12
synthetic complete for BY4743	4.88	nM	14.1552	< 1e-12
synthetic complete for BY4743	6	nM	13.9839	< 1e-12
synthetic complete for BY4743	0.78	uM	9.82738	0.0050982
synthetic complete for BY4743	200	uM	7.43855	0.0000000062643
synthetic complete for BY4743	100	mM	7.37655	0.00000038145
minimal media	9	nM	7.1473	0.0095095
synthetic complete for BY4743	3	uM	6.69837	0.000000054143
potassium disulfite	1.5	M	6.62405	0.000029488

DPH2

Condition	Conc	Unit	Fitness Defect	P-value
wiskostatin	29	uM	26.4557	< 1e-12
rapamycin	6	nM	25.0175	< 1e-12
rapamycin	4.88	nM	22.2666	< 1e-12
fk506	100	uM	13.4163	< 1e-12
LiCl	100	mM	12.2135	1.8985e-10
lovastatin	154.5	uM	10.7425	2.3372e-11
LiCl	150	mM	9.13103	5.6724e-11
LiCl	150	mM	9.02692	7.4987e-11
fk506	0.1	ug/ml	8.3455	4.8222e-10
fk506	50	uM	8.21291	6.9733e-10

DPH4

Condition	Conc	Unit	Fitness Defect	P-value
rapamycin	4.88	nM	15.021	< 1e-12
wiskostatin	29	uM	14.0749	< 1e-12
latrunculin	0.78	uM	13.9785	0.0025394
rapamycin	6	nM	13.7098	< 1e-12
rapamycin	9	nM	10.1906	0.0047463
latrunculin	0.78	uM	8.4612	0.006841
ph8	0		7.95596	6.1789e-06
ph8	0		7.20522	1.4541e-05
fk506	100	uM	6.69505	5.4675e-08
ph8	0		5.85677	8.0067e-05

DPH5

Condition	Conc	Unit	Fitness Defect	P-value
wiskostatin	29	uM	20.2135	< 1e-12
rapamycin	6	uM	19.6983	< 1e-12
rapamycin	4.88	nM	16.3793	< 1e-12
phosphatase inhibitor	3	uM	13.332	< 1e-12
methotrexate	250	uM	13.0659	< 1e-12
latrunculin	3	uM	10.4089	2.4015e-09
methotrexate	250	uM	9.35561	4.1646e-10
nitric oxide	800	uM	9.28355	4.8694e-10
cantharidin	200	uM	8.58799	2.47e-10
rapamycin	9	nM	7.69872	0.0082283

YLR143w

Condition	Conc	Unit	Fitness Defect	P-value
latrunculin	0.78	uM	17.7743	0.0015752
wiskostatin	29	uM	14.9808	< 1e-12
rapamycin	4.88	nM	14.1552	< 1e-12
rapamycin	6	nM	13.9839	< 1e-12
latrunculin	0.78	uM	9.82738	0.0050982
cantharidin	200	uM	7.43855	0.0000000062643
LiCl	100	mM	7.37655	0.00000038145
rapamycin	9	nM	7.1473	0.0095095
phosphatase inhibitor	3	uM	6.69837	0.000000054143
sorbitol	1.5	M	6.62405	0.000029488

YBR246w

Condition	Conc	Unit	Fitness Defect	P-value
wiskostatin	29	uM	28.5198	< 1e-12
rapamycin	6	nM	26.6861	< 1e-12
rapamycin	4.88	nM	23.8278	< 1e-12
cadmium chloride	7.81	uM	17.3297	< 1e-12
LiCl	100	mM	15.5075	0.0000000000036887
latrunculin	0.78	uM	10.6867	0.00087576
latrunculin	0.78	uM	7.70972	0.0082054
norcantharidin	2500	uM	6.87307	0.000000032399
methotrexate	250	uM	6.48657	0.0000003551
hygromycin	13.75	uM	6.07804	0.0000003411

Figure 3.4. Top ten sensitivity inducing conditions. Data obtained from genome-wide yeast fitness screen (http://fitdb.stanford.edu, Hillenmeyer et al., Science 2008) in which homozygous and heterozygous gene deletions were exposed to 1144 different chemical assays and scored for fitness. Top 10 conditions that induce sensitivity in homozygous *DPH1*, *DPH2*, *DPH4*, *DPH5*, *YLR143w* and *YBR246w* deletion strains are listed.

Query	Interactor	CoFit
DPH1	*RPS16A*	0.548
DPH1	*IMG1*	0.542
DPH1	*TUF1*	0.521
DPH1	*YER087w*	0.520
DPH1	*ELP3*	0.501
DPH1	*RPL24B*	0.500
DPH1	*RPS30A*	0.496
DPH1	*SPT21*	0.493
DPH1	*SSQ1*	0.493
DPH1	*TOS1*	0.491

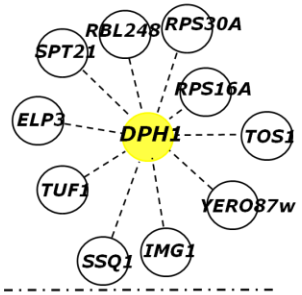

Query	Interactor	CoFit
DPH4	***YLR143w***	0.650
DPH4	**DPH5**	0.632
DPH4	***DPH2***	0.614
DPH4	***MAL1***	0.611
DPH4	***YPR092w***	0.584
DPH4	***LAP3***	0.577
DPH4	***SYT1***	0.572
DPH4	***PUS7***	0.568
DPH4	***YPR091c***	0.567
DPH4	**PBP1**	0.566

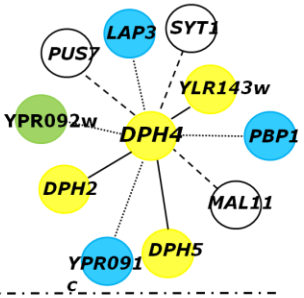

Query	Interactor	CoFit
YLR143w	***DPH4***	0.650
YLR143w	***DPH5***	0.633
YLR143w	***YER119c-A***	0.544
YLR143w	***YBR246w***	0.524
YLR143w	***OSH3***	0.515
YLR143w	***DPH2***	0.494
YLR143w	***LAP3***	0.477
YLR143w	***SCS2***	0.453
YLR143w	***DNF2***	0.443
YLR143w	***YPR092w***	0.442

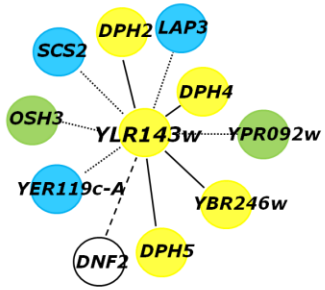

Query	Interactor	CoFit
DPH2	***OSH3***	*0.669*
DPH2	***YPR091c***	*0.629*
DPH2	***SWH1***	*0.628*
DPH2	***DPH4***	0.614
DPH2	***YBR246w***	0.596
DPH2	***SLM1***	0.596
DPH2	***NIF3***	0.581
DPH2	***CAF40***	0.572
DPH2	***YPR092w***	0.572
DPH2	***NDE1***	0.560

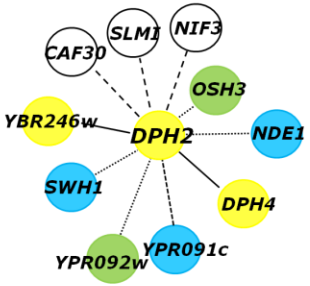

Query	Interactor	CoFit
DPH5	***YLR143w***	0.633
DPH5	***DPH4***	0.632
DPH5	***YBR246w***	0.574
DPH5	***YER119c-A***	0.533
DPH5	***ENT5***	0.529
DPH5	***PBP4***	0.498
DPH5	***SCS2***	0.495
DPH5	***OSH3***	0.492
DPH5	***PBP1***	0.489
DPH5	***DPH2***	0.484

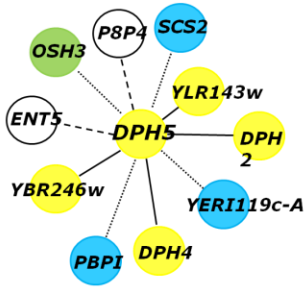

Query	Interactor	CoFit
YBR246w	***ISW1***	0.717
YBR246w	***YPR092w***	0.598
YBR246w	***DPH2***	0.596
YBR246w	***NDE1***	0.584
YBR246w	*DPH5*	0.574
YBR246w	***SVF1***	0.562
YBR246w	***DPH4***	0.553
YBR246w	***OSH3***	0.552
YBR246w	***YMR31***	0.548
YBR246w	***SWH1***	0.541

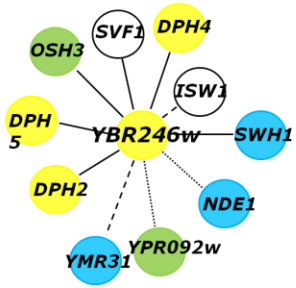

Likelihood (P-values) for GO terms related to
YLR143w (2e-03) and ***YBR246w*** (9e-04):

- peptidyl-histidine modification
- peptidyl-diphthamide metabolism
- peptidyl-diphthamide biosynthesis from peptidyl-histidine

Gene interaction types

- typical of 1 query only
- shared by 2 & 4 queries
- *DPH*-specific (5/6 queries)

Figure 3.5. FitDB based co-fitness values of *bona fide DPH* genes and correlated ORFs *YLR143w* and *YBR246w*. Collection of top 10 hits of genes that phenocluster with the indicated query ORFs (*DPH1*, *DPH2*, *DPH4*, *DPH5*, *YLR143w* and *YBR246w*). Data is derived from FitDB and is based on genome-scale co-fitness defect analysis of homozygous yeast deletion mutants in response to 1144 different conditions. Enriched GO terms for diphthamide related ORFs *YLR143w* and *YBR246w* are indicated with p-values ranging from 2×10^{-3} (*YLR143w*) to 9×10^{-4} (*YBR246w*). Genes, whose deletions most significantly correlate with the indicated query strains (yellow, central nodes) are grouped according to the type of interactions they undergo, e.g. unique (white), shared (blue/green) and *DPH*-specific profiles (yellow).

3.3 Conclusion

Genetic interaction studies are useful tools for investigating the function of uncharacterized genes and allocating them to specific cellular pathways. Complementary to this are the fields of chemical-genetic interactions as well as environmental-genetic interactions. Gathering data for gene-gene interactions together with gene deletion responses to chemical and environmental stresses has resulted in an immense collection of genetic data available to date that culminates in a genetic interaction network of a cell (Costanzo et al. 2010; Hillenmeyer et al. 2010).

Here we report that data mining of two different screens using yeast ORF deletion collections resulted in the finding of two novel candidate genes for diphthamide synthesis. Initially, genetic interaction studies with the help of SGA analysis provided first clues for a subset of genes that are related to diphthamide synthesis including *DPH1-DPH5* and two novel ORFs, *YLR143w* and *YBR246w* (Koh et al. 2010). The findings were reinforced with the help of the FitDB containing data from approximately 6 million single events of chemical and environmental stress responses (Hillenmeyer et al. 2008).

Both protein products of *YLR143w* and *YBR246w* are located in the cytoplasm like Dph1-Dph5 (Huh et al. 2003). While no specific function has been proposed for *YLR143w* yet, (Botet et al. 2008) reported that the deletion mutant is a strong sordarin suppressor. *YBR246w* on the other hand, has been implicated in several distinct pathways. Sequence analysis revealed that *YBR246w* contains four WD40 domains and is involved in endosomal recycling as the product of *ERE1* that partners with the protein

encoded by the *ERE2* gene (Shi et al. 2011) as well as the regulation of levels of ribosomal DNA transcription aka *RRT2* (Hontz et al. 2009; Shi et al. 2011), (Shi et al. 2011). Neither pathway seems to be directly connected to diphthamide synthesis, however it could indicate a multiple role for *YBR246w* in cellular processes. Furthermore, while our research was ongoing, the putative human homologue of *YBR246w*, WDR85 (WD repeat domain 85), was suggested to be involved in the diphthamide synthesis pathway (Carette et al. 2009) and very recently was reported to be necessary for the final amidation step converting diphthine into the end product of the modification pathway, diphthamide ((Su et al. 2011).

Analysis of the protein sequence of YLR143w on the other hand revealed an N-terminal Alpha_ANH_like_IV domain, which is predicted to bind ATP. Seeing that the amidation of diphthine is likely ATP-dependant, this might highlight a central role for *YLR143w* in the final step of diphthamide formation.

Taken together, the FitDB and DRYGIN profiles emphasize a shared phenotypic pattern for the *DPH* genes together with *YBR246w* and *YLR143w*, which are tightly clustered within the diphthamide gene network. Thus in the subsequent experiments we chose to further investigate the role of *YLR143W* and *YBR246w* in diphthamide synthesis.

CHAPTER 4

Investigating the role of *YLR143w* and *YBR246w* in diphthamide biosynthesis

4 Investigating the role of *YLR143w* and *YBR246w* in diphthamide biosynthesis

4.1 Introduction

As described in the previous chapter, data mining of two independent genetic interaction screens indicated that two novel ORFs, *YLR143w* and *YBR246w*, are closely related to *bona fide* diphthamide synthesis genes, *DPH1-DPH5*. The aim of the experiments described in this chapter was to investigate a putative role for both candidate genes in the post-translational modification of His^{699} on eEF2 in *S.cerevisiae*.

In order to address this question we exposed *YLR143w* and *YBR246w* mutant strains to *in vivo* and *in vitro* assays involving diphthamide indicator drugs, diphtheria toxin (DT) and the antifungal, sordarin, to investigate whether they phenocopy *bona fide DPH* genes. Futhermore, epitope tagged eEF2 from *YLR143w* and *YBR246w* mutant strains was analyzed via mass spectrometry to identify whether the lack of either gene affects diphthamide formation. A putative interaction between Ylr143w and Ybr246w and known diphthamide synthesis proteins, Dph1, Dph2 and Dph5, as well as eEF2, the protein carrying the posttranslational modification, was analyzed by co-immunoprecipitation. As mentioned in chapter 1 (section 1.5), the lack of diphthamide on eEF2 was shown to play a role in translational fidelity (Ortiz et al. 2006a; Bar et al.

2008). Hence, the level of frameshifting in cells lacking either of our candidate ORFs was compared to *DPH* deletion strains and the isogenic wild-type.

At the point of this research we were not aware of any findings regarding the direct involvement of *YBR246w* in diphthamide formation, hence for the purpose of readability our data will be presented without considering recent findings by Su et al. (2011) mentioned in the introduction (section 1.9). However, in the discussion we will present recent developments in identifying the function of *YBR246w* within the diphthamide pathway and compare our findings to the published work of Su et al. (2011).

4.2 Results

4.2.1 *YLR143w* and *YBR246w* phenocopy diphthamide synthesis genes

The unmodified His^{699} on yeast eEF2 protects from diphtheria toxin (DT) as well as sordarin, therefore we assayed *YLR143w* and *YBR246w* for their response towards both cytotoxic agents in order to gain insight into their diphthamidation properties. In order to assay for DT, the strains were transformed with vector pLMY101 carrying the F2 fragment (the cytotoxic ADP-ribosylase fragment of the toxin, DTA) under the expression of the conditional *GAL1* promoter. Ten-fold serial cell dilutions were spotted on selective media containing either galactose, to induce DTA expression from the *GAL1* promoter, or glucose, which serves as the control and inhibits the release of the toxin. Figure 4.1A shows that *YLR143w* and *YBR246w* are sensitive to the endogenous expression of DTA from the strong *GAL1* promoter, in contrast to *dph1Δ*, which cannot be killed by the toxin. *In vivo* DTA expression from the multi copy vector, pLMY101, under the control of the strong *GAL1* promoter, results in the intracellular release of high levels of the toxin. We therefore decided to downregulate endogenous DT expression by cloning the DTA fragment from pLMY101 into the single copy pGALS vector, p415-GALS (Mumberg et al. 1994). This *GALS* promoter is truncated and lowers expression levels up to 50 fold compared to the *GAL1* promoter. By exchanging the strong promoter for a weak one together with switching from a multi copy to a single copy vector, we sought to reduce the expression of endogenous DTA to a level which might result in a reduced toxin sensitivity of *YLR143w* and *YBR246w*

compared to the wild-type strain. In collaboration with Dr. Christian Baer, University of Kassel, we altered the level of galactose from 2% to 0.1% while simultaneously replacing it with raffinose as a carbon source, which does not induce the *GALS* promoter, thereby downregulating the *GALS* promoter and further decreasing DTA expression. Figure 4.1B clearly demonstrates an increased resistance towards very low levels of DT in the *YLR143w* and *YBR246w* strain compared to the isogenic wild-type. These results further support our hypothesis that deletion of either candidate ORF leads to the accumulation of diphthine, which even though a target for DT is less efficiently ADP-ribosylated compared to diphthamide.

When exposed to another diphthamide indicator drug the lack of Ylr143w and Ybr246w showed a significant resistance to levels of 10 µg/ml sordarin, which is cytotoxic to the wild-type strain (Figure 4.1C). In fact, *ylr143w* and *ybr246w* mutant strains are as insensitive to the action of sordarin as *bona fide DPH* genes, *DPH1-DPH5*. Though we are aware that the list of sordarin resistant yeast deletion mutants is rather large and that the resistance of both candidate ORFs towards sordarin might be independent of the diphthamide pathway, we decided to further investigate their potential as diphthamide biosynthesis genes.

The action of both compounds, DT and sordarin, on yeast eEF2 is dependent on the formation of diphthamide. Unmodified His^{699} cannot be targeted by either agent, whereas the mature modification, diphthamide, serves as a potent recognition motif on eEF2 and results in its inactivation by DT and sordarin. Interestingly, the acid hydrolysis product of diphthamide, diphthine, which is the second intermediate in the pathway, can still be recognized and targeted by DT even though less efficiently than

the complete diphthamide modification. Therefore we hypothesized that the DT sensitive phenotype of *YLR143w* and *YBR246w* towards endogenous expression of high levels of the toxin might be due to the accumulation of diphthine rather than diphthamide, which would explain the dose-dependant resistance towards DT.

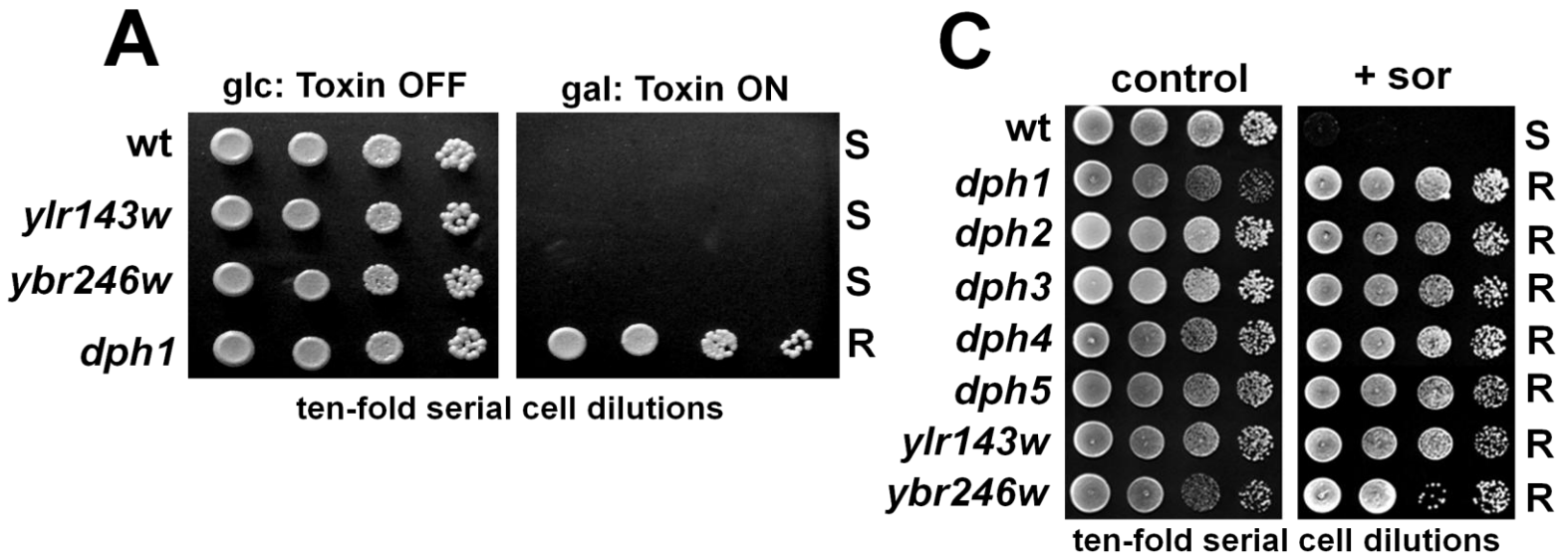
A
glc: Toxin OFF
gal: Toxin ON
wt
ylr143w
ybr246w
dph1
S
S
S
R
ten-fold serial cell dilutions
C
control
+ sor
wt
dph1
dph2
dph3
dph4
dph5
ylr143w
ybr246w
S
R
R
R
R
R
R
R
ten-fold serial cell dilutions
B
pSU8 (CEN/ARS)
GALS
DTA
0
2
2
0
1
1
0.1
1.9
% gal
% raf
wt
dph1
dph5
ylr143w
ybr246w
S
R
R
S
S
S
R
R
S
RS
S
R
R
RS
PR
ten-fold serial cell dilutions

Figure 4.1. *DPH6* and *DPH7* deletion strains copy traits typically related to the bona fide diphthamide mutants *dph1-dph5*.

(A) DT phenotype. Indicated strains were tested for sensitivity to intracellular expression of DTA, the cytotoxic ADP ribosylase fragment of DT. This assay involved galactose-inducible expression of DTA from the multicopy vector pLMY101 (see text for details). Serial cell dilutions were replica plated onto glucose (glc) as a control and galactose (gal), which induces expression of DTA. Growth was for 3 days at 30°C. DTA sensitive (S) and resistant (R) phenotypes are indicated. (B) Downregulation of DTA expression. As indicated, yeast *dph* mutants and wild-type control (wt) were tested for sensitivity to intracellular expression of DTA. This *in vivo* assay involved galactose-inducible expression from vector pSU8 (see Materials and Methods). Serial cell dilutions were replica spotted onto raffinose (2% raf) and galactose-inducing conditions using concentrations (2, 0.2 and 0.1% gal) suited to achieve gradual down-regulation of DTA toxicity. Growth was for 3 days at 30°C. DTA sensitive (S) resistant (R), partially resistant (PR) and reduced sensitive (RS) phenotypes are indicated. (C) Sordarin resistance. Ten-fold serial cell dilutions of the indicated yeast strains, BY4741 wild-type (wt) background and its dph1-dph7 gene deletion derivatives were grown on YPD plates in the absence (control) or presence (+ sor) of 10 μg ml^{-1} sordarin. Growth was assayed for 3 d at 30°C. Sordarin resistant (R) and sensitive (S) responses are indicated.

4.2.2 *YLR243w* and *YBR246w* cannot be ADP-Ribosylated *in vitro*

Seeing that the cytotoxicity of DT is specifically dependant on the diphthamide modification (in contrast to sordarin, which can be blocked by other pathways as indicated by the collection of sordarin resistant yeast gene deletions), we decided to confirm the *in vivo* DT sensitivity of *YLR143w* and *YBR246w* in an *in vitro* assay. In collaboration with Dr. Shihui Liu (National Institute of Health, Bethesda, USA) we performed an *in vitro* ADP-ribosylation assay in presence of DT (20 nM) with biotin labeled NAD as the cofactor. Isogenic wt strain together with gene deletions of *DPH1*, *DPH5*, *YLR143w* and *YBR246w* were assayed for their ADP-ribosylation property (Figure 4.2). Interestingly, similar to the *DPH* genes, neither *YLR143w* nor *YBR246w* could be ADP-ribosylated *in vitro*. Uptake of biotin labeled NAD was only observed in the wt strain, showing that eEF2 from *YLR143w, YBR246w* as well as *DPH1* and *DPH5* could not be ADP-ribosylated by DT *in vitro*. In concert with our *in vivo* results, these findings imply that *YLR143w* and *YBR246w* display a defect in diphthamide synthesis.

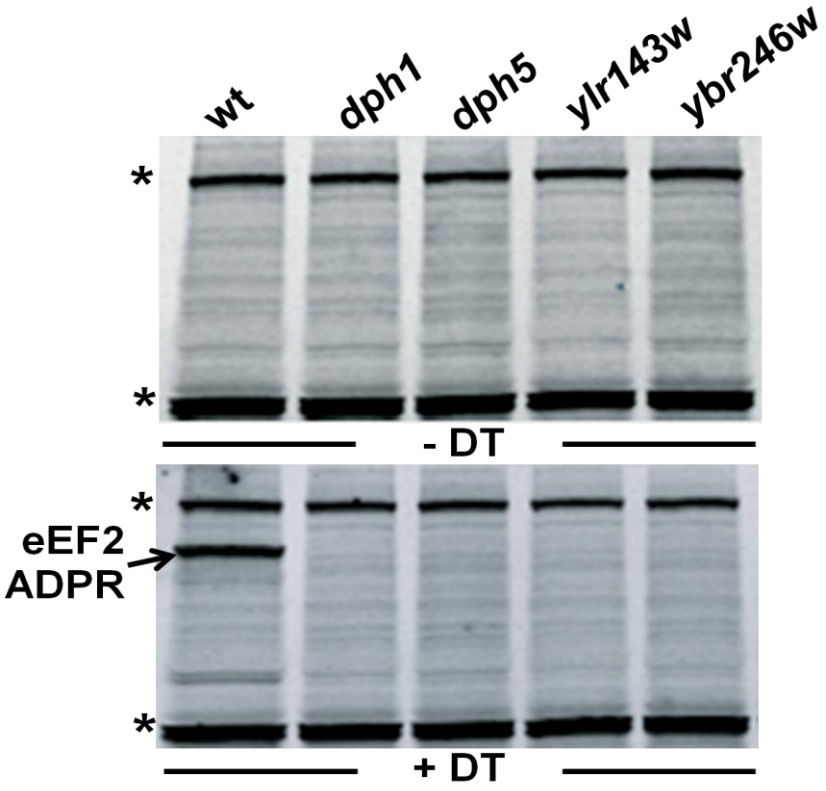

Figure 4.2. *ylr143w* and *ybr246w* demonstrate a lack of *in vitro* ADP-ribose acceptor activity.

Cell extracts obtained from *dph1, dph5, ylr143w and ybr246w* mutant and wild-type (wt) strains were incubated with (+DT) or without (-DT) 20 nM diphtheria toxin in the presence of biotin-NAD (10 μM) at 37°C for 1 hour. The transfer of biotin-ADP-ribose to eEF2 was detected by Western blotting using a streptavidin-conjugate. Two unknown non- specific bands (indicated by *) served as internal controls for even sample loading. Data generated by Dr. Shihui Liu.

4.2.3 eEF2 tandem affinity purification

In order to clarify the involvement of our candidate ORFs in diphthamide synthesis we isolated eEF2 from yeast deletion strains and analyzed the modification on His^{699} via mass spectrometry. To address the question, deletions of *DPH1* and *YLR143w* were tested in an *EFT2*-TAP (*Euroscarf*) strain, which allows the tandem affinity purification (TAP) of the protein. The TAP tag contains a protein A binding site followed by a CBP (calmodulin binding protein) domain. These two distinct motifs are separated by a TEV linker domain and allow two consecutive purification steps, which enable the isolation of proteins from crude extracts (for details see Methods). Seeing that TAP purification is a very elaborate process we decided to first investigate *YLR143w* in order to verify that the method is applicable for our strains. The TAP results are demonstrated in Figure 4.3, which highlights how the impurities of the first elution (after TEV protease cleavage) disappear after the second purification step and result in a single band of isolated TAP-tagged eEF2 protein. Though with a lower yield compared to the first elution, the purified protein can be directly trypsin digested in liquid. We isolated eEF2-TAP from wild-type strain and *DPH1* and *YLR143w* mutant strains and performed mass spectrometry, which detected His^{699} in the tryptic peptide 686-VNILDVTLHADAIHR-700. Unfortunately, we failed to detect any modification on His^{699} from any of the samples (MS spectra of unmodified wt, *dph1* and *ylr143w* peptide are included in the appendix). This was expected for the *DPH1* mutant, which impairs diphthamide formation completely, but not for the wild-type sample. After repeating the TAP isolation of eEF2 on new samples and switching from in liquid trypsinisation to in gel digest we still were unable to detect diphthamide in the wild-type

or any other modification of the histidine precursor. It was possible that the large size of the TAP tag (~21kDa) might interfere with the diphthamide formation on eEF2 given that the C-terminal end of the protein is in close proximity to His^{699} in the folded protein (see Figure 1.1 in the introduction). Therefore we decided to repeat the experiment with a smaller tag, which would avoid interference with diphthamide formation.

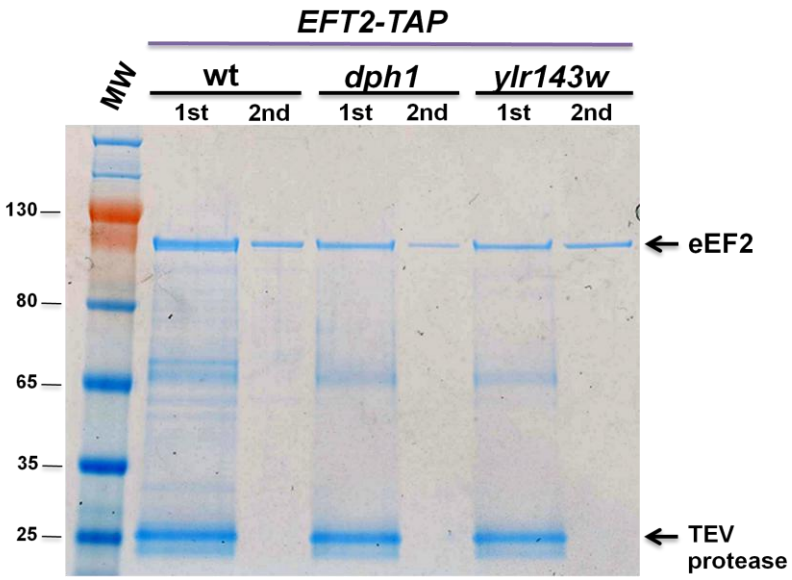

Figure 4.3. Tandem affinity purification (TAP) of eEF2.

Total protein extracts of wild-type (wt), *dph1* and *ylr143w* variants of an *EFT2*-TAP strain were used for TAP isolation of tagged eEF2 constructs. The first purification step with IgG coated sepharose beads binds the protein A domain of the TAP tag and is followed by the first elution in presence of TEV protease. The second purification step involved calmodulin affinity beads, which bind to the CBP (calmodulin binding protein) domain of the TAP tag and results in the isolation of a single band of eEF2. TAP eluates were run on SDS-PAGE and visualized with coomassie blue staining.

4.2.4 Mass spectrometry identifies *YLR143w* and *YBR246w* as diphthamide synthesis genes

In order to clarify the involvement of the candidate ORFs, *YLR143w* and *YBR246w*, in diphthamide synthesis we decided to isolate his-tagged eEF2 from strains lacking both genes and analyzing the modification of His^{699} via mass spectrometry. As a control, eEF2 from wild-type strain as well as *dph1Δ* (blocking the modification at the initial step) and *dph5Δ* (arresting diphthamidation after the formation of the ACP-intermediate) were also investigated. The eEF2-His6 construct expressed from plasmid pTKB612 was previously shown to complement an *eft1eft2* double mutant and therefore considered biologically functional. Isolation of His-tagged eEF2 from crude protein preps was performed using magnetic anti-His tag Dynabeads® (Invitrogen). Compared to the TAP-purification method above, His6-tag isolation in *S.cerevisiae* is not very clean, however when samples were run on an SDS-PAGE 4-12% Bis-Tris precast gel (Invitrogen) an enriched band with the right size of ~100kDa for eEF2 was detected (Figure 4.4). A section of the eEF2 band was excised and in gel digestion with trypsin was performed (see Methods). Mass spectrometry and data analysis was performed in collaboration with Prof. Mike Stark and Dr. Sara ten Have, University of Dundee.

Tryptic peptides were fractionated by LC-MS (Liquid Chromatography-MS) linked up to the mass spectrometer. They enter the first stage, which performs a survey scan for parent ions (m/z 335-1800). The top 15 most intense ions from each survey are then sent to the second stage, where they are fragmented to give the b and y ion series and a spectrum showing the ions that are obtained is produced. The actual spectra that

we are presenting are composites made by combining the signal from all spectra obtained for each parent ion, i.e. a particular ion may appear many times in a series of survey scans as its peak elutes from the LC step and be sequences many times as a result. Normally the spectra are identified and annotated by the software. In our case this had to be done manually by Dr. Sara ten Have by sifting through the data to identify parent ion masses that matched what we expected (see below) and then looking in the MS/MS spectrum for ions matching what was predicted. This was probably due to complications associated with the type of modification and the effect on the m/z. Parent ions can be singly or multiply charged, which gives a series of parent ion masses such as [M+H]+, [M+2H]2+, [M+3H]3+ etc. Dr. ten Have then used molecular mass calculator (MolE, http://library.med.utah.edu/masspec/mole.htm) to calculate the exact mass from a formula (see Table 4.1.). The assignment of each modification is by matching multiple lines in the MS/MS spectrum to predicted values for one modification and verifying whether they are different from any other modification or not.

	[M+H]+ (mono)	[M+2H]2+ (mono)	[M+3H]3+ (mono)
Unmodified	1686.9285	843.9682	562.9814
Diphthamide	1829.0397	915.0238	610.3518
Diphthamide-(CH3)3HN+	1769.9656	885.4867	590.6604
Diphthine	1830.0238	915.5158	610.6798
Diphthtine - (CH3)3HN+	1770.9496	885.9787	590.9884
ACP intermediate	1787.9762	894.4920	596.6639

Table 4.1. Expected m/z values for the different stages of His699 modification. Molecular mass calculator (MolE, http://library.med.utah.edu/masspec/mole.htm) was used to calculate the m/z values of singly or multiply charged parent ion masses ([M+H]+, [M+2H]2+, [M+3H]3+). The different stages of yeast eEF2 His699 modifications are listed with the diphthine and diphthamide values before and after the neutral loss of the trimethylamino group. Data provided by Prof. Mike Stark and Dr. Sara ten Have.

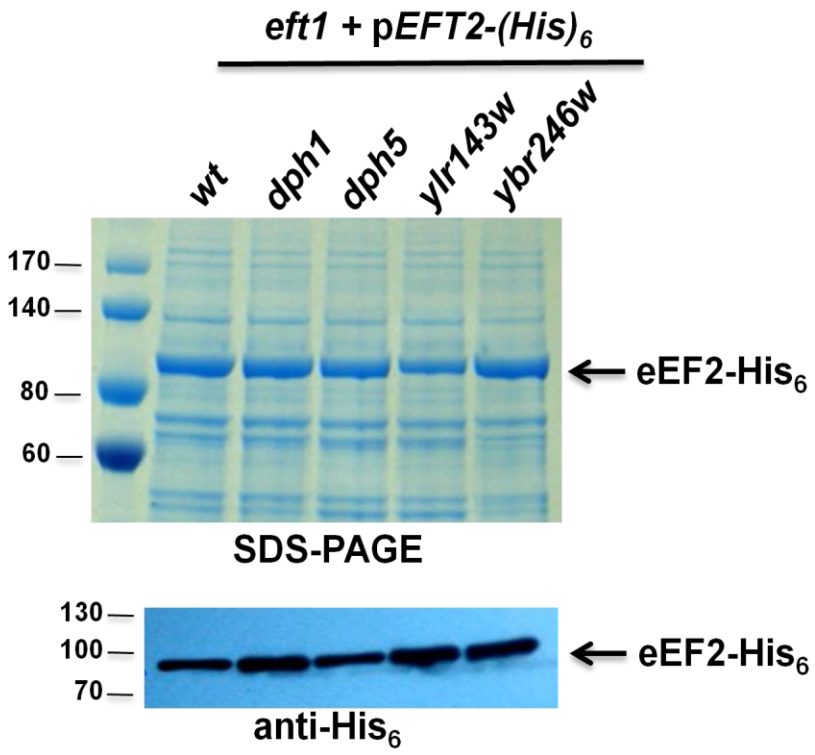

Figure 4.4. eEF2-His6 isolation and immunodetection.

Total protein extracts of wt, *dph1*, *dph5*, *ylr143w* and *ybr246w* variants of the background strain *eft1+pEFT2-(His)*$_6$ were used for anti-His isolation with magnetic beads (Dynabeads®, Invitrogen). The enriched eEF2-His6 s were run on SDS-PAGE (top panel) and visualizes with coomassie blue staining. The bottom panel demonstrates immunoblot detection of the *eft1+pEFT2-(His)*$_6$ construct with anti-His6 antibody.

The modified histidine in eEF2 is located in the tryptic peptide 686-VNILDVTLHADAIHR-700 (Figure 4.5A) and, as expected, unmodified versions of this peptide were readily detected in eEF2 prepared from the *dph1*Δ strain (Figure 4.5C). Unmodified peptide was also found in eEF2 prepared from the *dph5*Δ, *ybr246w*Δ and *ylr143*Δ strains as well as in eEF2 from the wild-type strain (Figure 4.5). Although we cannot accurately quantitate the relative levels, examination of extracted ion chromatograms for the doubly and triply charged species of the unmodified peptide suggests that by far the highest level was seen in the *dph1*Δ strain, with lower, though highly significant levels, in the other three mutants and less in the wild-type strain (Figure 4.6).

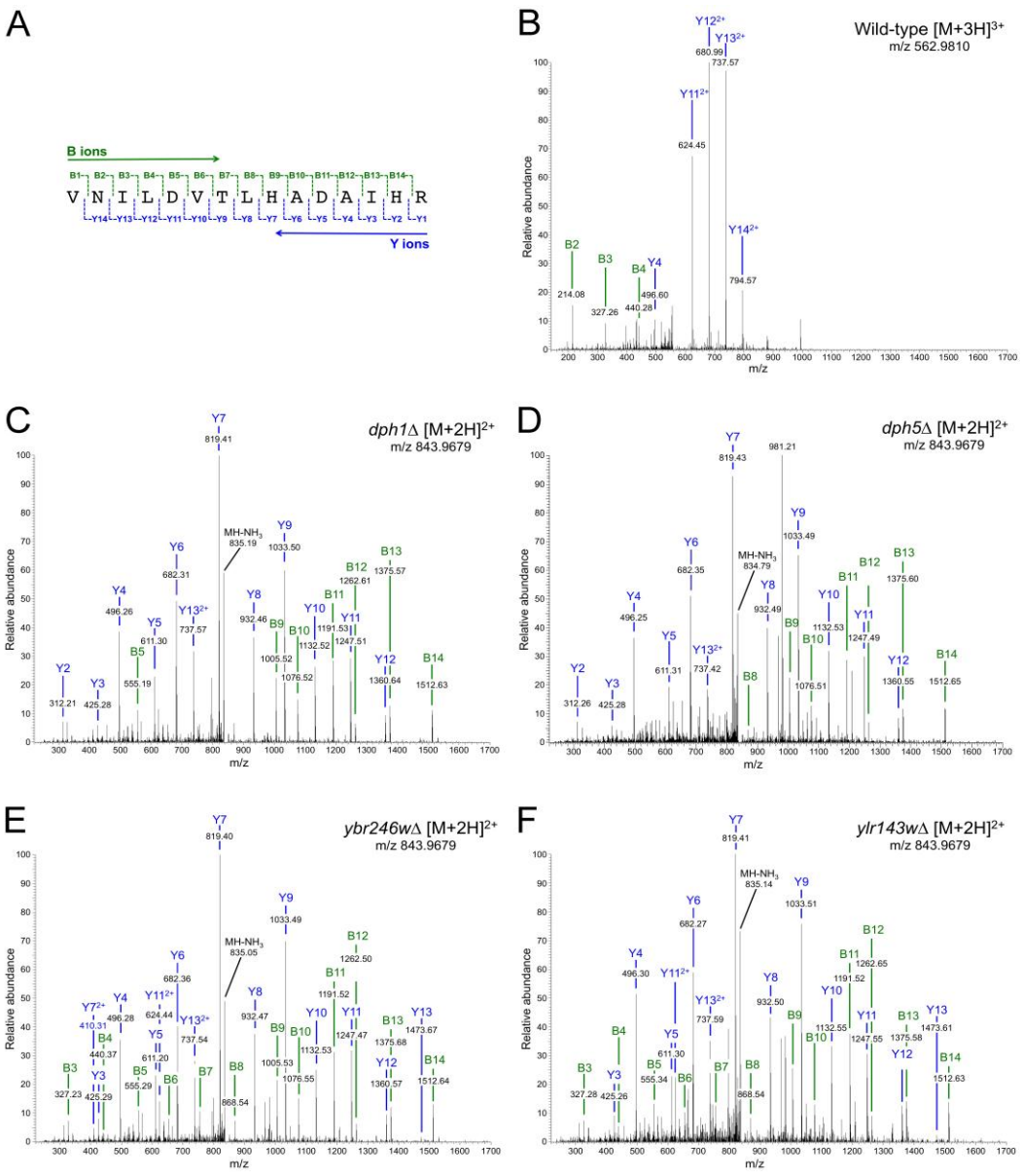

Figure 4.5. MS/MS spectra of unmodified eEF2 peptide 686-VNILDVTLHADAIHR-700 from wild-type and mutant yeast strains. (A) Cartoon showing how the B and Y ions seen in the MS/MS spectra map onto the tryptic peptide containing His-699. Y1 to Y13 and B14 ions contain His-699 and their m/z values are therefore informative regarding the modification state of His-699. (B-F) MS/MS spectra of unmodified peptide in eEF2 obtained from the indicated yeast strains: the parent ion m/z and charge state is indicated in each case. Data generated by Dr. Sara ten Have.

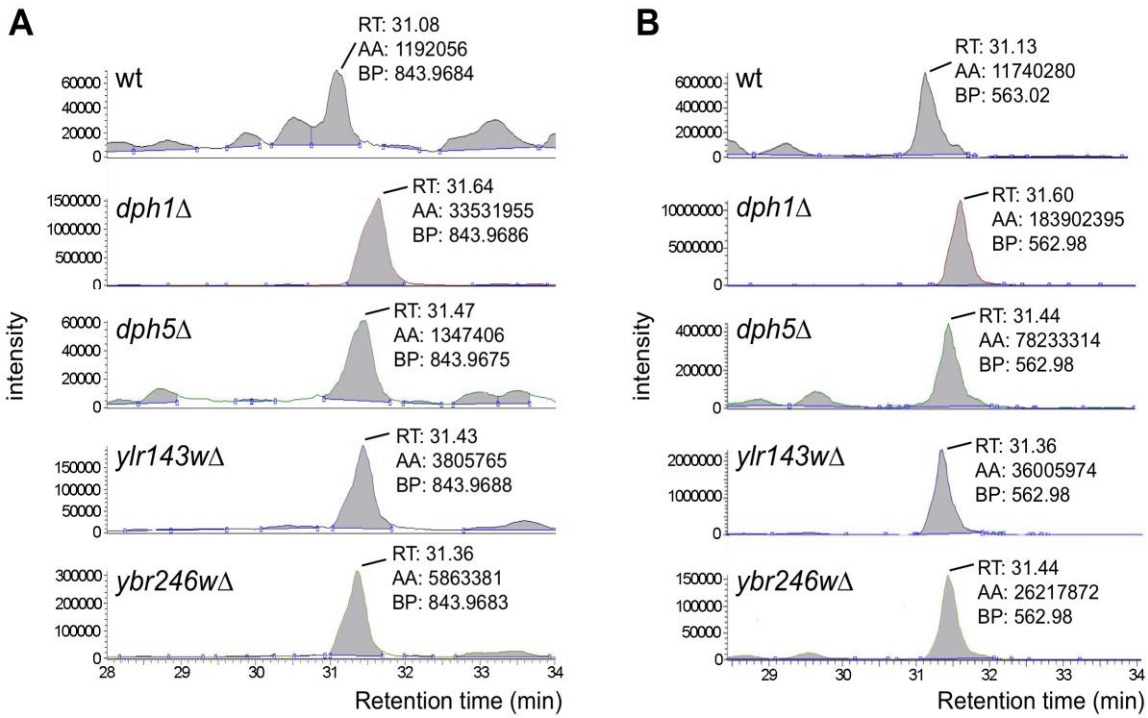

Figure 4.6. Extracted ion chromatograms of unmodified eEF2 peptide 686-VNILDVTLHADAIHR-700. In (A), peaks corresponding to doubly-charged ions (m/z unmodified peptide 843.97, extracted mass range 843.8-844.0) are shown while triply-charged ions (m/z unmodified peptide 562.98, extracted mass range 562.5-563.2) are shown in (B). The yeast strain to which each chromatogram pertains is indicated. Note that in (B) an intensity of 580,000 corresponding to unmodified peptide with m/z 562.98 was not resolved from a different, more abundant ion with m/z 563.02 in the wt sample. Peak annotations are as follows: RT, retention time; AA, peak area; BP, parent ion m/z. Data generated by Dr. Sara ten Have. Data generated by Dr. Sara ten Have.

In addition to the unmodified peptide, we readily detected diphthamide-modified peptide in eEF2 prepared from the wild-type yeast strain (Figure 4.7A), but failed to detect this in any of the mutants. Instead, ACP-modified peptide was found in eEF2 prepared from the *dph5*Δ strain (Figure 4.7B), as expected, given its known role in generating diphthine from the ACP intermediate (Zhu et al. 2010). In contrast, eEF2 from the *ybr246w*Δ mutant generated spectra consistent with the presence of diphthine on His^{699}, in which the m/z values for both the parent ions and the daughter ions in the MS/MS spectra were higher in a manner consistent with the 0.984 Da extra mass associated with diphthine rather than diphthamide modification (Figure 4.7C). Furthermore, the quite different elution times of the diphthine-modified and diphthamide-modified peptide evident from the extracted ion chromatograms (Figure 4.8) is consistent with differently modified forms.

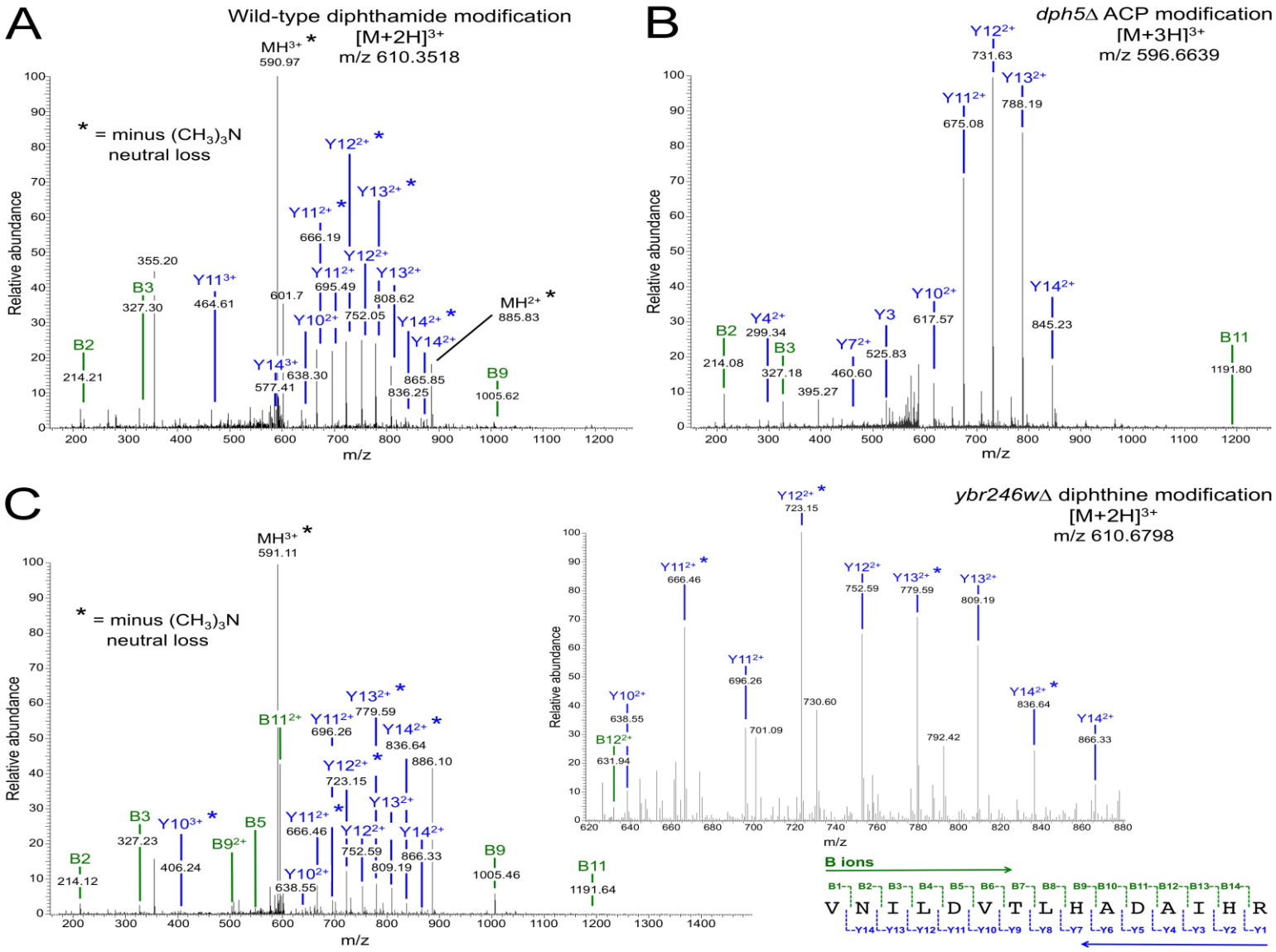
A
Wild-type diphthamide modification
[M+2H]3+
m/z 610.3518
MH3+ *
590.97
* = minus (CH3)3N
neutral loss
Y12 2+ *
Y13 2+ *
Y11 2+ *
666.19
Y12 2+
Y11 2+
695.49
Y13 2+
808.62
355.20
B3
327.30
Y11 3+
464.61
601.7
Y10 2+
752.05
Y14 2+ *
MH2+ *
885.83
Y14 2+
Y14 3+
638.30
577.41
865.85
836.25
B2
214.21
B9
1005.62
Relative abundance
m/z
B
dph5Δ ACP modification
[M+3H]3+
m/z 596.6639
Y12 2+
731.63
Y13 2+
788.19
Y11 2+
675.08
Y10 2+
617.57
Y14 2+
845.23
Y4 2+
299.34
B2
214.08
B3
327.18
Y3
525.83
Y7 2+
460.60
395.27
B11
1191.80
Relative abundance
m/z
C
ybr246wΔ diphthine modification
[M+2H]3+
m/z 610.6798
MH3+ *
591.11
* = minus (CH3)3N
neutral loss
Y13 2+ *
B11 2+
Y11 2+
779.59
696.26
Y14 2+ *
836.64
Y12 2+ *
723.15
886.10
Y13 2+
B3
327.23
Y10 3+ *
B5
Y11 2+ *
666.46
Y12 2+
Y14 2+
752.59
866.33
B9 2+
406.24
809.19
B2
214.12
Y10 2+
638.55
B9
1005.46
B11
1191.64
Relative abundance
m/z
Y12 2+ *
723.15
Y11 2+ *
666.46
Y12 2+
752.59
Y13 2+ *
779.59
Y13 2+
809.19
Y11 2+
696.26
Y14 2+ *
836.64
Y14 2+
866.33
Y10 2+
638.55
730.60
B12 2+
631.94
701.09
792.42
Relative abundance
m/z
B ions
V N I L D V T L H A D A I H R
Y14 Y13 Y12 Y11 Y10 Y9 Y8 Y7 Y6 Y5 Y4 Y3 Y2 Y1

Figure 4.7. MS/MS spectra of diphthamide, ACP and diphthine-modified eEF2 peptide 686-VNILDVTLHADAIHR-700 from wild-type and mutant yeast strains. Spectra are shown for (A) diphthamide-modified peptide from the wild-type yeast strain; (B) ACP-modified peptide from the *dph5*Δ mutant; (C) diphthine-modified peptide in the *ybr246w*Δ strain. In (A) and (C) * indicates neutral loss of trimethylamino during MS/MS. The insets in (C) show greater detail for the more crowded part of the MS/MS spectrum. The cartoon in the bottom right corner indicates how the B and Y ions are derived from the peptide sequence. Data generated by Dr. Sara ten Have.

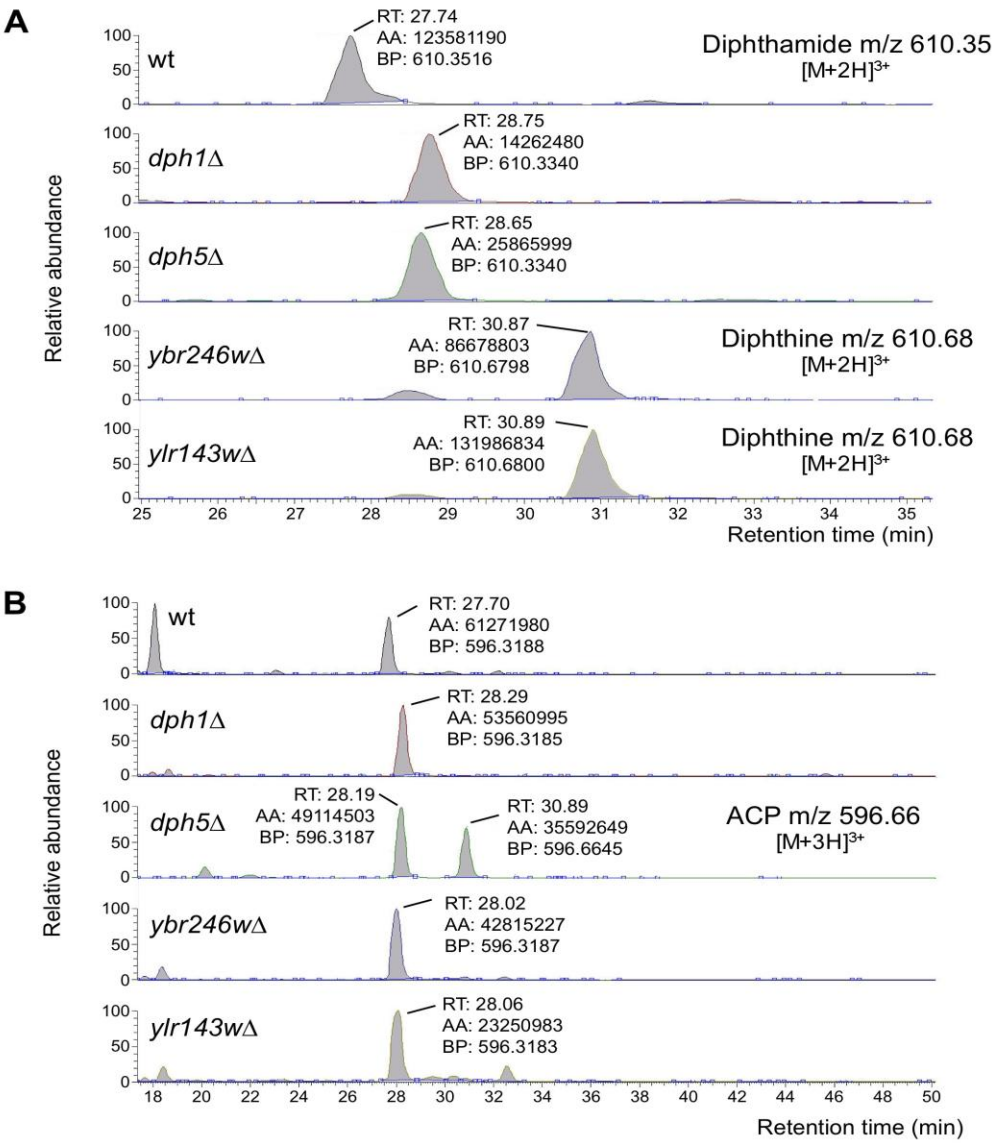

Figure 4.8. Extracted ion chromatograms of modified eEF2 peptide 686-VNILDVTLHADAIHR-700. (A) Peaks corresponding to triply-charged ions (m/z diphthine-modified peptide 610.68, m/z diphthamide-modified peptide 610.35, extracted masses 610.2-610.9). (B) Triply-charged ions (m/z ACP-modified peptide 596.66, extracted masses 596.2-596.8). Peak annotations are as follows: RT, retention time; AA, peak area; BP, parent ion m/z. Data generated by Dr. Sara ten Have. Data generated by Dr. Sara ten Have.

As noted in previous studies (Zhang et al. 2008), some of the ions in our MS/MS spectra had undergone neutral loss of the trimethylammonium group during MS/MS (Figure 4.7), as indicated by loss of 59.1103 mass units. Two types of spectra corresponding to the peptide with modified His^{699} were seen when eEF2 from the *ylr143w*Δ strain was analysed. In some spectra (Figure 4.9A), the parent ion m/z and MS/MS data indicated the presence of diphthine as in the *ybr246w*Δ mutant, with some daughter ions again showing neutral loss of the trimethylammonium group during MS/MS as noted above. However, we also detected peptide in which the elimination of the trimethylammonium group had occurred prior to analysis, as indicated by the lower parent ion m/z (Figure 4.9B) and MS/MS spectrum in which all assignable peaks corresponded to ions lacking the trimethylammonium group. Such trimethylammonium group elimination prior to mass spectrometry was observed previously when *Pyrococcus horikoshii* EF2 modified with diphthine was generated in an *in vitro* reaction (Zhu et al. 2010), indicating that the modification at least in *P. horikoshii* might be unstable. In contrast to the *ylr143w* deletion strain, we failed to detect any pre-mass spectrometry loss of the trimethylammonium group when eEF2 from the *ybr246w*Δ mutant was analysed, suggesting that the two samples, though both modified with diphthine, are somehow different. Figure 4.8 shows extracted ion chromatograms for ions with m/z values corresponding to the His^{699}-containing peptide modified with diphthamide or diphthine (Figure 4.8A) or with ACP (Figure 4.8B), indicating that the ACP modified peptide was only present in the *dph5*Δ mutant, the diphthine modified peptide was only present in the *ybr246w*Δ and *ylr143w*Δ mutants and the diphthamide-modified peptide was only seen in the wild-type strain. While we have not accurately

quantitated the relative levels of each modified peptide, the extracted ion chromatograms suggest that the levels of diphthine-modified peptide in the two mutant samples are broadly similar to the level of diphthamide-modified peptide in the wild-type sample (Figure 4.8). Hence we here present clear evidence that deletion of *YLR143w* as well as *YBR246w* result in the accumulation of diphthine-modified eEF2 and are therefore involved in the final amidation step of diphthamide synthesis. Based on the above evidence we propose to name the novel ORFs *DPH6* and *DPH7*, respectively.

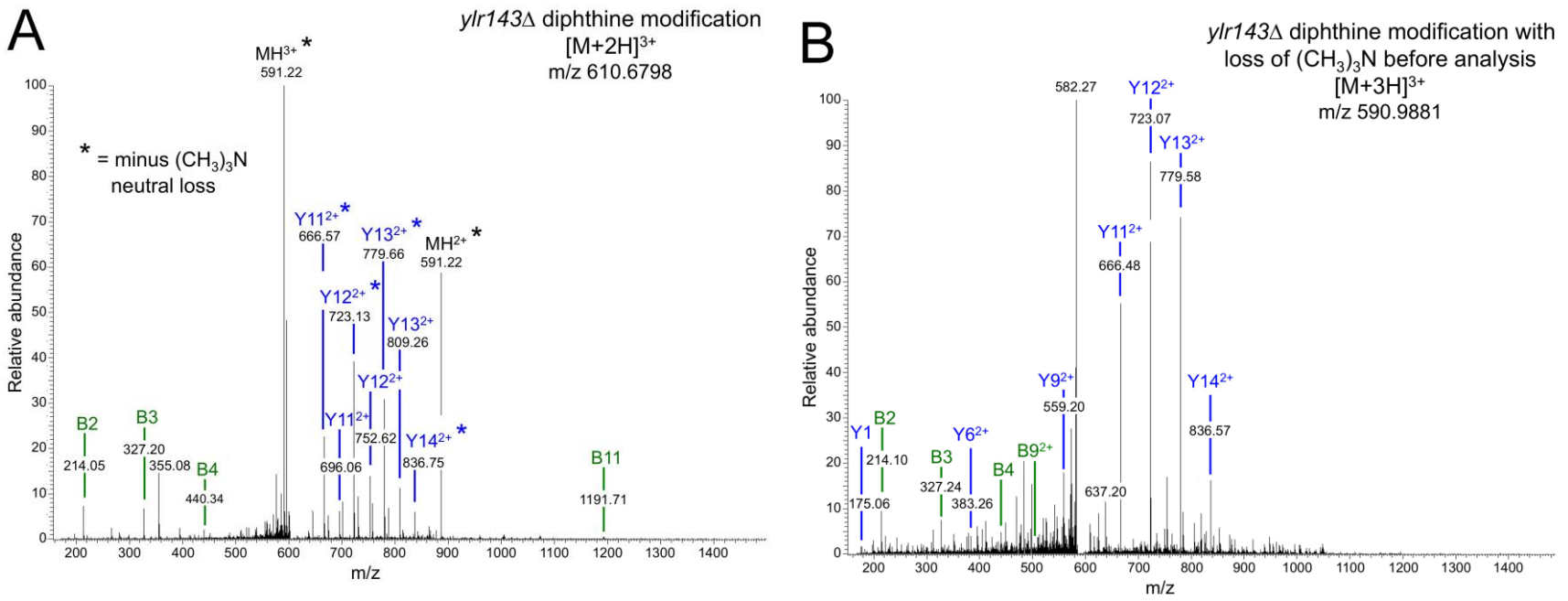

Figure 4.9. MS/MS spectra of diphthine-modified eEF2 peptide 686-VNILDVTLHADAIHR-700 from *ylr143w* mutant yeast strains. Spectra are shown for (A) diphthine-modified peptide in the *ylr143w*Δ strain and (B) diphthine-modified peptide in the *ylr143w*Δ strain with loss of the trimethylamino group before analysis in the mass spectrometer indicated by the parent ion m/z. In each case the parent ion m/z and charge state is indicated. In (A) * indicates neutral loss of trimethylamino during MS/MS. Data generated by Dr. Sara ten Have.

4.2.5 The *YLR143w/DPH6* gene product

Analysis of the Ylr143w/Dph6 protein sequence revealed three conserved domains that point towards its function as an enzyme (Figure 4.10). Firstly, the amino-terminal 225 residues contain an Alpha_ANH_like_IV domain (cd1994 in the NCBI Conserved Domain Database (Marchler-Bauer et al. 2011)). This domain, which is a member of the adenine nucleotide alpha hydrolase superfamily, is found in a range of proteins including N-type ATP pyrophosphatases and ATP sulfurylases and is predicted to bind ATP. Two domains (eu_AANH_C1: cd06155 and eu_AANH_C2: cd06166) that are related to the YjgF-YER057c-UK114 family of proteins present in bacteria, archaea, and eukaryotes are located in the C-terminal portion of Ylr143w/Dph6. These domains show sequence and/or structural similarity to several proteins including chorismate mutase and promote homotrimerisation, which forms an inter-subunit cleft that has been proposed to bind small molecule ligands (Sinha et al. 1999; Volz 1999; Burman et al. 2007). Key residues shown to be important for homotrimerisation and ligand binding in human UK114 such as phe-89, asn-93, pro-105 and arg-107 (Mistiniene et al. 2005) appear to be conserved in Ylr143w, and the conserved arg-107 has been shown to form a bidentate salt bridge with the carboxylic acid group of ligands bound to TdcF, an *Escherichia coli* YjgF-YER057c-UK114 family member with a likely role in 2-ketobutyrate metabolism (Burman et al. 2007). Although many proteins containing these domains are annotated as ribonucleases because of a ribonuclease activity that has been associated with mammalian UK114, these domains are also found in a range of proteins involved in nucleotide and amino acid metabolism (Sinha et al.

1999; Volz 1999; Burman et al. 2007; Lambrecht et al. 2012). It is therefore likely that Dph6 is directly involved in diphthine amidation and that this step is an ATP-dependent process, with perhaps ammonia or glutamine acting as the source of the amide group. The recent finding that *Salmonella enterica* YjgF has an enamine/imine deaminase activity that is conserved even in human UK114 (Lambrecht et al. 2012) suggests that Ylr143w/Dph6 may use one of its YjgF-YER057c-UK114 related domains to generate ammonia for diphthamide formation. It will be interesting to determine why Dph6 contains two such domains. However, definitive proof that Dph6 directly catalyses diphthamide formation will require demonstration of the biochemical activity in an *in vitro* assay system.


A
1
Adenine nucleotide alpha hydrolase
YjgF-YER057c-UK114
YjgF-YER057c-UK114
685

B

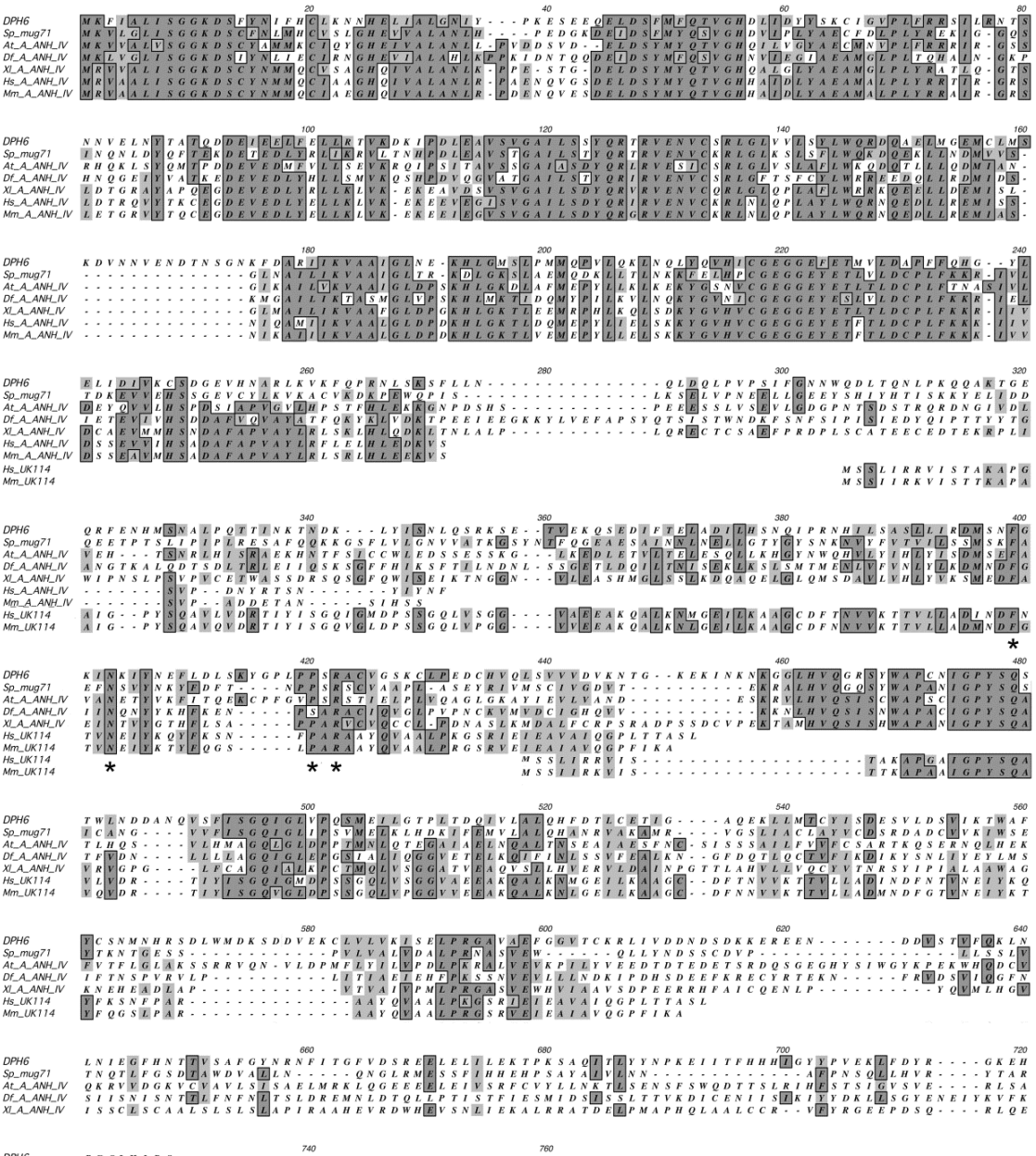
DPH6
Sp_mug71
At_A_ANH_IV
Df_A_ANH_IV
Xl_A_ANH_IV
Hs_A_ANH_IV
Mm_A_ANH_IV
Hs_UK114
Mm_UK114

Figure 4.10. Conservation of the *YLR143w/DPH6* gene product.

(A) Representation of Ylr143w/Dph6 indicating the conserved adenine nucleotide alpha hydrolase (cd1994) and YjgF-YER057c-UK114 related (cd06155, cd06166) domains discussed in the main text. (B) The Ylr143w/Dph6 amino acid sequence was aligned using Clustal with representative examples of putative homologues from other organisms. Sequences are as follows : *YLR143w*, *S. cerevisiae* Ylr143w; Sp_mug71, *Schizosaccharomyces pombe*; At_A_AAH_IV, *Arabidopsis thaliana* endoribonuclease; Df_A_AAH_IV, *Dictyostelium fasciculatum* endoribonuclease L-PSP domain-containing protein; Xl_A_AAH_IV, *Xenopus laevis* ATP binding domain 4; Hs_A_AAH_IV, Human ATP binding domain containing protein 4; Mm_A_AAH_IV, mouse ATP binding domain containing protein; Hs_UK114, human ribonuclease UK114/p14.5/L-PSP; Mm_UK114, mouse UK114/p14.5/L-PSP. Note that the last two sequences appear twice in the alignment so that the sequence relationships to each of the YjgF- YER057c-UK114 related domains in the non-mammalian proteins can be shown. *, conserved residues shown to be important for trimerisation and ligand binding.

4.2.6 The *YBR246w/DPH7* gene product

Unlike Dph6, which has not been analysed to this date, two seemingly disparate functions have already been proposed for *DPH7/YBR264w*, neither of which are obviously related to diphthamide biosynthesis. Firstly, *YBR246w* has been implicated as a negative regulator of RNA polymerase I and named *RRT2* (Hontz et al. 2009). Consistently, the Ybr246w protein interacts with a second protein (Rrt4) identified in the same genetic screen (Hontz et al. 2009). While effects on RNA polymerase I activity might result from changes in eEF2 function associated with its incomplete modification on his-699, no other components of the diphthamide biosynthetic pathway were identified in the same screen (Hontz et al. 2009). Secondly, the *YBR246w/DPH7* product has been proposed to function in retromer-mediated recycling of proteins from the yeast endosome back to the plasma membrane and hence named *ERE1* (**e**ndosomal **re**cycling) to reflect this role (Shi et al. 2011). A variety of evidence supports this role including impaired recycling of the arginine permease (Can1) and the Mup1 methionine transporter in ESCRT-mutant cells when *YBR246w* was deleted, association of a pool of Ybr246w protein with membranes that increased in ESCRT-mutant cells, and presence of Ybr246w in a complex with internalized Can1 in ESCRT-mutant cells (Shi et al. 2011). The possible connection between retromer-mediated recycling and diphthamide biosynthesis is not immediately clear.

Ybr246w has four clearly-defined WD40 repeats and a secondary structure predicted to consist of exclusively beta-sheet elements. A possible human homologue (WDR85) was previously implicated in diphthamide biosynthesis (Carette et al. 2009)

and has been proposed to function in the first step of the pathway. Figure 4.11 shows an alignment of Ybr246w with human WDR85 and other potential homologues from a range of different eukaryotes. While the predicted protein structure is highly suggestive of a role as an adaptor protein rather than a catalyst of a biochemical transformation, it remains to be demonstrated whether Ybr246w and its homologues function in multiple, disparate processes (as suggested by the yeast studies), or if these functions are somehow linked through effects on eEF2 modification and function.

A


1
WD40
WD40
WD40
WD40
387

B

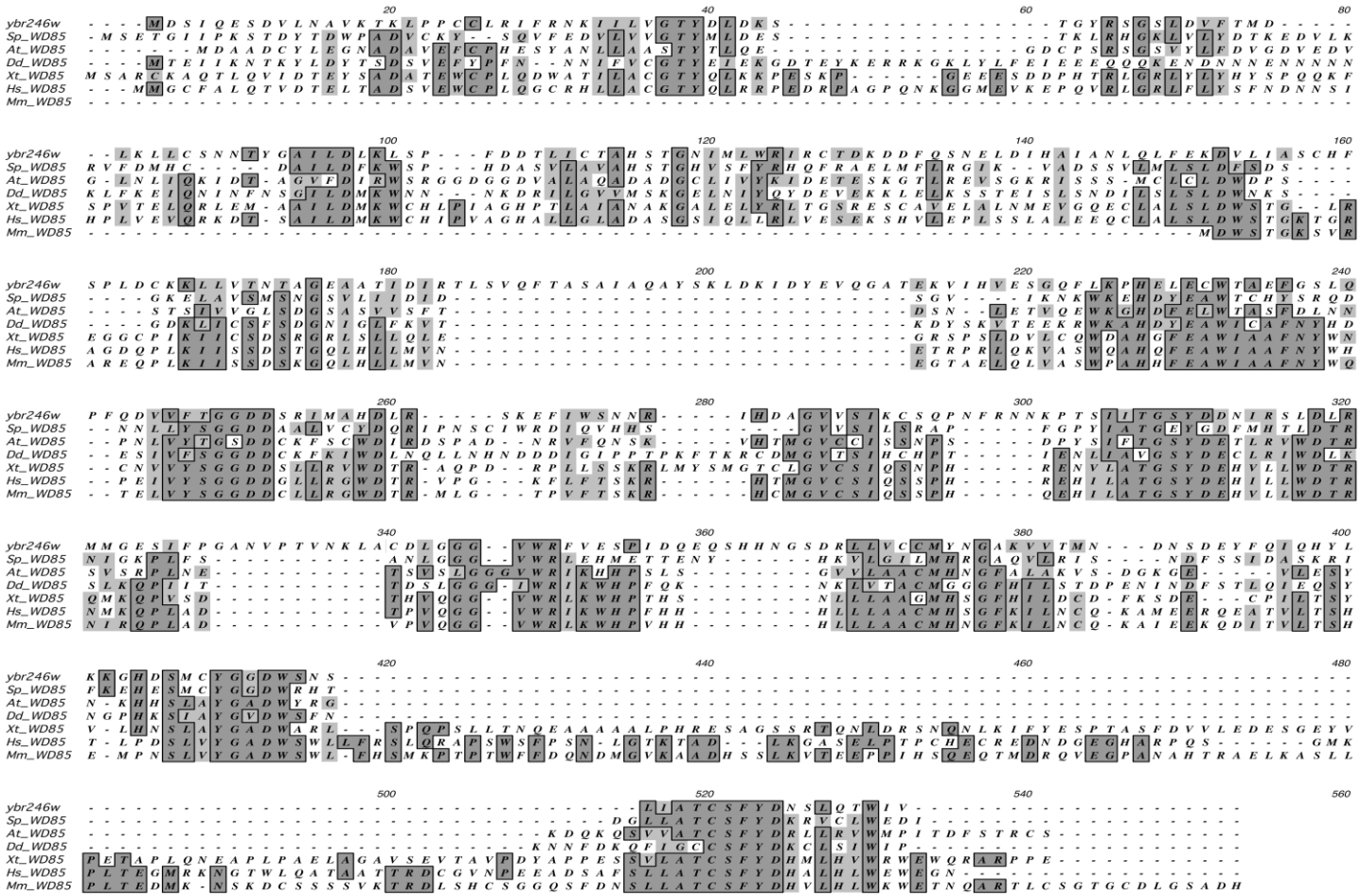
ybr246w
Sp_WD85
At_WD85
Dd_WD85
Xt_WD85
Hs_WD85
Mm_WD85

Figure 4.11. Conservation of the YBR246w/DPH7 gene product.

(A) Representation of Ybr246w/Dph7 showing the location of the conserved WD40 domains. (B) The Ybr246w/Dph7 amino acid sequence was aligned using Clustal with representative examples of putative homologues from other organisms. Sequences are as follows: *YBR246w, S. cerevisiae* Ybr246w Sp_WD85, *Schizosaccharomyces pombe* WD repeat protein; At_WD85, *Arabidopsis thaliana* WD40 domain-containing protein; Dd_WD85, *Dictyostelium discoideum* WD40 repeat-containing protein; Xt_WD85, *Xenopus tropicalis* WD repeat-containing protein 85-like; Hs_WD85, Human WD repeat-containing protein 85; Mm_WD85, mouse unnamed protein.

4.2.7 Ylr143w and Ybr246w do not directly interact with each other or other Dph proteins

Given that the mass spectrometry results clearly identified that *YLR143w/DPH6* and *YBR246w/DPH7* are necessary for the amidation of diphthine, we decided to investigate whether either gene interacts with other diphthamide synthesis genes. To do so, co-immunoprecipitation of tagged constructs were performed with C-terminal TAP-tagged *YLR143w/DPH6* and *YBR246w/DPH7*. Both constructs were readily detected in immunoblot assays where Ylr143w-TAP is accompanied by a smaller degradation product. *DPH1*, *DPH2* and *DPH5* were C-terminally HA-tagged, however neither construct co-purified with Ylr143w-TAP (Figure 4.12A). Furthermore, Co-IP of Dph2-HA and Dph5-HA with Ybr246w-TAP showed that they also do not interact directly. As a control for anti-HA immunoblot detection after the co-IP a positive-HA sample was loaded and readily detected at the right size. We therefore conclude that neither *YLR143w/DPH6* nor *YBR246w/DPH7* directly interact with *bona fide* diphthamide synthesis genes *DPH1*, *DPH2* and *DPH5*.

In order to confirm these findings, we repeated the co-IP with c-terminal Myc-tagged *YLR143w/DPH6* and *YBR246w/DPH7*, which is a smaller tag compared to the 21kDa TAP tag. In collaboration with Dr. Christian Baer, University of Kassel, we readily detected Ylr143w-c-Myc and Ybr246w-c-Myc in immuno blots, both of which are accompanied by smaller degradation products (Figure 4.12B). In line with the above findings, Dph5-HA construct did not co-purify with either of the two ORFs. Furthermore, co-IP of Ylr143w-HA with Ybr246w-c-Myc showed that they also do not directly interact with each other. As a positive control, co-IP of Elp2-c-Myc with Kti12-

HA was performed in parallel. Taken together, Co-IP analysis revealed that *YLR143w/DPH6* and *YBR246w/DPH7* do not directly interact with each other nor with diphthamide synthesis genes *DPH1*, *DPH2* and *DPH5*.

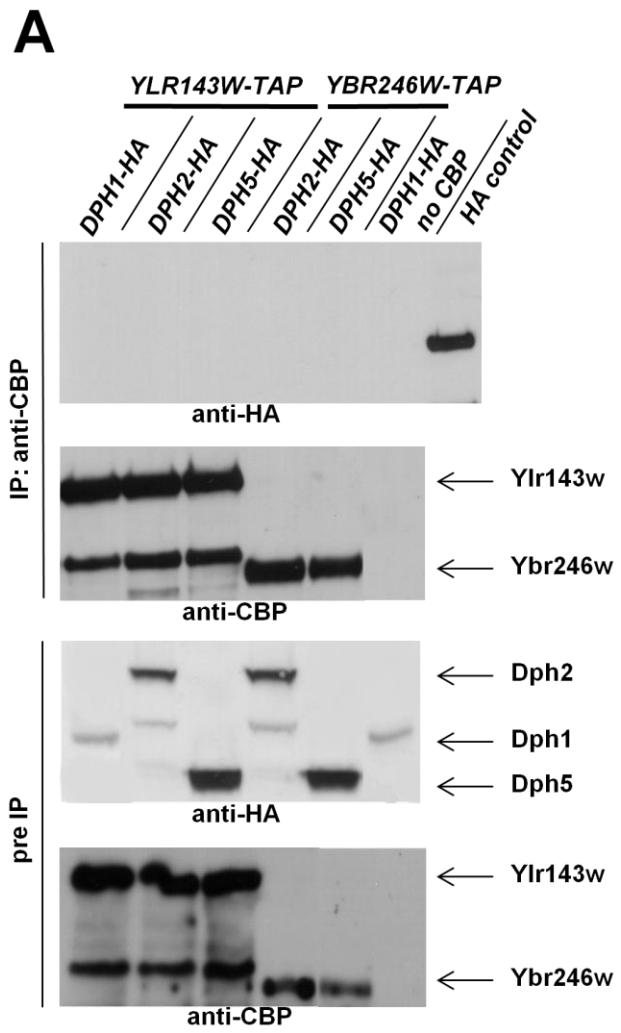
A
YLR143W-TAP
YBR246W-TAP
DPH1-HA
DPH2-HA
DPH5-HA
DPH2-HA
DPH5-HA
DPH1-HA
no CBP
HA control
IP: anti-CBP
anti-HA
Ylr143w
Ybr246w
anti-CBP
pre IP
Dph2
Dph1
Dph5
anti-HA
Ylr143w
Ybr246w
anti-CBP

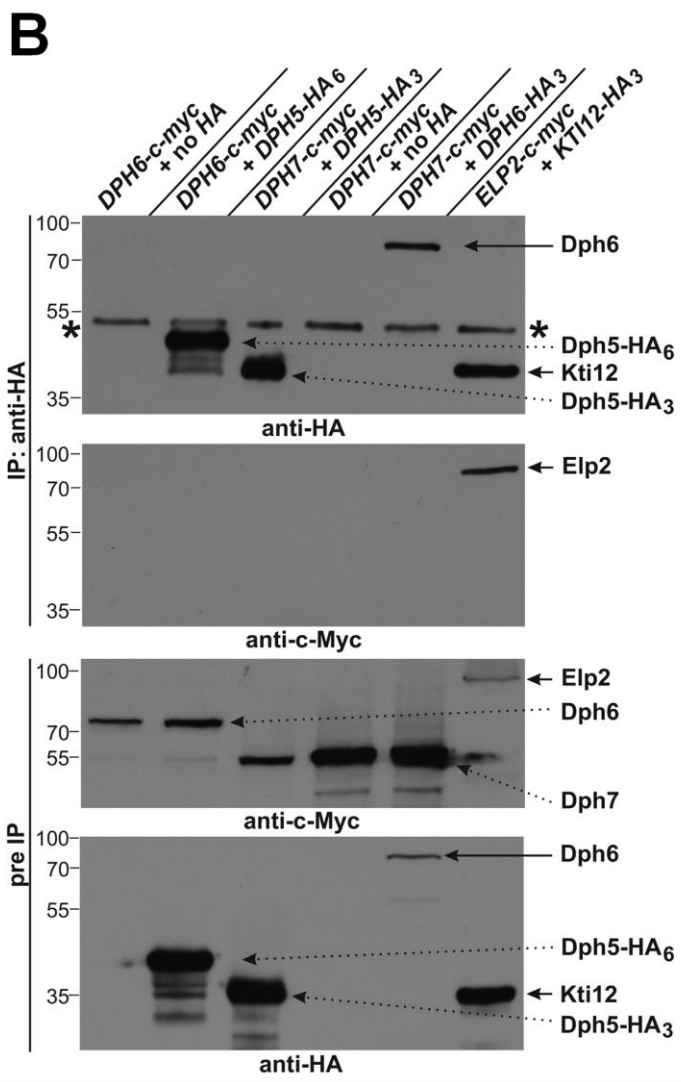
B
DPH6-c-myc + no HA
DPH6-c-myc + DPH5-HA6
DPH7-c-myc + DPH5-HA3
DPH7-c-myc + no HA
DPH7-c-myc + DPH6-HA3
ELP2-c-myc + KTI12-HA3
IP: anti-HA
100
70
55
35
Dph6
Dph5-HA6
Kti12
Dph5-HA3
anti-HA
Elp2
anti-c-Myc
pre IP
Dph7
anti-c-Myc
anti-HA

Figure 4.12. Ylr143w and Ybr246w do not interact with each other and *bona fide* diphthamide synthesis proteins Dph1, Dph2 and Dph5. (A) Failure to detect interaction by co-immune precipitation between Dph6 or Dph7 and either Dph1, Dph2 or diphthine synthase Dph5, factors integral to the first two steps of diphthamide synthesis. Co-immunoprecipitations were performed using magnetic beads (Dynabeads, Invitrogen) coupled to anti-CBP antibodies (Santa Cruz Biotechnology) specific for the calmodulin binding peptide (CBP) of the TAP-tag. The indicated strains expressed *DPH6-TAP* or *DPH7-TAP* in conjunction with HA-tagged versions of *DPH1*, *DPH2* or *DPH5*. The presence of the respective proteins within the immune precipitates (IP) was assessed using anti-HA and anti-CBP Western blots or anti-HA immune blots on total protein extracts obtained prior to the IP protocol (preIP). (B) Failure to detect Dph6-Dph7 interaction by co-immunoprecipitation. Co-immunoprecipitations using the anti-HA-antibody were performed with the indicated strains expressing *DPH6-c- myc* or *DPH7-c-myc* on their own or in parallel with HA-tagged versions of *DPH5* or *DPH6*, respectively. A strain co-producing c-Myc- and HA- and tagged versions of the Elp2 subunit (*ELP2-c-myc*) of the Elongator complex, and Kti12 (*KTI12-HA*), a protein known to interact with Elongator, was used as internal positive control. The presence of the respective proteins was assessed in individual anti-c-Myc and anti-HA immunoblots both in the IPs (top two panels) and crude extracts (pre IP; bottom two panels). The asterisk denotes an unspecific band that originates from the anti-HA-antibody present in the IPs. Figure B generated by Dr. Christian Baer.

4.2.8 Ylr143w/Dph6 interacts with eEF2 independent of Ybr246w/Dph7

As the sequence analysis (section 1.2.5) implicates a direct role for *YLR143w/DPH6* in the conversion of diphthine into diphthamide, we were intrigued to investigate whether it binds to eEF2 during the process. Furthermore, we wished to determine if deletion of *YBR246w/DPH7* would affect the putative interaction between eEF2 and Ylr143w/Dph6, given that the protein structure predicts a role in mediating protein-protein interactions (section 1.2.6). Co-immunoprecipitation (co-IP) was performed with His6-tagged eEF2 from plasmid pTKB612 together with C-terminal tagged Dph6-HA (Figure 4.13). Interestingly a faint eEF2-his6 band was detected after co-IP with anti-HA coupled Dynabeads® (Invitrogen). Though the interaction of *DPH6* with *EFT2* is not very strong, it nevertheless is clearly detectable after co-IP analysis, which indicates that Dph6 binds to a fraction of the isolated eEF2. Furthermore, the direct interaction is not altered by the deletion of *DPH7*. Taken together, this data suggests that Dph6 directly interacts with eEF2 in a Dph7-independent manner, indicating that it does not mediate the interaction. Furthermore, we also exclude a role for *DPH7* in regulating *DPH6* gene expression seeing that as Dph6 protein levels are unaltered in the *DPH7* deletion strain.

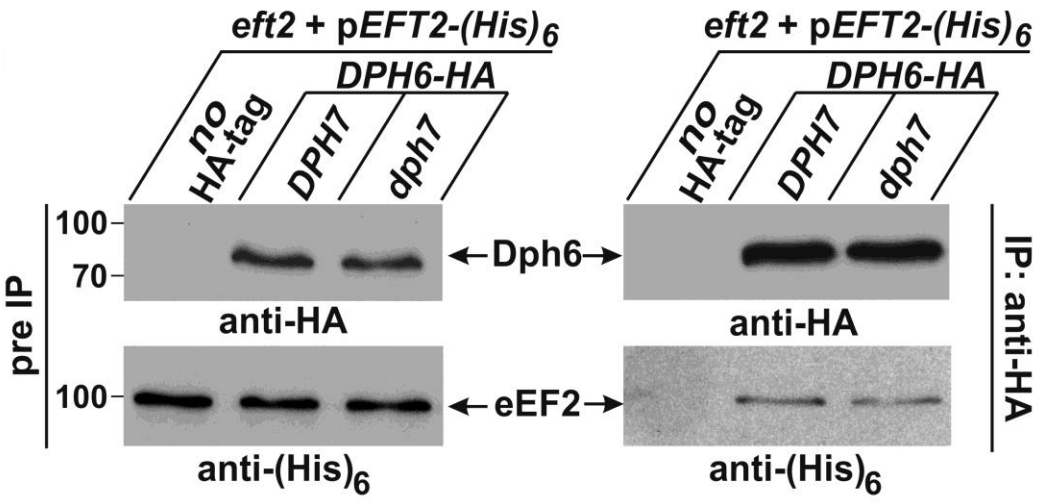

Figure 4.13. eEF2 interacts with Dph6 in a fashion that is independent of Dph7.

Yeast strains co-expressing $(His)_6$-tagged eEF2 with Dph6-HA in the background of wild-type (*DPH7*) *dph7* mutant strains were subjected to immune precipitations (IP) using the anti-HA antibody. Strains expressing $(His)_6$-tagged eEF2 on their own served as IP controls (no HA-tag). Subsequently, the precipitates were probed with anti-HA (top right panel) and anti-$(His)_6$ antibodies (bottom right panel) to check for the content of Dph6-HA. The content of HA-tagged Dph6 as well as (His)6-marked eEF2 in the protein extracts prior to IP (pre-IP) was examined on individual immuno blots using anti-HA (top left panel) and anti-$(His)_6$ antibodies (bottom left panel), respectively. Absence of Dph7 does not affect the Dph6•eEF2 interaction.

4.2.9 Deletion of *DPH7* enhances interaction between Dph5 and eEF2

Interestingly, Carette et al. (2009) reported that lack of WDR85, the putative mammalian homolog of *YBR246w/DPH7*, increases binding of Dph5 to eEF2. We confirmed this finding by co-immunoprecipitation of HA-tagged Dph5 and His6-tagged eEF2 expressed from plasmid pTKB612. Figure 4.14 highlights that deletion of *DPH7* results in a significant increase of interaction between Dph5 and EF2. Therefore we demonstrate that rather than mediating the interaction between Dph6 and eEF2, Dph7 regulates binding of the diphthine synthase, Dph5, to the translation elongation factor. Moreover, the same increase in binding of Dph5 to eEF2 could be observed by deleting *DPH1*, which lacks the ACP-intermediate that serves as a substrate for Dph5 mediated methylation. Furthermore, the lack of *DPH6* also seems to slightly increase Dph5-eEF2 binding. Therefore we conclude that eEF2 carrying an unmodified His^{699} residue (*DPH1* mutant) or the diphthine intermediate (*DPH7* mutant) displays a significantly increased affinity to Dph5.

Seeing that the interaction between the methyltransferase, Dph5, and the translation elongation factor, eEF2, seems to be altered in diphthamide synthesis mutants, we decided to examine the effect of Dph5 overexpression on *dph1-dph5* as well as *dph6* and *dph7* deletion strains. Figure 4.15 depicts the overexpression of Dph5, which is expressed under the control of the inducible *GAL1* promoter (plasmid pGAL-DPH5). While increased Dph5 levels do not show any effect on the wild-type strain and the *dph6* mutant, it proved to be detrimental to strains lacking any diphthamide modification (*dph1-dph4*) as well as the *dph7* mutant. This cytotoxic effect of Dph5 overexpression is in line with the above mentioned Dph5-eEF2 interaction profiles.

However, it must be noted that we did not investigate whether the effect of Dph5 overexpression on d*ph1-dph7* deletion strains was cytocidal or cytostatic.

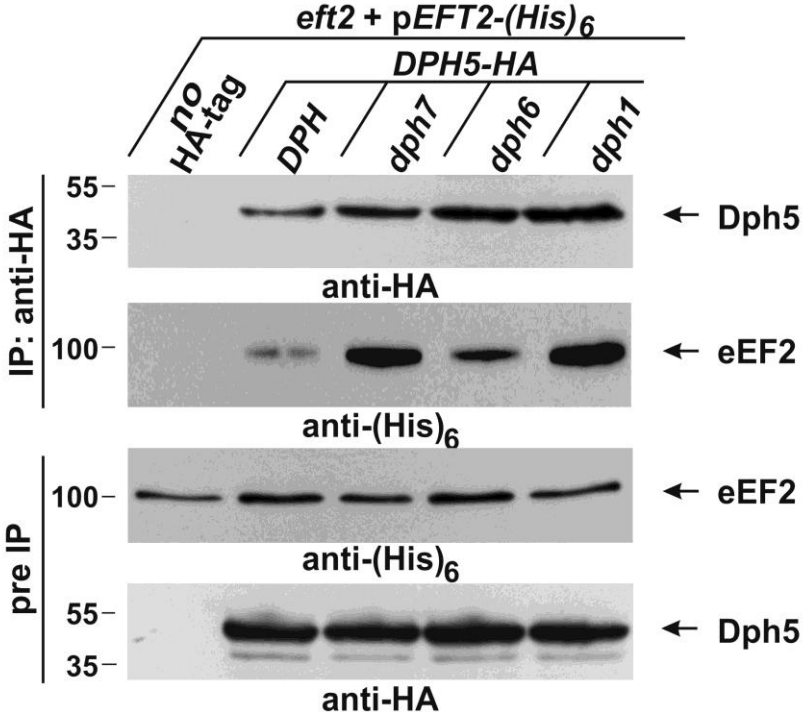

Figure 4.14. eEF2 interaction with Dph5 is dramatically enhanced by elimination of Dph7 or Dph1. Yeast strains co-expressing $(His)_6$-tagged eEF2 with Dph5-HA in the background of wild-type (*DPH*) and *dph* mutant strains (*dph7*, *dph6* and *dph1*) were subjected to immune precipitations (IP) using the anti-HA antibody. Strains expressing $(His)_6$-tagged eEF2 on their own served as IP controls (no HA-tag). Subsequently, the precipitates were probed with anti-HA and anti-$(His)_6$ antibodies as indicated to check for the content of Dph5-HA and eEF2-$(His)_6$, respectively (all indicated by arrows). The content of HA-tagged Dph5 as well as $(His)_6$-marked eEF2 in the protein extracts prior to IP (pre-IP) was examined on individual immuno blots. Note that Dph5•eEF2 interaction is strongly enhanced by inactivating *DPH7* or *DPH1*. Data generated by Dr. Christian Baer.

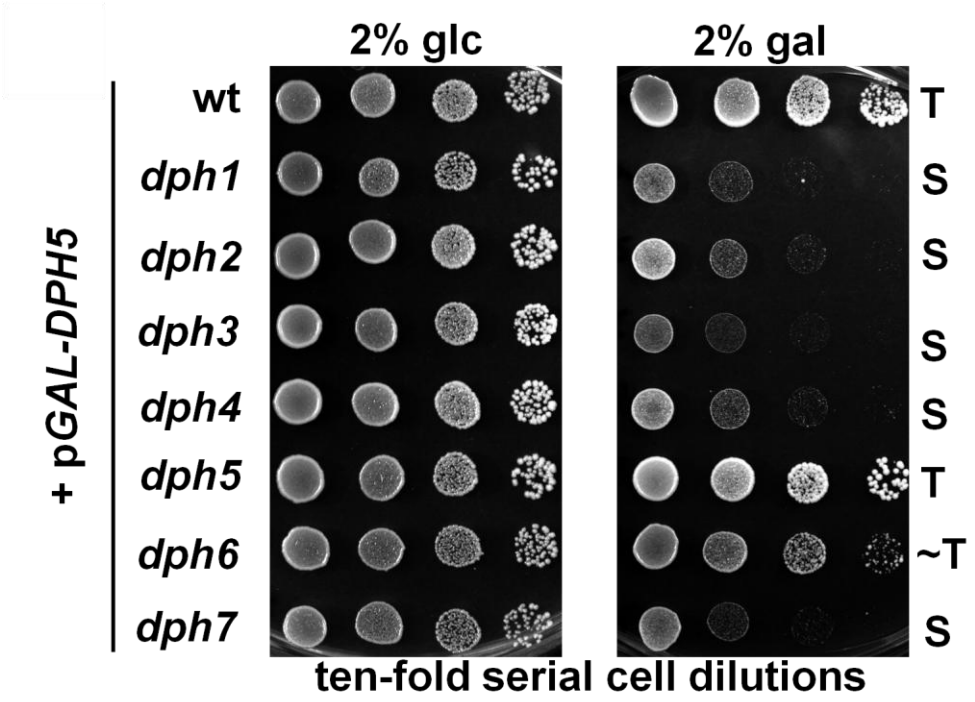

Figure 4.15. ***DPH5*** **overexpression in** ***dph1-dph4*** **and** ***dph7*** **mutants causes cytotoxicity and a severe cell growth defect.** Cells of yeast strains with the indicated genetic backgrounds and maintaining plasmid p*GAL-DPH5* for galactose inducible overexpression of diphthine synthase Dph5 were serially diluted and replica spotted onto glucose (2% glc) and galactose (2% gal) media to assay their response to *DPH5* overexpression. Growth was for 3 days at 30°C. Unaltered (T), slightly weakened tolerance (~T) and sensitive (S) responses are indicated. Note that *dph1-dph4* and *dph7* mutants are extremely sensitive to *DPH5* overexpression.

4.2.10 Excess Dph6 cannot by-pass the trimethylation step

Even though the diphthamide synthesis pathway has been dissected into three distinct steps, it has not been shown to happen in sequence. Therefore is the trimethylation by Dph5 a necessary step for the final amidation of diphthine? To answer this question we performed a simple test, where we overexpressed *DPH6* in a *DPH5* deletion strain. Overexpression of *DPH6* was achieved by cloning the gene into a multi copy plasmid carrying the strong *GAL1* promoter. The resulting pSU7 plasmid readily complements the *dph6* mutant and increases Dph6 levels in the *dph5* mutant in addition to endogenous levels of the protein. Lack of the methyltransferase abolishes the trimethylation of the carboxylgroup in the ACP-intermediate. We next asked whether lack of methylation could be overcome by overexpression of the putative diphthine amidase. To do so, the strains were exposed to sordarin as an indicator drug for diphthamidation of eEF2. Figure 4.16 highlights that increasing levels of Dph6 in a *DPH5* mutant strain does not alter its sordarin phenotype and the strain remains resistance to the cytotoxic agent. Therefore we conclude that the putative diphthine amidase, *DPH6*, cannot by-pass the trimethylation step in order to form diphthamide.

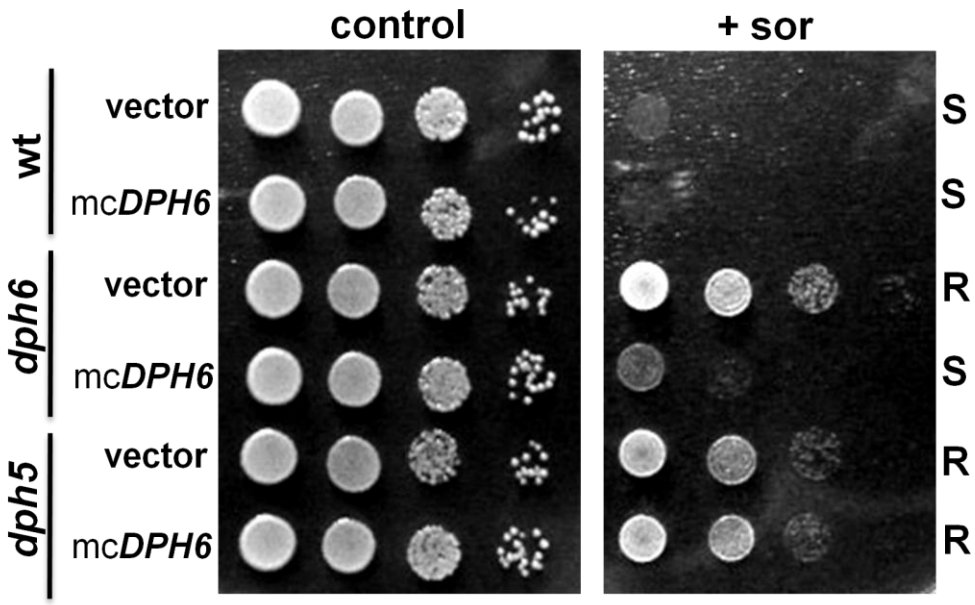

Figure 4.16. *DPH6* overexpression does not rescue the sordarin phenotype of a *DPH5* mutant. Ten-fold serial cell dilutions of the indicated yeast strains, wild-type (wt) background and its *dph5* and *dph6* gene deletion derivatives were transformed with either a multi copy *DPH6* vector (mc*DPH6*, pSU7) or an empty control vector (vector) and grown on YPD plates in the absence (control) or presence (+ sor) of 10 μg ml^{-1} sordarin. Growth was assayed for 2 d at 30°C. Sordarin resistant (R) and sensitive (S) responses are indicated.

4.2.11 Physiological role of diphthamide

Though the exact role for diphthamide on eEF2 has not been defined yet, it has been reported that amino acid substitution of His^{699} confer a thermosensitive growth phenotype (Kimata and Kohno 1994; Ortiz and Kinzy 2005). We observed the growth of *DPH* mutants, *dph1-dph7*, in liquid as well as on solid media but failed to detect growth defects at normal temperatures (30°C) or at an increased cultivation temperature of 39°C (Figure 4.17). The only exception was the *DPH3* mutant, which is involved in multiple cellular pathways and displays a severe growth phenotype at 39°C.

Furthermore, diphthamide deficiency has been shown to affect translational fidelity. Data from our own group (Bar et al. 2008) as well as from Ortiz et al. (2006) demonstrates that deletion of *DPH2*, *DPH1* as well as *DPH5*, which arrests the pathway at the first step and after formation of the ACP intermediate, respectively, results in an increase in -1 frameshifting during translation. Therefore we investigated the lack of *DPH6* and *DPH7* on translation fidelity by using the same approach as described by Ortiz et al. (2006). Here we take advantage of programmed ribosomal frameshifting seen during viral translation (Dinman 1995; Farabaugh 1996). In the interest of increasing the efficiency of genome packaging, RNA viruses contain overlapping ORFs, which require the ribosome to switch the reading frame in order to translate the shifted genes. To examine the level of frameshifting we transformed reporter plasmids carrying the *lacZ* gene in the 0 frame (pJD204.0), +1 frame (pJD204.+1) and -1 frame (pJD204.-1) (Harger et al. 2001; Ortiz et al. 2006a). The level of -1 and +1 frameshifting is measured relative to read-outs from the 0 frame plasmid. Both candidate genes, *DPH6* and *DPH7*, as well as *DPH1-DPH5* knock out strains were

transformed with the translation reporter plasmids and three different colonies of each strain were assayed for beta-galactosidase activity of the reporter gene (for details see Methods). The readouts from the +1 frameshift reporter plasmid vary within a wide range and therefore are not significantly different from the isogenic wild-type strain (Figure 4.18). -1 frameshifting however was significantly increased in *dph6* and all *dph* mutants, with the exception of *dph4* (Figure 4.19). Though together with *dph7 dph4* displays an elevated level of -1 frameshifting, it is not significantly different from the wild-type strain. The *DPH6* deletion results in the most significant increase of translational fidelity and indicates a central role in the maintenance of eEF2 function during translation regulation.

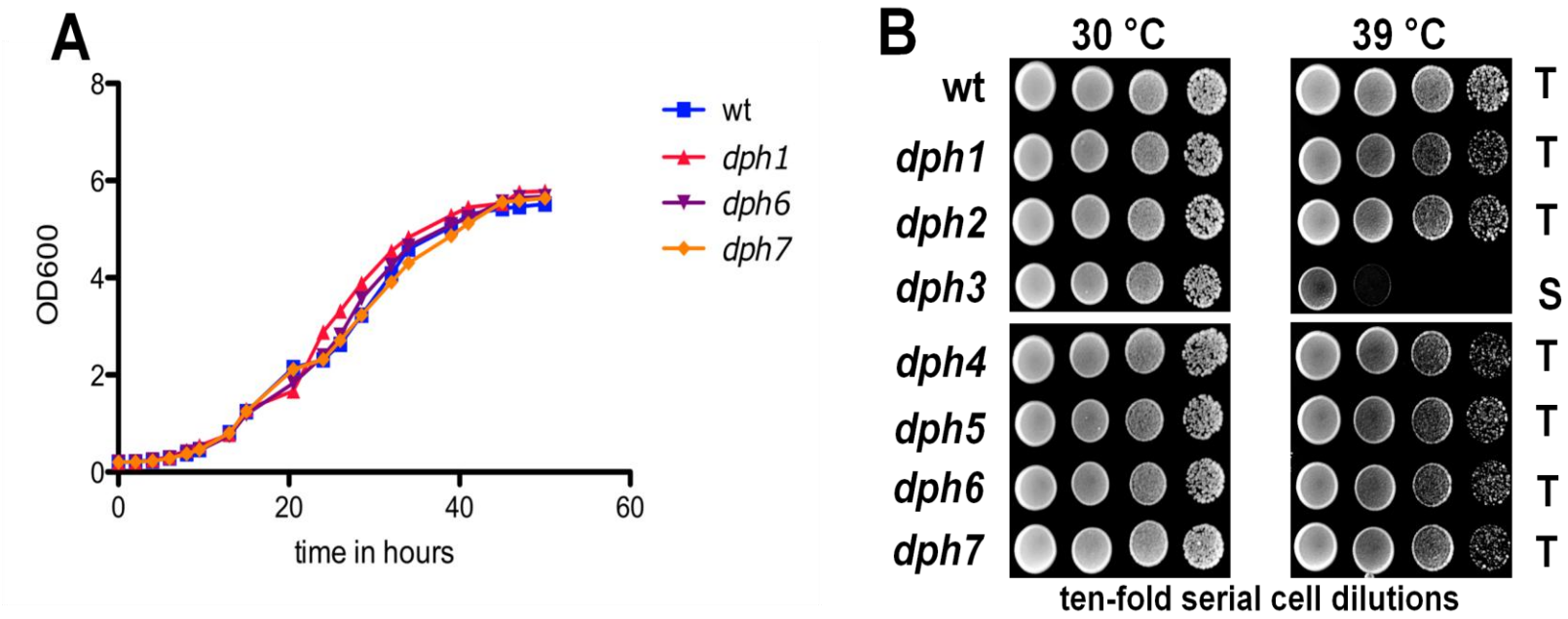

Figure 4.17. Lack of effect of *dph1-dph7* gene knockouts on growth performance and viability. (A) The wild-type parental strain and diphthamide deficient mutants *dph1*, *dph6* and *dph7* were grown in YNB minimal media supplemented with His, Met, Ura, Leu to cover the auxotrophic markers (Table S2) under standard laboratory conditions over a period of 50 h. OD600 was monitored at 2 h intervals. (B) To address a potential temperature sensitive phenotype, ten-fold serial cell dilutions of the indicated strains were spotted on YPD plates and grown at 30°C or 39°C. Note that only the *dph3/kti11* mutant, which affects additional biosynthetic pathways apart from diphthamide biosynthesis shows temperature sensitivity (S) while the other *dph* mutants tolerate high (T) temperatures.

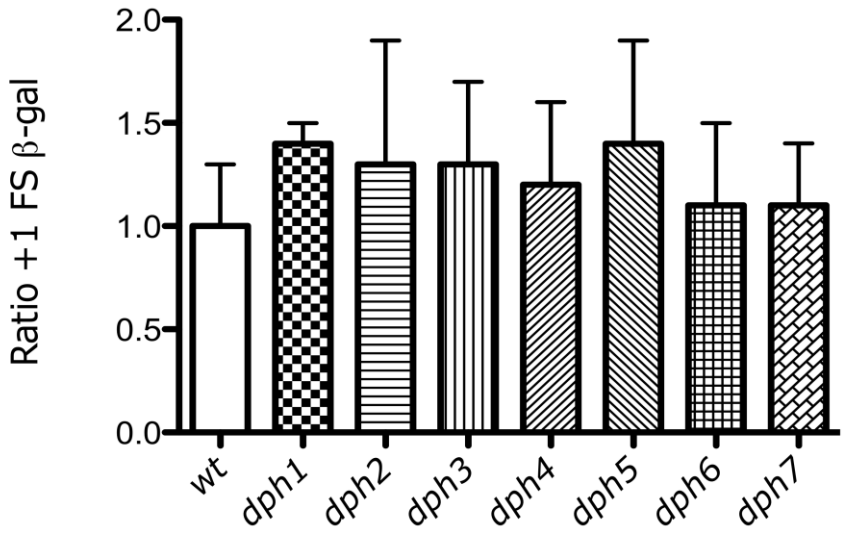

Figure 4.18. Ribosomal frameshift analysis reveals no significant increase in +1 frameshifting. Strains with the indicated genetic backgrounds were transformed with control (pJD240.0) or *lacZ* +1 frameshift (pJD240.+1) plasmids to monitor *lacZ* expression through β-galactosidase (β-Gal) production using O-nitrophenol-D-galactopyranoside assays and to score translation efficiency (pJD240.0) and fidelity (pJD240.+1). Ribosomal +1 frameshifts are expressed relative to the level of overall translation efficiency with statistical significance determined by one-way ANOVA followed by Dunnett's multiple comparison. None of the mutant backgrounds showed a significant increase in ribosomal +1 frameshifting relative to wild-type (wt).

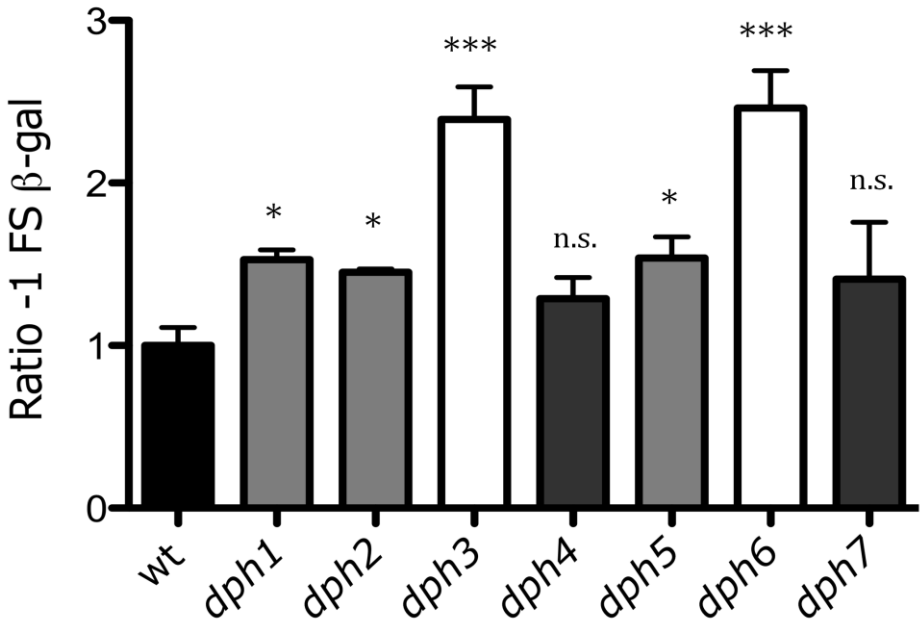

Figure 4.19. Ribosomal frameshift analysis reveals erroneous translation in dph1-dph7 mutants. Strains with the indicated genetic backgrounds were transformed with control (pJD240.0) or *lacZ* -1 frameshift (pJD240.-1) plasmids to monitor *lacZ* expression through β-galactosidase (β-Gal) production using O-nitrophenol-D-galactopyranoside assays and to score translation efficiency (pJD240.0) and fidelity (pJD240.-1). Ribosomal -1 frameshifts are expressed relative to the level of overall translation efficiency with statistical significance determined by one-way ANOVA followed by Dunnett's multiple comparison. With the exception of *dph4* and *dph7*, post-hoc comparison found that all other mutant backgrounds showed a significant increase in ribosomal -1 frameshifting relative to wild-type (wt) yeast cells (*=$P < 0.05$; ***= $P < 0.001$; ns. = not significant).

4.3 Discussion

The experiments presented in this chapter were performed to investigate the role of two candidate ORFs, *YLR143w/DPH6* and *YBR246w/DPH7,* in diphthamide synthesis. As mentioned above, while our work was in progress, Su et al. (2011) reported that *YBR246w/DPH7* is required for the final step of diphthamide synthesis. Here we discuss how our data support these recent findings and provide more evidence to further specify its role in the diphthamide pathway. Furthermore, the role of *YLR143w/DPH6* in the amidation of diphthine to complete diphthamide synthesis will be discussed.

Initially, exposing deletion mutants of both ORFs to diphthamide indicator drugs revealed that they phenocopy diphthamide synthesis genes by displaying resistance to the antifungal, sordarin, as well as failing to serve as a target for DT-mediated (20nM) *in vitro* ADP-Ribosylation. However, in contrast to *DPH1-DPH5* mutants, endogenous overexpression of the bacterial toxin inhibits cell growth and renders *YLR143w/DPH6* and *YBR246w/DPH7* sensitive to DT. Lowering the level of endogenous DT expression via a truncated *GALS* promoter showed that both mutants are clearly more resistant to the action of DT compared to the wild-type. Su et al. (2011) recently reported that *YBR246w/DPH7* mutants can be ADP-Ribosylated *in vitro* when exposed to levels of 10μM of toxin, a 500 fold higher dose than used in our assay. As mentioned in the introduction, the second intermediate in the pathway, diphthine, lacking the amide group, can still be ADP-ribosylated, although at a lower rate in comparison to diphthamide-modified eEF2 (Moehring et al. 1984; Chen and Bodley

1988). The dose-dependant effect of DT on *YLR143w/DPH6* and *YBR246w/DPH7*, which are sensitive to endogenous overexpression of DT but are not affected by low levels of the toxin *in vitro*, lead to the hypothesis that both genes might be involved in the final step of diphthamide formation.

To address the question whether *YLR143w/DPH6* and *YBR246w/DPH7* are indeed involved in the diphthamide pathway, we isolated His_6 tagged eEF2 from strains lacking either ORF and performed mass spectrometry to identify which post-translational modification was present in the deletion mutants. Our mass spectrometry analysis clearly shows that in yeast strains lacking either *YLR143w/DPH6* or *YBR246w/DPH7*, modification of his-699 progresses only as far as diphthine. Thus Dph6 and Dph7 are both required for the final amidation step required to generate diphthamide. Our work is therefore consistent with that of Su et al. (2011), who while our study was in progress reported that Ybr246w/Dph7 is required for conversion of diphthine to diphthamide. In eEF2 isolated from the *ybr246w/dph7* mutant we only detected loss of the trimethylamino group of diphthine during mass spectrometry, in eEF2 isolated from the *ylr143w/dph7* mutant we observed loss of the trimethylamino group before analysis of the peptide. This suggests that diphthine-modified eEF2 in the *ylr143w/dph6* mutant is somehow more labile and prone to elimination of the trimethylamino group. Previously, it was suggested that similar lability of diphthine on EF2 from the archaon *P. horikoshii* might be due to the local amino acid context of the modified residue in EF2 and that sequence differences between eukaryal and archaeal EF2 could explain why diphthine-modified eEF2 from yeast appeared stable in the *ybr246w/dph7* knockout strain (Su et al. 2011). Furthermore, we detected unmodified

his-699 peptide in eEF2 extracted from all the strains examined and not just in the *dph1*Δ mutant that is blocked in the first step of the diphthamide biosynthetic pathway. Thus even in wild-type strains, not all eEF2 appears to be modified. The presence of higher levels of unmodified eEF2 in *ybr246w/dph7*, *ylr143w/dph6* and possibly also *dph5* in comparison to wild-type yeast could indicate some sort of feedback control mechanism whereby the first step of the diphthamide biosynthetic pathway is downregulated if significant levels of eEF2 with modification intermediates, e.g. ACP or diphthine, accumulate.

Prompted by our mass spectrometry results, we examined whether either novel diphthamide synthesis protein interacts with each other or *bona fide DPH* genes and eEF2. Co-immunoprecipitation of tagged constructs revealed that *YLR143w/DPH6* and *YBR246w/DPH7* do not interact with each other or with *DPH1*, *DPH2* and *DPH5*. However, Ylr143w/Dph6 directly binds to eEF2 suggesting that it is the favored candidate for the amidase, which converts diphthine into diphthamide. In line with this, sequence analysis of *YLR143w/DPH6* revealed three conserved domains, which indicate that it functions as an enzyme. The N-terminal region contains a Alpha_ANH_like_IV domain (cd1994 in the NCBI Conserved Domain Database), a member of the adenine nucleotide alpha hydrolase superfamily, which is proposed to bind ATP. The C-terminal region carries two concerved domains related to the YjgF-YER057c-UK114 protein family (eu_AANH_C1: cd06155 and eu_AANH_C2: cd06166). These domains are found in a range of proteins involved in nucleotide and amino acid metabolism (Volz 1999; Burman et al. 2007; Lambrecht et al. 2012). We therefore consider it likely that

Dph6 is directly involved in diphthine amidation and that this step is an ATP-dependent process, with perhaps ammonia or glutamine acting as the source of the amide group.

Sequence analysis revealed that *YBR246w/DPH7* contains four WD40 domains and is involved in two seemingly diphthamide-unrelated processes: firstly it was shown to act in endosomal recycling as the product of the *ERE1* gene (Shi et al. 2011) and secondly as a negative regulator of RNA polymerase I (*RRT2*) (Hontz et al. 2009; Shi et al. 2011). Though the putative mammalian homologue, WDR85, was proposed to act in the first step of diphthamide formation (Carette et al. 2009), our data, in line with recent findings reported by Su et al. (2011), clearly demonstrate that it is necessary for the final step of diphthine amidation. The four conserved WD40 repeats in *YBR246w/DPH7* suggest that it acts in mediating protein-protein interaction. Though it does not bind to Ylr143w/Dph6, our data suggest a regulatory role for Ybr246w/Dph7 in modulating the interaction between Dph5 and eEF2, where the *ybr246w/dph7* mutant shows a significant increase in interaction between the diphthine synthase and the translation elongation factor. We hypothesize that Ybr246w/Dph7 might be necessary to displace Dph5 from eEF2 in order to allow the diphthamide synthesis to progress into the final amidation step. This notion is supported by the finding that the mammalian homolog, WDR85, shows a similar effect on Dph5-eEF2 interaction. Furthermore, we demonstrate that elevated levels of Dph5 are cytotoxic to *dph1-dph4* cells as well as the *ybr246w/dph7* mutant. It appears that the Dph5 is inhibitory to the translation factor when diphthamide synthesis is incomplete. Therefore we conclude that Dph5 does not only act as a methyltransferase but also binds to eEF2 when diphthamidation is incomplete and inhibits its function in translation elongation. In agreement with this, we

demonstrate that the lack of *DPH1* resulting in an unmodified His^{699} also promotes binding of Dph5 to eEF2. In addition, the detrimental effect of Dph5 overexpression on the *ybr246w* mutant contributes to our hypothesis that *YBR246w* is necessary to displace Dph5 from eEF2 before diphthine can be converted to diphthamide by Ylr143w/Dph6. Whereas in the *ylr143w/dph6* cell, endogenous levels of Ybr246w are present to antagonize the toxicity of increased Dph5 levels and rescue eEF2 function. This would predict a better accessibility of the His^{699} residue in the *ylr143w/dph6* mutant compared to the *ybr246w* mutant, which is confirmed in the finding that cells lacking *YLR143w/DPH6* are more sensitive to the action of endogenous expression of DT.

Moreover, our mass spectrometry data not only clarifies the involvement of *YLR143w/DPH6* and *YBR246w/DPH7* in diphthamide synthesis but also showed a loss of the trimethylamino group in both mutant strains. While eEF2 analysis from *ybr246w* cells displayed this chemical change only during the mass spectrometry, eEF2 from *ylr143w/dph6* showed partial loss of the trimethylamino group before analysis. Hence the diphthine modification in the *ylr143w/dph6* is more labile than in the *ybr246w/dph7* mutant. It is possible that Ybr246w/Dph7 displaces Dph5 in the *ylr143w/dph6* cell thereby rendering it more prone to elimination, whereas in a *ybr246w/dph7* mutant Dph5 occupies and stabilizes the diphthine modification. The proposed model for Ybr246w/Dph7 function in diphthamide synthesis will need further biochemical examination to confirm our hypothesis, however the previous findings of its involvement in endosomal recycling and regulation of RNA transcription might implicate Ybr246w/Dph7 in multiple cellular processes. Nevertheless, we present extensive data suggesting Ylr143w/Dph6 as the more likely candidate for the amidase

and Ybr246w/Dph7 as a regulator of the interaction between Dph5 and eEF2 and therefore we have named the former *DPH6* and the latter *DPH7*.

Though the pathological relevance of diphthamide as an effector of the cytotoxic drugs, diphtheria toxin, sordarin and ricin, has been extensively studied, its physiological role remains elusive. However, data from our own group and others have demonstrated that *DPH1*, *DPH2* and *DPH5* mutants display a significant increase in -1 frameshifting (Ortiz et al. 2006a; Bar et al. 2008). Furthermore, mouse models of *DPH1*, *DPH3* and *DPH4* indicate a crucial role for the diphthamide modification in embryonic development and tumourignesis (Chen and Behringer 2004a; Liu et al. 2006; Webb et al. 2008). It appears that the function of the posttranslational modification on eEF2 becomes more apparent in higher organisms, where the regulation of translation is a tightly regulated process. In support of this, we examined -1 frameshifting in all *bona fide* diphthamide synthesis genes as well as the novel *DPH6* (*YLR143w*) and *DPH7* (*YBR246w*) ORFs. Our assay resulted in a similar incidence of -1 frameshifting in *DPH2* and *DPH5* cells as reported by Ortiz et al. (2006) and further demonstrates that apart from *DPH4* and *DPH7*, all other diphthamide deficient mutants display a significant increase in -1 frameshifting. Though the ratio of -1 frameshifting in *dph4* and *dph7* is statistically not significant, it is elevated compared to the wild-type. We therefore propose that diphthamide on eEF2 is necessary for maintaining the correct reading frame during translation and that together with other *DPH* genes, *DPH6* is crucial in this capacity.

CHAPTER 5

DISCUSSION

5 Discussion

The research presented here is centered upon diphthamide, a unique post-translational modification on translation elongation factor 2 (EF2) from archaea and eukarya (Moehring et al. 1984; Chen et al. 1985a). As the name implies, eEF2 is a key player in the elongation cycle of *de novo* protein synthesis and facilitates the translocation of the newly synthesized polypeptide within the ribosome. Since it was first discovered in 1974, diphthamide has been subject to extensive studies revealing its chemical structure and the involvement of at least 5 proteins, Dph1-Dph5, in a three step biosynthesis pathway (Pappenheimer 1977; Liu and Leppla 2003a). However, the physiological role for this complex modification remains elusive. While diphthamide-deficient yeast display mild phenotypes, mouse models of *DPH1*, *DPH3* and *DPH4* are embryonically lethal and display developmental delays (Chen and Behringer 2004b; Liu et al. 2006; Webb et al. 2008). Furthermore, *DPH1* is allelic with *OVCA1*, a tumour suppressor gene that is strongly linked to ovarian and breast cancer formation. Mouse embryonic fibroblasts (MEFs) lacking *OVCA1* display cell proliferation defects, which could explain the defects in embryogenesis (Chen and Behringer 2004b). Therefore the crucial role of diphthamide on eEF2 seems to be more apparent in multi-cellular organisms, however the conserved diphthamide synthesis pathway allows us to investigate this unique post-translational modification in *S. cerevisiae*. This research was aimed at dissecting diphthamide biosynthesis further by investigating the first and the final step of the pathway.

5.1 Dph1 mutagenesis reveals a central role for the iron-sulfur enzyme

The initial step of eEF2 diphthamidation is the transfer of an ACP (3-amino-3carboxylgroup) radical from SAM (S-adenosylmethionine) onto the imidazole ring of the histidine precursor and in eukaryotes involves four proteins, Dph1-Dph4 (Chen and Bodley 1988). Our group together from data from other groups demonstrated that Dph1, Dph2 and Dph3 form a complex, where all partner proteins interact with each other and co-purify in protein immunoblots (Fichtner et al. 2003a; Liu et al. 2004a; Bar et al. 2008). Furthermore, the homologous Dph1 and Dph2 form a heterodimer where the archael counterpart of Dph1, PhDph2 (*P. horikoshii* Dph2), was recently reported to serve as an iron-sulfur containing enzyme that catalyzes the cleavage of the ACP group from SAM. Extensive structural and spectrometric data revealed that PhDph2 has three distinct domains each containing a conserved cysteine residue (Cys59, Cys163 and Cys287), which cluster at the center of the protein and present the binding sites for the iron-sulfur cluster (Zhang et al. 2010; Zhu et al. 2011).

Here we aimed at dissecting the eukaryotic homologue of PhDph2 in *S. cerevisiae* (ScDph1) in order to map functional regions of Dph1. By introducing progressive truncations in intervals of 30aa from the N- and the C-terminal end we hoped to identify the shortest deletion mutant that confers loss of function and therefore the minimal function unit of this protein. Surprisingly we observed that the smallest

truncation of only 30aa from either end renders Dph1 inactive in terms of diphthamide biosynthesis. Furthermore, the conserved regions containing the first and the third cysteine residue proved to be crucial for the interaction of Dph1 with either Dph2 or Dph3. Despite the fact that all N- and C- teminal truncations (N1-N4 and C1-C4) were not able to form diphthamide, the interaction between Dph1 and Dph2 as well as Dph1 and Dph3 remained intact as long as the conserved regions containing the cysteine residues were present. Since only the full-length Dph1 was able to form diphthamide, we hypothesize that the smallest truncation changes the structure of the protein, which might interfere with the formation of the triangular mold necessary for binding of the iron-sulfur cluster. It appears that the conformation of Dph1 is as important as the three conserved cysteine residues for binding of the [4Fe-4S] in order to facilitate cleavage of the ACP radical and its subsequent translocation to the histidine precursor.

The first step of archael diphthamide synthesis only requires the action of PhDph2 *in vitro*, which functions in the form of a homodimer. In eukaryotes on the other hand, the homologous Dph1 and Dph2 form a heterodimer with Dph2 only containing the first and the third conserved cysteine residue found in PhDph2 (Zhang et al. 2010). Therefore ScDph1 is the yeast counterpart to bacterial PhDph2, however ScDph2 is likely to have evolved from this same ancestral protein. A similar investigation of the Dph2 protein from Chinese Hamster ovary cells (CgDph2, *C. griseus*) showed that an N-terminal truncation of 158aa, which removes the first conserved cysteine residue and only leaves the second C-terminal one, has no effect on CgDph2 function and is as active as the wild-type protein (Roy et al. 2010). This finding does not agree with the proposed model by Zhu et al. (2011) who recently

reported that at least two of the three cysteine residues in PhDph2 are necessary for binding of the [4Fe-4S] cluster and that mutation of a single Cys residue does not affect diphthamide formation however the double mutant is inactive. Together with our observation that in contrast to Dph2, Dph1 is sensitive to a truncation as small as 30aa, we believe that Dph2 is not likely to act as the primary iron-sulfur binding enzyme, which generates the ACP radical from SAM. Furthermore, by mutating one of the PhDph2 subunits, Zhu et al. (2011) showed that a heterodimer with one wildtype and one mutated PhDph2 subunit, which could not bind the [4Fe-4S] construct, was more stable than the unaltered homodimer. Though the reason for this is unclear, it was suggested that a single bound iron-sulfur cluster might be thermodynamically more stable than the homodimer with two such clusters. If this proves to be the case, it might provide an explanation as to why archael PhDph2 evolved into the closely related Dph1 and Dph2 in yeast and higher organisms, where the former is likely to act as the main [4Fe-4S] cluster binding enzyme. Though Dph2 activity is essential for diphthamide formation, it might have a structural or regulatory function as opposed to the catalytic activity of Dph1. Since the Dph1-Dph2 heterodimer is fundamental to the diphthamide pathway, one could speculate that Dph2 stabilizes the structure, which is necessary to shape the triangular mold for binding of the iron-sulfur scaffold.

Though X-ray crystallography of PhDph2 has provided valuable insight in the mechanism of action which generates the ACP radical, it will be interesting to elucidate the structure of the Dph1-Dph2 heterodimer as well as the Dph1-Dph2-Dph3 complex in eukaryotes to clarify the function of each protein in diphthamide formation.

5.2 Data mining of genetic interaction database reveals novel *DPH* genes

The analysis of toxin-resistant mutants in yeast and Chinese hamster ovary cells (CHO) cells identified 5 diphthamide synthesis genes, *DPH1-DPH5*, which are involved in the first and second step of the pathway (Pappenheimer 1977; Liu et al. 2004a). However, no specific enzyme was identified for the final conversion of diphthine into diphthamide. While our study was in progress, Su et al. (2011) reported a novel candidate gene, *YBR246w*, which plays a role in the final step. We here present our data, which are in agreement with the above mentioned publication and report the finding of a novel gene, *YLR143w*, which is likely to be the amidase that catalyzes the conversion of diphthine into the final product.

Data mining of two independent yeast screens revealed two candidate ORFs, *YLR143w/DPH6* and *YBR246/DPH7*, that share genetic and phenotypic traits of *bona fide* diphthamide synthesis genes. As determined by data collected in the DRYGIN database (Koh et al. 2010) *DPH6* and *DPH7* are closely linked to the genetic interaction landscape of *DPH1*, *DPH2*, *DPH4* and *DPH5*. Furthermore, both ORFs phenocluster with Dph1-Dph5 according FitDB, a data collection of fitness defects of yeast deletion mutant (Hillenmeyer et al. 2008). We further looked into the phenotypic similarity by demonstrating that like Dph1-Dph5, Dph6 and Dph7 are resistant to the diphthamide indicator drugs sordarin as well as DT (diphtheria toxin) in low levels. However, the sensitivity to elevated DT levels prompted the question of how Dph6 and Dph7 are

different from Dph1-Dph5 and whether they are indeed involved in the diphthamide pathway. Isolation of eEF2 from *dph6* and *dph7* mutant strains and subsequent mass spectrometry clearly shows that both gene products are necessary for the progression of diphthine into diphthamide. Therefore our data confirms the findings recently reported by (Su et al. 2011).

To further investigate the role of *DPH6* and *DPH7* in diphthamide synthesis we investigated whether either protein directly interacts with other Dph proteins or eEF2. Though neither Dph6 nor Dph7 interact with Dph1, Dph2 or Dph5, we observed binding of Dph6 to eEF2 in protein immunoblots. Dph7 on the other hand acts as a modulator of the interaction between Dph5 and eEF2. In other words, Dph5-eEF2 binding is elevated in the absence of Dph7, a finding also observed with its putative mammalian homologue, WDR85 (Carette et al. 2009). In addition, elevated levels of Dph5 are cytotoxic to *dph1-dph4* and *dph7* mutant strains. We hypothesize that Dph7 is necessary to displace Dph5 from eEF2 and that this is crucial for the progression of the diphthamide pathway from diphthine to the final product. We propose that in the *DPH6* deletion strain, endogenous levels of Dph7 rescue the cytotoxic phenotype of Dph5 overexpression by downregulating binding of Dph5 to eEF2. This hypothesis could be confirmed by repeating the same experiment in a *dph6/dph7* double mutant, where we would expect to see toxicity conferred by Dph5 overexpression. It is likely that Dph5 not only acts as a methyltransferase, but also serves as a checkpoint enzyme, which is inhibitory to eEF2 and the diphthamide pathway when intermediate forms of the peptide (ACP intermediate or diphthine) are present. In agreement with this, *DPH1* mutated strains with unmodified eEF2 promote binding of Dph5 to eEF2. This model (Figure

5.1) is reinforced by our mass spectrometry data, where all samples contained unmodified His_{699}, but the highest levels were found in the *dph6* and *dph7* and possibly *dph5* mutant strains. In sum, we demonstrate that the post-translational modification of eEF2 by the seven diphthamide synthesis genes, Dph1-Dph7, is not a linear process but contains some sort of feedback loop which regulates the progression of the pathway.

The findings reported in this study clearly favour Dph6 as the enzyme that catalyzes the final step of the diphthamide pathway. Not only does Dph6 directly bind to eEF2, but it also contains a putative ATP-binding site, which is necessary for the ATP-dependant amidation of diphthine. Structure analysis of Dph7 however, revealed four conserved WD40 repeats, which are indicative of proteins, which mediate protein-protein interaction, a feature that is in agreement with the above mentioned regulatory function. Nevertheless, definite proof that Dph6 is indeed the amidase involved in the final step can be gained by reconstructing the amidation of diphthine *in vitro* in presence of Dph6 alone.

It should be noted that the protein interaction profiles for Dph6 and Dph7 presented here have been generated by co-immunoprecipitation experiments only. Though this method is widely used it generally detects high affinity protein-protein interactions only and has its limitations. The use of epitope tags might interfere with proper folding of the tagged protein and alter the outcome of the co-immunoprecipitation. In addition, prior to co-purifying interacting proteins the cells are lysed in order to harvest the proteins, which then are processed further in different binding and elution buffers, which might not present an ideal environment for transient protein interactions. Hence, if Dph6 and Dph7 interact with other component of the

diphthamide pathway in a transient manner, they might have escaped our detection via co-immunoprecipitation. In order to address this issue several methods could be explored to verify the findings presented in this study. The traditional yeast-two-hybrid (Y2H) approach is an alternative assay, which allows detection of protein interactions *in vivo* (Berggard et al. 2007). Here, the expression of a downstream reporter gene is dependent on transcription factors (for example *Gal4*), which binds to an upstream activating sequence (UAS). In order to detect protein interactions, the transcription factor is split into a bait and a target sequence, which are used to c-terminally tag the two proteins of interest. If the bait protein and the target protein interact, the transcriptional activator is assembled and drives the expression of the reporter gene, which in turn is a measure for the protein-protein interaction of the bait protein with the target protein. The Y2H method does not only allow detection of protein interactions *in vivo*, but also amplifies the signal by using a reporter gene. Alternatively, chemical crosslinking of interacting proteins with the use of bifunctional reagents, such as carbodiimide, allow to freeze putative protein complexes by coupling the carboxyl group from one protein to the lysine group of another protein (Melcher 2004). This enables the analysis of low affinity interactions before they dissociate. Taken together, co-immunoprecipitation has its limitations for detecting weakly interacting proteins, therefore verifying our results with an alternative method would provide further evidence for our proposed model for the diphthamide pathway.

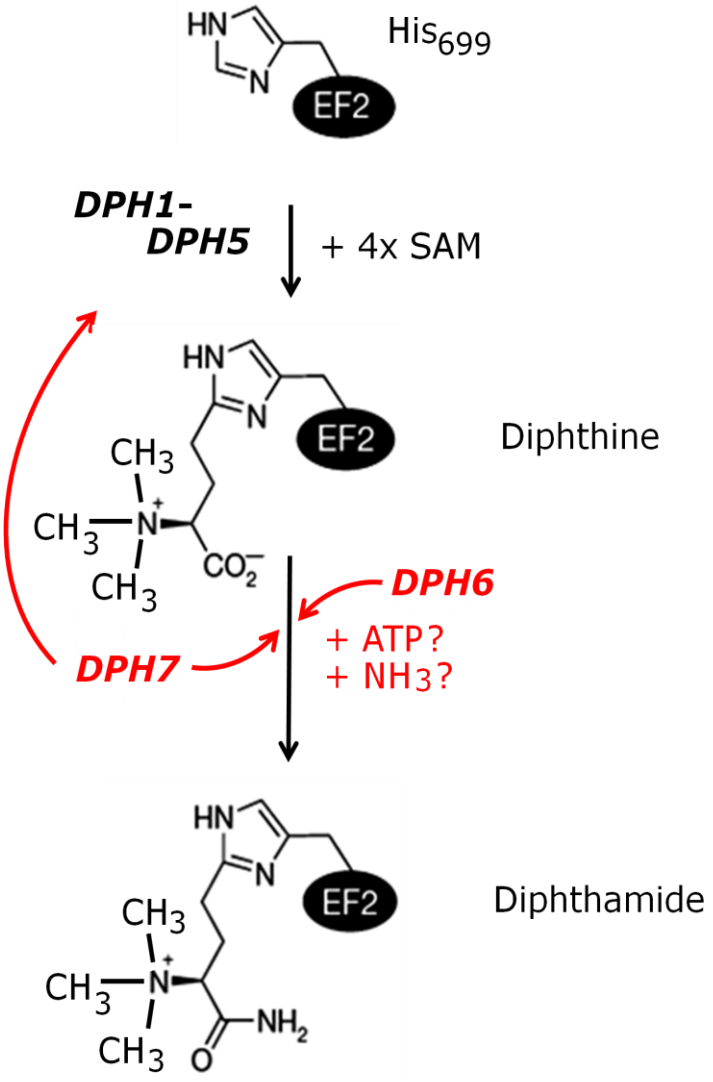

Figure 5.1. Model for the diphthamide pathway incorporating the proposed novel roles of Dph5, Dph6 and Dph7. Diphthamide pathway showing the interaction of Dph5 with unmodified eEF2 and the proposed role of Dph7 in displacement of Dph5 prior to diphthine amidation.

5.3 The physiological role of diphthamide in normal cellular function

Though the diphthamide pathway has been implemented in cancer formation, embryonic development as well as cell proliferation control, the normal physiological role for this post-translational modification (PTM) is unclear. The three step pathway represents one of the most complicated PTMs and its final product, diphthamide, was first identified as the unique target for bacterial toxins (Robinson et al. 1974; Van Ness et al. 1980b). However, it seems unlikely that seven gene products, Dph1-Dph7, would be recruited to form a complex modification on eEF2, just so it could serve as a target for lethal bacterial toxins. In regard to the physiological role of diphthamide, deletion mutants of *DPH1*, *DPH2* and *DPH5* have previously been shown to increase -1frameshifting (Ortiz et al. 2006a; Bar et al. 2008). Here we demonstrate that apart from *dph4* and *dph7* all *bona fide* Dph proteins together with the novel diphthamide protein, Dph6, significantly increase the incidence of -1 frameshifting. We therefore conclude that diphthamidation of eEF2 is crucial for maintaining the correct reading frame during translation. These findings are consistent with (Liu et al. 2012), who very recently reported that lack of diphthamide on eEF2 in mammalian cells significantly elevated -1frameshifting. The diphthamide modification is located at the tip of domain IV of eEF2, a region that protrudes into the ribosomal decoding center and has been suggested to interact with the codon-anticodon interface of tRNA and mRNA (Stark et al. 2000; Spahn et al. 2004). eEF2 function is strictly dependant on conformational changes, which allow its translocation activity. Therefore it is likely that the

diphthamide modification contributes to the maintenance of the eEF2 conformation, which in turn is fundamental to its role in translation. In line with this, Liu et al. (2012) demonstrated that the use of a specific eEF2 antibody, which does not target the site of diphthamidation directly, has an increased reactivity to eEF2 lacking diphthamide in contrast to the wildtype, which indicates conformational changes that influence the accessibility for the antibody.

Despite the elevated -1frameshifting incidence in *dph4* and *dph7* mutant strains, they were statistically not significant. The uni-reporter plasmids used in our assay with a single reporter gene readout resulted in a wide range of fluctuation for the same strain. The error bars (as shown in figure 4.18 and 4.19) especially for the -1 frameshifting assay of the *dph7* mutant could be corrected with a dual-reporter construct, where the reference gene demonstrates the level of total translation and the relative -1 frameshifting incidence is measured from the second reporter gene, which is in -1 frame. This presents a favourable alternative to the uni-reporter assay and we would expect *dph4* and *dph7* mutant strains to phenocopy the other *DPH* genes in regard to the incidence of errors in translation.

The specific role of maintaining the fidelity of mRNA translation would explain why the lack of the modification on eEF2 has such a deleterious effect on embryonic development, a stage where protein synthesis is a tightly controlled process. In the unicellular organism *S. cerevisiae* however, though increased -1 frameshifting is clearly measurable, it is not lethal to yeast as demonstrated by the viability of *dph1-dph7* mutants. Therefore the crucial physiological role of diphthamide may only be apparent in muticellular organisms.

Interestingly, frameshifting events are present in organisms from archaea, eubacteria as well as eukarya (Dinman 2006). Though first discovered in RNA-viruses, which routinely use -1 programmed ribosomal frameshifting (PRF) to achieve alternative read-through of overlapping ORFs, it has been demonstrated that higher organisms as well as bacteria apply frameshifting as an intrinsic part of their translation machinery (Brierley 1995; Farabaugh 1996). Computational analyses of the *S. cerevisiae* genome predicted 10340 putative -1 PRF motifs, with 1275 out of the 6353 yeast genes containing at least one statistically significant -1 PRF signal (Jacobs et al. 2007). Out of nine tested motifs eight were shown to result in significant -1 PRF levels *in vivo*. However, unlike viruses yeast frameshifting events do not result in alternative gene products, but redirect ribosomes to premature stop codons, which leads to the degradation of the reporter mRNA via the NMD (nonsense-mediated mRNA decay) pathway. More recently, (Belew et al. 2011) demonstrated that the regulation of mRNA abundance via -1 operational ribosomal frameshifting (-1 RF) in *S. cerevisiae* is not only determined via the NMD pathway but also the no-go decay pathway (NGD). The fact that approximately 11% of yeast genes contain at least one -1 RF indicates that frameshifting is a widely-spread post-transcriptional mechanism for the regulation of mRNA abundance and stability. This is not only the case for yeast genomes, but across 25 analysed eukaryotic genomes so far, 8-12% of genes have been shown to contain at least one -1 RF (data collected in PRF database: PRFdB at http://prfdb.umd.edu/) (reference) (Belew et al. 2008). In the context of diphthamidation of eEF2, the significant increase of -1 frameshifting in diphthamide-deficient yeast as well as mammalian cells indicates that the post-translational modification of eEF2 is necessary

to regulate the level of -1 frameshifting, thereby affecting the abundance and stability of mRNA. It is likely that in the unicellular yeast deregulation of the affected mRNA levels is less severe compared to higher organisms, which especially during embryonic development are dependant on a tightly controlled translation machinery.

An outstanding issue in the field is how in humans, *OVCA1/DPH1*, and the subsequent lack of eEF2 diphthamidation leads to formation of ovarian and breast cancer. Liu et al. (2012) reported that the loss of function of *OVCA1* is unlikely to have other effects than the lack of diphthamide formation on eEF2. Together with our observation that diphthamide-deficient strains are prone to errors in translation fidelity, it is likely that the lack of diphthamidation of eEF2 deregulates its function and the resulting increase in -1 frameshifting significantly degrades affected mRNA levels, which in turn promote cancer formation. *OVCA1* would therefore acts as a tumour suppressor gene by allowing the post-translational modification of the translation factor and could thereby prevent these frameshift errors during protein biosynthesis. It would therefore be interesting to investigate mRNA levels in *OVCA1* deficient mammalian cells to investigate which specific mRNAs are significantly degraded in absence of the tumour suppressor gene.

5.4 Concluding remarks and future directions

In conclusion, the work presented here contributes to a better understanding of the diphthamide biosynthesis pathway and its role in normal cell physiology. Our data provides a better insight into the role of Dph1 in the first step of eEF2 diphthamidation.

Furthermore, by mining data collected in extensive genetic and phenotypic studies, we identified the novel and until now uncharacterized member of the *DPH* gene family, *DPH6*. We here present genetic, phenotypic and biochemical analyses of Dph6 and Dph7 and present a model for their role in the final step of diphthamide formation.

However, in order to further explore the diphthamide pathway a number of potential experiments have been proposed. These include structural analysis of the Dph1-Dph2-Dph3 complex in eukaryotic cells to clarify how these proteins interact with each other in order to facilitate the initial step of the pathway. *In vitro* reconstruction of the conversion of diphthine to diphthamide with the help of Dph6, would give definite proof that it is indeed the missing amidase as indicated by our study. Furthermore, investigating the putative homologues of *DPH6* and *DPH7* in mammalian cell lines and in a mouse model would clarify if they phenocopy the defects in embryogenesis and cell proliferation seen in *DPH1*, *DPH3* and *DPH4* deficient mice. In addition, a *DPH6* and *DPH7* mouse model would give insight into their role in the context of cancer formation. Given the implication of this unique post-translational modification on eEF2 in cancer formation, embryogenesis and cell proliferation control it is crucial to further our knowledge on the role of diphthamide in translation regulation.

CHAPTER 6

MATERIALS and METHODS

6 Materials and Methods

6.1 Materials

6.1.1 *Escherichia coli* strains

Strain	Genotype	Source
DH5α	*supE44 ΔlacU169 (Φ80LacZΔM15) hsdR17 recA1 endA1 gyrA96 thi-1 relA1*	Gibco BRL

6.1.2 *Saccharomyces cerevisiae* strains

Strain	Discription	Source/Reference
BY4741	MATa *his3Δ1 leu2Δ0 met15Δ0 ura3Δ0*	Euroscarf, Frankfurt
Y02262	BY4741 *dph1*Δ::*kanMX4*	Euroscarf, Frankfurt
Y05041	BY4741 *dph2*Δ::*kanMX4*	Euroscarf, Frankfurt
CBY12	BY4741 *dph3*Δ::*SpHIS5*	(Baer et al. 2008)
Y06909	BY4741 *dph4*Δ::*kanMX4*	Euroscarf, Frankfurt
Y04121	BY4741 *dph5*Δ::k*anMX4*	Euroscarf, Frankfurt
Y03386	BY4741 *ybr246w*Δ::*kanMX4*	Euroscarf, Frankfurt
Y13386	BY4742 *ybr246w*Δ::*kanMX4*	Euroscarf, Frankfurt
BY4742	MATa *his3Δ1 leu2Δ0 lys2Δ0 ura3Δ0*	Euroscarf, Frankfurt
Y04100	BY4741 y*lr143w*Δ::*kanMX4*	Euroscarf, Frankfurt
Y14100	BY4742 *ylr143w*Δ::*kanMX4*	Euroscarf, Frankfurt
SUY7	BY4741 y*lr143w*Δ::*kanMX4 dph1*Δ::*KlLEU2*	This study
SUY8	BY4741 *ylr143w*Δ::*kanMX4 dph5*Δ::*KlLEU2*	This study
SUY9	BY4741 *ybr246w*Δ::*kanMX4 dph1*Δ::*KlLEU2*	This study
SUY10	BY4741 *ybr246w*Δ::*kanMX4 dph5*Δ::*KlLEU2*	This study
SUY11	BY4741 *ybr246w*Δ::*kanMX4 ylr143w*Δ::*KlURA3*	This study
SUY12	BY4741 *ybr246w*Δ::*kanMX4 ylr143w*Δ::*KlURA3 dph1*Δ::*SpHIS5*	This study
SUY13	BY4741 *ybr246w*Δ::*kanMX4 ylr143w*Δ::*KlURA3 dph5*Δ::*SpHIS5*	This study
SUY3	BY4741 *eft1*Δ::*kanMX4* + pTKB612 ($eEF2^{HIS}$)	This study
SUY4	BY4741 *eft1*Δ::*kanMX4 ylr143w*Δ::*KlURA3* + pTKB612 ($eEF2^{HIS}$)	This study
SUY5	BY4741 *eft1*Δ::*kanMX4 dph1*Δ::*KlURA3* + pTKB612 ($eEF2^{HIS}$)	This study
SUY6	BY4741 *eft1*Δ::*kanMX4 dph5*Δ::*KlURA3* + pTKB612 ($eEF2^{HIS}$)	This study
SUY14	BY4741 *eft1*Δ::*kanMX4 ybr246w*Δ::*KlURA3* + pTKB612 ($eEF2^{HIS}$)	This study
CBY41	W303-1a *KTI11-c-myc*::*SpHIS5*	Baer *et al.* (2008)
CBY42	W303-1a *DPH1-HA*::*KanMX6*	(Baer et al. 2008)
CBY43	W303-1a *DPH2-c-myc*::*SpHIS5*	Baer *et al.* (2008)

SUY15	CBY43 *DPH1-HA*::*KanMX6*	This study
SUY16	SUY15 C1 truncation of *DPH1-HA*::*KanMX6*	This study
SUY17	SUY15 C2 truncation of *DPH1-HA*::*KanMX6*	This study
SUY18	SUY15 C3 truncation of *DPH1-HA*::*KanMX6*	This study
SUY19	SUY15 C4 truncation of *DPH1-HA*::*KanMX6*	This study
SUY20	CBY43 *kanMX6*::*pGAL1-HA-DPH1*	This study
SUY21	SUY20 N1 truncation of *kanMX6*::*pGAL1-HA-DPH1*	This study
SUY22	SUY20 N2 truncation of *kanMX6*::*pGAL1-HA-DPH1*	This study
SUY23	SUY20 N3 truncation of *kanMX6*::*pGAL1-HA-DPH1*	This study
SUY24	SUY20 N4 truncation of *kanMX6*::*pGAL1-HA-DPH1*	This study
SUY25	CBY41 *DPH1-HA*::*KanMX6*	This study
SUY26	SUY25 C1 truncation of *DPH1-HA*::*KanMX6*	This study
SUY27	SUY25 C2 truncation of *DPH1-HA*::*KanMX6*	This study
SUY28	SUY25 C3 truncation of *DPH1-HA*::*KanMX6*	This study
SUY29	SUY25 C4 truncation of *DPH1-HA*::*KanMX6*	This study
SUY30	CBY41 *kanMX6*::*pGAL1-HA-DPH1*	This study
SUY31	SUY30 N1 truncation of *kanMX6*::*pGAL1-HA-DPH1*	This study
SUY32	SUY30 N2 truncation of *kanMX6*::*pGAL1-HA-DPH1*	This study
SUY33	SUY30 N3 truncation of *kanMX6*::*pGAL1-HA-DPH1*	This study
SUY34	SUY30 N4 truncation of *kanMX6*::*pGAL1-HA-DPH1*	This study
YSC1178-YLR143w	BY4741 *YLR143w-TAP*::*His3MX6*	Open Biosystems
YSC1178-YBR246w	BY4741 *YBR246w-TAP*::*His3MX6*	Open Biosystems
SUY35	YSC1178-YLR143w *DPH1-HA*::*KanMX6*	This study
SUY36	YSC1178-YLR143w *DPH2-HA*::*KanMX6*	This study
SUY37	YSC1178-YLR143w *DPH5-HA*::*KanMX6*	This study
SUY38	YSC1178-YBR246w *DPH2-HA*::*KanMX6*	This study
SUY39	YSC1178-YBR246w *DPH5-HA*::*KanMX6*	This study
SUY40	YSC1178-YBR246w *YLR143w-HA*::*KanMX6*	This study
CBKY1	SUY43 *ybr246wΔ::URA3*	
CBKY2	SUY43 *ylr143wΔ::URA3*	Dr. Christian Baer
CBKY3	SUY43 *dph1Δ::URA3*	
CBKY5	BY4741 *DPH5-3HA::kanMX6*	Dr. Christian Baer
CBKY6	SUY43 *DPH6-(HA)$_3$::KanMX6*	Dr. Christian Baer
CBKY7	BY4741 *YLR143w-3c-myc::kanMX6*	Dr. Christian Baer
CBKY8	BY4741 *YBR246w-9c-myc::HIS3MX6*	Dr. Christian Baer
CBKY9	BY4741 *DPH5-3HA::kanMX6; YBR246w-9c-myc::HIS3MX6*	Dr. Christian Baer
CBKY10	BY4741 *YLR143w-3HA::kanMX6; YBR246w-9c-myc::HIS3MX6*	Dr. Christian Baer
CBKY11	BY4741 *YLR143w-3c-myc::kanMX6; DPH5-6HA::HIS3MX6*	Dr. Christian Baer
CBKY12	SUY43 but *ybr246wΔ::HIS3*	Dr. Christian Baer
CBKY13	BY4741 *HIS3MX::P$_{GAL1}$-3HA-DPH6*	Dr. Christian Baer
CBKY14	BY4741 *HIS3MX::P$_{GAL1}$-3HA-DPH6; dph5Δ::KanMX4*	Dr. Christian Baer
CBKY15	BY4741 *HIS3MX::P$_{GAL1}$-3HA-DPH6; dph7Δ::KanMX4*	Dr. Christian Baer
SUY41	YSC1178-YLR143w + pTKB612 (eEF2^{HIS})	This study
SUY42	YSC1178-YBR246w + pTKB612 (eEF2^{HIS})	This study
SUY43	SUY3 *DPH5-HA::His3MX6*	This study
SUY44	SUY14 *DPH5-HA::His3MX6*	This study
SUY45	BY4741 *dph1Δ::KlURA3*	This study
SUY46	BY4741 *dph2Δ::KlURA3*	This study
SUY47	BY4741 *dph3Δ::KlURA3*	This study

SUY48	BY4741 *dph4Δ::KlURA3*	This study
SUY49	BY4741 *dph5Δ::KlURA3*	This study
SUY50	BY4741 *ylr143wΔ::KlURA3*	This study
SUY51	BY4741 *ybr246wΔ::KlURA3*	This study

6.1.3 Plasmids

Plasmid	Discription	Source/Reference
pLMY101	*AmpR, URA3, 2μ,* Diphtheria Toxin (DT) F2 fragment insert, *GAL1* promoter	generous gift from Dr. Collier (Mattheakis et al., 1992)
pSU1	pYCPlac111, *GAL1* promoter	This study
pSU2	pYCPlac111, *GAL1* promoter and DT insert from pLMY101	This study
pSU3	pYEPlac181, *GAL1* promoter	This study
pSU4	pYEPlac181, *GAL1* promoter and DT insert from pLMY101	This study
pSU5	pYES2/CT, mouse *Ovca1* insert from pCMV-*OVCA1*-myc-His	This study
pSU6	pYCPlac111, YLR143w insert	This study
pSU7	pYEPlac181, YLR143w insert	This study
pSU8	p415-GALS, DT insert from pLMY101	This study
pSU9	p416-GALS, DT insert from pLMY101	This study
p415-GALS	pRS415, *LEU2, CEN-ARS, GALS* promoter	Mumberg et al. 1994
p416-GALS	pRS416, *URA3, CEN-ARS, GALS* promoter	Mumberg et al. 1994
pTKB612	*EFT2*-6xHis tag, *LEU2, CEN-ARS, TEF5* promoter, *Amp*R	Jorgensen et al. 2002
pYM1	C-terminal 3HA epitope tag plasmid, *kanMX6* selectable marker	(Knop et al. 1999)
pYM2	C-terminal 3HA epitope tag plasmid, *HIS3MX6* selectable marker	(Knop et al. 1999)
pYM3	C-terminal 6HA epitope tag plasmid, *klTRP1* selectable marker	(Knop et al. 1999)
pYM4	C-terminal 3Myc epitope tag plasmid, *kanMX6* selectable marker	(Knop et al. 1999)
pYM5	C-terminal 3Myc epitope tag plasmid, *HIS3MX6* selectable marker	(Knop et al. 1999)
pYM6	C-terminal 9Myc epitope tag plasmid, *klTRP1* selectable marker	(Knop et al. 1999)
pGAL-*DPH5*	YEp BG1805: p*GAL1-DPH5-HA-(His)6 URA3 2μ*	Open Biosyst.
YCplac111	*Amp*R, *CEN4 ARS1 LEU2* yeast-*E.coli* shuttle vector	Gietz and Sugino (1988)
YEplac181	*Amp, LEU2, 2μ*, yeast-*E.coli* shuttle vector	Gietz and Sugino (1988)
YEplac195	AmpR, URA3, 2μ, yeast-*E.coli* shuttle vector	Gietz and Sugino (1988)
YDpKl-Leu	*Amp*R pUC9_ derivative, *K. lactis LEU2*	D.Jablonowski
YDpSp-His	*Amp*R pUC9_ derivative, *S. pombe HIS3*	D.Jablonowski
YDpKl-Ura	*Amp*R pUC9_ derivative, *K. lactis URA3*	D.Jablonowski
pJET1.2	*Amp*R, *2μ, E. coli* blunt-end cloning vector	Fermentas

pYES2	*Amp*R, *URA3, 2μ,* Yeast-E.coli shuttle vector	Invitrogen
pJD204.0	pRS316, *lacZ* reporter (control), *URA3, CEN-ARS, Amp*R	+ kindly provided by G. Kinzy, Robert Wood Johnson Medical School, Piscataway, USA (Harger et al. 2001)
pJD204.-1	pRS316, *lacZ* reporter (-1 frameshift), *URA3, CEN-ARS, Amp*R	kindly provided by G. Kinzy, Robert Wood Johnson Medical School, Piscataway, USA (Harger et al. 2001)
pJD204.+1	pRS316*, lacZ* reporter (+1 frameshift), *URA3, CEN-ARS, Amp*R	kindly provided by G. Kinzy, Robert Wood Johnson Medical School, Piscataway, USA (Harger et al. 2001)

6.1.4 Oligonucleotides

Designation	Sequence	Use
FW-*DPH1*	TTGGAATCGTATTGAGCGGTAGAC	*DPH1* deletion diagnosis
RV-*DPH1*	GACAATTTAGTTTCGCCTGCAAGCC	*DPH1* deletion diagnosis
FW-*DPH2*	ACGGATCTAAACATGGCAAGGAAGG	*DPH2* deletion diagnosis
RV-*DPH2*	CATTTTGGCGGCTAATTTCCAAGGC	*DPH2* deletion diagnosis
FW-*DPH3*	CGCTATAAAGAGCTTCTCATCGC	*DPH3* deletion diagnosis
RV-*DPH3*	CGTTTTCCATCAGTGCACTTGG	*DPH3* deletion diagnosis
FW-*DPH4*	GCCAAAAGATAAGCGCAATCAAC	*DPH4* deletion diagnosis
RV-*DPH4*	CAACCTCTTTTATATACACCATTC	*DPH4* deletion diagnosis
FW-*DPH5*	GATCTTGGTTATCCGCTCGTAAGGG	*DPH5* deletion diagnosis
RV-*DPH5*	GCTATATAATCTCCTCCAGGATCGC	*DPH5* deletion diagnosis
FW-*YLR143w*	CCAAAAAGAGTAGGCCTATGAGAGG	*YLR143w* deletion diagnosis
RV-*YLR143w*	CTTGGTCTTTAGCTTATTCAGGTGC	*YLR143w* deletion diagnosis
FW-*YBR246w*	GCAGAGACACCAACCAGTTGACACC	*YBR246w* deletion diagnosis
RV-*YBR246w*	CTATTGGCAGGAGCCAGCAGGGAG	*YBR246w* deletion diagnosis
FW-ko*DPH1*	ATGGCAACGAAATAATCCACAAGCAAAAGAGTAGAACGACGGCCAGTGAATTCCCGG	*DPH1* gene deletion
RV-ko*DPH1*	AAACTATTTAAACTATTCAATCGCATGTTTCGGAGTAGCTTGGCTGCAGGTCGACGG	*DPH1* gene deletion
FW-ko*DPH2*	GATCGTGCAAAGGTTGAAAAATGGCGACGGCCAGTGAATTCCCGG	*DPH2* gene deletion

RV-ko*DPH2*	GTCGAGGGAAACAAATTATAAGAGTCAGCTTGGCTGCAGGTCGACGG	*DPH2* gene deletion
FW-ko*DPH3*	ACATACCACGACTGTAAGCACATCATTTGTACAATACATTACCAGCTGAACGACGGCCAGTGAATTCCCGG	*DPH3* gene deletion
RV-ko*DPH3*	CTTTATTTCTATTTGTATTCTCGATCTAGCCTCTCATCTTTAGGCAGCAGAGCTTGGCTGCAGGTCGACGG	*DPH3* gene deletion
FW-ko*DPH4*	CTTTCTTTTGGTGTGAAAATTTAGCGCGACGGCCAGTGAATTCCCGG	*DPH4* gene deletion
RV-ko*DPH4*	GCTCAATTTCCCCTCCCATTTTCAGCTTGGCTGCAGGTCGACGG	*DPH4* gene deletion
FW-ko*DPH5*	ATGCTTTATTTGATCGGACTTGGTCTCTCGTACAAATCAGACATTACCGTCGACGGCCAGTGAATTCCCGG	*DPH5* gene deletion
RV-ko*DPH5*	ATAAAAAAGAAACTACACATGAGCGTGTGCATTACCTTTACTCGTCGCTGAGCTTGGCTGCAGGTCGACGG	*DPH5* gene deletion
FW-ko*YLR143w*	CAATAAGTCAGTATCATGAAGTTTATAGCATTAATATCAGGTGGGAAGCGACGGCCAGTGAATTCCCGG	*YLR143w* gene deletion
RV-ko*YLR143w*	CATTTGGAGTTAGGAACGAATATGCAACCCAAAGCGGTGTTCTTTACCAGCTTGGCTGCAGGTCGACGG	*YLR143w* gene deletion
FW-ko*YBR246w*	CTACATCCACCTCTAGCTGGTTTTTGCATAGCTATACATATGGACCGACGGCCAGTGAATTCCCGG	*YBR246w* gene deletion
RV-ko*YBR246w*	CTAAACTATCCATGTTTGCAAGGAATTATCATAAAATGAGCATGTTGAGCTTGGCTGCAGGTCGACGG	*YBR246w* gene deletion
S2-*DPH1*	GAATATGATACTAACTATTTATACATATGTAACAGGAAGACAAGTGACAACAAAAACTATTTAAAATCGATGAATTCGAGCTCG	*DPH1* epitope tagging (C-terminal)
S3-*DPH1*	ATCCAATGGATTATTACGAAGCTAAAGGATACGGGCGTGGGGAAACTCCGAAACATGCGATTGAACGTACGCTGCAGGTCGAC	*DPH1* epitope tagging (C-terminal)
S2-*DPH2*	TAAATAGTTTATTAGTTAAAATCTTGGATTTAAATAGAGAAGTCGAGGGAAACAAATTATAAGAGATCGATGAATTCGAGCTCG	*DPH2* epitope tagging (C-terminal)
S3-*DPH2*	GTATTTCCGGTGTCGCACGTGGTTATGGATTTGATCGCGAAGACGCTATGAAAAAGGAAAACAAACGTACGCTGCAGGTCGAC	*DPH2* epitope tagging (C-terminal)
S2-*DPH3*	TGCGTTGCTAAGTCATATAGCTCTTTCTTTATTTCTATTTGTATTCTCGATCTAGCCTCTCATCTATCGATGAATTCGAGCTCG	*DPH3* epitope tagging (C-terminal)
S3-*DPH3*	AAGACTTGGCTGAGTACTACGAAGAGGCAGGCATCCACCCCCCTGAGCCTATTGCCGCT	*DPH3* epitope tagging

	GCTGCCCGTACGCTGCAGGTCGAC	(C-terminal)
S2-*DPH4*	CTATAAACAGATTTATCTGATATGCTCAATTTCCCCTCCCATCGATGAATTCGAGCTCG	*DPH4* epitope tagging (C-terminal)
S3-*DPH4*	GAAGGTTAATTTTGACATCGAGGAAGAGCAAGAAGGACAACGTACGCTGCAGGTCGAC	*DPH4* epitope tagging (C-terminal)
S2-*DPH5*	GGCCCGATTCGTTTGGGATCGAATTGTTACCCGACTGAAAGGATCGATGAATTCGAGCTCG	*DPH5* epitope tagging (C-terminal)
S3-*DPH5*	CGGCATGGGTCCCACCCACAGAAGACGACAGCGACGAGCGTACGCTGCAGGTCGAC	*DPH5* epitope tagging (C-terminal)
S2-*YLR143w*	GCGTATATCTATTAAGTTTATAAAATATAAGGCCTACATTTGGAGATCGATGAATTCGAGCTCG	*YLR143w* epitope tagging (C-terminal)
S3-*YLR143w*	GATTACCGTGGTAAAGAACACCGCTTTGGGTTGCATATTCGTTCCCGTACGCTGCAGGTCGAC	*YLR143w* epitope tagging (C-terminal)
S3.1-*DPH1*	TCAATAAACCACTATTAACACCATATGAGGCTAGTGTCTTACTAAAGAAACGTACGCTGCAGGTCGAC	DPH1 truncation and epitope tagging (C-terminal)
S3.2-*DPH1*	TTATTCTAAGTGAAGTTTTTCCCCAAAAGCTCGCAATGTTCGATCAAATTGATGTTTTTGTTCAGCGTACGCTGCAGGTCGAC	DPH1 truncation and epitope tagging (C-terminal)
S3.3-*DPH1*	GTAGACAAGGTAATTTAAACACTGTAAAAAACTTGGAAAAAAACCTGATCCGTACGCTGCAGGTCGAC	DPH1 truncation and epitope tagging (C-terminal)
S3.4-*DPH1*	TCACTAGAGAAGGATACGATCAAAAGCAACTCGTGGAAGTTAGAGCAGAGGCCATTGAAGTCGCTCGTACGCTGCAGGTCGAC	DPH1 truncation and epitope tagging (C-terminal)
F4- *DPH1*	AGAAATATAAATTCCTCATCCTGTGTTATAGAGAATCTTGGTGTTATCATTATAGTTCAGAAGTGGAATTCGAGCTCGTTTAAAC	DPH1 truncation and epitope tagging (N-terminal)
R3- *DPH1*	CCAATAAATCTTCTTCTTGGTTGTTTTTTAGATTCTGTAGAGCCACTCATGCACTGAGCAG	DPH1 truncation and

	CGTAATCTG	epitope tagging (N-terminal)
R3.1- *DPH1*	TTGTAGTTAGAGGGCAATAATTTGATGGCTTCATTCAACTCTTTGTCATTGCACTGAGCAGCGTAATCTG	DPH1 truncation and epitope tagging (N-terminal)
R3.2- *DPH1*	TCACTTATAATCAATGAGTAAATCAGCAAACCTTCAGGCATCTGTAGGGCTATTCTTTTAGCATTGCACTGAGCAGCGTAATCTG	DPH1 truncation and epitope tagging (N-terminal)
R3.3- *DPH1*	TCATCAATACAGCATGCACCATAAGACACATCCCCCATTACTAGAGTTTCGCACTGAGCAGCGTAATCTG	DPH1 truncation and epitope tagging (N-terminal)
R3.4- *DPH1*	AGTACTTTAATCTTTGTAACGTCAATAGGAACTAAACACGAATGAGCGTAGCACTGAGCAGCGTAATCTG	DPH1 truncation and epitope tagging (N-terminal)

6.1.5 Antibodies

All antibodies used in this study were obtained from Santa Cruz. For western blot detection of proteins and for coupling of Dynabeads (Invitrogen) prior to use in co-immunoprecipitation assays the following antibodies were used: monoclonal primary antibodies anti-HA, anti-c-Myc, anti-His6 and anti-CBP. The corresponding secondary antibodies were: anti-mouse, anti-rabbit and anti-goat.

6.1.6 Cultivation of bacterial strains

E. coli cultures were grown in Luria-Bertani (LB) medium containing 0.5% (w/v) Bacto yeast extract, 1% (w/v) Bacto tryptone and 0.5% (w/v) sodium chloride. To select plasmids LB was supplemented with ampicillin to a final concentration of 100 μg/ml. *E. coli* strains were grown at 37°C, while the liquid cultures were shaken during incubation.

6.1.7 Cultivation of yeast strains

S. cerevisiae strains were routinely grown at 30°C for 2-3 days in YEPD (Yeast Extract, Peptone, Dextrose) medium containing 1% (w/v) Bacto yeast extract, 2% (w/v) dextrose and 2% (w/v) Bacto peptone. Minimal synthetic medium (SD) consisted of 0.81% (w/v) Difco yeast nitrogen base without amino acids and 2% (w/v) dextrose (Sherman 1991). Strains with auxotrophic markers were propagated by addition of the following amino acids to the SD medium: adenine hemi-sulphate (40mg/l), L-leucine (120mg/l), L-histidine (20mg/l), L-tryptophan (20mg/l), L- methionine (20mg/l) and Uracil (20mg/l). 2% (w/v) Agar-Agar were added to the media before autoclaving to prepare plates.

6.2 Methods

6.2.1 Isolation of plasmid DNA from bacterial cultures

Plasmid extraction from over night bacterial culture was performed using Plasmid Mini Kit1 (OMEGA Bio-TEK) according to manufacturer's instructions.

6.2.2 Isolation of genomic DNA from yeast cultures

Isolation of yeast genomic DNA was performed after the desired strain was grown in 5ml liquid selective culture over night at 30°C. The cells were collected by spinning at 4000 rpm for 2-3 min. The pellet was washed with 1ml distilled water before they were centrifuged at 4000 rpm. The cells were resuspended in 200 µl breaking buffer (2% Triton X100, 1% SDS, 100mM NaCl, 10mM Tris/HCl pH8.0, 0.1mM EDTA), 200 µl Phenol-Chloroform-Isoamyl alcohol and a volume of 250ml of glass beads were added, before breaking the cells open in the bead beater for 1min. This mix was centrifuged for 5 min. at 14000 rpm before 150 µl of the clear phase on top was harvested. The DNA was precipitated by addition of 1ml 96% ethanol and gently inverted before the supernatant was dried and resuspended in 300µl 1x TE (0.1M Tris-HCl pH8 and 1mM EDTA).

6.2.3 Transformation protocols for E.coli

6.2.3.1 *E.coli* transformation (chemical)

1-2 µl of plasmid was added to 120 µl chemically competent *E.coli* cells (DH5α). This mix was incubated on ice for 30 min. before heat shocked at 42°C for 90 sec. Following this, the cells were chilled on ice for 2 min. before the addition of 1 ml Luria Broth. The *E.coli* were incubated at 37°C for one hour while shaking. Finally the cells were collected by centrifugation for 1 min. at 14000 rpm before they were spread on LB/Amp plates containing 100µg/ml Ampicillin. Colonies were allowed to grow over night at 37°C.

6.2.3.2 *E.coli* transformation (electroporation)

1-2 ml plasmid was added to 120 ml electrocompetent *E.coli* and transferred into a cuvette. An electric pulse of 2.5V was applied followed by the addition of 1 ml Luria Broth. The transformed *E.coli* were allowed to incubate at 37°C for one hour before they were collected by centrifugation and spread onto LB/Amp plates containing 100µg/ml Ampicillin. Colonies were allowed to grow over night at 37°C.

6.2.4 *S. cerevisiae* transformation procedures

6.2.4.1 Short transformation protocol for S. cerevisiae

This protocol was adapted from (Chen et al. 1992) and was routinely performed for plasmid transformation into yeast. Liquid yeast culture was grown over night and a 250 µl aliquot was pelleted by centrifugation at 4000rpm for 5 min. The pellet was

resuspended in 100 µl of one step transformation mix (800 µl 40% (w/v) PEG (polyethylene glycol, MW 3350), 200 µl 1M lithium acetate, 100 µl 1M DTT), 5 µl of 10mg/ml single stranded salmon sperm DNA (previously denatured at 95°C for 10 min) and 1µg of plasmid DNA. The mixture was vortexed and heat shocked at 42°C for 30min. The transformed yeast cells were collected by centrifugation at 4000rpm for 3 min. and washed with 1 ml sterile water. After centrifugation (4000rpm for 3 min.) the cells were resuspended in 100 µl sterile water and plated on appropriate media. The transformed cells were allowed to incubate at 30°C for 2-3 days.

6.2.4.2 High efficiency transformation protocol for *S. cerevisiae*

The yeast transformation protocol was based on (Schiestl and Gietz 1989) and was used for endogenous gene disruption or for N- and C-terminal epitope tagging. 40ml of liquid culture (grown from an overnight culture) were incubated at OD_{600} 0.5 and allowed to grow until OD_{600} 1.5. The cells were collected at 4000rpm for 5 min. and washed with 30 ml sterile water before they were collected again (centrifugation at 4000rpm for 5 min). The pellet was resuspended in 100 µl Lithium Acetate (100mM) and incubated at 30°C for 30 min while shaking. 100 µl aliquot was used for each single transformation. The cells in the aliquot were collected (centrifugation at 8000rpm for 15sec) and the pellet was resuspended in the transformation mix (240 µl 50% (w/v) PEG (polyethylene glycol), 36 µl Lithium acetate (1M), 50 µl single stranded salmon sperm DNA (previously denatured at 95°C for 10 min) and 34 µl DNA (precipitated and purified PCR product). This transformation mix was incubated at 30°C for 30 min followed by a heat shock step of 50 min at 42°C. The transformed cells were pelleted at 8000 rpm for 15 sec and resuspended in 1 ml fresh YEPD. In order to allow the

antibiotic marker to be expressed the mix was incubuated at 30°C for 2-3 hours while shaking. The cells were harvested and washed with 1 ml sterile water before they were plated on appropriate media and allowed to grow for 2-3 days.

6.2.5 Polymerase chain reaction

6.2.5.1 *Taq* polymerase PCR protocol

Routine PCR reactions were carried out using KAPA*Taq* polymerase (Kapa Biosystems) according to manufacturer's instructions with 1µM of each primer and under normal PCR conditions. Typical cycling conditions were an initial 95°C denaturation step for 1 min; 25-35 cycles of denaturation at 95°C for 30 sec followed by annealing at a primer-dependent temperature for 30 s, an elongation step at 72°C for 1 min/kb and a final extension at 72°C for 10 min. All PCR reactions were carried out using Sesoquest Thermo-Cycler PCR machines.

6.2.5.2 Proofreading PCR

Phusion high-fidelity polymerase and high-fidelity buffer (USB) were used according to manufacturer's instructions when its proofreading property was desired. In contrast to KAPA*Taq* polymerase reactions, the elongation step was reduced to 20 sec per kb.

6.2.5.3 Sequencing PCR

Sequencing PCR was performed using the following mix: 2 µl primer, 4 µl plasmid, 1 µl Big Dye (provided by PNACL sequencing service), 3 µl sequencing buffer and 2 µl distilled water. The PCR conditions were: initial denaturation step: 94°C for 5 min, followed by cycles of 96°C for 10 sec and annealing and extension step: 60°C for 4min, and the final step: 15°C for ∞. The denaturation, annealing and elongation cycle was repeated 29 times. Following sequencing PCR, the product was purified using Performa DTR Gel Filtration Cartridges (Edge BioSystems) according to manufacturer's instructions before sending for sequencing by PNACL (University of Leicester sequencing service).

6.2.5.4 Yeast colony PCR

In order to test freshly transformed yeast, colony PCR was performed without prior DNA isolation from the colony. A very small amount of yeast cells was picked from a colony and transferred into a 0.2 ml PCR tube containing 10 µl 1x SPZ solution. 1x SPZ solution stock was previously prepared as follows: for a 50 ml SPZ stock 30 ml 2M sorbitol, 4.05 ml (1M) Na2HPO4, 0.95 ml NaH2PO4 and 15ml water was mixed and frozen at -20°C. 2.5 mg/ml Zymolyase 100-T was added to 1x SPZ solution before use. The yeast cells suspended in SPZ solution were incubated for 30 min at 37°C then 5 min 95°C in a PCR Thermo-Cyler. 90 µl sterile water was added and after mixing 2 µl of this template was used for a 20 µl PCR reaction with KAPA*Taq* polymerase.

6.2.6 Agarose gel electrophoresis

In order to visualize DNA or to separate a pool of different sized DNA fragments from each other, samples were routinely run on a 0.8 – 2 % agarose gel depending on the size of the fragments. To do so the samples were first mixed with 0.25x their volume of 5x loading dye containing 10% (w/v) Ficoll type 400, 0.1 M EDTA, 0.2% (v/v) bromophenol blue and 0.5% (w/v) SDS. Agarose was melted in 1x TBE buffer (90 mM Tris base, 90 mM boric acid, 2 mM EDTA pH 8.0) and the solution was supplemented with ethidium bromide (0.5 μg/ml) prior to polymerization. 1x TBE buffer was also used as running buffer. The appropriate DNA molecular ladders (GeneRuler, Fermentas) were run in parallel to allow determination of the size of the fragments. After the samples had run for the desired amount of time they were visualized using a UV light transilluminator.

6.2.7 DNA isolation from agarose gels

The elution of DNA bands from agarose gels was performed using Gel Extraction Kit (OMEGA Bio-TEK) according to manufacturer's instructions.

6.2.8 Restriction Digestion

Restriction digestion of DNA samples was performed using restriction enzymes from Fermentas or New England Biolabs together with the according buffers according to manufacturer's instructions.

6.2.9 Ethanol precipitation of PCR products

In order to concentrate DNA, ethanol precipitation of PCR products was performed. To do so the PCR product was mixed with 0.1x the starting volume 3M sodium acetate (pH 4.8) and 2x the volume ice cold 100% ethanol. This mixture was incubated at -20°C for 30 min. The precipitated DNA was centrifuged at 4°C and 13000 rpm for 30 min. The supernatant was discarded and the DNA was washed with 1 ml ice cold 70% ethanol and centrifuged again at 4°C and 13000 rpm for 5 min. The ethanol was discarded and the precipitated DNA was dried before it was resuspended in 34 µl 1x TE (0.01M Tris-HCl pH8 and 1mM EDTA).

6.2.10 Ligation

Ligation reactions of blunt-end DNA or sticky-end DNA was performed using T4-DNA ligase (5U/µl) and 10x reaction buffer (Fermentas). The ligation mix (1 µl ligase, 1 µl buffer, 4 µl distilled water, 3 µl insert and 1 µl plasmid DNA) was incubated either at RT for 2 hours or at 16°C over night before transformation into *E. coli*. Vector and insert DNA were typically used at a 1:3 ratio.

6.2.11 Gene manipulation procedures

6.2.11.1 PCR-based *in vivo* epitope tagging

N- and C-terminal tagging of a desired gene was performed according to previously published *in vivo* PCR-based one step epitope tagging protocols by (Knop et al. 1999) using appropriate S3/S2 primers (listed under 6.1.4). S2/S3 primers were

designed with a 50bp 5' overhang which is homologous to the upstream region of the desired gene and were used to amplify a desired cassette containing a marker gene and a tag. Epitope tagging occurred *in vivo* homologous recombination after the PCR product was transformed following the high efficiency procedure mentioned in 6.2.4.2. Tagged genes were confirmed via PCR using ORF specific primers (listed under 6.1.4) as well as western blot detection with appropriate antibodies.

6.2.11.2 PCR-based *in vivo* gene deletion

Gene deletions were performed using *in vivo* PCR-based one step gene disruption protocol described by (Wach et al. 1994) using the desired marker plasmids, YDpKl-Leu, YDpKl-Ura or YDpSp-His(Jablonowski et al. 2001) and the appropriate knock-out primers (listed under 6.1.4) as previously described in. Knock-out primers were designed with a 5'overhang homologous to the upstream and downstream region of the desired ORF. The amplified knock-out cassette was transformed using the high efficiency protocol described under 6.2.4.2 and gene deletion occurred in vivo via homologous recombination. Gene deletions were

confirmed via PCR from genomic DNA using ORF specific primers (listed under 6.1.4).

6.2.12 Phenotype assays for *S. cerevisiae*

6.2.12.1 Sordarin phenotype

In order to test *S. cerevisiae* strains for their sordarin phenotype, YEPD agar media was supplemented with 20 µg/ml sordarin sodium salt from *Sordaria araneosa* (Sigma-Aldrich) when glucose was the carbon source and 5 µg/ml sordarin when glucose was the carbon source. The strains were allowed to grow for 2-4 days before they were assed for their sordarin phenotype.

6.2.12.2 Diphtheria toxin (DT) phenotype

In order to test the DT phenotype *S. cerevisiae* strains they were transformed with the *URA3* plasmid pLMY101, a kind gift from R. John Collier (Harvard Medical School, Boston, Mass.). This plasmid allows DT F2 fragment expression under the transcriptional control of yeast *GAL1* promoter, which allows conditional expression of the toxin on galactose-inducing medium. In order to reduce the level of DT expression, *BamH1* fragment with the DT F2 insert from pLMY101 was cloned into *GAL-S* vectors p415-*GALS* and p416-*GALS* (Mumberg et al. 1994) respectively, which are *CEN-ARS* plasmids carrying a truncated *GALS* promoter. The resulting p415-*GALS*-DT (pSU8) and p416-*GALS*-DT (pSU9), allowed conditional DT expression on galactose-inducing medium.

6.2.12.3 Frameshift reporter assay

Translational frameshift reporter assay involved the *lacZ* reporter plasmids pJD204.0 (wildtype control), pJD204.-1 (-1 frame) and pJD204.+1 (+1 frame) (Harger et al. 2001) (kindly provided by G. Kinzy, Robert Wood Johnson Medical School, Piscataway, USA). Translational fidelity was assayed as previously described by Ortiz *et al.* 2006 (Ortiz et al. 2006b). For measurement of β-galactosidase readouts from the *lacZ* reporter gene, three biological replicates (three different colonies from the plasmid transformations) of each strain were used for two technical replicates. Overnight cultures grown in SD media were used for the assay. 800µl of liquid culture was washed with sterile water and collected by centrifugation at 4000 rpm for 5 min. The pellet was resuspended in 1ml Z-buffer (for a 10ml Z-buffer stock: 60 mM Na_2PO_4, 40 mM Na_2HPO_4, 10 mM KCl, 1 mM $MgSO_4$, pH 7.0 before addition of 50 mM β-mercaptoethanol, 400 µl 0.1% (w/v) SDS 600 µl chloroform). The reaction was started by addition of 200 ml ONPG (4 mg/ml in Z-buffer without β-mercaptoethanol) and incubated at 30°C, while the time was measured until the solution started turning yellow. The reaction was stopped by adding 400 µl 1M Na_2CO_3 and the sample was centrifuged at 4000 rpm for 5 min. The supernatant was collected and the OD_{400} and OD_{550} was measured. β-galactosidase activity was calculated using the following formula:

Activity = $1000*(OD_{420}-(1.75*OD_{550})/(time*volume*OD_{600})$

In order to minimize measurement errors the above protocol was adjusted by using protein extracts instead of the cell solution. Total protein extracts from the yeast strains transformed with the lacZ reporter plasmids were prepared according to the protocol described under 6.2.13.1. The protein extracts were used for measurement of β-galactosidase activity on the same day they were prepared to avoid protein degradation during storage and thawing. 5-10 µl of the protein extract was mixed with 800 µl Z-buffer (without β-mercaptoethanol or chloroform). The reaction was started by addition of 200 µl of ONPG (4 mg/ml in Z-buffer without β-mercaptoethanol or chloroform) and the mix was incubated at 30°C until the solution turned yellow. The reaction was stopped by addition of 400 µl 1 M Na_2CO_3 and the OD_{420} was measured. β-galactosidase activity (unit = nM cleaved ONPG / min / mg protein) was calculated using the following formula:

Activity = ((OD_{420}*1.4)/0.0045)/(amount of protein*extract volume*time)

6.2.13 Protein biochemistry

6.2.13.1 Isolation of whole cell protein extract from yeast

To prepare whole cell protein extract yeast strains were grown overnight in the appropriate media. This culture was used to inoculate a fresh 50 ml culture and allowed to grow until OD_{600} 1.5 was reached. The cells were harvested at 4°C and 4000rpm for 5 min and washed twice with 30 ml sterile water. The pellet was resuspended in 400 µl breaking buffer (50mM Hepes-KOH pH7.3, 60mM Sodium acetate, 5mM Manganese acetate, 0.1% Triton X100, 10% Glycerol, 1mM Sodium fluoride, 20mM

Glycerophosphate, 1mM DTT) supplemented with Proteinase inhibitor cocktail (Roche). ~300µl volume of glass beads were added and the cells were broken in a bead beater for 1 min. at highest speed. This was followed by centrifugation at 4°C and 13000rpm for 5 min. to separate and harvested the supernatant containing the extracted protein. After another round of centrifugation at 4°C and 13000rpm for 20-30 min. The clear supernatant was collected and used for consequent experiments. The protein concentration of each sample was measured using the NanoDrop spectrometer.

6.2.13.2 Polyacrylamide gel electrophoresis

In order to separate a pool of proteins from each other they were run SDS-PAGE gels alongside an appropriate pre-stained protein ladder (PageRuler, Fermentas). If not otherwise stated, SDS-PAGE gels were composed of a 5% stacking gel (5% (v/v) acryl amide, 125mM Tris/HCl pH 6.8, 0.1% (w/v) SDS) and a 12% separation gel (12% (v/v) acryl amide, 375mM Tris/HCl pH 8.8, 0.1% (w/v) SDS). Prior to loading, protein samples were denatured in 1x Laemmli buffer (0.25M Tris-HCl, pH 6.8, 4% (w/v) SDS, 20% (v/v) ß-mercaptoethanol, 0.02% (w/v) bromphenol blue, 40% (v/v) glycerol) and heated to 90°C for 10 min. Proteins samples were run in 1x running buffer ((0.025 Tris-HCl, 0.192M glycine, 0.1% SDS) at 200 volts until the desired seperation of the pre-stained band in the protein ladder was reached.

6.2.13.3 Western blotting

Routinely 60 µg of each protein sample along with an appropriate marker (GeneRuler, Fermentas) was run on SDS-PAGE gels and used in the Western blot

assay. The proteins were transformed from the gel to a PVDF membrane (Millipore) activated by 20% (v/v) methanol in 1x running buffer (0.025 Tris-HCl, 0.192M glycine, 0.1% SDS) and blotted for 1 -2 hours at 100 volts using transfer buffer (0.025 Tris-HCl, 0.192M glycine, 0.1% SDS, 20% (v/v) methanol). The transfer was performed in wet conditions using a Bio-Rad apperatus. After the transfer the PVDF membrane was incubated in blocking solution (5%(w/v) milk in 1x TBST (20mM Tris/HCl pH7.6, 137mM Sodium chloride, 0.3% Tween 20) for 30min. Following this the membrane was incubated for 2 hours in 5%(w/v) milk in 1x TBST containing the desired primary antibody in dilution of 1:1000 – 1:10 000 according to manufacturer's instructions. After three wash steps with 1x TBST for 15min., the membrane was incubated for 2 hours with the appropriate secondary antibody diluted in 5%(w/v) milk in 1x TBST according to manufacturer's instructions. After three wash steps with 1x TBST for 15min., the protein bands were then visualized using the ECL-Amersham Bioscience according to manufacturer's instructions.

6.2.13.4 Stripping PVDF membranes

In order to remove the antibodies from proteins blotted onto a PVDF membrane and to repeat immuno detection of the same samples, the membrane was stripped of the bound antibodies by incubation in 1% SDS in 0.1M glycine at pH 2.8. After a 30 min. incubation the membrane was washed four times for 15min. in 1x TBST (20mM Tris/HCl pH7.6; 137mM Sodium chloride, 0.3% Tween 20).

6.2.13.5 Co-Immunoprecipitation

Detection of N- and C-terminal HA and c-myc tagged proteins in co-immune precipitation (co-IP) assays was performed using magnetic Dynabeads (Invitrogen, #101-03D). To do so total protein extracts were prepared as described under 6.2.13.1. A small aliquot of the whole cell protein extract (routinely 50 µl) was set aside for detection of the proteins in the pre-IP sample. First, Dynabeads were coupled with the desired antibody according to manufacturer's instructions. 3 mg of total protein was applied to Dynabeads and immunoprecipitated according to manufacturer's instructions. IP and pre-IP samples were loaded on SDS-PAGEs (10-15%) and detected via Western blot using the appropriate antibodies.

6.2.13.6 TAP purification

Tandem affinity purification was performed according to (Rigaut et al. 1999) and (Puig et al. 2001). The TAP tag allows a tandem of two consecutive purification steps: first the Protein A domain at the C-terminal end of the TAP tag is immunoprecipitated with Dynabeads previously coupled with IgG primary antibody. The bound protein is eluted by cleavage of the linker sequence by AcTEV Protease (Invitrogen). The second purification step is performed with CBP-coupled Dynabeads, which binds the CBP domain of the TAP tag.

A total volume of 2 litres of yeast culture was inoculated from overnight cultures and grown to OD600 1.5. The cells were harvested by centrifugation at 4000rpm for 20 min and washed twice with sterile water. Cell pellets were frozen at -80°C overnight before they were disrupted at the following day. The cell pellet was resuspended in 10

ml buffer (10mM K-HEPES pH7.9, 10mM KCl, 1.5mM MgCl2, 0.5mM DTT, 0.5mM PMSF, 2mM benzamidine, Complete Protease Inhibitor Cocktail (Roche) and the cells were disrupted with the bead beater. The crude extract was adjusted 10 200 mM KCl by addition of the appropriate amount of 2 M KCl. Two consecutive centrifugation steps were performed at 4°C: 35000rpm for 30 min followed by 45000rpm for 1hr. The cleared extract was dialyzed against buffer D (20mM K-HEPES pH7.9, 50mM KCl, 0.2mM EDTA pH8.0, 0.5mM DTT, 20% glycerol, 0.5mM PMSF, 2 mM benzamidine) for 4hrs at 4°C. The dialyzed volumes of the samples varied from 7 - 10 ml and was frozen at -80°C overnight before the actual TAP purification was performed.

200 µl IgG Sepharose beads were washed with 5 ml IPP150 buffer (10 mM Tris-Cl at pH 8.0, 15 0mM NaCL, 0.1% NP-40) at RT for 5 min. before the IPP150 buffer was removed. Each 10 ml extract buffer was adjusted by addition of 50 µl 2M Tris-HCl at pH 8.0, 200 µl 5M NaCl and 100 µl NP-40. 10ml of this adjusted extract was added to the washed IgG Sepharose beads and incubated at 4°C while gently shaking. The unbound liquid was removed and the beads with the bound protein were washed three times with 10 ml IPP150 buffer. Following this the beads were washed once with 10 ml TEV-cleavage buffer (10mM Tris-HCl at pH8.0, 150mM NaCl, 0.1% NP-40, 0.5mM EDTA and 1mM DTT) at 16°C. The liquid was removed and the bound protein was eluted by incubation with 1 ml TEV cleavage buffer and 100 units of AcTEV Protease (Invitrogen) for 2hrs at 16°C. The eluate was collected and the remaining eluate was washed out with 200 µl TEV cleavage buffer. 200 µl calmodulin affinity beads were prepared by washing with 5 ml IPP150 buffer in a new column. The IPP150 buffer was removed and the eluate was prepared by adding 3 volumes of IPP150 calmodulin-

binding buffer (10 mM β-mercaptoethanol, 10 mM Tris-HCl at pH 8.0, 150 mM NaCl, 1 mM MgAc, 1 mM imidazole 2 mM $CaCl_2$ and 0.1% NP-40) and 1 µl of 1M $CaCl_2$ per ml of eluate. The adjusted eluate was transferred to the calmodulin affinity beads and incubated for 2hrs at 4°C while rotating. The unbound material was removed and the beads were washed three times with 10 ml IPP150 calmodulin-binding buffer. The bound protein was eluted in fractions of 200 µl with IPP150 calmodulin elution buffer (10 mM β-mercaptoethanol, 10 mM Tris-HCl at pH 8.0, 150 mM NaCl, 1 mM MgAc, 1 mM imidazole 2 mM $CaCl_2$ and 0.1% NP-40, 2 mM EGTA).

6.2.13.7 *In vitro* ADP-Ribosylation

In vitro ADP-Ribosylation assays were performed by Dr. Shihui Liu at the National Institute of Health, Bethesda, USA. Yeast cell extracts were prepared as described previously (Liu and Leppla 2003b). ADP-ribosylation reactions were performed at 37^{o}C for 1 hour in a volume of 40 µl ADP-ribosylation buffer (20 mM Tris-HCl, pH 7.4; 1 mM EDTA; 50 mM DTT) containing 50 µg of yeast extract, 50 ng fully-nicked DT, and 10 µM 6-Biotin-17-NAD (Trevigen). Samples were then mixed with SDS sample buffer, boiled for 5 min and run on 4−25 % SDS-PAGE gels (Invitrogen). The proteins were transferred to nitrocellulose membranes and western blotting was performed using streptavidin-IR conjugate (Rockland Immunochemicals, Gilbertsville, PA) and scanned on an Odyssey Infrared Imager (LICOR Biosciences, Lincoln, NE). Two unknown non-specific bands (indicated by *) served as the even loading controls.

6.2.13.8 Expression and purification of His6-tagged eEF2

BY4741 wt strain as well as *dph1*, *dph5*, *ylr142w* and *ybr246w* mutant strains were transformed with *LEU*-marked pTKB612 plasmid (Jorgensen et al. 2005), which expresses His-tagged eEF2. Jorgensen *et al.* showed that the eEF2-His construct can complement a *eft1*Δ *eft2*Δ double mutant confirming that the construct is functional. In order to express and purify eEF2 for MS/MS analysis 750ml of yeast culture were grown in YPD to an OD_{600} 2.0 and harvested by centrifugation. The pellet was resuspended in 3ml B60 buffer without DTT (50mM Hepes-KOH pH 7.3, 60mM KAc, 5mM MgAc, 0.1% Triton X100, 10% Glycerol, 1mM NaF, 20mM Glycerophosphate, Protease Inhibitor complete tablet (Roche)) and cells were lysed in a bead beater. The lysate was centrifuged twice at 13 500rpm for 30 min. and the protein concentration measured with a NadoDrop spectrophotometer. 5mg total protein was applied to 2mg anti-His-tag-Dynabeads and purified according to manufacturer's instructions (Invitrogen, #101-03D). The identity of the purified protein was confirmed by Western Blot using anti-6xHis antibody (Abcam, #ab18184).

6.2.13.9 Analysis of Diphthamide pathway modifications of eEF2 by mass spectrometry

Crude yeast eEF2 preparations were separated by SDS-PAGE using 4-12% Bis-Tris precast gels (Invitrogen, Carlsbad, USA) and the area of the gel containing eEF2 was excised after staining with Instant Blue Coomassie (Expedeon, Cambridge, UK). In-gel digests were performed using trypsin, subsequent to reduction and alkylation with dithiothreitol and iodoacetamide, with the resulting peptides cleaned over C18

columns. Peptides were then analysed via HPLC-MS/MS using a Dionex U300 HPLC (Dionex California) with a 15 cm PepMap C18 column coupled to a Thermo Orbitrap Velos mass spectrometer (Thermo Fisher Scientific, Bremen, Germany). The peptides were eluted from the C18 column at 300 nL/min over 120 min using a linear 5-90%(v/v) acetonitrile gradient. The Orbitrap Velos was operated in positive ion mode, with an ion source voltage of 1.2 kV and capillary temperature 200°C, using a lock mass of 445.120024. The initial survey scan was performed at 60000 resolution, FTMS scanning from 335-1800 Da. The top 15 most intense ions were selected for MS/MS sequencing, using collision-induced dissociation (CID; MS/MS charge state 1+ rejected, >2+ accepted). Protein identification was performed using MaxQuant 1.2.2.5 (Cox and Mann 2008) against a proteome database generated from the *Saccharomyces* Genome database (Cherry et al.) in 2010. Manual annotation of the modified peptide spectra corresponding to the modified eEF2 peptide and generation of extracted ion chromatograms were done using the Thermo Xcalibur software for spectra visualisation. Mass spectrometry analyses was performed and analysed at the University of Dundee in collaboration with Prof. Mike Stark and Dr. Sara ten Have.

6.2.14 Bioinformatic data mining of *DPH* genes

DRYGIN database (http://drygin.ccbr.utoronto.ca/, (Baryshnikova et al. 2010; Costanzo et al. 2010; Koh et al. 2010), which is based on quantitative genetic interactions of *S. cerevisiae* derived from the SGA double-mutant arrays conducted in the C. Boone lab, University of Toronto, was used to identify putative Dph synthesis genes.

In addition, Yeast Fitness Data Base, FitDB (http://fitdb.stanford.edu/fitdb.cgi), was used for data mining in order to identify genes that phenocluster with known Dph genes. The gene-gene relationship studies in FitDB are based on homozygous co-fitness profiling according to Hillenmeyer *et al.* (2008 and 2010) (Hillenmeyer et al. 2008; Hillenmeyer et al. 2010).

6.2.15 Multi-alignment tool

DNA sequences of the desired ORFs were obtained from NCBI website (http://www.ncbi.nlm.nih.gov/gene/) and aligned with the help of the multi-alignment tool, Jalview (http://www.jalview.org/) from the University of Dundee.

6.2.16 Statistical Analysis

The relative values for +1 and -1 frameshifting were statistically analyzed using one-way ANOVA followed by Dunnett's multiple comparison post test and was performed with Graphpad Prism 5.0 software (Roy et al. 2010).

APPENDICES

7 Appendices

7.1 Appendix 1: Mass spectrometry analyses of TAP-isolated eEF2 from wt, *dph1*Δ and *ylr143w*Δ strains

The following spectra from mass spectrometric analysis of TAP-isolated eEF2 tryptic peptide 686-VNILDVTLHADAIHR-700 of wildtype, *dph1*Δ and *ylr143w*Δ mutant strains only show unmodified His_{699}.

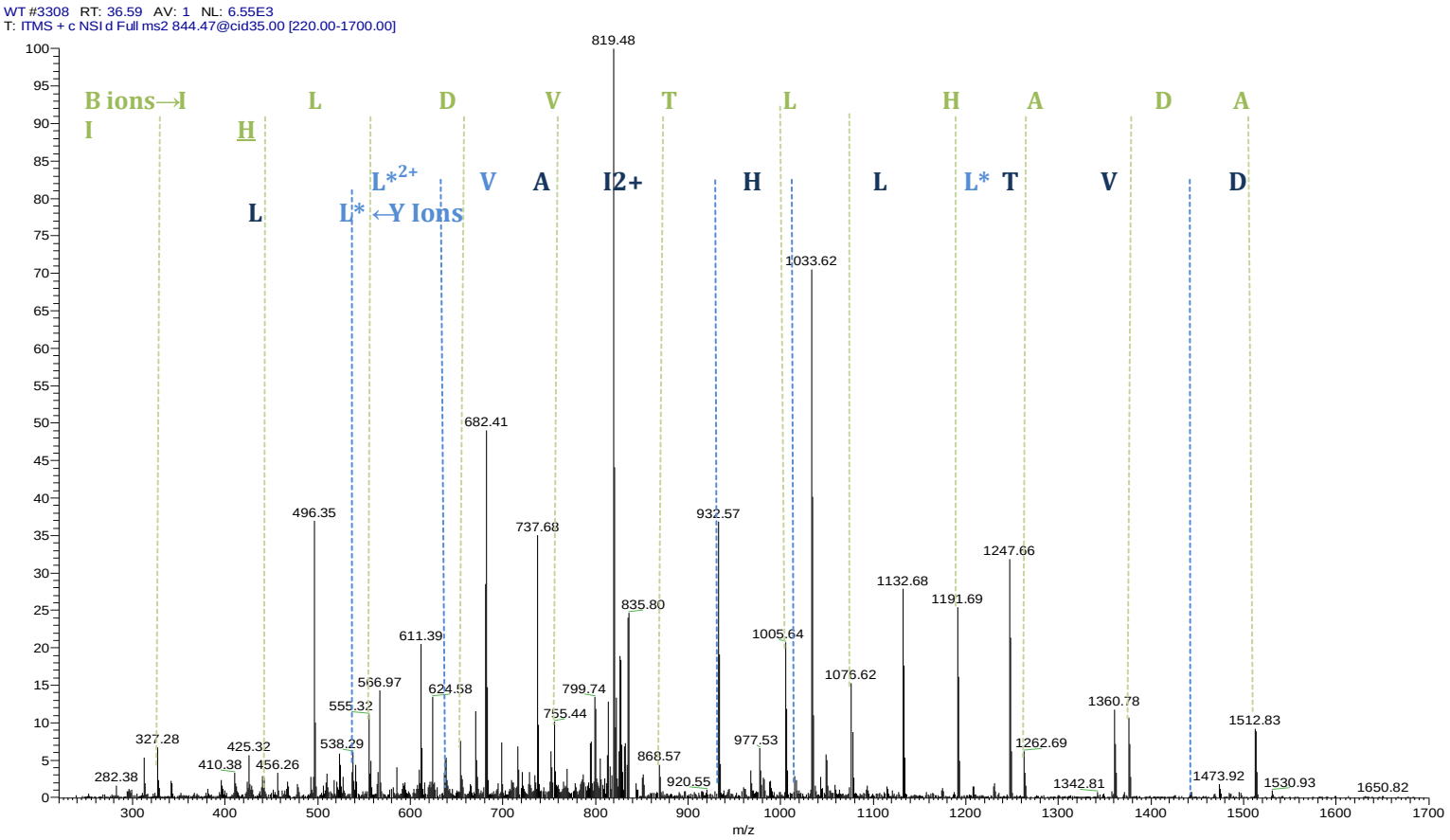

Figure A2. Mass spectrometry spectra of wildtype unmodified His_{699} in eEF2 tryptic peptide.

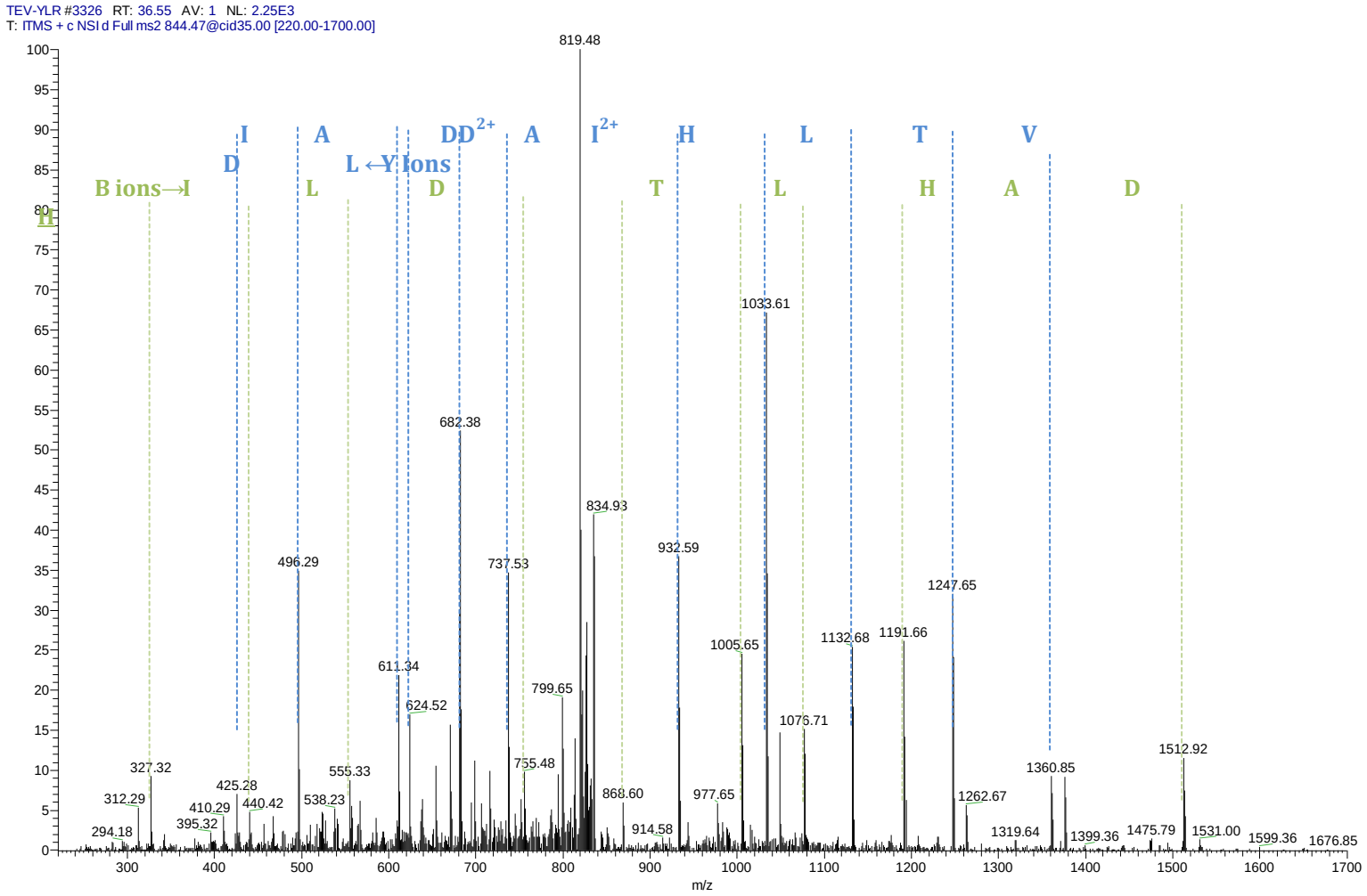

Figure A3. Mass spectrometry spectra of *ylr143wΔ* unmodified His_{699} in eEF2 tryptic peptide.

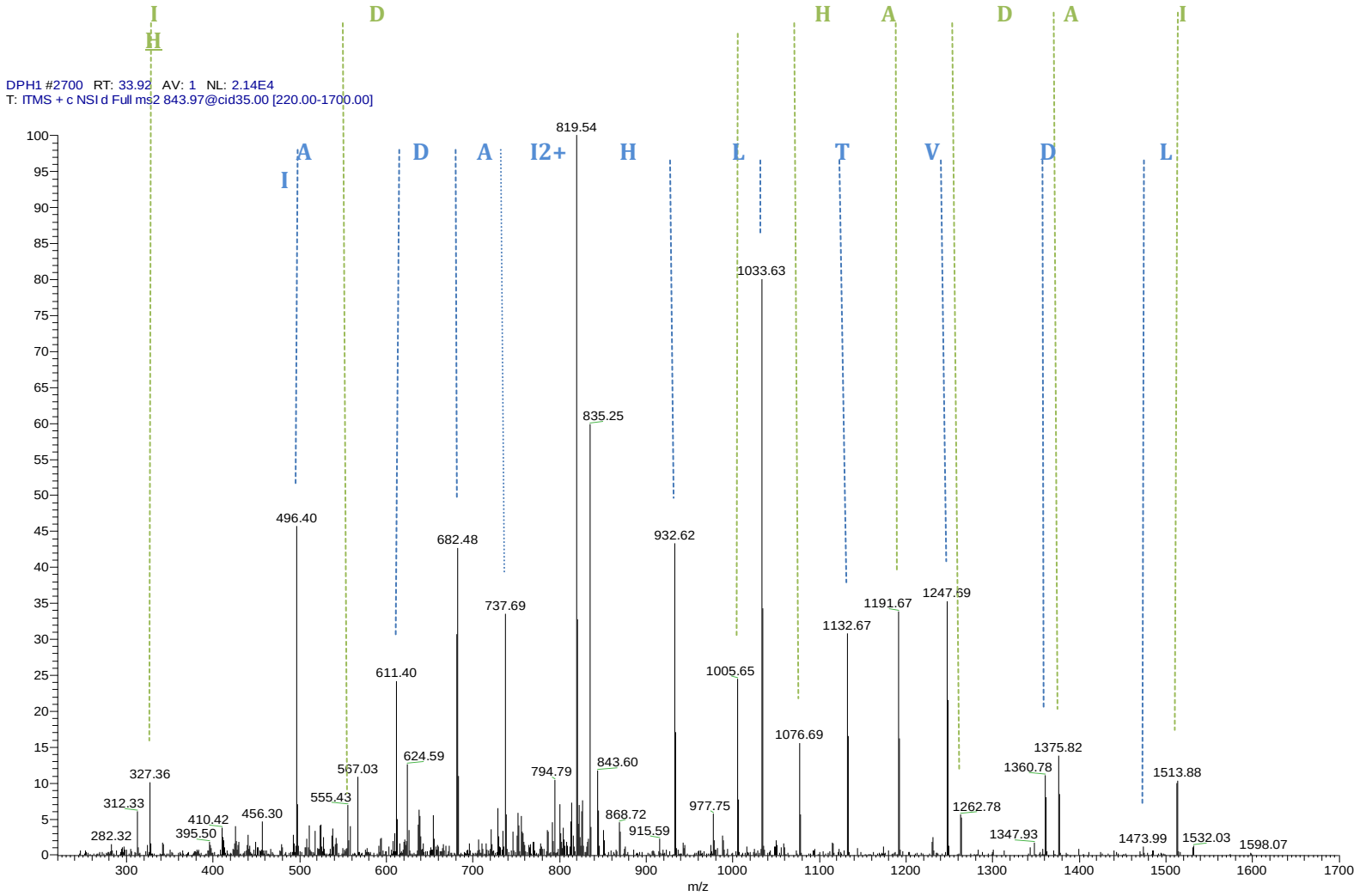

Figure A4. Mass spectrometry spectra of *dph1*Δ unmodified His_{699} in eEF2 tryptic peptide.

7.2 Appendix 2: The amidation step of diphthamide biosynthesis in yeast requires DPH6, a gene identified through mining the DPH1-DPH5 interaction network

OPEN ACCESS Freely available online

PLOS | GENETICS

The Amidation Step of Diphthamide Biosynthesis in Yeast Requires *DPH6*, a Gene Identified through Mining the *DPH1-DPH5* Interaction Network

Shanow Uthman[1☯], Christian Bär[1,2☯¤], Viktor Scheidt[2], Shihui Liu[3], Sara ten Have[4], Flaviano Giorgini[1], Michael J. R. Stark[4]*, Raffael Schaffrath[1,2]*

1 Department of Genetics, University of Leicester, Leicester, United Kingdom, **2** Institut für Biologie, FG Mikrobiologie, Universität Kassel, Kassel, Germany, **3** Laboratory of Parasitic Diseases, National Institute of Allergy and Infectious Diseases, National Institutes of Health, Bethesda, Maryland, United States of America, **4** Centre for Gene Regulation and Expression, College of Life Sciences, MSI/WTB Complex, University of Dundee, Dundee, Scotland

Abstract

Diphthamide is a highly modified histidine residue in eukaryal translation elongation factor 2 (eEF2) that is the target for irreversible ADP ribosylation by diphtheria toxin (DT). In *Saccharomyces cerevisiae*, the initial steps of diphthamide biosynthesis are well characterized and require the *DPH1-DPH5* genes. However, the last pathway step—amidation of the intermediate diphthine to diphthamide—is ill-defined. Here we mine the genetic interaction landscapes of *DPH1-DPH5* to identify a candidate gene for the elusive amidase (*YLR143w/DPH6*) and confirm involvement of a second gene (*YBR246w/DPH7*) in the amidation step. Like *dph1-dph5*, *dph6* and *dph7* mutants maintain eEF2 forms that evade inhibition by DT and sordarin, a diphthamide-dependent antifungal. Moreover, mass spectrometry shows that *dph6* and *dph7* mutants specifically accumulate diphthine-modified eEF2, demonstrating failure to complete the final amidation step. Consistent with an expected requirement for ATP in diphthine amidation, Dph6 contains an essential adenine nucleotide hydrolase domain and binds to eEF2. Dph6 is therefore a candidate for the elusive amidase, while Dph7 apparently couples diphthine synthase (Dph5) to diphthine amidation. The latter conclusion is based on our observation that *dph7* mutants show drastically upregulated interaction between Dph5 and eEF2, indicating that their association is kept in check by Dph7. Physiologically, completion of diphthamide synthesis is required for optimal translational accuracy and cell growth, as indicated by shared traits among the *dph* mutants including increased ribosomal −1 frameshifting and altered responses to translation inhibitors. Through identification of Dph6 and Dph7 as components required for the amidation step of the diphthamide pathway, our work paves the way for a detailed mechanistic understanding of diphthamide formation.

Citation: Uthman S, Bär C, Scheidt V, Liu S, ten Have S, et al. (2013) The Amidation Step of Diphthamide Biosynthesis in Yeast Requires *DPH6*, a Gene Identified through Mining the *DPH1-DPH5* Interaction Network. PLoS Genet 9(2): e1003334. doi:10.1371/journal.pgen.1003334

Editor: Gregers Rom Andersen, Aarhus University, Denmark

Received September 23, 2012; **Accepted** January 7, 2013; **Published** February 28, 2013

Funding: We gratefully acknowledge support for this work from the Wellcome Trust (083524/Z/07/Z), by a grant from the U.S. National Institute of Allergy and Infectious Diseases Intramural Programme to SL (1ZIAAI000929-09), by joint research grants from the Biotechnology and Biological Sciences Research Council (BBSRC) to MJRS (BB/F0191629/1) as well as RS (BB/F019106/1), and by the HOPE Against Cancer Foundation for Leicestershire and Rutland through a OVCA1/DPH1 related PhD studentship (RM33G0118) awarded to SU. CB received support from the Department of Genetics, University of Leicester, and the Institute of Biology, Division of Microbiology, University of Kassel, Germany. RS gratefully acknowledges support from the Feodor Lynen Fellowship Alumnus Programme of the Alexander von Humboldt Foundation (3.1-3 FLFDEU-1037031), Bonn Bad Godesberg, Germany, and from the Royal Society (2008/R2 grant), UK. The funders had no role in study design, data collection and analysis, decision to publish, or preparation of the manuscript.

Competing Interests: The authors have declared that no competing interests exist.

* E-mail: m.j.r.stark@dundee.ac.uk (MJRS); schaffrath@uni-kassel.de, rs240@le.ac.uk (RS)

¤ Current address: Molecular Oncology Program, Spanish National Cancer Centre (CNIO), Melchor Fernandez Almagro 3, Madrid, Spain

☯ These authors contributed equally to this work.

Introduction

Regulation of biological processes by posttranslational modification can involve the function, distribution and interaction capabilities of the modified protein [1–3]. Though most modification pathways such as phosphorylation and ubiquitin conjugation target many different proteins, some exceptional ones uniquely target just a single polypeptide [4]. One prominent example is diphthamide formation on eukaryal translation elongation factor 2 (eEF2) [5]. Strikingly, this modification is pathobiologically important because it is hijacked for eEF2 inhibition by sordarin fungicides and by diphtheria toxin (DT) produced by pathovarieties of *Corynebacterium diphtheriae* that cause the severe human disease syndrome diphtheria [6–8]. Both agents efficiently block protein synthesis by inactivating the essential function of the modified translation factor, via stalling the diphthamide modified form of eEF2 on ribosomes and irreversible ADP ribosylation of eEF2, respectively [9–12]. Diphthamide itself is a highly modified histidine residue on eEF2 – 2-[3-carboxyamido-3-(trimethylamino)-propyl]-histidine – which is conserved from yeast (H_{699}) to man (H_{715}) (Figure 1) [5,8,13]. Intriguingly, it is absent from the bacterial eEF2 analog, EF-G, thus conferring immunity on the DT producer.

Among the archaea and eukarya, diphthamide formation involves a conserved biosynthetic pathway, which has been extensively dissected in *Saccharomyces cerevisiae* via isolation of

Author Summary

Diphthamide is an unusual modified amino acid found uniquely in a single protein, eEF2, which is required for cells to synthesize new proteins. The name refers to its target function for eEF2 inactivation by diphtheria toxin, the disease-inducing agent produced by the pathogen *Corynebacterium diphtheriae*. Why cells require eEF2 to contain diphthamide is unclear, although mice unable to make it fail to complete embryogenesis. Cells generate diphthamide by modifying a specific histidine residue in eEF2 using a three-step biosynthetic pathway, the first two steps of which are well defined. However, the enzyme(s) involved in the final amidation step are unknown. Here we integrate genomic and molecular approaches to identify a candidate for the elusive amidase (Dph6) and confirm involvement of a second protein (Dph7) in the amidation step, showing that failure to synthesize diphthamide affects the accuracy of protein synthesis. In contrast to Dph6, however, Dph7 may be regulatory. Our data strongly suggest that it promotes dissociation of eEF2 from diphthine synthase (Dph5), which carries out the second step of diphthamide synthesis, and that Dph5 has a novel role as an eEF2 inhibitor when diphthamide synthesis is incomplete.

mutant strains that confer resistance to growth inhibition by DT and sordarin. This has led to the identification of the diphthamide synthesis genes *DPH1-DPH5* [7,12,14–16] (Figure 1). The first step in diphthamide synthesis involves transfer of a 3-amino-3-carboxypropyl (ACP) radical from S-adenosyl-methionine (SAM) to the histidine imidazole ring, generating the ACP modified intermediate of eEF2 [17–19]. ACP radical transfer requires the proteins Dph1-Dph4 [16], where Dph1 and Dph2 are paralogous iron-sulfur cluster containing partner proteins that copurify and interact with Dph3, potentially as part of a multimeric complex [6,20–22]. Dph3 and Dph4 are thought to chaperone Dph1-Dph2 by maintaining their iron-sulfur clusters in redox states required for proper ACP radical generation. In line with this, Dph3 and Dph4 have electron carrier activities [23,24], while Dph3 (also known as Kti11 [25]) additionally partners with Elongator subunit Elp3 [6,20], an iron-sulfur cluster and radical SAM enzyme with roles in protein and tRNA modifications [26–28].

Formation of diphthine, the second pathway intermediate (Figure 1), requires trimethylation of the amino group in ACP and is catalyzed in yeast by diphthine synthase Dph5, using SAM as methyl donor [29–31]. Intriguingly, reconstitution of archaeal Dph5 activity has shown that the trimethylamino group formed in diphthine is prone to elimination in vitro [32]. Finally, the carboxyl group of diphthine is amidated by an elusive ATP dependent diphthamide synthetase (Figure 1). Once fully modified, diphthamide can be efficiently targeted by NAD^+-dependent ADP ribosylase toxins including DT, *Pseudomonas* exotoxin A [33] and *Vibrio* cholix toxin [34]. However, the intermediate diphthine is also a very weak substrate for inhibitory ADP ribosylation [29,31]. Together with data showing that growth inhibition by sordarin also depends on *DPH1-DPH5* [6,7], translation factor eEF2 constitutes an 'Achilles heel' for yeast, study of which has provided important insight into the pathobiological relevance of posttranslational protein modification [35].

Physiologically, the function of the diphthamide modification is enigmatic. Yeast mutants unable to synthesize diphthamide confer elevated frequency of ribosomal frameshifting [6,36] but are viable and grow normally [14], although substitution of the modified histidine in eEF2 by other amino acids confers growth defects in some instances [37]. However, loss of diphthamide synthesis leads to delayed development and is embryonic lethal in homozygous *DPH3* knockout mice [38–40]. Together with the association of mammalian *DPH1* with tumorigenesis [16,38] as well as neuronal and embryonic development, this indicates that diphthamide modification plays an important biological role. Whether or not this implies structural or regulatory roles for diphthamide modified eEF2 remains to be seen, but the latter notion is intriguing given the possibility of endogenous cellular ADP ribosylases that target eEF2 [4].

Interestingly, no DT resistant yeast mutants have been identified to date that affect the final amidation step in the pathway, probably because diphthine is targetable, albeit ineffi-

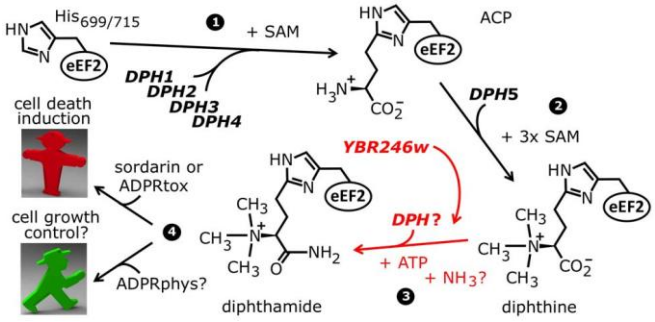

Figure 1. The biosynthetic pathway for modification of eEF2 by diphthamide. For roles played by the *bona fide* diphthamide genes *DPH1–DPH5* in steps 1 and 2 of the pathway, see main text. The ill-defined step 3, conversion of diphthine to diphthamide by amidation, is highlighted (red label). It likely involves ATP and ammonium cofactors in a reaction catalyzed by unidentified *DPH* gene product(s). Step 4 indicates diphthamide can be hijacked for eEF2 inactivation and cell death induction by antifungals, i.e. sordarin and bacterial ADP ribosylase toxins (ADPRtox); alternatively, it has been reported to undergo cell growth related physiological ADP ribosylation (ADPRphys?) by elusive cellular modifier(s). ACP, 2-[3-amino-carboxyl-propyl]-histidine; SAM: S-adenosylmethionine.
doi:10.1371/journal.pgen.1003334.g001

ciently, by ADP ribosylation [29,31]. Thus amidase-deficient mutants may display DT sensitivity in vivo and thereby escape identification in screens for DT resistant yeast mutants.

Indication that additional proteins are involved in diphthamide biosynthesis has come from recent work on WDR85 and its potential yeast ortholog *YBR246w* [41,42], while our preliminary investigation of the yeast *DPH1* genetic interaction network [13] implicated both *YBR246w* and *YLR143w* as novel proteins potentially involved in the diphthamide pathway. Here we further exploit yeast genome-wide genetic interaction and chemical genomics databases [43,44] to demonstrate that *YLR143w* (*DPH6*) and *YBR246W* (*DPH7*) cluster tightly with all known members of the diphthamide gene network. We find that *dph6* and *dph7* mutants phenocopy sordarin and DT traits typical of the *bona fide dph1-dph5* mutants, which are defective in the first two steps of diphthamide synthesis. Importantly, we show that *DPH6* and *DPH7* deletions block the final amidation step of the diphthamide pathway, cause diphthine modified forms of eEF2 to accumulate and consequently abolish ADP ribose acceptor activity upon DT treatment. Thus conversion of diphthine to diphthamide depends on Dph6 and Dph7.

Results

Yeast Gene Interaction Databases Predict Diphthamide Functions for *YLR143w* (*DPH6*) and *YBR246w* (*DPH7*)

To identify factors involved in the terminal amidation step of the diphthamide modification pathway (Figure 1), we took advantage of synthetic genetic array (SGA) screens, which previously enabled systematic mapping of genetic interactions among yeast deletion collections using high-density arrays of double mutants [45,46]. SGA analysis provides the set of genetic interactions for a given gene – the genetic interaction profile – and thereby the phenotypic signatures indicative of functions of both known genes and unassigned ORFs [47]. For example, genes with similar interaction profiles are often functionally related in shared biochemical pathways and/or protein complexes [48,49]. Consistent with this, SGA analysis revealed that the diphthamide gene network members have highly correlated interaction profiles and tightly cluster in the global genetic interaction landscape from yeast [45].

Since our preliminary examination of the yeast genetic interaction landscape placed two uncharacterized yeast ORFs, *YLR143w* and *YBR246w*, within the diphthamide gene network [13], we next examined this network in more detail by mining the SGA DRYGIN database for quantitative *S. cerevisiae* genetic interactions [44,50]. We compared *DPH1*, *DPH2*, *DPH4*, *DPH5*, *YLR143w* and *YBR246w* gene interactions with every array ORF represented in the SGA network and deposited at DRYGIN, ranking the similarity between all possible pairwise profiles according to their Pearson correlation coefficient (PCC; see Table S1 for full details). As expected, the other known *DPH* genes scored significantly highly among the correlation profiles generated for each specific *DPH* query gene, consistently being ranked among the top ten genetic interactors (Figure 2A). Strikingly, *YLR143w* and *YBR246w* were among the top interactors of *DPH1*, *DPH2*, *DPH4* and *DPH5*, while the most correlated interactors for *YLR143w* and *YBR246w* included each other and several *bone fide DPH* genes (Figure 2A). Such highly correlated interaction patterns suggest that *YLR143w* and *YBR246w* are both functionally interrelated and qualify as candidate ORFs of the pathway for eEF2 modification by diphthamide. In line with this notion, the two eEF2 encoding gene copies, *EFT1* and *EFT2*, also ranked among the top ten interactors of *DPH1*, *DPH2* and *DPH5* (Figure 2A).

For independent validation of these correlations, we searched the FitDB yeast fitness database [51], which contains genome-scale phenotypic profiles for diploid yeast deletion collections in response to more than 1100 different growth conditions [43,52]. Here, scoring gene interaction profiles by homozygous co-sensitivity revealed that among the top loci to phenocluster with *YBR246w* are *DPH2*, *DPH4* and *DPH5*, while top interactors of *YLR143w* include *DPH4*, *DPH5*, *YBR246w* and *DPH2* (Figure 2B). A similar pattern of interaction is shown by *DPH5* (Figure 2B), *DPH2* and *DPH4* (data not shown). Based on correlated interaction profiles, FitDB ascribes GO terms enriched for processes concerning peptidyl-diphthamide biosynthesis from peptidyl-histidine to *YLR143w* and *YBR246w* with p-values of 2×10^{-3} and 9×10^{-4} respectively (Figure 2C). Collectively, the FitDB and DRYGIN profiles thus provide robust phenotypic signatures suggesting novel roles in the diphthamide pathway for *YBR246w* and *YLR143w*, which are tightly clustered within the *DPH* gene network (Figure 2C). This notion is consistent with a recent report that *YBR246w* and its mammalian homolog, WDR85, have a diphthamide related function [41,42]. Since *YLR143w* is as yet unassigned in the *Saccharomyces* genome database (SGD), based on the evidence below that *YLR143w* and *YBR246w* are indeed diphthamide synthesis genes we have named them *DPH6* (*YLR143w*) and *DPH7* (*YBR246w*).

DPH6 and *DPH7* Deletions Cause Phenotypes Typical of *Bona Fide* Diphthamide Mutants

To verify the predicted roles for *DPH6* and *DPH7* in the diphthamide pathway, we next examined strains deleted for these ORFs for phenotypes specifically linked to defects in diphthamide formation on eEF2, namely sordarin resistance and response to DT [6,7]. Sordarin traps eEF2 on the 80S ribosome [53], blocking mRNA translation elongation and yeast cell growth [54] in a fashion that depends on diphthamide synthesis [6,7]. As a result, diphthamide mutants *dph1-dph5* efficiently protect against sordarin inhibition [6,7]. Like *dph1-dph5*, *dph6* and *dph7* mutants showed robust resistance towards sordarin at 10 μg/ml, a concentration inhibitory to the wild-type (Figure 3A). This resistance was comparable to that shown by eEF2 substitution mutants *efi2*H_{699}I and *efi2*H_{699}N (Figure 3A), which lack the His_{699} acceptor residue for diphthamide modification [37]. Thus *DPH6* and *DPH7* are novel sordarin effectors, a feature they share with the diphthamide synthesis genes *DPH1-DPH5* [6,7].

Diphthamide modification plays a key effector role for inhibitory ADP ribosylation of eEF2 by DT, hence *dph1-dph5* mutants in both yeast and mammalian cells confer resistance towards DT [14,16]. We therefore compared DT-dependent ADP ribosylation of eEF2 in vitro between wild-type cells and *dph1*, *dph5*, *dph6* and *dph7* mutants. While the translation factor from wild-type cells was efficiently modified by the toxic ADP ribosylase (Figure 3B), eEF2 extracted from *dph1*, *dph5*, *dph6* and *dph7* mutants could not be ADP ribosylated by exogenously added DT under the conditions used (Figure 3B). Such lack of ADP ribose acceptor activity in vitro strongly suggests defects in the diphthamide pathway and that *DPH6* and *DPH7* encode novel functions required for diphthamide formation. To further address this experimentally, we assayed the response of *dph6* and *dph7* mutants to intracellular expression of the ADP ribosylase domain of DT (DTA) using *GALS*, a truncated variant of the *GAL1* promoter [55]. When DTA expression was induced by 0.1% galactose, *dph6* and *dph7* mutants were indeed found to show some protection against DTA in contrast to wild-type cells (Figure 3C),

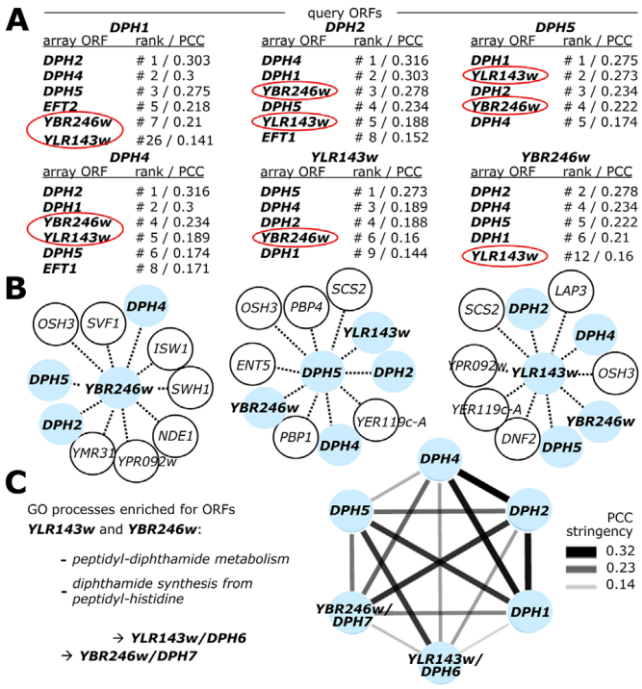

Figure 2. Genome-wide gene interaction databases identify additional diphthamide related candidate genes: *YLR143w*/*DPH6* and *YBR246w*/*DPH7*. (A) SGA database (DRYGIN). Genetic interaction profiles among *DPH1*, *DPH2*, *DPH4*, *DPH5*, *YBR246w* and *YLR143w* query gene deletion strains and 3885 or 4457 array ORF mutants were extracted from data for a total of ~1700 query strains deposited at DRYGIN (for full details, see excel spread sheet in Table S1). Ranking of top interactors for each query ORF was according to PCC (Pearson correlation coefficient) determination. For simplicity, array ORFs *DPH1*, *DPH2*, *DPH4*, *DPH5*, *EFT1*, *EFT2* (shown in bold) as well as potentially diphthamide related candidate loci *YLR143w* and *YBR246w* (red circles) are listed that score repeatedly as significantly high interactors of the query ORFs. (B) Yeast Fitness database (FitDB). Genes whose deletions phenocluster with the six query ORFs above were extracted from FitDB, which is based on genome-scale co-fitness defect analysis of homozygous yeast deletion mutants in response to greater than 1144 different conditions. For simplicity, the top ten interactors for three of the six query genes (*DPH5*, *YLR143w* and *YBR246w*: pale blue central nodes) above are depicted. (C) Representation of the tightly clustered and expanded *DPH1-DPH7* gene network where nodes (pale blue) correspond to individual *DPH* gene family members and edges connect gene pairs by PCC>0.14. Enhanced gene interaction strength is proportional to PCC stringency. Enriched GO process likelihoods in the diphthamide modification pathway are listed as P-values for the identified candidates *DPH6*/*YLR143w* and *DPH7*/*YBR246w*.
doi:10.1371/journal.pgen.1003334.g002

consistent with defects in diphthamide formation. However, at a higher level of expression on 2% galactose, they showed wild-type like sensitivity to DTA whereas *dph1* and *dph5* mutants remained fully resistant (Figure 3C). This suggests that eEF2 forms from *dph6* or *dph7* mutants, although not substrates in vitro (Figure 3B), can nonetheless be ADP ribosylated in vivo if DTA is expressed at a sufficiently high level [30]. While our work was in progress, eEF2 from a *ybr246w/dph7* mutant was shown to be a very weak substrate for ADP ribosylation when treated with 10 mM DT [42], a 500-fold increase in concentration over that used in our in vitro ADP ribosylation assays (Figure 3B). Thus eEF2 from the *dph6* or *dph7* mutants is resistant to sordarin and shows a vastly reduced ability to be ADP-ribosylated by DT, strongly suggesting that the diphthamide pathway is defective. Since the intermediate diphthine can serve as a sub-optimal substrate for ADP ribosylation using excess levels of DT or upon overexpressing its toxic ADP ribosylase domain from inside cells [29,31], the properties of eEF2 from *dph6* and *dph7* mutants are consistent with a defect in the final step of the pathway that converts diphthine to diphthamide. Our analysis is therefore entirely consistent with the above database predictions and indicates *DPH6* and *DPH7* constitute novel candidate loci for diphthamide biosynthesis.

Mass Spectrometry Reveals Diphthine Accumulation in *dph6* and *dph7* Mutants Due to a Block in the Terminal Amidation Step of the Diphthamide Pathway

Given the above evidence, we next examined whether eEF2 prepared from cells deleted for either *DPH6* or *DPH7* carried any modification on His_{699}, the eEF2 residue that is modified to

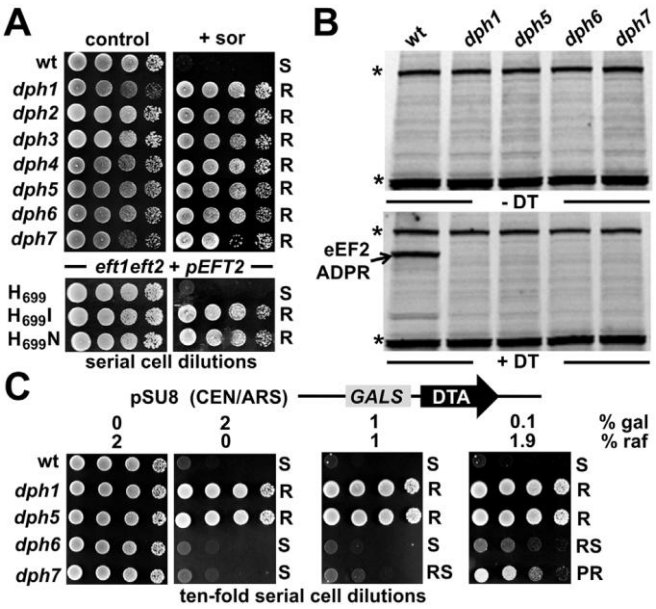

Figure 3. ***DPH6*** **and** ***DPH7*** **deletion strains copy traits typically related to the** ***bona fide*** **diphthamide mutants** ***dph1-dph5.*** (A) Sordarin resistance. Ten-fold serial cell dilutions of the indicated yeast strains, BY4741 wild-type (wt) background and its *dph1-dph7* gene deletion derivatives (upper panels) as well an MKK-derived *eft1 eft2* double deletion background maintaining plasmid p*EFT2* wild-type or H_{699} substitution (H_{699} N and H_{699}I) alleles of *EFT2* (lower panels), were grown on YPD plates in the absence (control) or presence (+sor) of 10 μg ml^{-1} sordarin. Growth was assayed for 3 d at 30°C. Sordarin resistant (R) and sensitive (S) responses are indicated. (B) Lack of in vitro ADP ribose acceptor activity of eEF2. Cell extracts obtained from *dph1*, *dph5*, *dph6* and *dph7* mutant and wild-type (wt) strains were incubated with (+DT) or without (−DT) 20 nM diphtheria toxin in the presence of biotin-NAD (10 μM) at 37°C for 1 hour. The transfer of biotin-ADP-ribose to eEF2 was detected by Western blotting using a streptavidin-conjugate. Two unknown non-specific bands (indicated by *) served as internal controls for even sample loading. (C) DT phenotype. As indicated, yeast *dph* mutants and wild-type control (wt) were tested for sensitivity to intracellular expression of DTA, the cytotoxic ADP ribosylase fragment of DT. This in vivo assay involved galactose-inducible expression from vector pSU8 (see Materials and Methods). Serial cell dilutions were replica spotted onto raffinose (2% raf) and galactose-inducing conditions using concentrations (2, 0.2 and 0.1% gal) suited to achieve gradual down-regulation of DTA toxicity. Growth was for 3 days at 30°C. DTA sensitive (S) resistant (R), partially resistant (PR) and reduced sensitive (RS) phenotypes are indicated.

doi:10.1371/journal.pgen.1003334.g003

generate diphthamide. eEF2 preparations made from wild-type and gene deletion strains expressing His_6-tagged eEF2 were digested with trypsin and examined by mass spectrometry. The His_6-tagged form was chosen as the source of eEF2 since expression rescued the inviability of an *eft1 eft2* double mutant lacking eEF2 function, and it is thus considered to be biologically active [56]. Strains lacking either *DPH1*, in which the first step of diphthamide biosynthesis is blocked, or lacking *DPH5* (encoding diphthine synthase), were used respectively as controls for complete lack of modification and presence of ACP, the first intermediate in the diphthamide pathway [14,16,30,32]. All strains expressed similar levels of His_6-tagged eEF2 (data not shown).

The modified histidine in eEF2 (His_{699}) is located in the tryptic peptide 686-VNILDVTLHADAIHR-700 and, as expected, unmodified versions of this peptide were readily detected in eEF2 prepared from the *dph1* mutant (Figure S1C). Unmodified peptide was also found in eEF2 prepared from *dph5*, *dph6* and *dph7* deletion strains as well as from wild-type cells (Figures S1 and S2). Thus even in wild-type cells not all of the eEF2 is modified by diphthamide. In addition to the unmodified peptide, we readily detected diphthamide-modified peptide in eEF2 prepared from the wild-type strain (Figure 4A), but failed to detect this in any of the mutants. Instead, ACP-modified peptide was found in eEF2 prepared from the *dph5* mutant (Figure 4B), as expected given its known role in generating diphthine [32] from the ACP intermediate in the pathway.

In contrast, eEF2 from the *dph7* mutant generated spectra consistent with the presence of diphthine on His_{699}, in which the m/z values for both the parent ions and the daughter ions in the MS/MS spectra were higher in a manner consistent with the 0.984 Da extra mass associated with presence of a carboxyl group in diphthine rather than the amide group in diphthamide (Figure 4C). Thus each of the doubly-charged daughter ions in Figure 4C is larger by an m/z of ~0.5 than the corresponding ion in the wild-type spectrum (Figure 4A). Furthermore, the quite

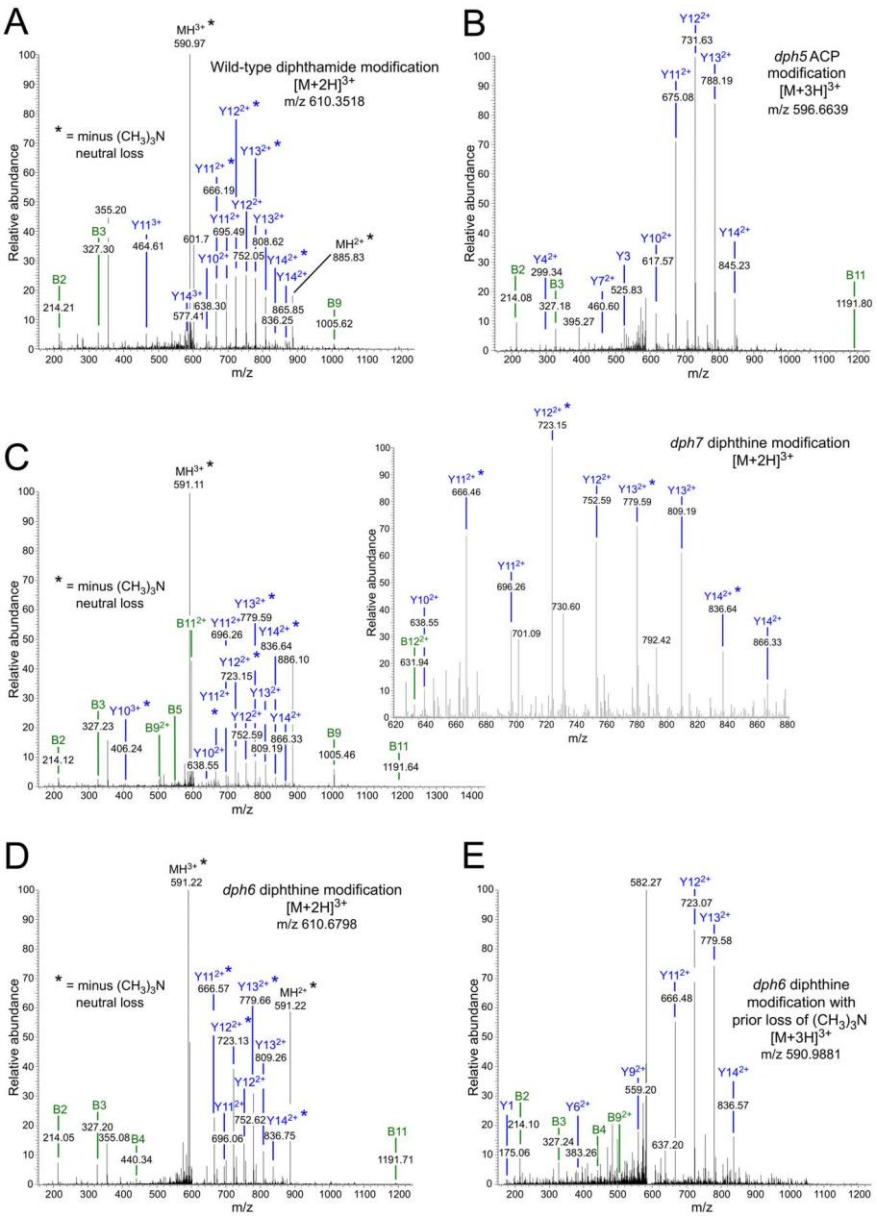
A
Wild-type diphthamide modification
[M+2H]3+
m/z 610.3518
* = minus (CH3)3N neutral loss
B
dph5 ACP modification
[M+3H]3+
m/z 596.6639
C
dph7 diphthine modification
[M+2H]3+
* = minus (CH3)3N neutral loss
D
dph6 diphthine modification
[M+2H]3+
m/z 610.6798
* = minus (CH3)3N neutral loss
E
dph6 diphthine modification with prior loss of (CH3)3N
[M+3H]3+
m/z 590.9881
Relative abundance
m/z

Figure 4. MS/MS spectra of diphthamide-, ACP-, and diphthine-modified EF2 peptide 686-VNILDVTLHADAIHR-700 from wild-type and mutant yeast strains. Spectra are shown for (A) diphthamide-modified peptide from the wild-type yeast strain; (B) ACP-modified peptide from the *dph5Δ* mutant; (C) diphthine-modified peptide in the *dph7Δ* strain; (D) diphthine-modified peptide in the *dph6Δ* strain; (E) diphthine-modified peptide in the *dph6Δ* strain with loss of the trimethylamino group before analysis in the mass spectrometer indicated by the parent ion m/z. In each case the parent ion m/z and charge state is indicated. In (A), (C) and (D), * indicates neutral loss of trimethylamino during MS/MS. The inset in (C) shows greater detail for the more crowded part of the MS/MS spectrum. Figure S2A indicates how the B and Y ions are derived from the peptide sequence.
doi:10.1371/journal.pgen.1003334.g004

different elution times of the diphthine-modified and diphthamide-modified peptide that are evident from the extracted ion chromatograms (Figure S3) are consistent with differently modified forms of eEF2. As noted in previous studies [32,33,36], some of the ions in our MS/MS spectra had undergone neutral loss of the trimethylamino group during MS/MS, as indicated by loss of 59.110 mass units.

Two types of spectra corresponding to the peptide with modified His_{699} were seen when eEF2 from the *dph6* mutant was analyzed. In some spectra (Figure 4D), the parent ion m/z and MS/MS data indicated the presence of diphthine as in the *dph7* mutant, with some daughter ions again showing neutral loss of the trimethylamino group during MS/MS as noted above. However, we also detected peptide forms in which elimination of the trimethylamino group had occurred prior to analysis, as indicated by the lower parent ion m/z (Figure 4E) and an MS/MS spectrum in which all assignable peaks corresponded to ions lacking the trimethylamino group. Such trimethylamino elimination prior to mass spectrometry was observed previously when diphthine-modified *Pyrococcus horikoshii* EF2 was generated in an in vitro reaction [32], indicating that this modification might be unstable. However, we failed to detect any pre-mass spectrometry loss of the trimethylamino group when eEF2 from the *dph7* mutant was analyzed. Thus while eEF2 from both mutants carries diphthine, the modification appears to be more labile in the *dph6* mutant and may be protected from trimethylamino elimination by the absence of Dph7.

Figure S3 shows extracted ion chromatograms for ions with m/z values corresponding to the His_{699} containing peptide modified with diphthamide, diphthine or with ACP, indicating that the ACP modified peptide was only present in the *dph5* mutant, the diphthine modified peptide was only present in *dph6* and *dph7* mutants, and diphthamide-modified peptide was only seen in wild-type cells. Our mass spectrometry analysis therefore shows that in yeast strains lacking either *DPH6* or *DPH7*, modification of His_{699} progresses only as far as diphthine. Thus both loci indeed qualify as novel diphthamide synthesis genes with likely roles in conversion of diphthine to diphthamide.

Protein–Protein Interactions Between Dph6, Dph7, Dph5, and EF2

Although Dph6 and Dph7 appear to function within the same step of the diphthamide synthesis pathway, using co-immune precipitation they were not found to interact either with one another or with Dph2 and Dph5, players involved in the two earlier pathway steps (Figure S4; Figure S5 and data not shown). However, in support of our evidence that Dph6 is a diphthamide biosynthetic factor, we observed by co-immune precipitation that Dph6-HA bound to a fraction of $(His)_6$-tagged eEF2 (Figure 5A). Intriguingly, this interaction was independent of Dph7 (Figure 5A), suggesting Dph7 may not mediate interaction between Dph6 and the translation factor. Dph7 is also unlikely to play an indirect role through regulation of *DPH6* gene expression because Dph6 protein levels were unaltered in the *DPH7* deletion strain (Figure 5A).

Inactivation of WDR85, the mammalian homolog of Dph7, was recently shown to dramatically enhance association of diphthine synthase Dph5 with eEF2 [41]. We therefore examined whether Dph7 impacts on the interaction between Dph5 and eEF2 in budding yeast. We found that a much higher level of affinity tagged eEF2 could be co-immune precipitated with HA-tagged Dph5 from extracts of the *dph7* mutant in comparison to wild-type extracts (Figure 5B). A smaller increase was also seen with the *dph6*

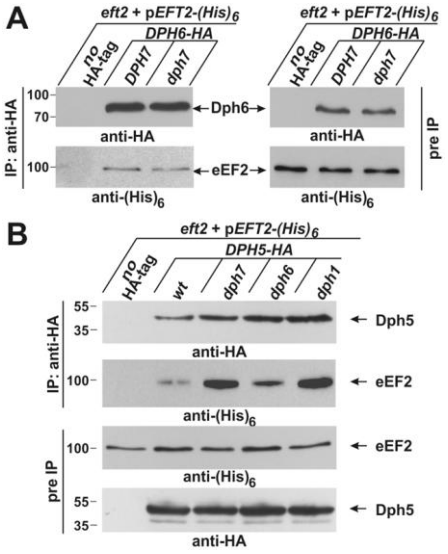

Figure 5. Co-immune precipitations reveal eEF2 interactions with Dph6 and Dph5. (A) eEF2 interacts with Dph6 in a fashion that is independent of Dph7. (B) eEF2 interaction with Dph5 is dramatically enhanced by elimination of Dph7 or Dph1. Yeast strains co-expressing $(His)_6$-tagged eEF2 with Dph6-HA (A) or Dph5-HA (B) in the background of wild-type (A: *DPH7* and B: wt) and *dph* mutant strains (A: *dph7*; B: *dph1*, *dph6* and *dph7*) were subjected to immune precipitations (IP) using the anti-HA antibody. Strains expressing $(His)_6$-tagged eEF2 on their own served as IP controls (A and B: no HA-tag). Subsequently, the precipitates were probed with anti-HA (A: top left panel; B: first panel) and anti-$(His)_6$ antibodies (A: bottom left panel) to check for the content of Dph6-HA (A) and Dph5-HA (B), respectively (all indicated by arrows). The content of HA-tagged Dph6 (A) and Dph5 (B) as well as $(His)_6$-marked eEF2 (A and B) in the protein extracts prior to IP (pre-IP) was examined on individual Western blots using anti-HA (A: top right panel; B: fourth panel) and anti-$(His)_6$ antibodies (A: bottom right panel; B: third panel), respectively. While absence of Dph7 hardly affected the Dph6●eEF2 interaction (A), Dph5●eEF2 interaction was strongly enhanced by inactivating *DPH7* or *DPH1* (B).
doi:10.1371/journal.pgen.1003334.g005

mutant (Figure 5B). This strongly suggests a conserved role for Dph7/WDR85 as a regulator of the Dph5•eEF2 interaction. Remarkably, we also found similarly enhanced binding of Dph5 to eEF2 in the *dph1* mutant, which has a defect in the first step of the diphthamide pathway and therefore lacks the ACP modification that is the immediate substrate of diphthine synthase (Figure 5B). Strikingly, *DPH5* overproduction from a galactose-inducible promoter was found to be highly detrimental to cells deleted for *DPH7* and to all mutants blocked at the first step of the pathway, but had little effect on the *dph6* mutant and no effect on wild-type or *dph5* cells (Figure 6A). Intriguingly, this cytotoxicity goes hand in hand with the enhanced Dph5•eEF2 interaction profiles we observed in *dph1*, *dph6* and *dph7* cells under conditions of wild-type *DPH5* copy number and normal Dph5 expression levels (Figure 5B). Taken together, our results suggest that binding of Dph5 to incompletely modified eEF2 may be inhibitory to the function of the translation factor. Our data also indicate that both unmodified eEF2, and diphthine-modified eEF2 in the absence of Dph7, show strongly enhanced binding to Dph5. Furthermore, since we failed to detect association between Dph5 and Dph6 despite demonstrating interaction of each with eEF2, it is likely that Dph5 and Dph6 do not bind concurrently to eEF2 and that their binding may therefore be mutually exclusive.

Physiological Implications of the Diphthamide Modification on eEF2

Although the precise biological function of diphthamide is unclear, its location at the tip of the eEF2 anticodon mimicry domain IV predicts a potentially important role in translation. Consistent with this, structure-function studies have shown that domain IV is sufficiently proximal for interaction with tRNA in the decoding P-site of the ribosome [57] and alterations of invariant tip residues, including H_{699} substitutions that cannot be diphthamide modified, confer biologically significant traits including thermosensitive growth defects [37,58]. Nonetheless, when compared to their wild-type parental strain, we found no significant changes in the growth performance of *dph1-dph7* mutants in either liquid or on solid media and at standard cultivation temperatures of 30°C (Figure S6). Even increasing the cultivation temperatures to 39°C had no discernable effect on *dph* cell growth except for the *dph3/kti11* mutant (Figure S6), which is known to be thermosensitive due to additional functions unrelated to diphthamide [6].

However, intrigued by previous reports that diphthamide defects can induce ribosomal frame-shifts [6,36], we next studied whether *DPH6* and *DPH7* deletions affect the accuracy of eEF2 in the translation process (Figure 6B). Using *lacZ*-based reporters to monitor programmed +1 and −1 frameshift signals derived from Ty elements [36,59], *dph1-dph7* mutants failed to induce significant ribosomal +1 frameshifts (data not shown). However, *dph1*, *dph2*, *dph3*, *dph5* and *dph6* mutants significantly enhanced *lacZ* expression dependent on a −1 frameshift, with *dph6* and *dph3* cells scoring as the top −1 frameshifters followed by lower but statistically significant effects in *dph1*, *dph2* and *dph5* mutants (Figure 6B). This confirms increased −1 frameshifting in *dph2* and *dph5* mutants seen previously [36] and demonstrates an even larger defect in *dph3* and *dph6* strains. Ribosomal −1 frameshift induction by *dph7* and *dph4*, though slightly increased in relation to wild-type controls, was considered statistically insignificant (Figure 6B). The −1 frameshifting phenotype shared between *dph6* and *bona fide dph* mutants is consistent with a role for diphthamide in promoting translational accuracy of eEF2. In line with a role for diphthamide in the fine tuning of translation elongation, growth assays performed under thermal and/or chemical stress conditions showed that certain *dph* mutants including *DPH6* and *DPH7* deletion strains displayed altered responses to translation elongation indicator drugs such as hygromycin, anisomycin or paromomycin (Figure S7). In conclusion, our data indicate that diphthamide mutant strains such as *dph6* increase ribosomal errors typical of −1 translational frameshifts and that the diphthamide modification function of Dph6, which is required for completion of diphthamide synthesis, is likely to assist eEF2 in reading frame maintenance during translation.

Discussion

We have presented genetic, phenotypic, mass spectrometric and biochemical analyses that clearly identify Dph6 as a novel protein required for the final step of diphthamide biosynthesis and that confirm a similar role for Dph7 as reported recently [41,42]. Thus in yeast strains lacking either *DPH6* or *DPH7*, modification of His_{699} on eEF2 progresses only as far as diphthine and these gene products are required for amidation of diphthine to generate diphthamide. Our findings are consistent both with a recent bioinformatics analysis that predicted a role for Dph6 in the diphthine to diphthamide conversion [60] and with the identification of Dph6 as yeast diphthamide synthetase reported by Su et al. [61] while we were revising our manuscript.

Dph6

Dph6 contains three conserved domains consistent with it functioning as an enzyme (Figure S8). The amino-terminal 225 residues constitute an Alpha_ANH_like_IV domain (cd1994 in the NCBI Conserved Domain Database [62], also known as DUF71), a member of the adenine nucleotide alpha hydrolase superfamily that is predicted to bind ATP. Many DUF71 proteins from archaea to mammals contain the highly conserved motif –E_{215}GG(D/E)XE_{220}– (Dph6 numbering), which has been proposed to be involved in substrate binding and catalysis and which is replaced by –ENGE(F/Y)H– in a group of related DUF71 proteins implicated in biotin synthesis [60]. Based on this we generated a *dph6* allele encoding two substitutions in this region (G216N, E220A) and tested its functionality by monitoring complementation of sordarin resistance in a yeast *dph6* knockout strain. Figure 7 clearly shows that this small change completely inactivates the function of Dph6, demonstrating that the Alpha_ANH_like_IV domain is critical for the conversion of diphthine to diphthamide. The C-terminal portion of Dph6 contains two domains related to the YjgF-YER057c-UK114 protein family (eu_AANH_C1: cd06155 and eu_AANH_C2: cd06166) that may promote homotrimerisation and formation of an inter-subunit cleft that has been proposed to bind small molecule ligands [63–65]. Several key residues in human UK114 required for homotrimerisation and ligand binding [66] are present in Dph6 (Figure S8) including arg-107, which in *E. coli* TdcF forms a bidentate salt bridge with the carboxylic acid group of bound ligands [63]. Deletion of residues 335–415 encompassing much of the YjgF-YER057c-UK114 region abolished the function of Dph6 as monitored by sordarin resistance (Figure 7), while truncation of Dph6 at the first of the two conserved domains by insertion of a *myc* tag also eliminated Dph6 function (Figure 7) despite detectable expression of the truncated polypeptide (data not shown), indicating that the YjgF-YER057c-UK114 domains are also important for Dph6 function and that the Alpha_ANH_-like_IV domain is nonfunctional on its own. Since *Salmonella enterica* YjgF has an enamine/imine deaminase activity that is conserved in human UK114 [67] it is possible that the YjgF-YER057c-UK114 domains in Dph6 are used to generate ammonia for diphthamide formation.

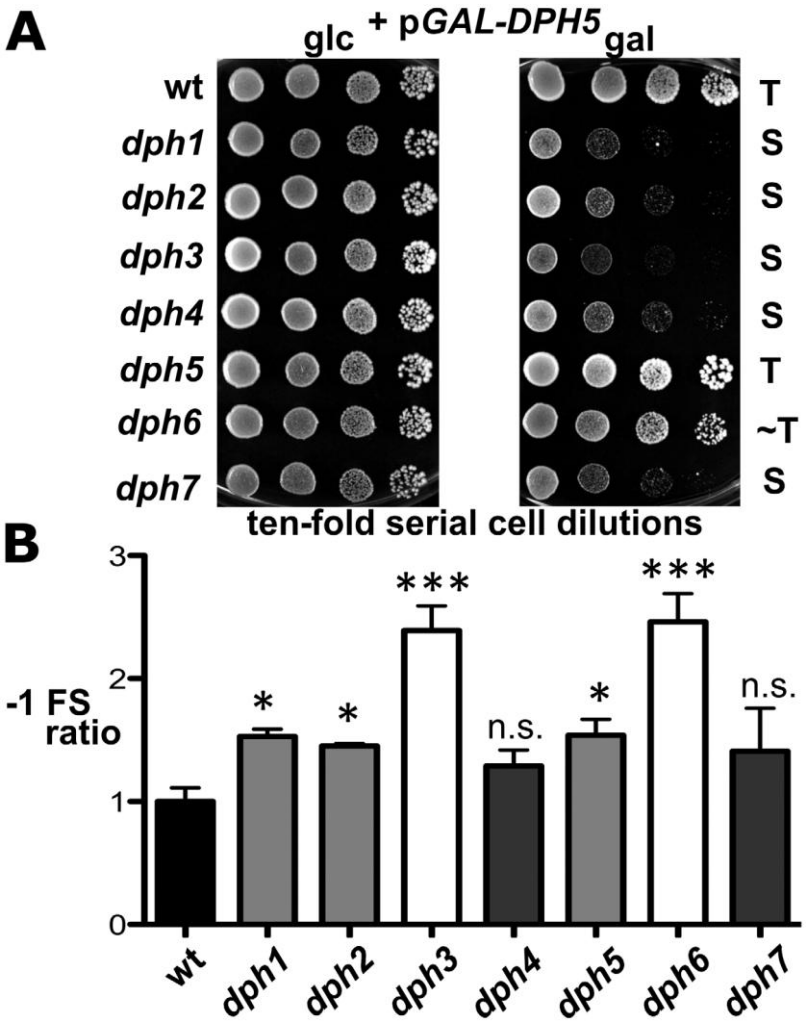

Figure 6. *dph* mutants show sensitivity to elevated diphthine synthase levels and confer reduced translational accuracy. (A) *DPH5* overexpression in *dph1-dph4* and *dph7* mutants causes cytotoxicity and a severe cell growth defect. Cells of yeast strains with the indicated genetic backgrounds and maintaining plasmid p*GAL-DPH5* for galactose inducible overexpression of diphthine synthase Dph5 were serially diluted and replica spotted onto glucose (2% glc) and galactose (2% gal) media to assay their response to *DPH5* overexpression. Growth was for 3 days at 30°C. Unaltered (T), slightly weakened tolerance (~T) and sensitive (S) responses are indicated. Note that *dph1-dph4* and *dph7* mutants are extremely sensitive to *DPH5* overexpression. (B) Ribosomal frameshift analysis reveals erroneous translation in *dph1-dph7* mutants. Strains with the indicated genetic backgrounds were transformed with control (pJD240.0) or *lacZ* −1 frameshift (pJD240.−1) plasmids [59] to monitor *lacZ* expression through β-galactosidase (β-Gal) production using *O*-nitrophenol-D- galactopyranoside assays and to score translation efficiency (pJD240.0) and fidelity (pJD240.−1). Ribosomal −1 frameshifts are expressed relative to the level of overall translation efficiency with statistical significance determined by one-way ANOVA followed by Dunnett's multiple comparison. With the exception of *dph4* and *dph7*, post-hoc comparison found that all other mutant backgrounds showed a significant increase in ribosomal −1 frameshifting relative to wild-type (wt) yeast cells (* = $P \leq 0.05$; *** = $P \leq 0.001$; ns. = not significant).
doi:10.1371/journal.pgen.1003334.g006

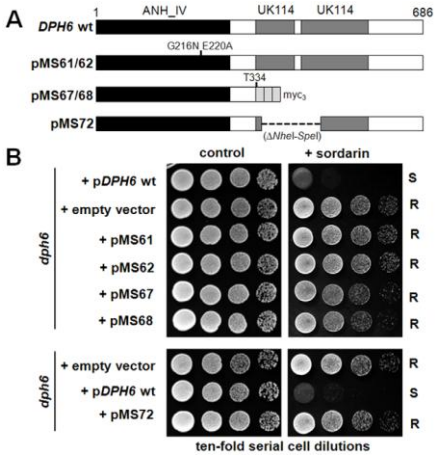

Figure 7. Both the Alpha_ANH_like_IV and YjgF-YER057c-UK114 domains in Dph6 are essential for its functionality. (A) Diagram showing the *DPH6* wild-type and mutant constructs tested in (B), indicating the Alpha_ANH_like_IV (ANH) and YjgF-YER057c-UK114 (UK114) domains and the position of point mutations, an in-frame deletion (- - - -) and triple myc epitope tag (myc_3) as appropriate. (B) Ten-fold serial cell dilutions of a *dph6* deletion strain carrying the constructs shown in (A) or the corresponding empty vector (top panel, pSU6 [wt *DPH6*]; lower panel, pSU7 [wt *DPH6*]: Table S3) were spotted onto SCD-Leu plates with or without 10 μg/ml sordarin and grown at 30°C for 3 days.
doi:10.1371/journal.pgen.1003334.g007

Taken together, these properties suggest a direct, ATP-dependent role for Dph6 in diphthine amidation proceeding via an adenylated intermediate and with ammonia acting as the source of the amide group. Such a direct role has now been demonstrated by Su et al., who have used an in vitro assay system to show that Dph6 has diphthamide synthetase activity [61]. Although proteins showing Dph6-like domain organization are readily identified in fungi, plants, amphibians and insects (Figure S8), they are largely absent from archaeal and mammalian proteomes. However, mammals and archaea have separate proteins showing strong similarity to either the adenine nucleotide alpha hydrolase domain or to the YjgF-YER057c-UK114 related regions (Figure S8 and data not shown), suggesting Dph6 functionality may be split between different polypeptides in these cases. It is therefore surprising that expression of the human *DPH6* ortholog in a yeast *dph6* mutant can restore diphthamide biosynthesis [61] despite lacking the YjgF-YER057c-UK114 domains that are essential in the yeast protein (Figure 7; [61]). Thus while the core function of the enzyme must therefore reside in the Alpha_ANH_like_IV domain, it will be interesting to determine the role of the YjgF-YER057c-UK114 domains in Dph6 from lower eukaryotes.

Dph7

Dph7 has four well-defined WD40 repeats (Figure S9) and its predicted structure consists exclusively of β-sheet elements [41,68]. Although its human homolog WDR85 has been implicated in the first step of diphthamide biosynthesis [41], our work and that of Su et al. [42] show that the pathway can proceed as far as diphthine in the absence of *DPH7* and that the block is therefore in conversion of diphthine to diphthamide. Furthermore, this block cannot be bypassed simply by introducing *DPH6* on a multicopy plasmid to increase the level of diphthamide synthetase (data not shown). How then might Dph7 contribute to diphthine amidation? Its domain structure suggests it could act as an adaptor molecule for diphthine amidation [42], but this notion is at odds with our failure to detect interaction between Dph7 and Dph6 (see above). Our intriguing finding that eEF2 binds much more Dph5 in the absence of Dph7 suggests an alternative role, namely that Dph7 is needed to displace Dph5 from diphthine-modified eEF2 to allow the amidation reaction to occur. Similar findings in mammalian cells upon inactivation of WDR85 support this notion [41]. Together with our data showing that viability of *dph1-dph4* and *dph7* cells is extremely sensitive to excess Dph5 in comparison to wild-type or *dph6* cells, it appears that binding of Dph5 to eEF2 is inhibitory to the function of the translation factor and negatively interferes with cell growth unless eEF2 carries the completed diphthamide modification. Perhaps in addition to catalyzing methylation of ACP-modified eEF2, Dph5 binds to newly-synthesised eEF2 to exclude it from functioning in translation until the diphthine amidation step takes place (Figure 8). Consistent with this proposal is our observation that the level of Dph5 associated with eEF2 in the *dph1* mutant, in which modification of His_{699} cannot be initiated, is drastically increased and virtually indistinguishable from the enhanced Dph5-eEF2 interaction seen when Dph7 is absent. Dph7 may be needed to displace Dph5 once diphthine has been generated so that Dph6 can carry out the diphthine to diphthamide conversion (Figure 8), a notion consistent with the sensitivity of the *dph7* mutant to *DPH5* overexpression. In contrast, the *dph6* mutant may tolerate Dph5 overexpression because Dph7 is present to displace it.

Two other seemingly unrelated functions have been previously proposed for *DPH7*. Firstly, it emerged from a genetic screen as a potential negative regulator of RNA polymerase I (Rrt2), although no other *DPH* genes were similarly identified [69]. Secondly, *DPH7* has been implicated in retromer mediated endosomal recycling and named *ERE1* [68]. The connection between endosomal recycling and diphthamide biosynthesis is currently unclear and it remains to be determined whether Dph7 is multifunctional or if these other roles are linked to its eEF2 modification function.

Diphthamide on eEF2 is the target for bacterial ADP-ribosylase toxins and also affects toxicity of sordarin and ricin, a ribosome inhibiting protein toxin from plants [70]. Although this emphasizes its pathological relevance, the physiological significance of diphthamide remains enigmatic and elusive. Nonetheless, the evolutionary conservation of the diphthamide pathway among eukaryotes and the embryonic lethality of mice that cannot synthesize diphthamide [38] strongly suggest that it is important in translation related processes. In support of this notion, evidence presented here and by others shows that diphthamide mutants cause increased translational frameshifting, a defect also observed in mammalian cells [6,36,71]. Diphthamide modification may have particular importance in multicellular organisms or when cells are stressed [4]. Mutation of mammalian diphthamide synthesis genes affects cell proliferation and development: inactivation of *DPH3/KTI11* is associated with tRNA modification defects and neurodegeneration and mutations in *DPH1/OVCA1* revealed a tumor suppressor role for this diphthamide synthesis gene in ovarian cancer [27,38–40,72]. Regardless of its physiological functions, our data indicate that the diphthamide pathway is more complex than originally anticipated and comprises, in

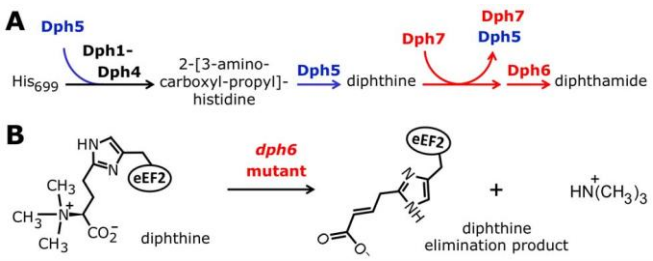

Figure 8. Model for the diphthamide pathway incorporating the proposed novel roles of Dph5, Dph6, and Dph7. (A) Diphthamide pathway showing interaction of Dph5 with unmodified eEF2 and the proposed role of Dph7 in displacement of Dph5 prior to diphthine amidation. (B) Elimination of the trimethylamino group in the absence of the proposed amidase Dph6 suggesting lability of diphthine in its absence.
doi:10.1371/journal.pgen.1003334.g008

addition to Dph1-Dph5, two further components, Dph6 and Dph7, which operate in the terminal amidation step (Figure 8). While it is now clear that Dph6 is diphthamide synthetase [61], in the future it will be important to understand why the archaeal and mammalian orthologs can dispense with the otherwise conserved YjgF-YER057c-UK114 domains and to define the precise role of Dph7. It will also be crucial to explore the potential role of diphthine synthase (Dph5) as a potential regulator of the entire pathway and the reasons for apparent lability of diphthine in the *dph6* mutant that is suggested by our data (Figure 8).

Materials and Methods

Strains, Media, Growth Conditions, and Growth Assays

Yeast strains used in this study are listed in Table S2 and plasmids in Table S3. Cultures were grown in complete (YPD) or minimal (SD) media [73] at 30°C unless otherwise stated. For phenotypic assays, YPD was supplemented with 10 µg/ml sordarin sodium salt from *Sordaria araneosa* (Sigma-Aldrich). Yeast transformations with plasmid DNAs were performed following the lithium acetate protocol [74]. Diphtheria toxin (DT) growth assays in vivo involved expression of the toxin's cytotoxic ADP ribosylase fragment (DTA) from vector pSU8 (p415-*GALS*-DTA), essentially as previously described for *dph1-dph5* mutants [6]. pSU8 was made by cloning the *Bam*HI fragment encoding DTA from pLMY101 [30] into plasmid p415-*GALS*, a single-copy *E. coli*-yeast shuttle vector with a truncated *GAL* promoter [55], which allows for conditional DTA induction on galactose-containing media. [55]. The translational frameshift reporter assay essentially involved previously published protocols together with the described *lacZ* reporter plasmids pJD204.0 (wild-type control), pJD204.−1 (−1 frame) and pJD204.+1 (+1 frame) [36,59]; the pJD204 plasmid series was kindly provided by T. Kinzy (UMDNJ, USA). The relative values for +1 and −1 frameshifting were statistically analyzed using one-way ANOVA followed by Dunnett's multiple comparison post test and was performed with Graphpad Prism 5.0 software essentially as previously described [75].

Gene Deletion and Epitope Tagging

Details of all primers used in numerous PCR dependent genomic manipulation experiments can be found in Table S4. Gene deletions were performed using in vivo PCR-based one step-gene disruption protocols in combination with marker plasmids YDpKl-L, YDpKl-U or YDpSp-H [76] and knockout primers (Table S4) including those previously described [6,25,77]. Gene deletions were confirmed via diagnostic PCR on genomic DNA preparations using target ORF-specific primer pairs (Table S4) as well as sordarin response assays. C-terminal tagging of *DPH1*, *DPH2*, *DPH5*, *DPH6/YLR143w* and *DPH7/YBR246* was performed according to previously published in vivo PCR-based epitope tagging protocols [78] using appropriate S3/S2 primer pairs (Table S4). Tagged genes were confirmed by Western blot detection with anti-HA or anti-c-Myc antibodies (Santa Cruz Biotechnology A-14 and F7, respectively). Detection of HA- or c-Myc-tagged Dph1, Dph2, Dph5, Dph6 and Dph7 as well as Dph3 and Elp2 in co-immune precipitation (Co-IP) assays were performed as previously described [6,77,79].

DPH6 Constructs

pSU6 was generated by insertion into YCplac111 [80] of a genomic PCR fragment including *DPH6* together with 829 bp of upstream and 59 bp of downstream sequence flanked by *Eco*RI and *Bam*HI sites incorporated using PCR primers (Table S4). The insert was verified by sequencing and shown to complement a *dph6* knockout strain. pSU7 was made by cloning the *DPH6* insert from pSU6 into YEplac181 [80]. To generate a G216N E220A *dph6* mutant, pSU6 was digested with *Age*I and *Bsm*BI and the small *DPH6* fragment replaced by an identical synthetic fragment (Integrated DNA Technologies) carrying the G216N E220A mutations, generating independent clones pMS61 and pMS62. The replaced region was verified by DNA sequencing. pMS67 and pMS68 were generated from pSU6 by replacing the *Bsm*BI-*Sal*I fragment carrying the C-terminal region of *DPH6* and downstream sequence with a synthetic *Bsm*BI-*Sal*I fragment in which codons 335–685 were replaced by sequence encoding the linker and triple *myc* tag from pYM23 [81]. To generate pMS72, the smaller *Nhe*I-*Spe*I fragment of pSU7 was excised and the large fragment ligated to generate an in-frame fusion that removed *DPH6* codons 347–471, checking the resulting fusion by DNA sequencing.

In Vitro ADP Ribosylation Assay

Yeast cell extracts were prepared as described previously [15]. ADP ribosylation reactions were performed at 37°C for 1 hour in a volume of 40 µl ADP ribosylation buffer (20 mM Tris-HCl, pH 7.4, 1 mM EDTA, 50 mM DTT) containing 50 µg of yeast extract, 50 ng fully-nicked DT and 10 µM 6-biotin-17-NAD (Trevigen). Samples were then mixed with SDS sample buffer, boiled for 5 min and run on 4–25% SDS-PAGE gradient gels (Invitrogen). The proteins were transferred to nitrocellulose

membranes and Western blotting was performed using streptavidin-IR conjugate (Rockland Immunochemicals, Gilbertsville, PA) and scanned on an Odyssey Infrared Imager (LICOR Biosciences, Lincoln, NE).

Expression and Purification of Affinity-Tagged eEF2-$(His)_6$

BY4741 wild-type yeast cells as well as *dph1*, *dph5*, *ybr142w/dph6* and *ybr246w/dph7* mutants thereof carrying an *eft2* null-allele were transformed with plasmid pTKB612 (a kind gift from A. R. Merrill, University of Guelph, Ontario, Canada), which expresses a $(His)_6$-tagged form of translation elongation factor eEF2 (Table S3) that is fully functional and able to complement an *eft1 eft2* double mutant [56]. In order to express and purify $(His)_6$-tagged eEF2 for MS/MS analysis, 750 ml of yeast culture were grown in YPD to an OD_{600} 2.0 and harvested by centrifugation. The pellet was resuspended in 3 ml B60 buffer (50 mM HEPES-KOH pH 7.3, 60 mM KOAc, 5 mM $Mg(OAc)_2$, 0.1% Triton X100, 10% (v/v) glycerol, 1 mM NaF, 20 mM glycerophosphate, complete protease inhibitor [Roche]) without DTT and cells were lysed in a bead beater. The lysate was centrifuged twice at 13,500 rpm for 30 min. and the protein concentration measured with a NanoDrop spectrophotometer. Five mg total protein was applied to 2 mg anti-$(His)_6$-tag Dynabeads (Invitrogen, #101-03D) and purified according to manufacturer's instructions. The identity of purified eEF2 fraction was confirmed by SDS-PAGE and Western blot analysis using an anti-$(His)_6$ antibody (Abcam, #ab18184).

Analysis of Diphthamide Pathway Modifications on eEF2 by Mass Spectrometry

Crude yeast eEF2 preparations from wild-type and *dph* mutants strains were separated by SDS-PAGE using 4–12% Bis-Tris precast gels (Invitrogen, Carlsbad, USA) and the area of the gel containing eEF2 was excised after staining with Instant Blue Coomassie (Expedeon, Cambridge, UK). In-gel digests were performed using trypsin, subsequent to reduction and alkylation with dithiothreitol and iodoacetamide, with the resulting peptides cleaned over C18 columns. Peptides were then analyzed via HPLC-MS/MS using a Dionex U300 HPLC (Dionex California) with a 15 cm PepMap C18 column coupled to a Thermo Orbitrap Velos mass spectrometer (Thermo Fisher Scientific, Bremen, Germany). The peptides were eluted from the C18 column at 300 nL/min over 120 min using a linear 5–90% (v/v) acetonitrile gradient. The Orbitrap Velos was operated in positive ion mode, with an ion source voltage of 1.2 kV and capillary temperature 200°C, using a lock mass of 445.120024. The initial survey scan was performed at 60000 resolution, FTMS scanning from 335–1800 Da. The top 15 most intense ions were selected for MS/MS sequencing, using collision-induced dissociation (CID; MS/MS charge state 1+ rejected, >2+ accepted). Protein identification was performed using MaxQuant 1.2.2.5 [82] against a proteome database generated from the *Saccharomyces* Genome database [83]. Manual annotation of the modified peptide spectra corresponding to the modified EF2 peptide and generation of extracted ion chromatograms were done using the Thermo Xcalibur software for spectra visualization.

Supporting Information

Figure S1 MS/MS spectra of unmodified eEF2 peptide 686-VNILDVTLHADAIHR-700 from wild-type and mutant yeast strains. (A) Cartoon showing how the B and Y ions seen in the MS/MS spectra map onto the tryptic peptide containing His-699. Y1 to Y13 and B14 ions contain His-699 and their m/z values are therefore informative regarding the modification state of His-699. (B–F) MS/MS spectra of unmodified peptide in eEF2 obtained from the indicated yeast strains: the parent ion m/z and charge state is indicated in each case.
(TIF)

Figure S2 Extracted ion chromatograms of unmodified EF2 peptide 686-VNILDVTLHADAIHR-700. In (A), peaks corresponding to doubly-charged ions (m/z unmodified peptide 843.97, extracted mass range 843.8–844.0) are shown while triply-charged ions (m/z unmodified peptide 562.98, extracted mass range 562.5–563.2) are shown in (B). The yeast strain to which each chromatogram pertains is indicated. Note that in (B) an intensity of 580,000 corresponding to unmodified peptide with m/z 562.98 was not resolved from a different, more abundant ion with m/z 563.02 in the wt sample. Peak annotations are as follows: RT, retention time; AA, peak area; BP, parent ion m/z.
(TIF)

Figure S3 Extracted ion chromatograms of modified eEF2 peptide 686-VNILDVTLHADAIHR-700. (A) Peaks corresponding to triply-charged ions (m/z diphthine-modified peptide 610.68, m/z diphthamide-modified peptide 610.35, extracted masses 610.2–610.9). (B) Triply-charged ions (m/z ACP-modified peptide 596.66, extracted masses 596.2–596.8). Peak annotations are as follows: RT, retention time; AA, peak area; BP, parent ion m/z.
(TIF)

Figure S4 Failure to detect interaction by TAP-based co-immune precipitation between Dph6 or Dph7 and either Dph2 or diphthine synthase Dph5, factors integral to the first two steps of diphthamide synthesis. Co-immune precipitations were performed using magnetic beads (Dynabeads, Invitrogen) coupled to anti-CBP antibodies (Santa Cruz Biotechnology) specific for the calmodulin binding peptide (CBP) of the TAP-tag. The indicated strains expressed *DPH6-TAP* or *DPH7-TAP* in conjunction with HA-tagged versions of either *DPH2* or *DPH5*. A strain co-expressing respectively, HA- and TAP-tagged variants of Dph1 and Dph3, step 1 pathway players previously shown to associate with one another [6,20] served as a positive internal control for interaction. The presence of the respective proteins within the immune precipitates (IP) was assessed using anti-HA and anti-CBP Western blots (A) or anti-HA immune blots on total protein extracts obtained prior to the IP protocol (preIP). (B). Asterisks indicate breakdown products of Dph2-HA, Dph3-TAPand Dph6-TAP.
(TIF)

Figure S5 Failure to detect Dph6-Dph7 interaction by co-immune precipitation. Co-immune precipitations using the anti-HA-antibody were performed with the indicated strains expressing *DPH6-c-myc* or *DPH7-c-myc* on their own or in parallel with HA-tagged versions of *DPH5* or *DPH6*, respectively. A strain co-producing c-Myc- and HA- and tagged versions of the Elp2 subunit (*ELP2-c-myc*) of the Elongator complex, and Kti12 (*KTI12-HA*), a protein known to interact with Elp2 [84], was used as internal positive control. The presence of the respective proteins was assessed in individual anti-c-Myc and anti-HA Western blots both in the IPs (top two panels) and crude extracts (pre IP; bottom two panels). The asterisk denotes an unspecific band that originates from the anti-HA-antibody present in the IPs.
(TIF)

Figure S6 Lack of effect of *dph1-dph7* gene knockouts on growth performance and viability. (A) The wild-type parental strain and diphthamide deficient mutants *dph1*, *dph6* and *dph7* were grown in YNB minimal media supplemented with His, Met, Ura, Leu to

cover the auxotrophic markers (Table S2) under standard laboratory conditions over a period of 50 h. OD_{600} was monitored at 2 h intervals. (B) To address a potential temperature sensitive phenotype, ten-fold serial cell dilutions of the indicated strains were spotted on YPD plates and grown at 30°C or 39°C. Note that only the *dph3/kti11* mutant, which affects additional biosynthetic pathways [6,85] apart from diphthamide biosynthesis [13] shows temperature sensitivity (S) (S) while the other *dph* mutants tolerate high temperatures (T).
(TIF)

Figure S7 Altered growth performance of *dph1-dph7* mutants in response to translation elongation indicator drugs under standard or elevated cultivation temperatures. Ten-fold serial cell dilutions of wild-type parental strain as well as diphthamide mutants *dph1-dph7* were replica spotted on YPD plates without (control) and supplemented with hygromycin (20 µg/ml), anisomycin (20 µg/ml) or paromomycin (1.5 mg/ml) and grown at 30°C (A) or 37°C (B). Reduced or improved performance of the *dph* mutants relative to wild-type behavior reflects respectively, enhanced sensitivity or improved tolerance towards the drug in question respectively.
(TIF)

Figure S8 Conservation of the *DPH6* gene product, Dph6. (A) Representation of Dph6 indicating the conserved adenine nucleotide alpha hydrolase (cd1994) and YjgF-YER057c-UK114 related (cd06155, cd06166) domains discussed in the main text. (B) The Dph6 amino acid sequence was aligned using Clustal with representative examples of putative orthologs from other organisms (identified by PSI-BLAST). Sequences are as follows (database accession numbers in parentheses): *DPH6*, *S. cerevisiae* Dph6/Ylr143w; Sp_mug71, *Schizosaccharomyces pombe* (NP 595310); At_A_AAH_IV, *Arabidopsis thaliana* endoribonuclease (NP 187098); Df_A_AAH_IV, *Dictyostelium fasciculatum* endoribonuclease L-PSP domain-containing protein (EGG21287); Xl_A_AAH_IV, *Xenopus laevis* ATP binding domain 4 (NP 001085655); Hs_A_AAH_IV, Human ATP binding domain containing protein 4 (NP 542381); Mm_A_AAH_IV, mouse ATP binding domain containing protein 4 (NP 079951); Hs_UK114, human ribonuclease UK114/p14.5/L-PSP (NP 005827); Mm_UK114, mouse UK114/p14.5/L-PSP (NP 0032313). Note that the last two sequences appear twice in the alignment so that the sequence relationships to each of the YjgF-YER057c-UK114 related domains in the non-mammalian proteins can be shown. *, conserved residues shown to be important for trimerisation and ligand binding [63,66].
(TIF)

Figure S9 Conservation of the *DPH7* gene product, Dph7. (A) Representation of Dph7 showing the location of the conserved WD40 domains. (B) The Dph7 amino acid sequence was aligned using Clustal with representative examples of putative orthologs from other organisms (identified by PSI-BLAST). Sequences are as follows (database accession numbers in parentheses): *DPH7*, *S. cerevisiae* Dph7/Ybr246w Sp_WD85, *Schizosaccharomyces pombe* WD repeat protein (CAA21429); At_WD85, *Arabidopsis thaliana* WD40 domain-containing protein (NP 201106); Dd_WD85, *Dictyostelium discoideum* WD40 repeat-containing protein (XP 646601); Xt_WD85, *Xenopus tropicalis* WD repeat-containing protein 85-like (XP 002942023); Hs_WD85, Human WD repeat-containing protein 85 (NP 620133); Mm_WD85, mouse unnamed protein (BAE 32074).
(TIF)

Table S1 SGA-based Excel spreadsheet extracted from the DRYGIN database for comprehensive presentation of genetic interactions between query genes *DPH1*, *DPH2*, *DPH4*, *DPH5*, *DPH6/YLR143w* and *DPH7/YBR246w* and array ORFs totaling 3885 (*DPH1*, *DPH2*, *DPH6/YLR143w* and *DPH7/YBR246w*) and 4457 (*DPH4* and *DPH5*). Genetic interaction profiles among the six queries were ranked according to Pearson Correlation Coefficient determination (PCC). Correlation scores of the top ten interactors identified with each query gene identified a tightly clustered and highly robust, SGA-based *DPH* gene network (Figure 2C).
(XLSX)

Table S2 Strains used or generated for this study.
(DOCX)

Table S3 Plasmids used or constructed for this study.
(DOCX)

Table S4 Primers and oligonucleotides used for this study.
(DOCX)

Acknowledgments

Thanks are due to Drs. Charles Boone and Michael Costanzo for their advice and assistance in SGA data analysis. In addition we thank Dr. Valérie de Crécy-Lagard for critical evaluation of the manuscript and sharing unpublished related data, Dr. Terri Goss Kinzy for providing essential biologicals and reagents, Natascha Mumdey and Dr. Wael Abdel-Fattah for technical assistance, and Jonas Teeuwen for help with Figure 8.

Author Contributions

Conceived and designed the experiments: SU CB SL FG MJRS RS. Performed the experiments: SU CB VS SL StH. Analyzed the data: SU CB SL VS StH FG MJRS RS. Contributed reagents/materials/analysis tools: SU CB VS SL StH MJRS. Wrote the paper: FG MJRS RS.

References

1. Ahrne E, Muller M, Lisacek F (2010) Unrestricted identification of modified proteins using MS/MS. Proteomics 10: 671–686.
2. Seet BT, Dikic I, Zhou MM, Pawson T (2006) Reading protein modifications with interaction domains. Nat Rev Mol Cell Biol 7: 473–483.
3. Walsh CT, Garneau-Tsodikova S, Gatto GJJ (2005) Protein posttranslational modifications: the chemistry of proteome diversifications. Angew Chem Int Ed Engl 44: 7342–7372.
4. Greganova E, Altmann M, Butikofer P (2011) Unique modifications of translation elongation factors. FEBS J 278: 2613–2624.
5. Van Ness BG, Howard JB, Bodley JW (1980) ADP-ribosylation of elongation factor 2 by diphtheria toxin. NMR spectra and proposed structures of ribosyl-diphthamide and its hydrolysis products. J Biol Chem 255: 10710–10716.
6. Bär C, Zabel R, Liu S, Stark MJ, Schaffrath R (2008) A versatile partner of eukaryotic protein complexes that is involved in multiple biological processes: Kti11/Dph3. Mol Microbiol 69: 1221–1233.
7. Botet J, Rodriguez-Mateos M, Ballesta JP, Revuelta JL, Remacha M (2008) A chemical genomic screen in *Saccharomyces cerevisiae* reveals a role for diphthamidation of translation elongation factor 2 in inhibition of protein synthesis by sordarin. Antimicrob Agents Chemother 52: 1623–1629.
8. Van Ness BG, Howard JB, Bodley JW (1980) ADP-ribosylation of elongation factor 2 by diphtheria toxin. Isolation and properties of the novel ribosyl-amino acid and its hydrolysis products. J Biol Chem 255: 10717–107120.
9. Dominguez JM, Gomez-Lorenzo MG, Martin JJ (1999) Sordarin inhibits fungal protein synthesis by blocking translocation differently to fusidic acid. J Biol Chem 274: 22423–22427.
10. Jørgensen R, Ortiz PA, Carr-Schmid A, Nissen P, Kinzy TG, et al. (2003) Two crystal structures demonstrate large conformational changes in the eukaryotic ribosomal translocase. Nat Struct Biol 10: 379–385.
11. Oppenheimer NJ, Bodley JW (1981) Diphtheria toxin. Site and configuration of ADP-ribosylation of diphthamide in elongation factor 2. J Biol Chem 256: 8579–8581.
12. Pappenheimer AM, Jr. (1977) Diphtheria toxin. Annu Rev Biochem 46: 69–94.
13. Uthman S, Liu S, Giorgini F, Stark MJR, Costanzo M, et al. (2012) Diphtheria disease and genes involved in formation of diphthamide, key effector of the

diphtheria toxin. In: Priti R, editor. Insight and Control of Infectious Disease in Global Scenario. Rijeka: InTech.
14. Chen JY, Bodley JW, Livingston DM (1985) Diphtheria toxin-resistant mutants of *Saccharomyces cerevisiae*. Mol Cell Biol 5: 3357–3360.
15. Liu S, Leppla SH (2003) Retroviral insertional mutagenesis identifies a small protein required for synthesis of diphthamide, the target of bacterial ADP-ribosylating toxins. Mol Cell 12: 603–613.
16. Liu S, Milne GT, Kuremsky JG, Fink GR, Leppla SH (2004) Identification of the proteins required for biosynthesis of diphthamide, the target of bacterial ADP-ribosylating toxins on translation elongation factor 2. Mol Cell Biol 24: 9487–9497.
17. Dunlop PC, Bodley JW (1983) Biosynthetic labeling of diphthamide in *Saccharomyces cerevisiae*. J Biol Chem 258: 4754–4758.
18. Lin H (2011) S-adenosylmethionine-dependent alkylation reactions: when are radical reactions used? Bioorg Chem 39: 161–170.
19. Moehring JM, Moehring TJ, Danley DE (1980) Posttranslational modification of elongation factor 2 in diphtheria-toxin-resistant mutants of CHO-K1 cells. Proc Natl Acad Sci USA 77: 1010–1014.
20. Fichtner L, Jablonowski D, Schierhorn A, Kitamoto HK, Stark MJ, et al. (2003) Elongator's toxin-target (TOT) function is nuclear localization sequence dependent and suppressed by post-translational modification. Mol Microbiol 49: 1297–1307.
21. Zhang Y, Zhu X, Torelli AT, Lee M, Dzikovski B, et al. (2010) Diphthamide biosynthesis requires an organic radical generated by an iron-sulphur enzyme. Nature 465: 891–896.
22. Zhu X, Dzikovski B, Su X, Torelli AT, Zhang Y, et al. (2011) Mechanistic understanding of *Pyrococcus horikoshii* Dph2, a [4Fe-4S] enzyme required for diphthamide biosynthesis. Mol Biosyst 7: 74–81.
23. Proudfoot M, Sanders SA, Singer A, Zhang R, Brown G, et al. (2008) Biochemical and structural characterization of a novel family of cystathionine beta-synthase domain proteins fused to a Zn ribbon-like domain. J Mol Biol 375: 301–315.
24. Thakur A, Chitoor B, Goswami AV, Pareek G, Atreya HS, et al. (2012) Structure and mechanistic insights into novel iron-mediated moonlighting functions of human J-protein cochaperone, Dph4. J Biol Chem 287: 13194–13205.
25. Fichtner L, Schaffrath R (2002) *KTI11* and *KTI13*, *Saccharomyces cerevisiae* genes controlling sensitivity to G1 arrest induced by *Kluyveromyces lactis* zymocin. Mol Microbiol 44: 865–875.
26. Greenwood C, Selth LA, Dirac-Svejstrup AB, Svejstrup JQ (2009) An iron-sulfur cluster domain in Elp3 important for the structural integrity of elongator. J Biol Chem 284: 141–149.
27. Huang B, Johansson MJ, Byström AS (2005) An early step in wobble uridine tRNA modification requires the Elongator complex. RNA 11: 424–436.
28. Paraskevopoulou C, Fairhurst SA, Lowe DJ, Brick P, Onesti S (2006) The Elongator subunit Elp3 contains a Fe_4S_4 cluster and binds S-adenosylmethionine. Mol Microbiol 59: 795–806.
29. Chen JY, Bodley JW (1988) Biosynthesis of diphthamide in Saccharomyces cerevisiae. Partial purification and characterization of a specific S-adenosylmethionine:elongation factor 2 methyltransferase. J Biol Chem 263: 11692–11696.
30. Mattheakis LC, Shen WH, Collier RJ (1992) *DPH5*, a methyltransferase gene required for diphthamide biosynthesis in *Saccharomyces cerevisiae*. Mol Cell Biol 12: 4026–4037.
31. Moehring TJ, Danley DE, Moehring JM (1984) In vitro biosynthesis of diphthamide, studied with mutant Chinese hamster ovary cells resistant to diphtheria toxin. Mol Cell Biol 4: 642–650.
32. Zhu X, Kim J, Su X, Lin H (2010) Reconstitution of diphthine synthase activity *in vitro*. Biochemistry 49: 9649–9657.
33. Zhang Y, Liu S, Lajoie G, Merrill AR (2008) The role of the diphthamide-containing loop within eukaryotic elongation factor 2 in ADP-ribosylation by *Pseudomonas aeruginosa* exotoxin A. Biochem J 413: 163–174.
34. Jorgensen R, Purdy AE, Fieldhouse RJ, Kimber MS, Bartlett DH, et al. (2008) Cholix toxin, a novel ADP-ribosylating factor from *Vibrio cholerae*. J Biol Chem 283: 10671–10678.
35. Uthman S, Kheir E, Bär C, Jablonowski D, Schaffrath R (2011) Growth inhibition strategies based on antimicrobial microbes/toxins. In: A M-V, editor. Science against Microbial Pathogens: Communicating Current Research and Technological Advances: Formatex Research Center, Spain. pp. 1321–1329.
36. Ortiz PA, Ulloque R, Kihara GK, Zheng H, Kinzy TG (2006) Translation elongation factor 2 anticodon mimicry domain mutants affect fidelity and diphtheria toxin resistance. J Biol Chem 281: 32639–32648.
37. Kimata Y, Kohno K (1994) Elongation factor 2 mutants deficient in diphthamide formation show temperature-sensitive cell growth. J Biol Chem 269: 13497–13501.
38. Chen CM, Behringer RR (2004) Ovca1 regulates cell proliferation, embryonic development, and tumorigenesis. Genes Dev 18: 320–332.
39. Liu S, Wiggins JF, Sreenath T, Kulkarni AB, Ward JM, et al. (2006) Dph3, a small protein required for diphthamide biosynthesis, is essential in mouse development. Mol Cell Biol 26: 3835–3841.
40. Webb TR, Cross SH, McKie L, Edgar R, Vizor L, et al. (2008) Diphthamide modification of eEF2 requires a J-domain protein and is essential for normal development. J Cell Sci 121: 3140–3145.
41. Carette JE, Guimaraes CP, Varadarajan M, Park AS, Wuethrich I, et al. (2009) Haploid genetic screens in human cells identify host factors used by pathogens. Science 326: 1231–1235.
42. Su X, Chen W, Lee W, Jiang H, Zhang S, et al. (2012) YBR246W is required for the third step of diphthamide biosynthesis. J Am Chem Soc 134: 773–776.
43. Hillenmeyer ME, Ericson E, Davis RW, Nislow C, Koller D, et al. (2010) Systematic analysis of genome-wide fitness data in yeast reveals novel gene function and drug action. Genome Biol 11: R30.
44. Koh JL, Ding H, Costanzo M, Baryshnikova A, Toufighi K, et al. (2010) DRYGIN: a database of quantitative genetic interaction networks in yeast. Nucleic Acids Res 38: D502–D507.
45. Costanzo M, Baryshnikova A, Bellay J, Kim Y, Spear ED, et al. (2010) The genetic landscape of a cell. Science 327: 425–431.
46. Tong AH, Evangelista M, Parsons AB, Xu H, Bader GD, et al. (2001) Systematic genetic analysis with ordered arrays of yeast deletion mutants. Science 294: 2364–2368.
47. Tong AH, Lesage G, Bader GD, Ding H, Xu H, et al. (2004) Global mapping of the yeast genetic interaction network. Science 303: 808–813.
48. Costanzo M, Baryshnikova A, Myers CL, Andrews B, Boone C (2011) Charting the genetic interaction map of a cell. Curr Opin Biotechnol 22: 66–74.
49. Dixon SJ, Costanzo M, Baryshnikova A, Andrews B, Boone C (2009) Systematic mapping of genetic interaction networks. Annu Rev Genet 43: 601–625.
50. DRYGIN [http://drygin.ccbr.utoronto.ca/]
51. FitDB [http://drygin.ccbr.utoronto.ca/]
52. Hillenmeyer ME, Fung E, Wildenhain J, Pierce SE, Hoon S, et al. (2008) The chemical genomic portrait of yeast: uncovering a phenotype for all genes. Science 320: 362–365.
53. Justice MC, Hsu MJ, Tse B, Ku T, Balkovec J, et al. (1998) Elongation factor 2 as a novel target for selective inhibition of fungal protein synthesis. J Biol Chem 273: 3148–3151.
54. Søe R, Mosley RT, Justice M, Nielsen-Kahn J, Shastry M, et al. (2007) Sordarin derivatives induce a novel conformation of the yeast ribosome translocation factor eEF2. J Biol Chem 282: 657–666.
55. Mumberg D, Muller R, Funk M (1994) Regulatable promoters of *Saccharomyces cerevisiae*: comparison of transcriptional activity and their use for heterologous expression. Nucleic Acids Res 22: 5767–5768.
56. Jorgensen R, Carr-Schmid A, Ortiz PA, Kinzy TG, Andersen GR (2002) Purification and crystallization of the yeast elongation factor eEF2. Acta Crystallogr D Biol Crystallogr 58: 712–715.
57. Spahn CM, Gomez-Lorenzo MG, Grassucci RA, Jorgensen R, Andersen GR, et al. (2004) Domain movements of elongation factor eEF2 and the eukaryotic 80S ribosome facilitate tRNA translocation. EMBO J 23: 1008–1019.
58. Ortiz PA, Kinzy TG (2005) Dominant-negative mutant phenotypes and the regulation of translation elongation factor 2 levels in yeast. Nucleic Acids Res 33: 5740–5748.
59. Harger JW, Meskauskas A, Nielsen J, Justice MC, Dinman JD (2001) Ty1 retrotransposition and programmed +1 ribosomal frameshifting require the integrity of the protein synthetic translocation step. Virology 286: 216–224.
60. de Crecy-Lagard V, Forouhar F, Brochier-Armanet C, Tong L, Hunt JF (2012) Comparative genomic analysis of the DUF71/COG2102 family predicts roles in diphthamide biosynthesis and B12 salvage. Biology Direct 7: 32.
61. Su X, Lin Z, Chen W, Jiang H, Zhang S, et al. (2012) Chemogenomic approach identified yeast YLR143W as diphthamide synthetase. Proc Natl Acad Sci USA 109: 19983–19987.
62. Marchler-Bauer A, Lu S, Anderson JB, Chitsaz F, Derbyshire MK, et al. (2011) CDD: a Conserved Domain Database for the functional annotation of proteins. Nucleic Acids Res 39: D225–D229.
63. Burman JD, Stevenson CE, Sawers RG, Lawson DM (2007) The crystal structure of *Escherichia coli* TdcF, a member of the highly conserved YjgF/YER057c/UK114 family. BMC Struct Biol 7: 30.
64. Sinha S, Rappu P, Lange SC, Mantsala P, Zalkin H, et al. (1999) Crystal structure of *Bacillus subtilis* YabJ, a purine regulatory protein and member of the highly conserved YjgF family. Proc Natl Acad Sci USA 96: 13074–13079.
65. Volz K (1999) A test case for structure-based functional assignment: the 1.2 A crystal structure of the yjgF gene product from *Escherichia coli*. Protein Sci 8: 2428–2437.
66. Mistiniene E, Pozdniakovaite N, Popendikyte V, Naktinis V (2005) Structure-based ligand binding sites of protein p14.5, a member of protein family YER057c/YIL051c/YjgF. Int J Biol Macromol 37: 61–68.
67. Lambrecht JA, Flynn JM, Downs DM (2012) Conserved YjgF protein family deaminates reactive enamine/imine intermediates of pyridoxal 5′-phosphate (PLP)-dependent enzyme reactions. J Biol Chem 287: 3454–3461.
68. Shi Y, Stefan CJ, Rue SM, Teis D, Emr SD (2011) Two novel WD40 domain-containing proteins, Ere1 and Ere2, function in the retromer-mediated endosomal recycling pathway. Mol Biol Cell 22: 4093–4107.
69. Hontz RD, Niederer RO, Johnson JM, Smith JS (2009) Genetic identification of factors that modulate ribosomal DNA transcription in *Saccharomyces cerevisiae*. Genetics 182: 105–119.
70. Gupta PK, Liu S, Batavia MP, Leppla SH (2008) The diphthamide modification on elongation factor-2 renders mammalian cells resistant to ricin. Cell Microbiol 10: 1687–1694.
71. Liu S, Bachran C, Gupta P, Miller-Randolph S, Wang H, et al. (2012) Diphthamide modification on eukaryotic elongation factor 2 is needed to assure

fidelity of mRNA translation and mouse development. Proc Natl Acad Sci USA 109: 13817–13822.
72. Nobukuni Y, Kohno K, Miyagawa K (2005) Gene trap mutagenesis-based forward genetic approach reveals that the tumor suppressor OVCA1 is a component of the biosynthetic pathway of diphthamide on elongation factor 2. J Biol Chem 280: 10572–10577.
73. Sherman F (1991) Getting started with yeast. Methods Enzymol 194: 3–21.
74. Gietz D, St Jean A, Woods RA, Schiestl RH (1992) Improved method for high efficiency transformation of intact yeast cells. Nucleic Acids Res 20: 1425.
75. Roy V, Ghani K, Caruso M (2010) A dominant-negative approach that prevents diphthamide formation confers resistance to *Pseudomonas* exotoxin A and diphtheria toxin. PLoS ONE 5: e15753. doi:10.1371/journal.pone.0015753
76. Jablonowski D, Fichtner L, Martin VJ, Klassen R, Meinhardt F, et al. (2001) *Saccharomyces cerevisiae* cell wall chitin, the *Kluyveromyces lactis* zymocin receptor. Yeast 18: 1285–1299.
77. Frohloff F, Jablonowski D, Fichtner L, Schaffrath R (2003) Subunit communications crucial for the functional integrity of the yeast RNA polymerase II elongator (gamma-toxin target (TOT)) complex. J Biol Chem 278: 956–961.
78. Knop M, Siegers K, Pereira G, Zachariae W, Winsor B, et al. (1999) Epitope tagging of yeast genes using a PCR-based strategy: more tags and improved practical routines. Yeast 15: 963–972.
79. Zachariae W, Shin TH, Galova M, Obermaier B, Nasmyth K (1996) Identification of subunits of the anaphase-promoting complex of *Saccharomyces cerevisiae*. Science 274: 1201–1204.
80. Gietz RD, Sugino A (1988) New yeast-*Escherichia coli* shuttle vectors constructed with *in vitro* mutagenized yeast genes lacking six-base pair restriction sites. Gene 74: 527–534.
81. Janke C, Magiera MM, Rathfelder N, Taxis C, Reber S, et al. (2004) A versatile toolbox for PCR-based tagging of yeast genes: new fluorescent proteins, more markers and promoter substitution cassettes. Yeast 21: 947–962.
82. Cox J, Mann M (2008) MaxQuant enables high peptide identification rates, individualized p.p.b.-range mass accuracies and proteome-wide protein quantification. Nat Biotechnol 26: 1367–1372.
83. Cherry JM, Hong EL, Amundsen C, Balakrishnan R, Binkley G, et al. (2012) *Saccharomyces* Genome Database: the genomics resource of budding yeast. Nucleic Acids Res 40: D700–D705.
84. Frohloff F, Fichtner L, Jablonowski D, Breunig KD, Schaffrath R (2001) *Saccharomyces cerevisiae* Elongator mutations confer resistance to the *Kluyveromyces lactis* zymocin. EMBO J 20: 1993–2003.
85. Jablonowski D, Schaffrath R (2007) Zymocin, a composite chitinase and tRNase killer toxin from yeast, Biochem Soc Trans 35: 1533–1537.

BIBLIOGRAPHY

8 Bibliography

Aevarsson, A., Brazhnikov, E., Garber, M., Zheltonosova, J., Chirgadze, Y., al-Karadaghi, S., Svensson, L.A., and Liljas, A. 1994. Three-dimensional structure of the ribosomal translocase: elongation factor G from Thermus thermophilus. *EMBO J* **13**(16): 3669-3677.

Agrawal, R.K., Heagle, A.B., Penczek, P., Grassucci, R.A., and Frank, J. 1999. EF-G-dependent GTP hydrolysis induces translocation accompanied by large conformational changes in the 70S ribosome. *Nat Struct Biol* **6**(7): 643-647.

Andersen, C.B., Becker, T., Blau, M., Anand, M., Halic, M., Balar, B., Mielke, T., Boesen, T., Pedersen, J.S., Spahn, C.M. et al. 2006. Structure of eEF3 and the mechanism of transfer RNA release from the E-site. *Nature* **443**(7112): 663-668.

Ayoubi, T.A. and Van De Ven, W.J. 1996. Regulation of gene expression by alternative promoters. *FASEB J* **10**(4): 453-460.

Baer, C., Zabel, R., Liu, S., Stark, M.J.R., and Schaffrath, R. 2008. A versatile partner of eukaryotic protein complexes that is involved in multiple biological processes: Kti11/Dph3. *Molecular Microbiology* **69**(5): 1221-1233.

Bar, C., Zabel, R., Liu, S., Stark, M.J., and Schaffrath, R. 2008. A versatile partner of eukaryotic protein complexes that is involved in multiple biological processes: Kti11/Dph3. *Mol Microbiol* **69**(5): 1221-1233.

Baryshnikova, A., Costanzo, M., Kim, Y., Ding, H., Koh, J., Toufighi, K., Youn, J.Y., Ou, J., San Luis, B.J., Bandyopadhyay, S. et al. 2010. Quantitative analysis of fitness and genetic interactions in yeast on a genome scale. *Nat Methods* **7**(12): 1017-1024.

Belew, A.T., Advani, V.M., and Dinman, J.D. 2011. Endogenous ribosomal frameshift signals operate as mRNA destabilizing elements through at least two molecular pathways in yeast. *Nucleic Acids Res* **39**(7): 2799-2808.

Belew, A.T., Hepler, N.L., Jacobs, J.L., and Dinman, J.D. 2008. PRFdb: a database of computationally predicted eukaryotic programmed -1 ribosomal frameshift signals. *BMC Genomics* **9**: 339.

Berchuck, A., Kohler, M.F., Hopkins, M.P., Humphrey, P.A., Robboy, S.J., Rodriguez, G.C., Soper, J.T., Clarkepearson, D.L., and Bast, R.C. 1994a. OVEREXPRESSION OF P53 IS NOT A FEATURE OF BENIGN AND

EARLY-STAGE BORDERLINE EPITHELIAL OVARIAN-TUMORS. *Gynecologic Oncology* **52**(2): 232-236.

Berchuck, A., Kohler, M.F., Marks, J.R., Wiseman, R., Boyd, J., and Bast, R.C. 1994b. THE P53 TUMOR-SUPPRESSOR GENE FREQUENTLY IS ALTERED IN GYNECOLOGIC CANCERS. *American Journal of Obstetrics and Gynecology* **170**(1): 246-252.

Berggard, T., Linse, S., and James, P. 2007. Methods for the detection and analysis of protein-protein interactions. *Proteomics* **7**(16): 2833-2842.

Botet, J., Rodriguez-Mateos, M., Ballesta, J.P., Revuelta, J.L., and Remacha, M. 2008. A chemical genomic screen in Saccharomyces cerevisiae reveals a role for diphthamidation of translation elongation factor 2 in inhibition of protein synthesis by sordarin. *Antimicrob Agents Chemother* **52**(5): 1623-1629.

Brierley, I. 1995. Ribosomal frameshifting viral RNAs. *J Gen Virol* **76 (Pt 8)**: 1885-1892.

Brigotti, M., Rambelli, F., Zamboni, M., Montanaro, L., and Sperti, S. 1989. Effect of alpha-sarcin and ribosome-inactivating proteins on the interaction of elongation factors with ribosomes. *Biochem J* **257**(3): 723-727.

Bruening, W., Prowse, A.H., Schultz, D.C., Holgado-Madruga, M., Wong, A., and Godwin, A.K. 1999. Expression of OVCA1, a candidate tumor suppressor, is reduced in tumors and inhibits growth of ovarian cancer cells. *Cancer Research* **59**(19): 4973-4983.

Burman, J.D., Stevenson, C.E., Sawers, R.G., and Lawson, D.M. 2007. The crystal structure of Escherichia coli TdcF, a member of the highly conserved YjgF/YER057c/UK114 family. *BMC Struct Biol* **7**: 30.

Carette, J.E., Guimaraes, C.P., Varadarajan, M., Park, A.S., Wuethrich, I., Godarova, A., Kotecki, M., Cochran, B.H., Spooner, E., Ploegh, H.L. et al. 2009. Haploid genetic screens in human cells identify host factors used by pathogens. *Science* **326**(5957): 1231-1235.

Chen, C.M. and Behringer, R.R. 2004a. Ovca1 regulates cell proliferation, embryonic development, and tumorigenesis. *Genes & Development* **18**(3): 320-332.

-. 2004b. Ovca1 regulates cell proliferation, embryonic development, and tumorigenesis. *Genes Dev* **18**(3): 320-332.

Chen, D.C., Yang, B.C., and Kuo, T.T. 1992. One-step transformation of yeast in stationary phase. *Curr Genet* **21**(1): 83-84.

Chen, J.Y. and Bodley, J.W. 1988. Biosynthesis of diphthamide in Saccharomyces cerevisiae. Partial purification and characterization of a specific S-

adenosylmethionine:elongation factor 2 methyltransferase. *J Biol Chem* **263**(24): 11692-11696.

Chen, J.Y., Bodley, J.W., and Livingston, D.M. 1985a. Diphtheria toxin-resistant mutants of Saccharomyces cerevisiae. *Mol Cell Biol* **5**(12): 3357-3360.

Chen, J.Y.C., Bodley, J.W., and Livingston, D.M. 1985b. DIPHTHERIA TOXIN-RESISTANT MUTANTS OF SACCHAROMYCES-CEREVISIAE. *Molecular and Cellular Biology* **5**(12): 3357-3360.

Cherry, J.M., Hong, E.L., Amundsen, C., Balakrishnan, R., Binkley, G., Chan, E.T., Christie, K.R., Costanzo, M.C., Dwight, S.S., Engel, S.R. et al. Saccharomyces Genome Database: the genomics resource of budding yeast. *Nucleic Acids Res* **40**(Database issue): D700-705.

Collier, R.J. 2001. Understanding the mode of action of diphtheria toxin: a perspective on progress during the 20th century. *Toxicon* **39**(11): 1793-1803.

Corda, D. and Di Girolamo, M. 2003. Functional aspects of protein mono-ADP-ribosylation. *EMBO J* **22**(9): 1953-1958.

Costanzo, M., Baryshnikova, A., Bellay, J., Kim, Y., Spear, E.D., Sevier, C.S., Ding, H., Koh, J.L., Toufighi, K., Mostafavi, S. et al. 2010. The genetic landscape of a cell. *Science* **327**(5964): 425-431.

Cox, J. and Mann, M. 2008. MaxQuant enables high peptide identification rates, individualized p.p.b.-range mass accuracies and proteome-wide protein quantification. *Nat Biotechnol* **26**(12): 1367-1372.

Deng, Q. and Barbieri, J.T. 2008. Molecular mechanisms of the cytotoxicity of ADP-ribosylating toxins. *Annu Rev Microbiol* **62**: 271-288.

Dever, T.E. and Green, R. 2012. The elongation, termination, and recycling phases of translation in eukaryotes. *Cold Spring Harb Perspect Biol* **4**(7): a013706.

Dinman, J.D. 1995. Ribosomal frameshifting in yeast viruses. *Yeast* **11**(12): 1115-1127.

-. 2006. Programmed Ribosomal Frameshifting Goes Beyond Viruses: Organisms from all three kingdoms use frameshifting to regulate gene expression, perhaps signaling a paradigm shift. *Microbe Wash DC* **1**(11): 521-527.

Dixon, S.J., Costanzo, M., Baryshnikova, A., Andrews, B., and Boone, C. 2009. Systematic mapping of genetic interaction networks. *Annu Rev Genet* **43**: 601-625.

Dominguez, J.M., Gomez-Lorenzo, M.G., and Martin, J.J. 1999. Sordarin inhibits fungal protein synthesis by blocking translocation differently to fusidic acid. *J Biol Chem* **274**(32): 22423-22427.

Farabaugh, P.J. 1996. Programmed translational frameshifting. *Microbiol Rev* **60**(1): 103-134.

Fendrick, J.L. and Iglewski, W.J. 1989a. Endogenous ADP-ribosylation of elongation factor 2 in polyoma virus-transformed baby hamster kidney cells. *Proc Natl Acad Sci U S A* **86**(2): 554-557.

-. 1989b. ENDOGENOUS ADP-RIBOSYLATION OF ELONGATION FACTOR-II IN POLYOMA VIRUS-TRANSFORMED BABY HAMSTER-KIDNEY CELLS. *Proceedings of the National Academy of Sciences of the United States of America* **86**(2): 554-557.

Fendrick, J.L., Iglewski, W.J., Moehring, J.M., and Moehring, T.J. 1992. Characterization of the endogenous ADP-ribosylation of wild-type and mutant elongation factor 2 in eukaryotic cells. *Eur J Biochem* **205**(1): 25-31.

Fernandez-Puentes, C., Benson, S., Olsnes, S., and Pihl, A. 1976. Protective effect of elongation factor 2 on the inactivation of ribosomes by the toxic lectins abrin and ricin. *Eur J Biochem* **64**(2): 437-443.

Fichtner, L., Jablonowski, D., Schierhorn, A., Kitamoto, H.K., Stark, M.J., and Schaffrath, R. 2003a. Elongator's toxin-target (TOT) function is nuclear localization sequence dependent and suppressed by post-translational modification. *Mol Microbiol* **49**(5): 1297-1307.

Fichtner, L., Jablonowski, D., Schierhorn, A., Kitamoto, H.K., Stark, M.J.R., and Schaffrath, R. 2003b. Elongator's toxin-target (TOT) function is nuclear localization sequence dependent and suppressed by post-translational modification. *Molecular Microbiology* **49**(5): 1297-1307.

Fichtner, L. and Schaffrath, R. 2002. KTI11 and KTI13, Saccharomyces cerevisiae genes controlling sensitivity to G1 arrest induced by Kluyveromyces lactis zymocin. *Mol Microbiol* **44**(3): 865-875.

Gomez-Lorenzo, M.G., Spahn, C.M., Agrawal, R.K., Grassucci, R.A., Penczek, P., Chakraburtty, K., Ballesta, J.P., Lavandera, J.L., Garcia-Bustos, J.F., and Frank, J. 2000. Three-dimensional cryo-electron microscopy localization of EF2 in the Saccharomyces cerevisiae 80S ribosome at 17.5 A resolution. *EMBO J* **19**(11): 2710-2718.

Guarente, L. 1993. Synthetic enhancement in gene interaction: a genetic tool come of age. *Trends Genet* **9**(10): 362-366.

Gupta, P.K., Liu, S., Batavia, M.P., and Leppla, S.H. 2008. The diphthamide modification on elongation factor-2 renders mammalian cells resistant to ricin. *Cell Microbiol* **10**(8): 1687-1694.

Harger, J.W., Meskauskas, A., Nielsen, J., Justice, M.C., and Dinman, J.D. 2001. Ty1 retrotransposition and programmed +1 ribosomal frameshifting require the integrity of the protein synthetic translocation step. *Virology* **286**(1): 216-224.

Hillenmeyer, M.E., Ericson, E., Davis, R.W., Nislow, C., Koller, D., and Giaever, G. 2010. Systematic analysis of genome-wide fitness data in yeast reveals novel gene function and drug action. *Genome Biol* **11**(3): R30.

Hillenmeyer, M.E., Fung, E., Wildenhain, J., Pierce, S.E., Hoon, S., Lee, W., Proctor, M., St Onge, R.P., Tyers, M., Koller, D. et al. 2008. The chemical genomic portrait of yeast: uncovering a phenotype for all genes. *Science* **320**(5874): 362-365.

Holmberg, L. and Nygard, O. 1994. Interaction sites of ribosome-bound eukaryotic elongation factor 2 in 18S and 28S rRNA. *Biochemistry* **33**(50): 15159-15167.

Honjo, T., Nishizuka, Y., and Hayaishi, O. 1968. Diphtheria toxin-dependent adenosine diphosphate ribosylation of aminoacyl transferase II and inhibition of protein synthesis. *J Biol Chem* **243**(12): 3553-3555.

Hontz, R.D., Niederer, R.O., Johnson, J.M., and Smith, J.S. 2009. Genetic identification of factors that modulate ribosomal DNA transcription in Saccharomyces cerevisiae. *Genetics* **182**(1): 105-119.

Huh, W.K., Falvo, J.V., Gerke, L.C., Carroll, A.S., Howson, R.W., Weissman, J.S., and O'Shea, E.K. 2003. Global analysis of protein localization in budding yeast. *Nature* **425**(6959): 686-691.

Jablonowski, D., Fichtner, L., Martin, V.J., Klassen, R., Meinhardt, F., Stark, M.J., and Schaffrath, R. 2001. Saccharomyces cerevisiae cell wall chitin, the Kluyveromyces lactis zymocin receptor. *Yeast* **18**(14): 1285-1299.

Jacobs, J.L., Belew, A.T., Rakauskaite, R., and Dinman, J.D. 2007. Identification of functional, endogenous programmed -1 ribosomal frameshift signals in the genome of Saccharomyces cerevisiae. *Nucleic Acids Res* **35**(1): 165-174.

Jager, D., Werdan, K., and Muller-Werdan, U. 2011. Endogenous ADP-ribosylation of elongation factor-2 by interleukin-1beta. *Mol Cell Biochem* **348**(1-2): 125-128.

Jensen, O.N. 2004. Modification-specific proteomics: characterization of post-translational modifications by mass spectrometry. *Curr Opin Chem Biol* **8**(1): 33-41.

Jorgensen, R., Merrill, A.R., and Andersen, G.R. 2005. The life and death of translation elongation factor 2. In *Translation UK Meeting*, pp. 1-6, Glasgow, SCOTLAND.

-. 2006. The life and death of translation elongation factor 2. *Biochem Soc Trans* **34**(Pt 1): 1-6.

Jorgensen, R., Ortiz, P.A., Carr-Schmid, A., Nissen, P., Kinzy, T.G., and Andersen, G.R. 2003. Two crystal structures demonstrate large conformational changes in the eukaryotic ribosomal translocase. *Nat Struct Biol* **10**(5): 379-385.

Kimata, Y. and Kohno, K. 1994. Elongation factor 2 mutants deficient in diphthamide formation show temperature-sensitive cell growth. *J Biol Chem* **269**(18): 13497-13501.

Knop, M., Siegers, K., Pereira, G., Zachariae, W., Winsor, B., Nasmyth, K., and Schiebel, E. 1999. Epitope tagging of yeast genes using a PCR-based strategy: more tags and improved practical routines. *Yeast* **15**(10B): 963-972.

Koh, J.L., Ding, H., Costanzo, M., Baryshnikova, A., Toufighi, K., Bader, G.D., Myers, C.L., Andrews, B.J., and Boone, C. 2010. DRYGIN: a database of quantitative genetic interaction networks in yeast. *Nucleic Acids Res* **38**(Database issue): D502-507.

Kong, F., Tong, R., Jia, L., Wei, W., Miao, X., Zhao, X., Sun, W., Yang, G., and Zhao, C. 2011. OVCA1 inhibits the proliferation of epithelial ovarian cancer cells by decreasing cyclin D1 and increasing p16. *Mol Cell Biochem* **354**(1-2): 199-205.

Lambrecht, J.A., Flynn, J.M., and Downs, D.M. 2012. Conserved YjgF protein family deaminates reactive enamine/imine intermediates of pyridoxal 5'-phosphate (PLP)-dependent enzyme reactions. *J Biol Chem* **287**(5): 3454-3461.

Lin, H. and Begley, T. 2011. Protein posttranslational modifications: chemistry, biology, and applications. *Mol Biosyst* **7**(1): 14-15.

Lin H., D.J., Jiang H. 2008. Post-translational modifications to regulate protein function. in *Wiley Encyclopedia of Chemical Biology* (ed. I. John Wiley & Sons).

Liu, S., Bachran, C., Gupta, P., Miller-Randolph, S., Wang, H., Crown, D., Zhang, Y., Wein, A.N., Singh, R., Fattah, R. et al. 2012. Diphthamide modification on eukaryotic elongation factor 2 is needed to assure fidelity of mRNA translation and mouse development. *Proc Natl Acad Sci U S A* **109**(34): 13817-13822.

Liu, S. and Leppla, S.H. 2003a. Retroviral insertional mutagenesis identifies a small protein required for synthesis of diphthamide, the target of bacterial ADP-ribosylating toxins. *Mol Cell* **12**(3): 603-613.

Liu, S., Milne, G.T., Kuremsky, J.G., Fink, G.R., and Leppla, S.H. 2004a. Identification of the proteins required for biosynthesis of diphthamide, the target of bacterial ADP-ribosylating toxins on translation elongation factor 2. *Mol Cell Biol* **24**(21): 9487-9497.

Liu, S., Wiggins, J.F., Sreenath, T., Kulkarni, A.B., Ward, J.M., and Leppla, S.H. 2006. Dph3, a small protein required for diphthamide biosynthesis, is essential in mouse development. *Mol Cell Biol* **26**(10): 3835-3841.

Liu, S.H. and Leppla, S.H. 2003b. Retroviral insertional mutagenesis identifies a small protein required for synthesis of diphthamide, the target of bacterial ADP-ribosylating toxins. *Molecular Cell* **12**(3): 603-613.

Liu, S.H., Milne, G.T., Kuremsky, J.G., Fink, G.R., and Leppla, S.H. 2004b. Identification of the proteins required for biosynthesis of diphthamide, the target of bacterial ADP-ribosylating toxins on translation elongation factor 2. *Molecular and Cellular Biology* **24**(21): 9487-9497.

Marchler-Bauer, A., Lu, S., Anderson, J.B., Chitsaz, F., Derbyshire, M.K., DeWeese-Scott, C., Fong, J.H., Geer, L.Y., Geer, R.C., Gonzales, N.R. et al. 2011. CDD: a Conserved Domain Database for the functional annotation of proteins. *Nucleic Acids Res* **39**(Database issue): D225-229.

Mattheakis, L.C., Shen, W.H., and Collier, R.J. 1992. DPH5, A METHYLTRANSFERASE GENE REQUIRED FOR DIPHTHAMIDE BIOSYNTHESIS IN SACCHAROMYCES-CEREVISIAE. *Molecular and Cellular Biology* **12**(9): 4026-4037.

Melcher, K. 2004. New chemical crosslinking methods for the identification of transient protein-protein interactions with multiprotein complexes. *Curr Protein Pept Sci* **5**(4): 287-296.

Mistiniene, E., Pozdniakovaite, N., Popendikyte, V., and Naktinis, V. 2005. Structure-based ligand binding sites of protein p14.5, a member of protein family YER057c/YIL051c/YjgF. *Int J Biol Macromol* **37**(1-2): 61-68.

Moehring, T.J., Danley, D.E., and Moehring, J.M. 1984. In vitro biosynthesis of diphthamide, studied with mutant Chinese hamster ovary cells resistant to diphtheria toxin. *Mol Cell Biol* **4**(4): 642-650.

Mumberg, D., Muller, R., and Funk, M. 1994. Regulatable promoters of Saccharomyces cerevisiae: comparison of transcriptional activity and their use for heterologous expression. *Nucleic Acids Res* **22**(25): 5767-5768.

Murphy, J.R. 1996. Corynebacterium Diphtheriae.

Oppenheimer, N.J. and Bodley, J.W. 1981. Diphtheria toxin. Site and configuration of ADP-ribosylation of diphthamide in elongation factor 2. *J Biol Chem* **256**(16): 8579-8581.

Ortiz, P.A. and Kinzy, T.G. 2005. Dominant-negative mutant phenotypes and the regulation of translation elongation factor 2 levels in yeast. *Nucleic Acids Res* **33**(18): 5740-5748.

Ortiz, P.A., Ulloque, R., Kihara, G.K., Zheng, H., and Kinzy, T.G. 2006a. Translation elongation factor 2 anticodon mimicry domain mutants affect fidelity and diphtheria toxin resistance. *J Biol Chem* **281**(43): 32639-32648.

Ortiz, P.A., Ulloque, R., Kihara, G.K., Zheng, H.Y., and Kinzy, T.G. 2006b. Translation elongation factor 2 anticodon mimicry domain mutants affect fidelity and diphtheria toxin resistance. *Journal of Biological Chemistry* **281**(43): 32639-32648.

Pappenheimer, A.M., Jr. 1977. Diphtheria toxin. *Annu Rev Biochem* **46**: 69-94.

Phillips, N., Ziegler, M., Saha, B., and Xynos, F. 1993. ALLELIC LOSS ON CHROMOSOME-17 IN HUMAN OVARIAN-CANCER. *International Journal of Cancer* **54**(1): 85-91.

Phillips, N.J., Ziegler, M.R., Radford, D.M., Fair, K.L., Steinbrueck, T., Xynos, F.P., and DonisKeller, H. 1996. Allelic deletion on chromosome 17p13.3 in early ovarian cancer. *Cancer Research* **56**(3): 606-611.

Puig, O., Caspary, F., Rigaut, G., Rutz, B., Bouveret, E., Bragado-Nilsson, E., Wilm, M., and Seraphin, B. 2001. The tandem affinity purification (TAP) method: a general procedure of protein complex purification. *Methods* **24**(3): 218-229.

Rigaut, G., Shevchenko, A., Rutz, B., Wilm, M., Mann, M., and Seraphin, B. 1999. A generic protein purification method for protein complex characterization and proteome exploration. *Nat Biotechnol* **17**(10): 1030-1032.

Robinson, E.A., Henriksen, O., and Maxwell, E.S. 1974. Elongation factor 2. Amino acid sequence at the site of adenosine diphosphate ribosylation. *J Biol Chem* **249**(16): 5088-5093.

Rodnina, M.V. and Wintermeyer, W. 2009. Recent mechanistic insights into eukaryotic ribosomes. *Curr Opin Cell Biol* **21**(3): 435-443.

Roy, V., Ghani, K., and Caruso, M. 2010. A dominant-negative approach that prevents diphthamide formation confers resistance to Pseudomonas exotoxin A and diphtheria toxin. *PLoS One* **5**(12): e15753.

Schiestl, R.H. and Gietz, R.D. 1989. High efficiency transformation of intact yeast cells using single stranded nucleic acids as a carrier. *Curr Genet* **16**(5-6): 339-346.

Schuijer, M. and Berns, E. 2003. TP53 and ovarian cancer. *Human Mutation* **21**(3): 285-291.

Schultz, D.C., Vanderveer, L., Berman, D.B., Hamilton, T.C., Wong, A.J., and Godwin, A.K. 1996. Identification of two candidate tumor suppressor genes on chromosome 17p13.3. *Cancer Research* **56**(9): 1997-2002.

Sherman, F. 1991. Getting started with yeast. *Methods Enzymol* **194**: 3-21.

Shi, Y., Stefan, C.J., Rue, S.M., Teis, D., and Emr, S.D. 2011. Two novel WD40 domain-containing proteins, Ere1 and Ere2, function in the retromer-mediated endosomal recycling pathway. *Mol Biol Cell* **22**(21): 4093-4107.

Sinha, S., Rappu, P., Lange, S.C., Mantsala, P., Zalkin, H., and Smith, J.L. 1999. Crystal structure of Bacillus subtilis YabJ, a purine regulatory protein and member of the highly conserved YjgF family. *Proc Natl Acad Sci U S A* **96**(23): 13074-13079.

Sitikov, A.S., Davydova, E.K., and Ovchinnikov, L.P. 1984. Endogenous ADP-ribosylation of elongation factor 2 in polyribosome fraction of rabbit reticulocytes. *FEBS Lett* **176**(1): 261-263.

Sjolinder, M., Uhlmann, J., and Ponstingl, H. 2002. DelGEF, a homologue of the Ran guanine nucleotide exchange factor RanGEF, binds to the exocyst component Sec5 and modulates secretion. *FEBS Lett* **532**(1-2): 211-215.

-. 2004. Characterisation of an evolutionary conserved protein interacting with the putative guanine nucleotide exchange factor DelGEF and modulating secretion. *Exp Cell Res* **294**(1): 68-76.

Skogerson, L. and Engelhardt, D. 1977. Dissimilarity in protein chain elongation factor requirements between yeast and rat liver ribosomes. *J Biol Chem* **252**(4): 1471-1475.

Spahn, C.M., Gomez-Lorenzo, M.G., Grassucci, R.A., Jorgensen, R., Andersen, G.R., Beckmann, R., Penczek, P.A., Ballesta, J.P., and Frank, J. 2004. Domain movements of elongation factor eEF2 and the eukaryotic 80S ribosome facilitate tRNA translocation. *EMBO J* **23**(5): 1008-1019.

Stark, H., Rodnina, M.V., Wieden, H.J., van Heel, M., and Wintermeyer, W. 2000. Large-scale movement of elongation factor G and extensive conformational change of the ribosome during translocation. *Cell* **100**(3): 301-309.

Su, X., Chen, W., Lee, W., Jiang, H., Zhang, S., and Lin, H. 2011. YBR246W is required for the third step of diphthamide biosynthesis. *J Am Chem Soc* **134**(2): 773-776.

Sun, J., Zhang, J., Wu, F., Xu, C., Li, S., Zhao, W., Wu, Z., Wu, J., Zhou, C.Z., and Shi, Y. 2005. Solution structure of Kti11p from Saccharomyces cerevisiae reveals a novel zinc-binding module. *Biochemistry* **44**(24): 8801-8809.

Taylor, D.J., Nilsson, J., Merrill, A.R., Andersen, G.R., Nissen, P., and Frank, J. 2007. Structures of modified eEF2 80S ribosome complexes reveal the role of GTP hydrolysis in translocation. *EMBO J* **26**(9): 2421-2431.

Thakur, A., Chitoor, B., Goswami, A.V., Pareek, G., Atreya, H.S., and D'Silva, P. 2012. Structure and mechanistic insights into novel iron-mediated moonlighting functions of human J-protein cochaperone, Dph4. *J Biol Chem* **287**(16): 13194-13205.

Tong, A. and Boone, C. 2005. Synthetic Genetic Array (SGA) Analysis in Saccharomyces cerevisiae. in *Yeast Protocols, Second Edition Methods in Molecular Biology*. The Humana Press Inc., Totowa, NJ, U. S. A .

Tong, A.H., Evangelista, M., Parsons, A.B., Xu, H., Bader, G.D., Page, N., Robinson, M., Raghibizadeh, S., Hogue, C.W., Bussey, H. et al. 2001. Systematic genetic analysis with ordered arrays of yeast deletion mutants. *Science* **294**(5550): 2364-2368.

Tong, A.H., Lesage, G., Bader, G.D., Ding, H., Xu, H., Xin, X., Young, J., Berriz, G.F., Brost, R.L., Chang, M. et al. 2004. Global mapping of the yeast genetic interaction network. *Science* **303**(5659): 808-813.

Triana-Alonso, F.J., Chakraburtty, K., and Nierhaus, K.H. 1995. The elongation factor 3 unique in higher fungi and essential for protein biosynthesis is an E site factor. *J Biol Chem* **270**(35): 20473-20478.

Uthman S., B.C.J.D., Schaffrath R. 2011. Growth Inhibition Strategies Based on Antimicrobial Microbes/Toxins. in *Science against Microbial Pathogens: Communicating Current Research and Technological Advances* (ed. A. Mendez-Vilas). Formatex Research Center.

Van Ness, B.G., Howard, J.B., and Bodley, J.W. 1980a. ADP-ribosylation of elongation factor 2 by diphtheria toxin. Isolation and properties of the novel ribosyl-amino acid and its hydrolysis products. *J Biol Chem* **255**(22): 10717-10720.

-. 1980b. ADP-ribosylation of elongation factor 2 by diphtheria toxin. NMR spectra and proposed structures of ribosyl-diphthamide and its hydrolysis products. *J Biol Chem* **255**(22): 10710-10716.

Volz, K. 1999. A test case for structure-based functional assignment: the 1.2 A crystal structure of the yjgF gene product from Escherichia coli. *Protein Sci* **8**(11): 2428-2437.

Wach, A., Brachat, A., Poehlmann, R., and Philippsen, P. 1994. New heterologous modules for classical or PCR-based gene disruptions in *Saccharomyces cerevisiae*. *Yeast* **10**(13): 1793-1808.

Webb, T.R., Cross, S.H., McKie, L., Edgar, R., Vizor, L., Harrison, J., Peters, J., and Jackson, I.J. 2008. Diphthamide modification of eEF2 requires a J-domain protein and is essential for normal development. *J Cell Sci* **121**(Pt 19): 3140-3145.

Wu, F., Zhang, J., Sun, J., Huang, H., Ji, P., Chu, W., Yu, M., Yang, F., Wu, Z., Wu, J. et al. 2008. Solution structure of human DESR1, a CSL zinc-binding protein. *Proteins* **71**(1): 514-518.

Yamaizumi, M., Mekada, E., Uchida, T., and Okada, Y. 1978. One molecule of diphtheria toxin fragment A introduced into a cell can kill the cell. *Cell* **15**(1): 245-250.

Yates, S.P., Jorgensen, R., Andersen, G.R., and Merrill, A.R. 2006. Stealth and mimicry by deadly bacterial toxins. *Trends Biochem Sci* **31**(2): 123-133.

Zabel, R., Bar, C., Mehlgarten, C., and Schaffrath, R. 2008. Yeast alpha-tubulin suppressor Ats1/Kti13 relates to the Elongator complex and interacts with Elongator partner protein Kti11. *Mol Microbiol* **69**(1): 175-187.

Zhang, Y., Liu, S., Lajoie, G., and Merrill, A.R. 2008. The role of the diphthamide-containing loop within eukaryotic elongation factor 2 in ADP-ribosylation by Pseudomonas aeruginosa exotoxin A. *Biochem J* **413**(1): 163-174.

Zhang, Y., Zhu, X., Torelli, A.T., Lee, M., Dzikovski, B., Koralewski, R.M., Wang, E., Freed, J., Krebs, C., Ealick, S.E. et al. 2010. Diphthamide biosynthesis requires an organic radical generated by an iron-sulphur enzyme. *Nature* **465**(7300): 891-896.

Zhu, X., Dzikovski, B., Su, X., Torelli, A.T., Zhang, Y., Ealick, S.E., Freed, J.H., and Lin, H. 2011. Mechanistic understanding of Pyrococcus horikoshii Dph2, a [4Fe-4S] enzyme required for diphthamide biosynthesis. *Mol Biosyst* **7**(1): 74-81.

Zhu, X., Kim, J., Su, X., and Lin, H. 2010. Reconstitution of diphthine synthase activity in vitro. *Biochemistry* **49**(44): 9649-9657.